Mitochondrial stress signalling and its impacts on physiology

THÈSE N^{O} 8433 (2018)

PRÉSENTÉE LE 1ER JUIN 2018

À LA FACULTÉ DES SCIENCES DE LA VIE
CHAIRE NESTLÉ EN MÉTABOLISME ÉNERGÉTIQUE
PROGRAMME DOCTORAL EN BIOTECHNOLOGIE ET GÉNIE BIOLOGIQUE

ÉCOLE POLYTECHNIQUE FÉDÉRALE DE LAUSANNE

POUR L'OBTENTION DU GRADE DE DOCTEUR ÈS SCIENCES

PAR

Adrienne Joëlle Laurence MOTTIS

acceptée sur proposition du jury:

Prof. D. Pioletti, président du jury
Prof. J. Auwerx, directeur de thèse
Prof. J.-C. Martinou, rapporteur
Prof. A. Ablasser, rapporteuse
Prof. C. Ewald, rapporteur

ÉCOLE POLYTECHNIQUE
FÉDÉRALE DE LAUSANNE
Suisse
2018

To Nick

To my grandmothers

If it does not challenge you, then it won't change you.

Acknowledgements

These 5 years of my PhD program have been an intense and breathtaking journey. I have not only gathered valuable knowledge, but I feel that it also helped my mind grow and it particularly taught me a lot about me as a person.

First and foremost, I would like to express my sincere gratitude towards Prof. Johan Auwerx, who encouraged me to start a PhD, back in the time when I was a master intern in his lab. He has been trusting me while at the same time helpfully guiding me in many different aspects of my PhD. I am very grateful for everything that he taught me, for the skills he helped me acquire, which among others are professionalism, preciseness, efficacy and conciseness, and especially for his support, particularly in the last months of my PhD. I sincerely wish to find a career path that will enable me to be as passionate as Johan, who in my eyes embodies an inexhaustible working force.

Secondly, I would like to thank Prof. Kristina Schoonjans for her encouragements, her understanding during different times of my PhD and for the friendly moments that we shared when she offered me a chance to teach in her biochemistry lecture. This experience truly was very much enjoyable and enriching to me.

I acknowledge Prof. Andrea Ablasser, Prof. Jean-Claude Martinou, Prof. Collin Ewald and Prof. Dominique Pioletti, who accepted to be members of my jury.

I would like to thank Dr. Davide D'amico for the close and enriching collaboration we have had over these almost 3 years, through which I have genuinely learned a huge amount of things.

I also acknowledge all collaborators, whose scientific help has been crucial for the achievement of the results of this thesis: Dr. Evan Williams, Prof. Ruedi Aebershold, Manuel Kulagin and Prof. Nicola Harris, Prof. Nicola Zamboni, Prof. Robert Williams, Prof. Andrew Dillin.

I would like to express my sincere gratitude towards all my colleagues who offered me their help and support throughout this PhD and truly contributed to me forging my scientific and professional maturity. I cannot find the words to express how indispensable were Dr. Pooja Jha and Dr. Elena Katsyuba's careful and constant support as well as their inputs, especially during the writing period of my PhD. My gratitude also goes to Dr. Laurent Mouchiroud, who introduced me to the world of *C. elegans* and gave me advice and support in many aspects of my PhD; to Dr. Pedro M Quiros, Dr. Olli Matilainen and Dr. Norman Moullan, who were always willing to generously and selflessly offer their help and guidance; to Dr. Maroun Bou Sleiman, whose generosity in helping me with R programing was an amazing support, and to my other bioinformatics colleagues, Hao Li and Alexis Bachmann.

I am very grateful to the people whose advice and assistance contributed to the achievement of this thesis in its written form: Dr. Pooja Jha, Dr. Davide D'Amico, Dr. Elena Katsyuba, Naveed Ziari, Dr. Laurent Mouchiroud, Charlotte Kern, Alexis Bachman and Dr. Hadrien Demagny.

Many thanks go to the people with whom I collaborated and had fruitful scientific discussions and brainstormings: Dr. Virginija Jovaisaite, Dr. Norman Moullan, Dr. Alessia Perino and Vera Lemos, Dr. Xu Wang and Dr. Sokrates Stein. I also would like to thank the people who taught and supervised me when I was a newcomer in the lab, Dr. Pénélope Andreux, Dr. Adriano Maida, Dr. Riekelt Houtkooper, Dr. Norman Moullan and Dr. Dongryeol Ryu.

My wish is also to sincerely thank people working in our lab who are of an indispensable help for the everyday work. I would like to thank Dr. Norman Moullan, who advised me, helped me technically and had much patience in listening to me so many times. Our administrative assistant Valérie Stengel, whose efficacy very often saves our life. A lot of my thankfulness is also destined to the technicians of our lab, whose work is indispensable: many thanks to Thibaud Clerc, whose technical help has been very valuable in the last months of my PhD, to Sabrina Bichet, to Roxane Pasquettaz, to Andréane Fouassier.

I also would like to thank the EDBB PhD program, in the names of Prof. Matteo Dal Perraro and Sonja Bodmer, whose help has always been very supportive. Sonja is one of these people, whose kindness and sympathy makes you forget about administrative hurdles.

I am really thankful to Prof. Stewart Cole and his team, in particular Raphaël Sommer and Dr. Claudia Sala, who hosted me in the kindest way and provided me with a P2 facility.

I would like to thank Roy Combes, Gisèle Ferrand and Arthur Humbert and several UDP collaborators, in particular Maud, Camille and Giacomo, for helping me throughout another adventure of my PhD study, the longevity study, and for technical help.

A PhD is not only a professional adventure, but it also constitutes firework in terms of personal development. People outside of my professional environment contributed in an undefinable way to the achievement of this PhD.

Nick, je n'ai aucun mot pour décrire le soutien, la compréhension, la disponibilité et les encouragements inconditionnels dont tu as fait preuve tout au long de ces 5 ans. Ton amour a été mon guide et tu as toujours su maintenir ma motivation et ma persévérance. Merci pour tout.

Je tiens aussi à exprimer à quel point je suis reconnaissante envers mes parents et mon frère, Yves, Emmanuelle et Laurent, qui ont toujours été là pour me soutenir pendant cette aventure, ont fait preuve d'une compréhension sans limites, m'ont aidée dans plein d'aspects différents. Je suis incroyablement chanceuse de vous avoir pour famille.

Je dois aussi une grande partie de mon développement personnel au long de ce doctorat à 3 femmes qui, chacune à leur manière, ont été des coaches : Cristina Francey, Joëlle Rossier et Jennifer Beeli Guhl.

Longue est la liste des personnes qui, par leurs mots, leurs gestes et leurs encouragements, m'ont soutenue et comprise durant ce doctorat. J'aimerais néanmoins mentionner quelques personnes qui m'ont tout particulièrement entourée durant ces années : mes grands-parents ; ma belle-sœur, mon beau-frère et leurs

enfants, Jennifer, Frédéric, Emily et Robin ; mes amies les plus proches, Aurélie, Léa, Pauline, Anne-Alexandra et Jeanne ; ma tante Joëlle ; mes voisins, Lara, Emmanuele et Mattia ; ma famille d'Espagne ; mes amis, Ingrid et Romain ; ma tante et mon oncle, Martine et Daniel ; Anita, Picky, Géraldine, Francisca et tous les Budry, Bastian et Valérie, Roland et Christiane.

I finally would like to express how lucky I am of having met people in this lab, who became such close friends. I am sure our friendship will persist in time: Elena, Sabrina, Pooja, Vera, Alessia, Pan and Giuseppe. Throughout these years of my PhD, we have shared strong moments, which will remain as bright memories. Elena, tu es comme une sœur pour moi, je ne peux pas imaginer ce doctorat sans toi, merci d'avoir été là.

Thanks to all current and former members of Auwerx and Schoonjans lab for an amazing working atmosphere.

Résumé

Dans le règne eucaryote, les mitochondries sont responsables de la respiration et de la production d'énergie au sein de la cellule et participent à de nombreux processus cellulaires, comme le métabolisme intermédiaire. Ainsi, la mitochondrie impacte directement sur certaines fonctions de l'organisme comme l'équilibre métabolique, la forme physique et le vieillissement. Par conséquent, le dysfonctionnement mitochondrial est impliqué dans de nombreuses maladies comme notamment les maladies neurodégénératives, l'obésité, le diabète et le cancer. Plusieurs réseaux de surveillance moléculaire assurent continuellement le bon fonctionnement des mitochondries. Parmi les réponses déclenchées par le stress moléculaire, la « mitochondrial unfolded protein response » (UPR^{mt}) (réponse mitochondriale aux protéines dénaturées) vise à maintenir et restaurer la protéostasie au sein de cette organelle. Une meilleure compréhension de la réponse cellulaire au stress mitochondrial pourrait contribuer à élargir notre connaissance fondamentale des processus physiologiques et pathologiques impliquant les mitochondries, pouvant potentiellement conduire à de nouvelles avancées thérapeutiques ciblant ces organelles.

Cette thèse porte sur la caractérisation mécanistique et physiologique de la réponse au stress mitochondrial dans différents organismes.

J'ai utilisé l'organisme modèle *Caenorhabditis elegans* pour rechercher de nouveaux régulateurs de l'UPR^{mt} et j'ai pu identifier la protéine liant le poly-A *pab-1.* A l'aide de profilage transcriptomique, nous avons montré que l'induction des gènes immunitaires est une conséquence commune à plusieurs types de stress mitochondriaux. Nous avons démontré que *pab-1* régule aussi bien l'activation de la réponse au stress mitochondrial que l'activation de l'immunité innée. De plus, *pab-1* est nécessaire pour la survie de *C. elegans* à certaines infections bactériennes. Des données transcriptomiques provenant de plusieurs tissus humains révèlent une conservation potentielle de ce rôle immunitaire chez l'orthologue humain de *pab-1*, *PABPC1*.

Chez la souris, j'ai étudié la régulation de la réponse au stress mitochondrial au moyen d'une combinaison d'approches expérimentales bioinformatiques et *in vivo*.

Une association d'analyses transcriptomiques et protéomiques dans la population génétique de référence murine BXD a révélé une forte co-régulation des orthologues du UPR^{mt} en conditions physiologique normale. A titre d'approche complémentaire, nous avons pharmacologiquement induit un stress mitochondrial chez des souris adultes et nouvellement nées. Compte tenu de l'ascendance bactérienne des mitochondries, l'antibiotique doxycycline (dox) a également des effets délétères sur ces organelles. Nous avons établi que la dox altère l'homéostasie protéique au sein des mitochondries ainsi que la consommation d'oxygène chez les souris adultes. Cependant, le stress mitochondrial induit par traitement post-natal à la dox ne présente pas d'effets durables sur la physiologie et la longévité des souris, contrairement à ce qui a été observé chez *C. elegans*.

La flore intestinale des mammifères joue un rôle important dans l'homéostasie de leur organisme. L'utilisation d'antibiotiques perturbe l'équilibre de la flore et se répercute sur le métabolisme, l'inflammation et le système nerveux. Afin d'écarter ces effets collatéraux, nous avons traité des souris sans flore avec de la dox afin de caractériser plus précisément la réponse aux conséquences purement liées au stress mitochondrial. Au moyen du profilage multi-omique, nous avons établi que les organes, dont le fonctionnement dépend fortement des mitochondries, présentent des signatures transcriptomiques et protéomiques spécifiques suite au traitement à la dox. Dans le rein, nous avons observé une inhibition de la traduction des protéines et de la voie liée à la cible mammifère de la rapamycin (mamalian Target of Rapamycin ou mTOR), accompagnée d'une activation de la réponse au stress intégré (Integrated Stress Response ou ISR). Dans le foie, la dox a conduit à un remodelage du métabolisme des lipides. Dans ces deux organes, les marqueurs de la réponse antivirale de l'interféron type I ont été induits par la dox au niveau trancriptionnel.

Cette thèse démontre que la réponse au stress mitochondrial représente un processus varié comprenant des aspects conservés à travers les espèces, les organes et les conditions.

Mots-clés : stress mitochondrial, protéines « poly(A)-binding », immunité innée, UPR^{mt}, régulation post-transcriptionelle, souris sans flore, protéostase, méthodes transcriptomiques et protéomiques, « integrated stress response »

Summary

Mitochondria are responsible for respiration and energy harvesting across the eukaryotic kingdom. They also take part in other cellular processes like intermediary metabolism. As a result, mitochondrial function directly impacts organismal features such as metabolic homeostasis, fitness and aging. Moreover, mitochondrial dysfunction is involved in numerous pathologies, such as neurodegenerative disease, obesity, diabetes and cancer. Several surveillance pathways constantly monitor mitochondria to ensure their proper function. Among the pathways triggered by stress, the mitochondrial unfolded protein response (UPR^{mt}) aims to restore proteostasis within this organelle. A better understanding of the cellular response to mitochondrial stress would expand our fundamental knowledge of physiological and pathological processes involving mitochondria, leading to potential new therapeutics that target these organelles.

This thesis focuses on the mechanistic and physiological characterization of the mitochondrial stress response in several organisms.

I used the model organism *Caenorhabtis elegans* to screen for novel players of the UPR^{mt} and found the poly(A)-binding protein *pab-1*. Using transcript profiling, we showed that the induction of immune genes is a common consequence of several mitochondrial stressors. We demonstrated that *pab-1* regulates the activation of the mitochondrial stress response and innate immunity as well. On top, *pab-1* is required for the survival of *C. elegans* upon bacterial infection. Transcriptomic data from multiple human tissues suggest that the human *pab-1* orthologue, *PABPC1,* has a conserved role in immunity.

In mice, I explored the regulation of the mitochondrial stress response using a combination of bioinformatics and *in vivo* experimental approaches. Combined transcriptomic and proteomic analyses in the BXD mouse genetic reference population revealed a tight co-regulation of the orthologues of the UPR^{mt} under normal physiological conditions. As a complementary approach, we triggered mitochondrial stress pharmacologically in newly born and adult mice. Due to the bacterial ancestry of mitochondria, the effects of the antibiotic doxycycline (dox) are also deleterious to this organelle. We found that dox impairs mitochondrial

proteostasis and oxygen consumption in adult mice. However, mitochondrial stress induced by post-natal dox treatment did not cause long-lasting effects on mouse physiology and longevity, which is very distinct from observations in *C. elegans.*

The mammalian gut flora plays an important role in organismal homeostasis. The use of an antibiotic causes perturbations of the microbiota, with repercussions on metabolism, inflammation, and the nervous system. To eliminate these confounding effects, we also treated germ-free mice with dox to characterize the response of the mouse to a so-called “pure” mitochondrial stress. Using multi-omics profiling, we found that organs highly dependent on mitochondria display specific transcriptomic and proteomic signatures following dox treatment. In the kidney, we observed an inhibition of translation and of the mTOR pathway, accompanied by an activation of the ATF4 integrated stress response (ISR). In the liver, dox led to a remodelling of lipid metabolism. In both organs, target transcripts of type I interferon anti-viral response were induced.

This thesis demonstrates that the response to mitochondrial stress is a multi-faceted process with conserved aspects across species, organs and conditions.

Keywords: mitochondrial stress, poly(A)-binding proteins, innate immunity, UPR^{mt}, post-transcriptional regulation, germ-free mice, proteostasis, transcriptomics, proteomics, integrated stress response

Contents

List of figures

List of tables

Chapter 1 Introduction

1.1 Mitonuclear communication in stress

Adapted from

Quiros PM*, Mottis A*, Auwerx J. Mitonuclear communication in homeostasis and stress. 2016 Nature reviews Molecular cell biology 17, 213-226. doi: 10.1038

*Co-first authors

1.1.1 Introduction

Mitochondria are derived from α-proteobacteria that were engulfed by the precursor of modern eukaryotic cells before evolving as endosymbionts over millions of years. These organelles have maintained some of their ancestral bacterial characteristics, such as a circular genome and the capacity to produce ATP — mitochondria are the core of energy metabolism within the cell (Friedman and Nunnari, 2014). During evolution, however, many of the proteobacterial genes were progressively transferred to the nuclear genome, while mitochondria acquired new components and functions from the host cell, resulting in profound changes in both the mitochondrial and nuclear genome and proteome (Wallace, 2009). Out of over 1,200 proteins present in mitochondria, only 13 are encoded by the mammalian mitochondrial DNA (mtDNA) (12 in *Caenorhabditis elegans*) (Mercer et al., 2011; Pagliarini et al., 2008). These 13 proteins constitute important components of all complexes of the electron transport chain (ETC) except for complex II, the components of which are exclusively encoded within the nuclear genome. Therefore, the nucleus and mitochondria must continuously coordinate the transcription and translation, as well as the translocation and import of mitochondrial proteins (Pagliarini et al., 2008).

Mitochondria are not only at the heart of cellular energy harvesting, however — they also regulate many aspects of intermediate metabolism, calcium buffering and processes such as apoptosis. Consequently, mitochondrial function is under tight nuclear control, through so-called ‘anterograde regulation’, which can decrease or increase mitochondrial activity, as well as promote mitochondrial biogenesis, depending on cellular needs. Conversely, mitochondria can generate a ‘retrograde response’ that signals to the nucleus to alter the expression of nuclear genes to modify cellular function and reprogram its metabolism. The integration of these anterograde (from nucleus to mitochondria) and retrograde (from mitochondria to nucleus) signals — also known as mitonuclear communication — constitutes a robust network that help cells to maintain homeostasis under basal conditions and enables their adaptation to a variety of stressors. However, mitonuclear communication is most often bidirectional and of a hormetic nature, combining anterograde and retrograde signals. Thus, retrograde signals generated in reaction to some mitochondrial stressors trigger particular nuclear responses, which will induce the specific expression of certain mitochondrial proteins; in turn, these proteins will

resolve the original perturbations in the mitochondria through ‘mitonuclear feedback’. Depending on the severity and nature of the initial stress signal, mitonuclear communication can also result in an ‘integrated stress response’, which can also be induced by other stress signals such as those originating from endoplasmic reticulum (ER) stress, triggering a global cellular response by decreasing protein synthesis. Moreover, mitonuclear stress can also trigger a ‘cell non-autonomous response’, which modulates the function of distant cells to facilitate an organismal response or adaptation to stress (Figure 1.1).

Mitochondria generate a wide variety of retrograde signals through which they regulate different cellular and organismal activities, and protect against mitochondrial dysfunction by activating the expression of nuclear genes involved in metabolic reprogramming or stress defence (Jazwinski, 2013). The retrograde response exists in all organisms, but the regulation and nature of the pathways involved can vary. Despite the pleiotropic nature of the retrograde signals, these pathways can be classified into energetic stress responses, calcium-dependent responses and reactive oxygen species (ROS) stress responses, depending on the trigger.

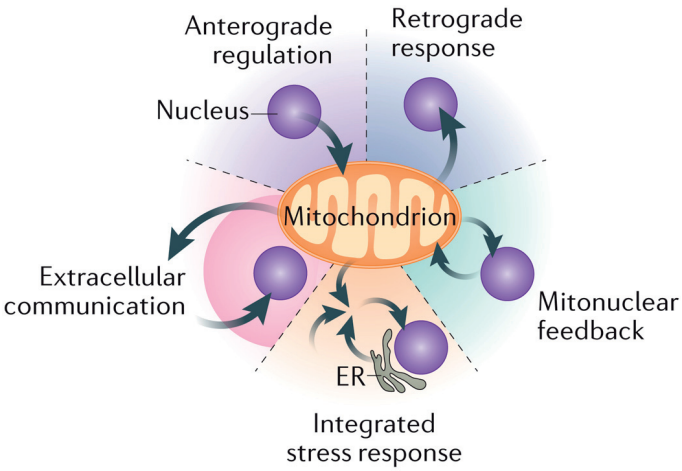

Figure 1.1 : Mitonuclear communication

Mitochondria and the nucleus communicate closely with each other. From a ‘mitocentric’ point of view, as illustrated here, signals sent from the nucleus to mitochondria constitute anterograde regulation, whereas those sent by mitochondria to the nucleus are defined as the retrograde response. Although mitonuclear feedback responses can be orchestrated bidirectionally, they usually originate from mitochondria and consequently induce a nuclear response that is specifically geared towards the mitochondria. The integrated stress response is a general cellular stress pathway that controls cytosolic protein synthesis; this stress response can be triggered in mitochondria, in the endoplasmic reticulum (ER) and in the cytosol. Mitonuclear communication can also be extracellular, as mitochondria can send extracellular cues known as mitokines, which affect nuclear regulation in a cell-non-autonomous manner.

1.1.2 Retrograde response

Energetic stress responses. The retrograde stress response was initially described in yeast, in which it regulates carbon and nitrogen metabolism (Liu and Butow, 2006). Yeast contains the retrograde response genes (RTG) 1–3, which induce different metabolic enzymes and thereby activate alternative metabolic pathways to counteract mitochondrial dysfunction (Sekito et al., 2000), including peroxisomal anaplerotic reactions such as the glyoxylate cycle (Jazwinski and Kriete, 2012). Independent of the induction of the RTG genes, other pathways, including the carbon catabolite-derepressing protein kinase (also known as Snf1; the yeast orthologue of AMPK), the target of rapamycin complex 1 (TORC1) pathway and the Sir2 pathway, can also be activated in response to energetic stress in yeast to prevent abnormal histone deacetylation and reprogram metabolism, and to regulate protein synthesis and improve protein homeostasis, respectively (Caballero et al., 2011; Friis et al., 2014; Heeren et al., 2009).

Although the absence of clear *RTG* orthologues in other species hindered the simple generalization of the retrograde signal, some pathways are activated in a similar fashion after mitochondrial stress, testifying to functional conservation. In *C. elegans*, mutations in the ETC subunits *isp-1* and *clk-1* activate AMPK subunit α-2 (Curtis et al., 2006), which transduces changes in cellular energy levels ensuing from mitochondrial stress (Apfeld et al., 2004). Defects in the TCA cycle also trigger the expression of glyoxylate cycle genes such as *gei-7* — a isocitrate lyase/malate synthase — through mechanisms that are ill-defined but that most likely involve *aak-2*, mediating the transition to mitochondria-independent energy production (Edwards et al., 2013; Gallo et al., 2011). Administration of α-ketoglutarate — a key TCA cycle intermediate — also mediates cellular adaptations leading to lifespan extension through TOR, *aak-2* and *daf-16* (Chin et al., 2014).

In mammals, the retrograde response has also been linked to mammalian TOR (mTOR) and AMPK; however, as mammalian cells lack the glyoxylate cycle, they use different anaplerotic reactions to adapt their metabolism to manage energy deficits. A decrease in mitochondrial ATP synthesis stimulates AMPK, promoting the activation of PGC1α, which stimulates mitochondrial energy metabolism and biogenesis (Garcia-Roves et al., 2008) (Figure 1.2). AMPK also triggers the mitochondrial quality control system, which regulates mitochondrial dynamics and induces mitophagy

(Egan et al., 2011). Similarly, reduced mTOR activity, such as under energetic stress (for example, during exercise and nutrient limitation), facilitates mitochondrial retrograde signaling, whereas its activation inhibits the retrograde response (Lerner et al., 2013).

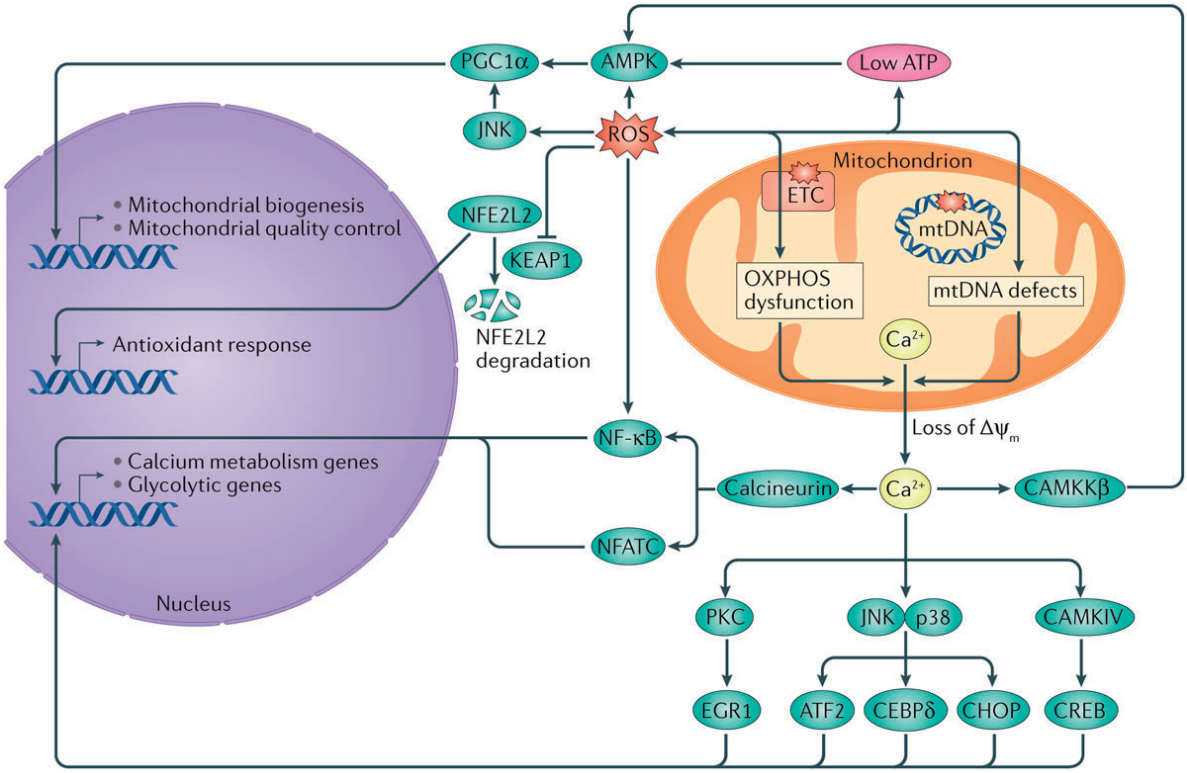

Figure 1.2 : The retrograde response

Defects in oxidative phosphorylation or mtDNA, by damage in electron transport chain (ETC) and mutations in the mtDNA, activate a retrograde response to the nucleus that can be triggered by a decrease in the level of ATP, increased signalling by reactive oxygen species (ROS) or the release of calcium ions (Ca2+) from mitochondria. Low ATP levels activate AMP-activated protein kinase (AMPK), which stimulates mitochondrial biogenesis and quality control. An increase in ROS also activates anterograde regulation through AMPK or the c-Jun N-terminal kinase (JNK) pathway, by activating PPAR gamma coactivator 1α (PGC1□□. Increased levels of ROS inhibits the KEAP1-mediated proteasomal degradation of nuclear factor erythroid 2-related factor 2 (NFE2L2) and facilitates the translocation of NFE2L2 to the nucleus and the subsequent activation of an antioxidant response. Loss of the mitochondrial membrane potential (Δψm) results in the release of calcium from mitochondria, inducing the expression of genes for calcium metabolism and glycolysis through two mechanisms. First, calcineurin translocates to the nucleus with nuclear factor κB (NF-κB), which can also be activated by ROS, and with nuclear factor of activated T cells (NFATc). Alternatively, calcium can activate several kinases, such as protein kinase C (PKC), JNK--p38 and calcium/calmodulin-dependent protein kinase type IV (CAMKIV), which, in turn, activate different transcription factors, such as EGR1, ATF2, cAMP response element-binding protein (CREB), CCAAT/enhancer-binding protein δ (C/EBPδ) and C/EBP homologous protein (CHOP). The release of calcium can also activate anterograde regulation though calcium/calmodulin-dependent protein kinase type IV (CAMKIV). ETC, electron transport chain; ROS, reactive oxygen species; mtDNA: mitochondrial DNA; OXPHOS: oxidative phosphorylation system.

Calcium-dependent stress responses. Mitochondria are essential to regulate the levels of intracellular calcium (Rizzuto et al., 2012). Different mitochondrial stressors, such as the loss of, or mutations in, mtDNA, disruption of ETC complexes and OXPHOS or treatment with **ionophores**, trigger the loss of mitochondrial membrane potential and the subsequent release of Ca^{2+} into the cytoplasm (Amuthan et al., 2002; Arnould et al., 2002; Luo et al., 1997; Srinivasan et al., 2015). Elevated levels of free cytosolic Ca^{2+} activate the phosphatase calcineurin, which activates the nuclear factor-κB (NF-κB) p105 subunit and nuclear factor of activated T cells (NFATc) (Biswas et al., 1999; Biswas et al., 2003; Formentini et al., 2012) (Figure 1.2). Both are transcription factors, which then translocate to the nucleus where they promote the synthesis of proteins involved in Ca^{2+} transport and storage (Amuthan et al., 2001; Biswas et al., 1999), and of glycolytic and gluconeogenic enzymes(Amuthan et al., 2001). Elevated Ca^{2+} also directly activates different calcium-regulated kinases, such as CaMKIV, Ca^{2+}-dependent protein kinase C, c-Jun amino-terminal kinase (JNK) and p38 mitogen-activated protein kinase (p38 MAPK), which, in turn, stimulate different transcription factors, such as CREB, EGR-1, cAMP-dependent transcription factor ATF2, CCAAT/enhancer-binding protein δ (C/EBPδ) and C/EBP homologous protein (CHOP) (Arnould et al., 2002; Biswas et al., 2003) (Figure 3). Which of these transcription factors is activated depends on the cell type and the activating stimulus; furthermore, activation not only facilitates mitochondrial adaptation, but also leads to pleiotropic responses affecting calcium metabolism, insulin signaling, glucose metabolism and cell proliferation (Amuthan et al., 2001; Biswas et al., 1999; Biswas et al., 2003; Formentini et al., 2012; Guha et al., 2010; Lim et al., 2006; Srinivasan et al., 2015; Woods et al., 2005; Wu et al., 2002).

ROS-dependent responses. Mitochondrial ROS are generated through aerobic metabolism, often resulting from defective ETC, and act directly by regulating redox biology and as a signaling molecule for numerous cellular processes, in normal as well as stress conditions (Schieber and Chandel, 2014; Shadel and Horvath, 2015). In *C. elegans*, mutation in *clk-1* — a mitochondrial hydrolase required for synthesizing the ETC component ubiquinone (Miyadera et al., 2001) — inhibits respiration and increases ROS levels, which stabilize and activate hypoxia-inducible factor 1 (HIF-1), a transcription factor regulating the adaptation to low oxygen levels (Lee et al., 2010). ROS also signal through the orthologue of stress-inducible p38 MAPK, PMK-1, which

phosphorylates and activates the transcription factor skinhead-1 (SKN-1), thereby promoting its nuclear localization (Inoue et al., 2005; Schmeisser et al., 2013; Zarse et al., 2012). These mechanisms induce the expression of adaptive ROS defense genes, such as superoxide dismutase and catalase (Zarse et al., 2012). CLK-1 itself can also act as a messenger of mitochondrial stress, as certain CLK-1 isoforms translocate to the nucleus following ROS formation and induce a protective program while inhibiting the mitochondrial unfolded protein response (UPR^{mt}) by binding chromatin, a property that is conserved in mammalian cells (Monaghan et al., 2015).

In *Drosophila melanogaster*, disruption of complex I of the ETC triggers a signaling cascade that involves ROS-mediated dimerization of the *D. melanogaster* homologue of the mammalian kinase ASK1, which promotes JNK signaling to the FOXO transcription factor and activates the cyclin-dependent kinase inhibitor Dacapo (Owusu-Ansah et al., 2008). In parallel, increased AMP levels arising from a decrease in mitochondrial ATP synthesis activate AMPK and p53, leading to the downregulation of cyclin E1 and subsequent G1 arrest as part of the G1–S cell-cycle checkpoint (Owusu-Ansah et al., 2008). Through the JNK pathway, ROS also activate the UPR^{mt} in flies with muscle-specific depletion of the complex I subunit NADH-ubiquinone oxidoreductase 75 kDa (ND75) (Owusu-Ansah et al., 2013) (see below).

In mammals, increases in ROS to levels that are not deleterious to cell function induce a retrograde signal to activate detoxification enzymes and antioxidant proteins in mitochondria and the cytosol (Chen and Kunsch, 2004; Kops et al., 2002; Lu et al., 2012; Tan et al., 2008). This activation is mediated by the binding of transcription factors such as nuclear factor erythroid 2-related factor 2 (NFE2L2, also known as NRF2, but not to be confused with GABPα mentioned above), to antioxidant response elements (Nguyen et al., 2009) (Figure 1.2). Increased levels of mitochondrial ROS were also reported to activate NF-κB, thereby promoting cellular proliferation and survival in cancer cells (Formentini et al., 2012). ROS can also induce mitochondrial biogenesis and the expression of genes involved in oxidative phosphorylation by promoting JNK--PGC1α signalling (Chae et al., 2013); and promote mitochondria fuel switching by mediating complex II phosphorylation (Acin-Perez et al., 2014) and metabolic reprogramming through mitochondrial uncoupling and AMPK activation (Shi et al., 2015).

1.1.3 Mitonuclear feedback and proteostasis

A well-conserved protein quality control system, comprising mainly chaperones and proteases encoded in the nucleus, exists in mitochondria to maintain mitochondrial proteostasis (Quiros et al., 2015). These proteins participate in the folding, assembly and turnover of mitochondrial proteins in both normal and stress conditions. Stresses that exceed the capacity of this protein quality control system are sensed by mitochondria and communicated to the nucleus to promote the expression of these quality control components, as well as other compensatory genes that have been implicated in restoring mitochondrial homeostasis through bidirectional communication between both organelles. Depending on the nature of the stressor, three different mitonuclear proteostasis responses have been described: the UPR^{mt}, which activates the expression of proteases, chaperones and other stress response genes; proteolytic stress responses, which specifically induce the expression of some mitochondrial proteases; and the heat shock response, which activates mitochondrial chaperones.

UPR^{mt}. The UPR^{mt} is a protective transcriptional response that promotes the expression of mitochondrial proteostasis genes to stabilize mitochondrial function and of metabolic genes to adapt to the provoking stress. The UPR^{mt} is triggered by mitochondrial proteotoxic stresses, such as the accumulation of unfolded proteins, impairment of the protein quality control system, mitonuclear imbalance, or inhibition of the ETC(Jovaisaite et al., 2014). The UPR^{mt} has been characterized most fully in *C. elegans*, in which it can be induced using RNAi directed against some nuclear-encoded mitochondrial proteins, such as cytochrome *c* oxidase (*cco-1*), a mitochondrial protein quality-control protease (*spg-7*), or several mitochondrial ribosomal proteins, typified by *mrps-5* (Durieux et al., 2011a; Houtkooper et al., 2013) (more on *mrps-5* below). Furthermore, doxycycline and chloramphenicol — antibiotics that target bacterial as well as mitochondrial translation owing to the evolutionary conservation of the machinery — activate the UPR^{mt} by depleting mitochondrial encoded ETC subunits, similarly to mtDNA depletion by ethidium bromide (Houtkooper et al., 2013). PARP inhibitors or NAD^+ precursors that activate SIRT1 and mitochondrial function, as well as the longevity compounds resveratrol and rapamycin, also activate the UPR^{mt} due to a mitonuclear imbalance, in this case

generated by enhancing the production of mtDNA-encoded ETC proteins (Gariani et al., 2015; Mouchiroud et al., 2013; Pirinen et al., 2014).

The UPR^{mt} in *C. elegans* involves the digestion by the matrix protease ClpP of unfolded or unassembled mitochondrial proteins into peptides, which are transported into the cytoplasm by the HAF-1 transporter (Haynes et al., 2010) (Figure 1.3). Through a poorly understood mechanism, the cytoplasmic accumulation of these peptides induces a transcriptional response co-ordinated by ATFS-1 (activating transcription factor associated with stress). ATFS-1 possesses a mitochondrial targeting sequence as well as a nuclear localization signal. In normal conditions it constantly shuttles to mitochondria, where it is degraded by the LonP protease; however, in response to mitochondrial stress, ATFS-1 import to mitochondria is attenuated, causing it to localize in the nucleus instead (Nargund et al., 2012). Here, ATFS-1 and two other factors, DVE-1 and ubiquitin-like 5 (UBL-5), induce the expression of several genes involved in mitochondrial quality control and cellular metabolism to restore proteostasis, including the mitochondrial chaperones *hsp-6*, *hsp-60 and dnj-10*, the i-AAA protease *ymel-1*, the mitochondrial fission factor *drp-1*, glycolytic genes such as *gpd-2*, detoxification genes such as the transcription factor *skn-1*, and the core components of the TIM23 complex, *tim-23* and *tim*-17 (Benedetti et al., 2006; Haynes et al., 2007; Haynes et al., 2010; Nargund et al., 2015; Nargund et al., 2012) (Figure 4a). During stress, ATFS-1 also limits the expression of other mitochondrial genes in the nucleus**,** such as those encoding TCA cycle enzymes and ETC subunits, by repressing their promoters (Nargund et al., 2015). To ensure that the expression of mitochondrial and nuclear ETC subunits is coordinated under stress conditions, certain splice variants of ATFS-1 are specifically imported into mitochondria during stress (through an unknown mechanism) where they repress the expression of mtDNA-encoded ETC subunits (Nargund et al., 2015) (Figure 1.3).

The UPR^{mt} has also been described in *D. melanogaster*, although it has been less extensively studied in this model. Overexpression of a mutated form of the mitochondrial ornithine transcarbamylase containing an internal deletion (ΔOTC), which causes mitochondrial protein overload, induces the expression of the *D. melanogaster* orthologues of the chaperones of HSP60 and mtHSP70 (Pimenta de Castro et al., 2012). Mild mitochondrial distress in muscle cells arising from the muscle-specific knockdown of ND75 from complex I in *D. melanogaster* also induces

the UPR^{mt} together with a mitohormesis response (Owusu-Ansah et al., 2013) (see below).

Several lines of evidence suggest a certain degree of conservation of the existence of the UPR^{mt} in vertebrates, including in humans. The first line of evidence comes from studies using cell lines. In monkey kidney COS7 cells, the mitochondrial protein overload generated by ΔOTC causes the activation of CHOP and C/EBPβ (Horibe and Hoogenraad, 2007; Zhao et al., 2002). Heterodimers of these transcription factors bind to conserved mitochondrial unfolded response elements and induce the expression of UPR^{mt} genes, including those encoding the chaperones HSP60, HSP10 and mtDNAJ, the proteases YME1L1, CLPP and PMPCB, the mitochondrial import complex subunit TIM17A and some mitochondrial enzymes, such as thioredoxin 2 (Aldridge et al., 2007). Knock-down of mitochondrial leucine-rich PPR motif-containing protein, which impairs complex IV, activates the UPR^{mt} by inducing mitonuclear imbalance in a neuroblastoma cell line and in worms (Kohler et al., 2015). Independent of CHOP, the mammalian mitochondrial deacetylase SIRT3 is also activated following mitochondrial proteotoxic stress; SIRT3 coordinates an antioxidant response and mitophagy (Papa and Germain, 2014) (Figure 1.3). Overexpression of ClpX, the regulatory subunit of complex ClpXP, is reportedly sufficient to induce the UPR^{mt} in C2C12 myoblasts (Al-Furoukh et al., 2015). Inhibition of Hsp90 chaperones in the mitochondria of a human glioblastoma cell line triggers the UPR^{mt} and autophagy, potentially by inducing CHOP and C/EBPβ and repressing NF-κB (Siegelin et al., 2011). Beside the induction of UPR^{mt}, overexpression of ΔOTC also leads to the activation of mitophagy, suggesting a communication between the different mitochondrial quality control systems (Jin and Youle, 2013).

Further evidence comes from several mouse models with mitochondrial dysfunction, in which the UPR^{mt} is induced, indicating that it seems to exert homeostatic functions in mammals. For instance, deficiency of aspartyl tRNA synthetase in mouse skeletal and heart muscle causes the loss of mitochondrial proteostasis, which in the heart activates the UPR^{mt} and promotes mitochondrial biogenesis (Dogan et al., 2014). Cardiomyocyte-specific deletion of the mitofusins in mice prevents mitochondrial fusion, thereby impairing mitophagy and causing the accumulation of dysfunctional mitochondria and the activation of the UPR^{mt} (Song et al., 2015). A mutation in the

mitochondrial helicase Twinkle, which causes multiple mtDNA deletions and late-onset mitochondrial disease in mice, induces a progressive OXPHOS deficiency accompanied by an increase in HSP60, mtHSP70 and CLPP protein levels in muscle (Khan et al., 2014). The histone deacetylase SIRT7, which has emerged as a master regulator of mitochondrial homeostasis (Ryu et al., 2014), can also promote, in conjunction with NRF1, the regenerative capacity of aged haematopoietic stem cells through a mechanism that potentially involves the UPR^{mt} (Mohrin et al., 2015). Finally, another indication in support of the conservation of the UPR^{mt} in mammals comes from work in the mouse BXD genetic reference population, where the expression of the prototypical UPR^{mt} gene network, comprising mammalian orthologues of six worm UPR^{mt} regulators, negatively correlates with the expression of *Cox5b/COX5B* and *Spg7/SPG7* — the mouse/human orthologues of worm *cco-1* and *spg-7* — suggesting that the low abundance of these genes triggers the UPR^{mt} in mammals as it does in *C. elegans* (Wu et al., 2014).

Heat shock response. Heat stress constitutes a threat for proteins in all cellular compartments (Akerfelt et al., 2010), but can also elicit a specific mitochondrial signal to the nucleus, causing the expression of the mitochondrial chaperones HSP10 and HSP60 in addition to regular heat shock proteins (Tan et al., 2015). In cultured cells, heat causes the translocation of the mitochondrial single-stranded DNA-binding protein 1 (SSBP1) in a complex with heat shock factor 1 (HSF1) into the nucleus, where, by recruiting the chromatin-remodelling factor BRG1, it induces the expression of mitochondrial and cytoplasmic/nuclear chaperones that are essential for maintaining the mitochondrial membrane potential and for survival following heat shock (Figure 1.3).

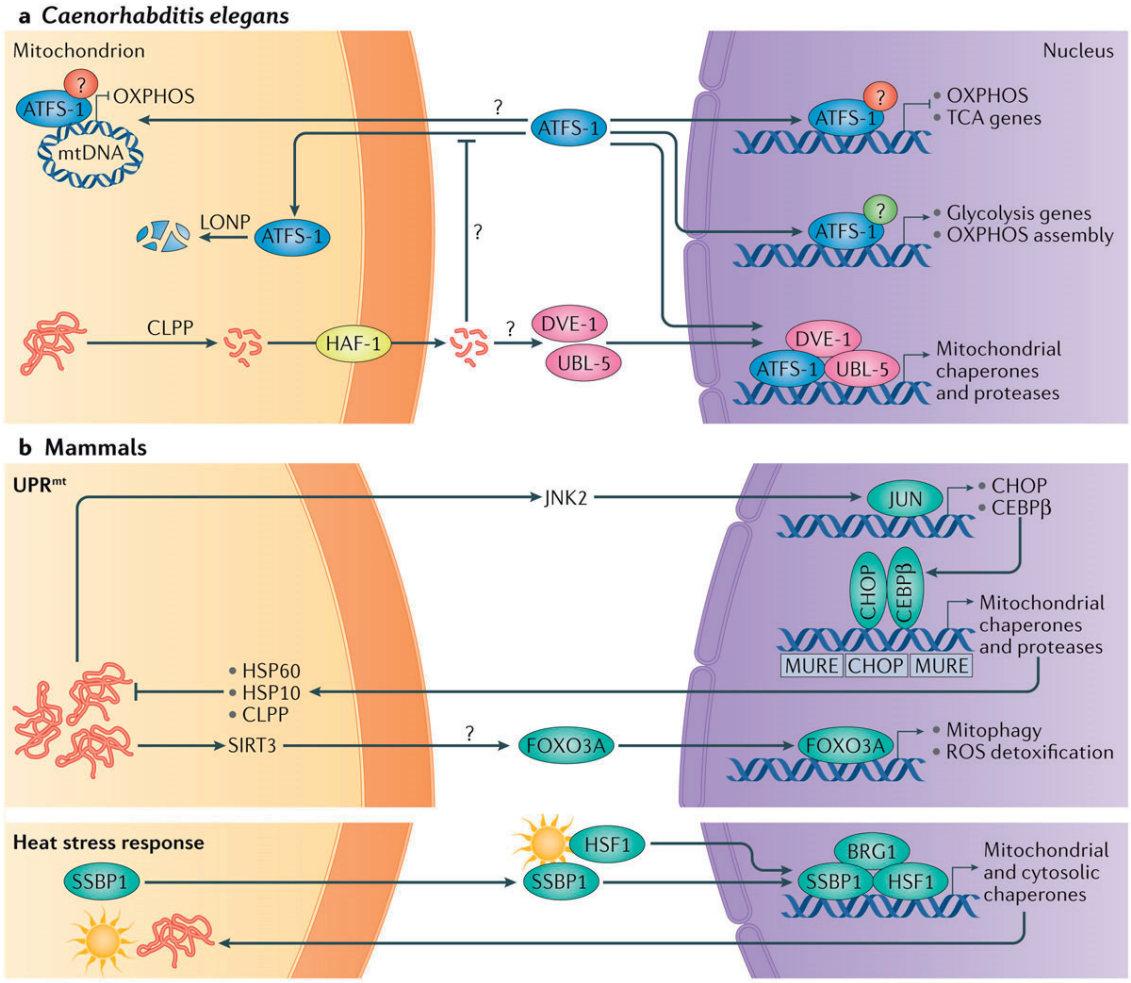

Figure 1.3 Mitonuclear feedback.

In worms, the ClpP-mediated cleavage of unfolded proteins in mitochondria initiates UPR^{mt} signalling. The efflux of short peptides through the mitochondrial transporter HAF-1 somehow inhibits mitochondrial protein import and, consequently, the transcription factor ATFS-1, which is normally imported into mitochondria and degraded by the Lon protease, translocates into the nucleus. Here, together with UBL-5 and DVE-1, it induces the expression of UPR^{mt} target genes — namely, chaperones and proteases — to restore proteostasis. ATFS-1 can also positively regulate glycolysis and assembly of the oxidative phosphorylation system, and negatively the expression of TCA cycle and oxidative phosphorylation genes. In response to mitochondrial stress, splice variants of ATFS-1 accumulate in mitochondria and repress the expression of mitochondrial genes involved in ETC.

b | In mammals, the activation of c-JUN by JNK2 leads to the induction of CHOP and C/EBPβ, which heterodimerize and activate UPR^{mt} genes. Mitochondrial proteotoxic stress also activates sirtuin 3 (SIRT3), which deacetylates FOXO3a, causing its translocation to the nucleus to induce the expression of ROS detoxification genes and mitophagy. The import of StAR from the mitochondrial outer membrane into the matrix induces, through an unknown mechanism, the expression of several proteases, which subsequently clear StAR from mitochondria. Heat causes single-stranded DNA-binding protein 1 (SSBP1) to translocate into the nucleus in association with heat shock factor HSF1 to bind the chromatin modifier BRG1 and induce the expression of mitochondrial and cytosolic chaperones. mtDNA: mitochondrial DNA; OXPHOS: oxidative phosphorylation system; TCA, tricarboxylic acid; ROS, reactive oxygen species. LonP: Lon protease; Afg3L2: AFG3-like AAA ATPase 2; Spg7: spastic paraplegia 7; Yme1l1: YME1 like 1 ATPase.

1.1.4 Integrated stress response

Mitochondrial stress can also activate the integrated stress response (ISR), which is a general cellular response that modulates global protein synthesis (Figure 5). This response is induced by different stress stimuli, including the ER unfolded protein response (UPR^{er}), the UPR^{mt}, oxidative stress, nutrient deprivation, viral double-stranded RNA or haem deficiencies (Harding et al., 2000; Harding et al., 2003). The key component of this stress response is the α subunit of eukaryotic translation initiation factor 2 (eIF2α); its phosphorylation by a number of different kinases, including general control non-derepressible-2 (GCN2), PKR-like ER-kinase, protein kinase double stranded RNA-dependent or haem-regulated inhibitor globally inhibits protein synthesis but concurrently facilitates the specific expression of stress-response genes (Donnelly et al., 2013), such as activating transcription factor 4 (ATF4) (Palam et al., 2011). ATF4, in turn, induces the expression of a wide range of stress proteins, such as CHOP, growth arrest and DNA damage-inducible protein (GADD34), ATF3, immunoglobulin heavy chain-binding protein (BiP; also known as GRP-78) or tribbles homolog 3 (TRIB3), to restore proper cellular function (Harding et al., 2000; Novoa et al., 2001; Ohoka et al., 2005).

The ISR and the phosphorylation of eIF2α as its pivot is highly conserved. In *C. elegans*, mutations in several ETC genes, such as *clk-1* or *isp-1*, induce ROS-mediated phosphorylation of eIF2α by the kinase GCN-2, thereby reducing cytosolic translation and the generation of new mitochondrial proteins (Baker et al., 2012). Activation of the ISR in this context appears crucial, as the loss of function of GCN2 affects mitochondrial activity and sensitizes cells to mitochondrial stress, with detrimental consequences (Baker et al., 2012).

In mammals, different mitochondrial stressors can activate the ISR. Arsenic-mediated mitochondrial stress, through eIF2α phosphorylation, impairs the function of the mitochondrial protein import complex and activates a gene expression program for maintaining mitochondrial proteostasis in mammals, as well as in *C. elegans* (Rainbolt et al., 2013). Altered or impaired expression of mtDNA in different mammalian cell types activates the GCN2-mediated ISR, triggering the expression of several different stress proteins, such as CHOP, TRIB3, ATF3 and hairy/enhancer-of-split related with YRPW motif protein (Michel et al., 2015). Tetracyclines such as doxycycline, which induce mitonuclear imbalance and mitochondrial dysfunction

(Houtkooper et al., 2013; Moullan et al., 2015), can also trigger the ATF4-mediated expression of stress genes (Bruning et al., 2014). The accumulation of unfolded proteins in the inner mitochondrial membrane generated by the loss of the serine protease HTRA2 in the brain also activates a CHOP-dependent ISR, protecting against neuronal cell death (Moisoi et al., 2009). In cultured cells, the outcome of the link between mitochondrial stress and the ISR can be protective or deleterious, most likely depending on the intensity and duration of the mitochondrial insults. In certain cells, inhibition of some mitochondrial ETC subunits activates an ATF4-dependent ISR, promoting cell viability and metabolic reprogramming (Evstafieva et al., 2014; Martinez-Reyes et al., 2012); however, the mitochondrial-dependent activation of the ISR is deleterious in other cell types, inhibiting cell proliferation or altering lipid metabolism (Silva et al., 2009; Viader et al., 2013).

Finally, beyond the prototypical ISR, other mechanisms aimed at controlling and decreasing global protein synthesis can be activated under conditions of mitochondrial stress, especially in yeast. In this organism, mitochondrial stress generated by loss of mitochondrial membrane potential or by defects in proteins of the mitochondrial import machinery decreases mitochondrial protein import, resulting in the aberrant cytosolic accumulation of newly synthesized unfolded mitochondrial peptides (Wang and Chen, 2015; Wrobel et al., 2015). This so-called mitochondrial precursor over-accumulation stress (mPOS) not only can lead to mitochondria-mediated cell death, but also can mitigate the stress by upregulating a large network of cytosolic genes to promote alternative pathways of protein synthesis and folding, as well as cell surviva l(Wang and Chen, 2015) (Figure 5). The mPOS response can also induce a UPR activated by mistargeting of proteins (UPRam), which protects the cell against defects in mitochondrial import by inhibiting protein synthesis and activating the proteasome (Wrobel et al., 2015).

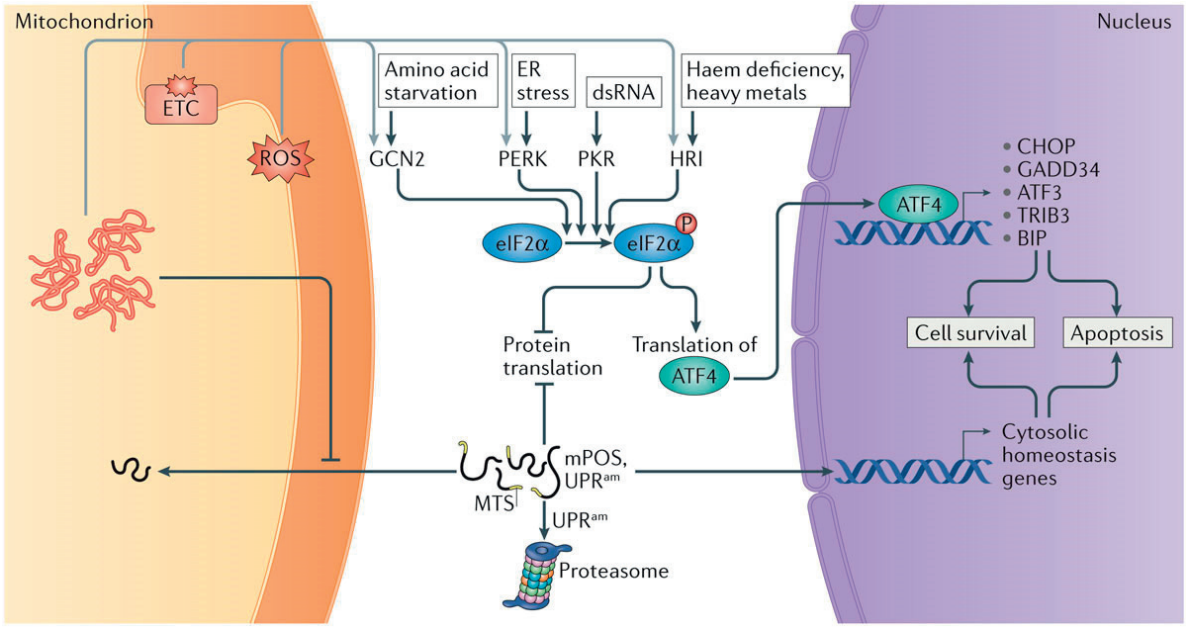

Figure 1.4 : The integrated stress response (ISR)

The central regulation node of the ISR is the translation initiation factor eIF2α, which, when phosphorylated, inhibits cytosolic translation. Four different kinases are known to phosphorylate eIF2α in response to various stresses: general control non-derepressible-2 (GCN2) is activated by amino acid starvation; PKR-like ER-kinase (PERK) is activated following endoplasmic reticulum (ER) stress; protein kinase double stranded RNA-dependent (PKR) is activated by dsRNA following viral infection; and haem-regulated inhibitor (HRI) is activated by heavy metals and haem deficiency. Defects in the electron transport chain (ETC), ROS and mitochondrial proteotoxic stresses can activate GCN2, PERK or HRI depending on the context. Phosphorylation of eIF2α promotes the selective translation of the transcription factor ATF4, which, in turn, promotes the expression of CHOP, GADD34, ATF3, BiP and TRIB3, as well as others transcription factors to restore cellular homeostasis. However, apoptosis can also ensue in the case of irreversible cellular damage. In conditions of mitochondrial stress, when protein import to mitochondria is slowed, newly translated mitochondrial polypeptides accumulate in the cytosol, inducing mitochondrial precursor over-accumulation stress (mPOS). This accumulation blocks translation and triggers UPR activated by mistargeting of proteins (UPRam), which activates the proteasomal degradation pathway and induces the expression of gene sets aimed at restoring cellular homeostasis. dsRNA: double-stranded RNA; ETC, electron transport chain; ROS, reactive oxygen species; MTS: mitochondrial targeting sequence.

1.1.5 Mitonuclear stress signalling and the immune response

Given their crucial functions in energy metabolism, mitochondria are the Achilles heel of cellular activities, constituting a prime target for attacks by pathogens and toxins that target mitochondrial activity and integrity (Arnoult et al., 2011). Furthermore, the proto-bacterial origin of mitochondria makes it tempting to speculate that cellular defence pathways against pathogens share similarities with those that defend against mitochondrial stress: when some molecules, such as mtDNA and formyl peptides, are released from damaged mitochondria, the immune system can be activated as it is during bacterial infection. The UPR^{mt} is involved in both

mitochondrial and immune surveillance to resolve mitochondrial stress and infection alike. Several bacterial species encountered by *C. elegans* induce mitochondrial dysfunction and consequently activate the UPR^{mt} as a protective response (Liu et al., 2014). Mutants in the UPR^{mt} genes *ubl-5*, *dve-1* and *atfs-1* display weakened immunity and reduced survival against bacteria that are commonly pathogenic for *C. elegans* (Hwang et al., 2014; Pellegrino et al., 2014). Following exposure to *Pseudomonas aeruginosa*, ATFS-1 induces the expression of genes encoding components of the innate immunity response such as lysozyme and antimicrobial peptides(Pellegrino et al., 2014). Immunity is also intimately linked to signalling by reactive oxygen species (ROS), as ROS activate *aak-2* and *hif-1*, leading to increased resistance of *C. elegans* to pathogenic strains of *Escherichia coli* (Hwang et al., 2014).

In mammals, mitochondrial stress also elicits an enhanced immune response. Moderate mitochondrial DNA stress induced by loss of function of transcription factor A, mitochondrial (TFAM), activates a cytosolic antiviral signal that enhances the expression of a subset of interferon-responsive genes (West et al., 2015). Mitochondria are also involved in antiviral defence through the mitochondria-associated viral sensor, a mitochondrial outer membrane protein that activates an antiviral signalling response (Arnoult et al., 2011). Mitochondrial-generated ROS contribute to the bactericidal activity of macrophages by activating cell surface Toll-like receptors (West et al., 2011). ROS also enhance immunity of mice heterozygous for a mutation in mitochondrial 5-demethoxyubiquinone hydroxylase — a protein involved in ubiquinone biosynthesis — against *Salmonella enterica* and tumour-cell grafts through the activation of hypoxia-inducible factor-1 α (Wang et al., 2010; Wang et al., 2012). Cellular protection against intracellular pathogens such as *Mycobacterium* spp. or *S. enterica* is furthermore dependent on mechanisms similar to mitophagy, the removal of defective mitochondria (Manzanillo et al., 2013). Conversely, extreme mitochondrial stress caused by TFAM deficiency in T cells causes lysosomal defects and an increased inflammatory response, which are recovered by restoring NAD^+ levels and mitochondrial function (Baixauli et al., 2015).

1.2 The innate immune response in *C. elegans*

1.2.1 *C. elegans* as a model organism

It has been over 40 years since Sydney Brenner first introduced the free-living nematode *Caenorhabitis elegans* for research use in the laboratory (Brenner, 1974). Indeed, its characteristics i.e. ease of maintenance, combined hermaphrodite and sexual reproduction, short life cycle (3 days at 20°C) and lifespan (about 20 days at 20°C) render it a very convenient model organism for eukaryotic biology. As an additional strength, *C. elegans* is a simple organism with a multi-tissues anatomy - comprising epidermis, muscles, reproductive system, intestine and nervous system - and a fixed number of 959 cells, whose complete lineage has been characterized and whose neuronal connections completely mapped (Sulston and Horvitz, 1977). Although the evolutionary distance from nematodes to humans is big, most of the essential pathways regulating homeostasis and development are present in *C. elegans* (Corsi et al., 2015). On top, the nematode genome possesses orthologues to 60-80% of human genes (Kaletta and Hengartner, 2006) and some pathologies not occurring naturally in worms can be modelled and studied in *C. elegans*, such as Alzheimer's disease and other degenerative diseases (Sorrentino et al., 2017). *C. elegans* has been used extensively in research and was therefore the first metazoan organism to be fully sequenced in 1998 (C. elegans Sequencing Consortium, 1998) . Furthermore, for *C. elegans* extremely powerful genetic tools, like whole genome RNA interference (RNAi) feeding libraries, have been developed (Kamath and Ahringer, 2003) that allow to modulate the expression of almost all genes with relative ease. It is therefore no surprise that the study of *C. elegans* enabled the discovery of many key biological processes, such as the discovery of microRNAs (Lee et al., 1993) and apoptosis genes (Hedgecock et al., 1983).

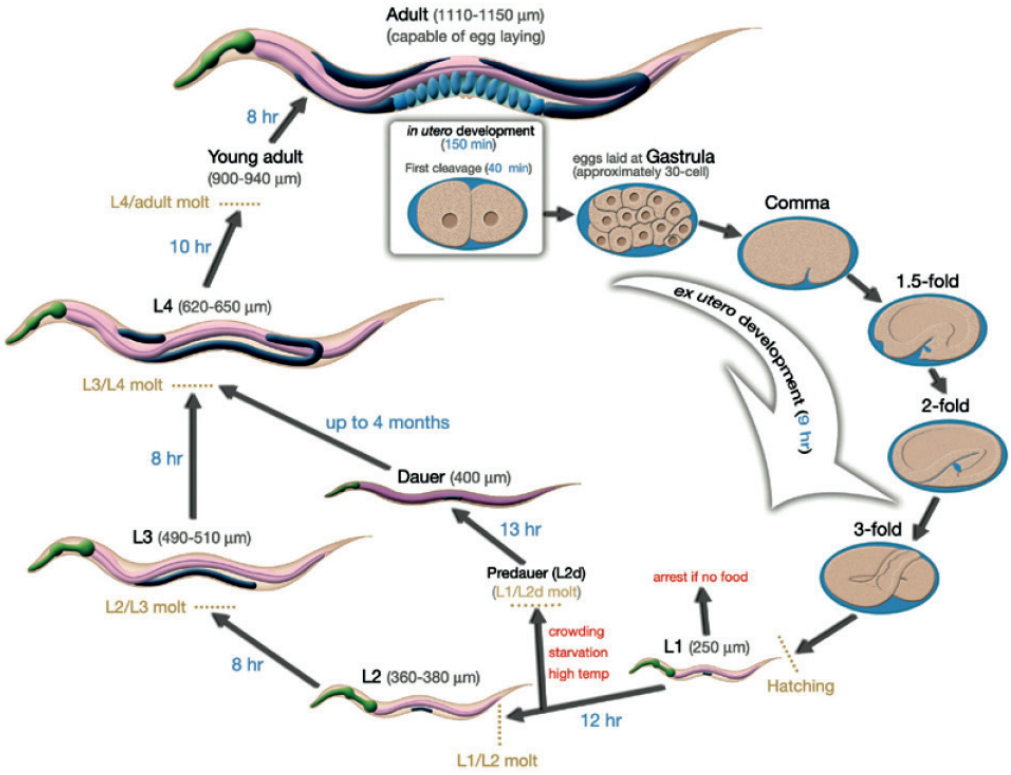

Figure 1.5 The life cycle of *C. elegans*

After hatching, the 4 larval stages and the adult stage of *C. elegans* are separated by molts. The indicated durations of the stages refer to growth at 22°C. This figure is adapted from the Worm Atlas (www.wormatlas.org).

1.2.2 General considerations about innate immunity in *C. elegans*

The activation of innate immunity in higher metazoans relies on pattern recognition receptors (PRRs), which are able to detect components of pathogens, called pathogen-associated molecular patterns (PAMPs), or components released from injured cells of the host, referred to as damage-associated molecular patterns (DAMPs) (Newton and Dixit, 2012). Amongst the best described PRRs are the Toll-like receptors (TLRs) (activated by viral or bacterial PAMPs, such as lipopolysaccharide), RIG-I-like receptors (RLRs) (responding to the presence of viral or bacterial nucleic acid in the cytoplasm) and NOD-like receptors (NLRs) (triggered by various PAMPS and DAMPs), which induce gene expression of innate immune effectors and pro-inflammatory cytokines mediated by NF-κB, type I interferon (IFN) and/or MAPK activation.

As an invertebrate, *C. elegans* does not possess any adaptive immune system and, as opposed to *Drosophila melanogaster* and higher organisms, the nematode does

not have specialized innate immune cells (Engelmann and Pujol, 2010). Thus, to fight pathogens, it mainly relies on immunity driven by epithelial cells at the body surface and in the intestine (Cohen and Troemel, 2015). Indeed, the main route of infection by bacteria, fungi and yeast is ingestion into the intestine, while some fungi and bacteria can affect the integrity of the epidermis or invade the germline through the vulva (Engelmann and Pujol, 2010). Activation of the innate immune response in worms mainly triggers the expression of effectors molecules (Engelmann and Pujol, 2010), such as (i) antimicrobial peptides of several classes, such as neuropeptide-like proteins (NLPs), (ii) lectins (*lec* and *clec* genes, binding carbohydrates on bacterial surface and involved in many species in recognition or effector functions), (iii) lysozymes (*lys* genes), (iv) caenopores (saponin-like proteins (spp) genes, killing bacteria by perforation of their membranes), and (v) ROS. Pathogenic defence also leads to upregulation of detoxification genes and efflux pumps (Shivers et al., 2008).

How the nematode recognizes pathogens is not clearly understood. The panel of the induced immune genes clearly depends on the pathogen and the type of infection, which proves selectivity of the response (Shivers et al., 2008; Tjahjono and Kirienko, 2017; Troemel et al., 2006). This suggests that worms might be able to detect features of the encountered pathogen to elicit an appropriate and specific response. However, surprisingly, no PRR able to directly recognize bacterial PAMPs has been identified in *C. elegans.* In addition, no obvious orthologues of NF-κB exist in worms. The only conserved member of the TLR family in the nematode, TOL-1, does not detect microbial components per se, but is involved in the activation of the neuronal arm of the immune response in *C. elegans* through the MAPK kinase cascade, (Pradel et al., 2007). TIR-1, a Toll-Interleukin 1 Receptor (TIR) domain adaptor protein, is required for the activation of the p38 MAPK cascade following pathogen attack, but the receptor activating TIR-1 is still unknown (Liberati et al., 2004). Beside immune gene induction, worms sense the presence of pathogenic bacteria, for example through detection of high CO_2 concentrations by specialized neurons (Bretscher et al., 2008), and as result escape the area, which is commonly referred to as “avoidance behaviour” (Zhang et al., 2005).

Since nematodes are bacteriophages, it appears logical that they cannot simply react against any bacterial features. Therefore, rather than by sensing directly pathogenic features, innate immunity in *C. elegans* seems to rely on the detection of impaired

cellular functions and homeostasis, which has been defined and well characterized in plants as “effector-triggered immunity” (Jones and Dangl, 2006). Indeed, the genetic impairment of essential cellular processes such as translation, mitochondrial respiration or proteasomal degradation induces immune gene reporters and triggers avoidance behaviour (Melo and Ruvkun, 2012).

While *C. elegans* reacts against its natural pathogens, it can also been used successfully to study the molecular mechanisms of pathogen virulence and immune response to human pathogens, which are not encountered naturally by *C. elegans* (Marsh and May, 2012). The focus of this introduction will be on the most abundantly studied pathogen in *C. elegans*, the Gram-negative bacteria *Pseudomonas aeruginosa*, an opportunistic pathogen of plants and animal (Cohen and Troemel, 2015). Studies using the nematode as a host for *P. aeruginosa* revealed very informative virulence mechanisms, that proved to be relevant to higher metazoan innate immunity (Alper et al., 2010; Kirienko et al., 2015). Therefore, the nematode represents a powerful genetic model to dissect and understand ancient and potentially conserved molecular mechanisms responsible for innate immunity (Irazoqui et al., 2010)

1.2.3 The many facets of the nematode innate immune response against *P. aeruginosa*

As for most human-pathogenic bacteria infecting the intestine of *C. elegans*, the central arm of immune activation upon *P. aeruginosa* infection signals through a MAPK cascade involving the p38 MAPK, PMK-1, and the transcription factors, ATF-7 and SKN-1/Nrf, the receptor initially activating the pathway still unknown (Ewbank and Pujol, 2016; Papp et al., 2012) (Figure 1.6). This leads to the expression of C-type lectins (*clec*), CUB-domain containing proteins (mainly extracellular proteases) and anti-microbial peptides (Troemel et al., 2006), as well as to the activation of neuronal circuitry, as mentioned above.

Many of the effects of *P. aeruginosa* infection are mediated by its Exotoxin A, which blocks host translation (Yates et al., 2006). As a result, two additional key players, the basic leucine zipper motif-containing transcription factor, ZIP-2, and the G protein-coupled receptor, FSHR-1, a distant orthologue of the gonadotropin receptor in vertebrates, activate distinct and partially overlapping sets of immune and

detoxification genes, in parallel to PMK-1 branch. ZIP-2 appears as an integrator of the effector-triggered immunity in *C. elegans*, since it also mediates the immune induction following genetic perturbations of mitochondria or histones in collaboration with CEBP-2, the orthologues of mammalian C/EBP-γ (Dunbar et al., 2012). Interestingly, ZIP-2 regulation is based on upstream open reading frames that allow translation of *zip-2* mRNA despite the translational block, a mechanism similar to the translational regulation of the stress-responsive mammalian transcription factor ATF4 (Lemaitre and Girardin, 2013).

Mitochondrial homeostasis appears as a central hub in the pathogenesis of and response to *P. aeruginosa* (Figure 1.6, orange section). Depending on the growth conditions of the bacteria, other virulence factors can be released, such as pyoverdin in “liquid killing” culture, which induces mitochondrial dysfunction and hypoxia as a consequence of its iron-scavenging action, and which activates the HIF-1 response as a result (Kirienko et al., 2013). In the regular “slow killing” condition relying on Exotoxin A virulence, the UPR^{mt} is activated upon the infection by several bacteria (Liu et al., 2014) and the UPR^{mt} transcription factor *atfs-1* also participates in immune gene expression (Pellegrino et al., 2014). As result, eliciting mitochondrial stress in a certain time window can improve the resistance of worms to subsequent *P.aeruginosa* infection (Nargund et al., 2012). Of note, ceramide and lipid metabolism is necessary for the signalling of this response (Liu et al., 2014). Mitophagy and autophagy also take part in the survival of *C. elegans* following *P. aeruginosa* infection, by removing damaged mitochondria (Kirienko et al., 2015) and preventing necrosis (Zou et al., 2014) respectively, thus rescuing the adverse effects of pathogenesis.

Finally, mitochondrial proline catabolic enzymes are essential in the modulation of ROS production to fight *P. aeruginosa* and elicit the PMK-1/SKN-1-dependent activation of detoxification genes (Tang and Pang, 2016). Mitochondrial insults caused by *P. aeruginosa* also lead the induction of surveillance genes belonging to the phylogenetically-conserved Ethanol and Stress Response Element (ESRE) network (Tjahjono and Kirienko, 2017). Genes belonging to this response contain the conserved ESRE motif and are induced following exposure to ethanol and other pleiotropic stresses (Kirienko and Fay, 2010).

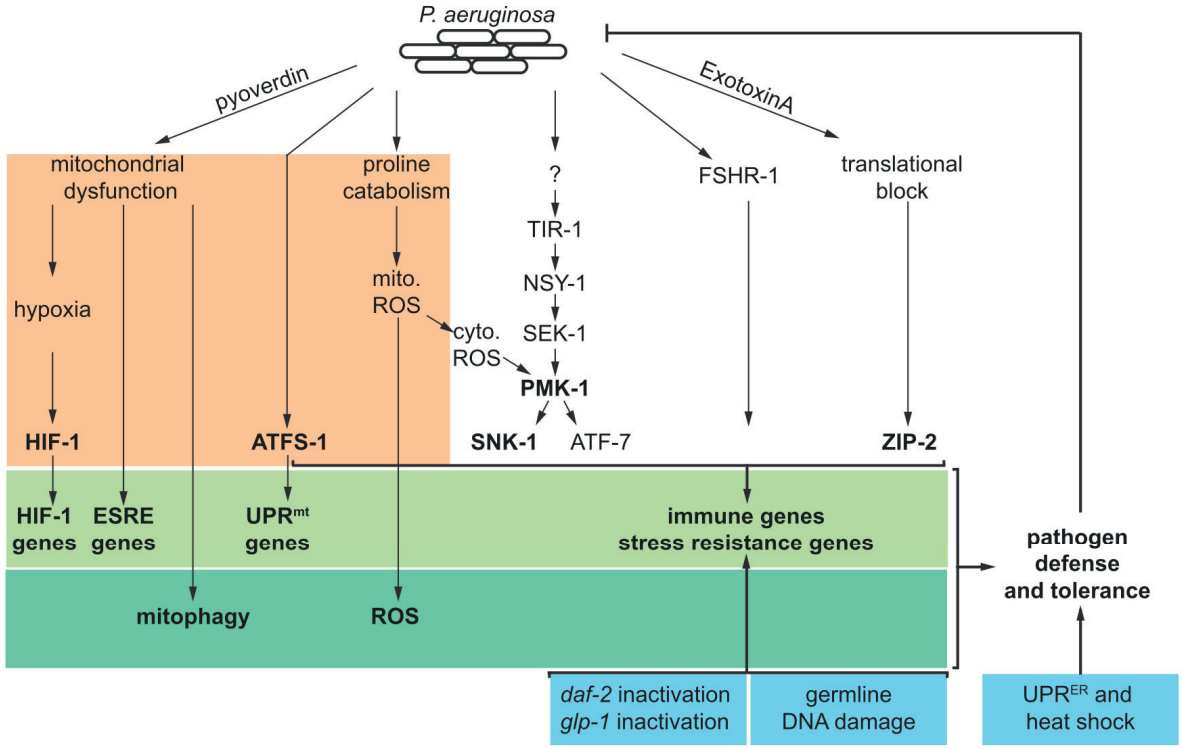

Figure 1.6 : The main defence mechanisms against *P. aeruginosa* in *C. elegans*

In green, the resulting effects of the signalling, which contribute to tolerance and defence against *P. aeruginosa*, light green representing the transcriptional responses. In orange, the mitochondria-related mechanisms. In blue, the longevity-related and systemic triggers of stress resistance.

As for ESRE, an additional layer of the innate immunity integrates the activation of other stress response and longevity pathways, such as the heat shock response and the unfolded protein response of the endoplasmic reticulum (UPR^{ER}) (Figure 1.6, blue sections). Worms with inactive *hsf-1* or *xbp-1*, the respective mediators of these responses, show a decreased resistance to *P. aeruginosa* (Richardson et al., 2010; Singh and Aballay, 2006). Amongst the most famous lifespan-extending manipulations are the mutation of the insulin-like growth factor receptor 1 homolog *daf-2*, as well as the ablation or impaired development of the germline through mutation of *glp-1* (Kenyon, 2010). These pro-longevity interventions also promote resistance to *P. aeruginosa* (Garsin et al., 2003). To exert this action, they depend on the FOXO homolog DAF-16 and PMK-1, which induce the expression of distinct stress response genes in parallel to each other (Troemel et al., 2006). Surprisingly, although *P. aeruginosa* does not appear to be a natural pathogen of *C. elegans*, it can interfere with the insulin signalling pathway by activating the *daf-2* receptor to inhibit host immunity, which is suggestive of an adaptive mechanism due to a

possible coevolution in the past in the frame of an ancient host-pathogen relationship (Evans et al., 2008).

Even if restricting to the response to *P. aeruginosa* only, one can already conclude that innate immunity in *C. elegans* integrates many of the arms of surveillance and longevity cellular signalling pathways. Although *P. aeruginosa* does not affect DNA integrity, while some pathogenic *Escherichia coli* strains do, it is interesting to mention that ultraviolet- or ionizing radiation-driven DNA-damage in the germline leads to the systemic activation of the ubiquitin proteasome system, as well as immune, heat and oxidative stress responses in distant somatic tissues (Ermolaeva et al., 2013). Of note, this systemic stress response, mediated by the ERK kinase MPK-1 in the germline and by PMK-1 in the soma, induces resistance to subsequent *P. aeruginosa* infection (Ermolaeva et al., 2013). This example demonstrates an additional layer of how innate immunity in the nematode uses cellular pathways to mount a coordinated and systemic resistance as a reaction to multiple triggers of surveillance.

Chapter 2 Thesis objectives

Mitochondria play a crucial role in cellular metabolism and viability. The altered function of these organelles has therefore been linked to various pathologies such as metabolic diseases, cancer and neurodegenerative disorders. The UPR^{mt} is part of the mitochondrial quality control system that guarantees protein homeostasis. It is thus relevant to investigate this particular stress pathway, as well as the response to mitochondrial stress in a broader sense, and their implications in physiology. However, compared to its equivalent UPR in the endoplasmic reticulum, the UPR^{mt} remains poorly characterized, particularly in mammals. My research project therefore focused on the study of the molecular regulators and mechanisms involved in UPR^{mt} and thereby also the mitochondrial stress response in a broader sense.

My first aim was to use *C. elegans* to perform a RNAi screening to find new candidate genes regulating UPR^{mt}. We identified new protein members, protein families and pathways modulating the UPR^{mt}. I focused on the study of an RNA-binding proteins, *pab-1*, and of its role in mitochondrial stress and innate immunity (Chapter 3) .

My second aim was to explore and characterize the mitochondrial stress response in mammals. With a combined approach using bioinformatics and *in vivo* experiments, our initial goal was to investigate whether UPR^{mt} is conserved in mice. Using the mouse genetic reference population and systems genetics, we documented the regulation of UPR^{mt} genes under normal physiological state (Chapter 4.1). As a complementary approach, I studied the mitochondrial response to stress induced by doxycycline treatment and examined its impact on physiology and longevity (Chapter 4.2). Finally, I characterized the response to doxycycline-induced mitochondrial stress, in a setting devoid of the interferences linked to perturbations of the microbiome in mice. I therefore treated germ-free mice with and without doxycycline and characterized the organ-specific response to mitochondrial stress using multi-omics approaches (Chapter 5), allowing me to distinguish stress induced on the "*mitobiome*" independent of effects on the "*microbiome*".

Chapter 3 The poly(A)-binding protein PAB-1 is required for mitochondrial stress signalling and defence against *Pseudomonas aeruginosa* in *C. elegans*

Adapted from

Mottis A, D'Amico D, Mouchiroud L, Li H, Jovaisaite V, Wolff S, Dillin A and §Auwerx J. In preparation.

§ Co-corresponding author

This project constituted my initial thesis project. I designed and performed the experiments and analysed the *C. elegans* transcriptomics data. I built and wrote the manuscript with guidance from JA and advices from DD. The screening was performed in collaboration in the laboratory of Andrew Dillin.

3.1 Abstract

How mitochondrial stress is signalled to remodel cellular pathways and to restore homeostasis is not yet totally understood. We performed a screen to identify suppressors of the mitochondrial unfolded protein response (UPR^{mt}), a pathway ensuring recovery of proteostasis following mitochondrial stress in *C. elegans* and identified *pab-1* as an essential player to elicit this transcriptional program. A major facet of the response to mitochondrial stress involves the induction of innate immunity genes, which critically depends on *pab-1*. In line with these observations, the loss of function of *pab-1* impedes the resistance of worms towards *Pseudomonas aeruginosa* infection in a manner partly dependent on *atfs-1*, the transcription factor governing UPR^{mt}.

3.2 Introduction

Mitochondria have historically been viewed as the seat of cellular energy harvesting. However, it is becoming increasingly clear that they are not only the powerhouses of

cell, but that they have pleiotropic functions, impacting on several cellular functions. Therefore, many aspects of mitochondrial function have to be closely monitored, including energy harvesting, mitochondrial dynamics balance, management of reactive oxygen species, as well as proteostasis. Some conserved surveillance pathways have ensued to monitor proteostasis within specific cellular compartments, thereby guaranteeing homeostasis of the whole cell and organism by extension. Such pathways include the unfolded protein response in the endosplasmic reticulum (UPR^{ER}) or the heat shock response in the cytosol. Amongst the specialized pathways aimed at restoring proteostasis, the mitochondrial unfolded protein response (UPR^{mt}), a pathway discovered and best characterized in *C. elegans*, is induced by the accumulation of misfolded proteins in mitochondria (Quiros et al., 2016). The UPR^{mt} is mainly governed by the stress-driven relocation of the transcription factor *atfs-1* from the mitochondria to the nucleus, where it induces the transcription of mitochondrial chaperones and proteases, such as *hsp-6*, *hsp-60* and *clpp-1,* to ultimately resolve the proteotoxic stress in mitochondria (Mottis et al., 2014).

Other safeguard mechanisms are specialized in the defence of the cell against pathogens and can crosstalk with cellular regulatory networks to detect and fight microorganisms. When the pathogenic Gram-negative bacteria, *Pseudomonas aeruginosa* colonizes the gut of *C. elegans*, it upregulates several innate immune genes as a result of downstream signalling by the p38 MAPK, PMK-1, the bZIP transcription factor, ZIP-2, and the G protein-coupled receptor, FSHR-1 (McEwan et al., 2012; Reddy et al., 2016; Troemel et al., 2006). An efficient way for nematodes to detect pathogenic bacteria is to sense the bacterial toxin-induced damage to cellular functions. Impairments of translation, proteasomal function or mitochondrial respiration lead to bacterial avoidance behaviour and expression of innate immune genes in *C. elegans* (Melo and Ruvkun, 2012). Therefore, when the transcription factor *atfs-1* relocalizes to the nucleus upon mitochondrial stress, or when ZIP-2 protein levels increase upon a block in translation, they transduce a stress signal to the nucleus, inducing a reparative transcriptional response of genes involved in proteostasis or innate immunity (Dunbar et al., 2012; Liu et al., 2014).

We here identify a new player in the integration of responses towards mitochondrial and pathogen stress: the cytoplasmic poly(A)-binding (PAB) protein *pab-1*. We used

doxycycline to inhibit mitochondrial translation and induce a mitochondrial stress typified by the UPR^{mt}(Houtkooper et al., 2013). We then screened for RNAi clones interrupting UPR^{mt} signalling and identified the poly-A binding protein, *pab-1*, as a regulator of mitochondrial surveillance. Using a genomics strategy, we found that the transcriptional signature of the *pab-1*-driven stress response is enriched in immune genes and subsequently demonstrated that *pab-1* is not only required to regulate the UPR^{mt} but also to provide resistance to *P. aeruginosa* infection, in a manner partly dependent on *atfs-1*. Of note, some degree of evolutionary conservation of this regulatory mechanism was suggested by the high correlation of the expression of the cytoplasmic PAB protein *PABPC1*, the closest human orthologue of *pab-1*, with innate immune and inflammatory gene sets in human genomics data. Altogether, our data point to a new mechanism for the regulation of immune and mitochondrial stress pathways, where *pab-1* might bind to A-rich sequence in these mRNAs, possibly stabilizing them and favouring their translation.

3.3 Results

3.3.1 *pab-1* is a positive regulator of the UPR^{mt}

We carried out an RNA-interference (RNAi) screening (Kamath and Ahringer, 2003) to identify proteins required for the activation of the UPR^{mt} upon mitochondrial stress, induced by doxycycline (dox), a bacterial and mitochondrial translation inhibitor (Houtkooper et al., 2013). We used the *hsp-6::gfp* reporter as a readout for the UPR^{mt} (Figure 3.1A) (Yoneda et al., 2004) and identified 189 out of 1809 pre-selected RNAi bacterial clones (from a custom made RNAi feeding library targeting transcription factors and chromatin modulators – see M&M for details) that decreased the GFP fluorescence upon dox treatment of *hsp-6::gfp* reporter worms, implying that the genes targeted by these clones are necessary for UPR^{mt} signalling. We systematically narrowed down to the most relevant hits through a few validation steps (Figure 3.1A). *First*, the RNAi hits were tested in *hsp-6::gfp* reporter worms using now, instead of a pharmacological, a genetic strategy to activate the UPR^{mt}, i.e. through the knock-down of the mitochondrial protease *spg-7*, a central player in mitochondrial protein quality control (PQC) (Yoneda et al., 2004). We visually evaluated the capacity of the 189 RNAi hits of the primary screen to reduce the GFP signal triggered by the suppression of this crucial PQC protease. We accordingly ranked them (Table 1) and selected the 8 best RNAi hits (Figure 3. 1B). As a *second* validation step, we quantified the GFP signal and selected 6 RNAi that attenuated the UPR^{mt} activation by at least 50% in *hsp-6::GFP* worms under *spg-7* silencing for further study (Figure 3.1C). It is worth noting that the demethylase *jmjd-3.1*, which was shown to regulate UPR^{mt} (Merkwirth et al., 2016), was amongst these 8 top hits. The *third* validation step relied on the use of the *rab-3::cco-1HP;ges-1::hsp-6::gfp* strain (Figure 3.1D), which displays a constitutive, cell-non-autonomous activation of the UPR^{mt} reporter in the intestine due to the stable silencing of the electron transport chain (ETC) subunit cytochrome c oxidase subunit *cco-1* (part of ETC Complex IV) in the neurons (Durieux et al., 2011a). Three candidates passed this final validation filter, i.e. *pab-1*, B0336.3 and *elt-2*. B0336.3 is a poorly characterized gene, whereas the *elt-2* RNAi was not specific for the UPR^{mt} as it also robustly attenuated the effect of tunicamycin on the UPR^{ER} (Supp. Figure 3.8C). In contrast, we found a more limited inhibitory effect of *pab-1* RNAi on UPR^{ER} activation (Supp. Figure 3.8C), which accordingly implies that it is more a selective mediator of mitochondrial stress

signalling, with equivalent effects on the UPR^{ER} as *atfs-1* (Supp. Figure 3.8C). Therefore, we focussed on *pab-1*, a cytosolic cytosolic poly(A)-binding protein for further validation studies. We established that *pab-1* RNAi was able to decrease the expression of several UPR^{mt} genes in wild type (WT) N2 worms treated with dox (Figure 3.1E). Mutation in several ETC subunits activates UPR^{mt} signalling (Benedetti et al., 2006; Yoneda et al., 2004); *pab-1* knock-down (KD) furthermore also reduced the induction of UPR^{mt} gene expression in *nuo-6* mutants of the NADH dehydrogenase subunit of ETC Complex I (Figure 3.1F). Taken together, our screening identified *pab-1* as a new regulator of the UPR^{mt}.

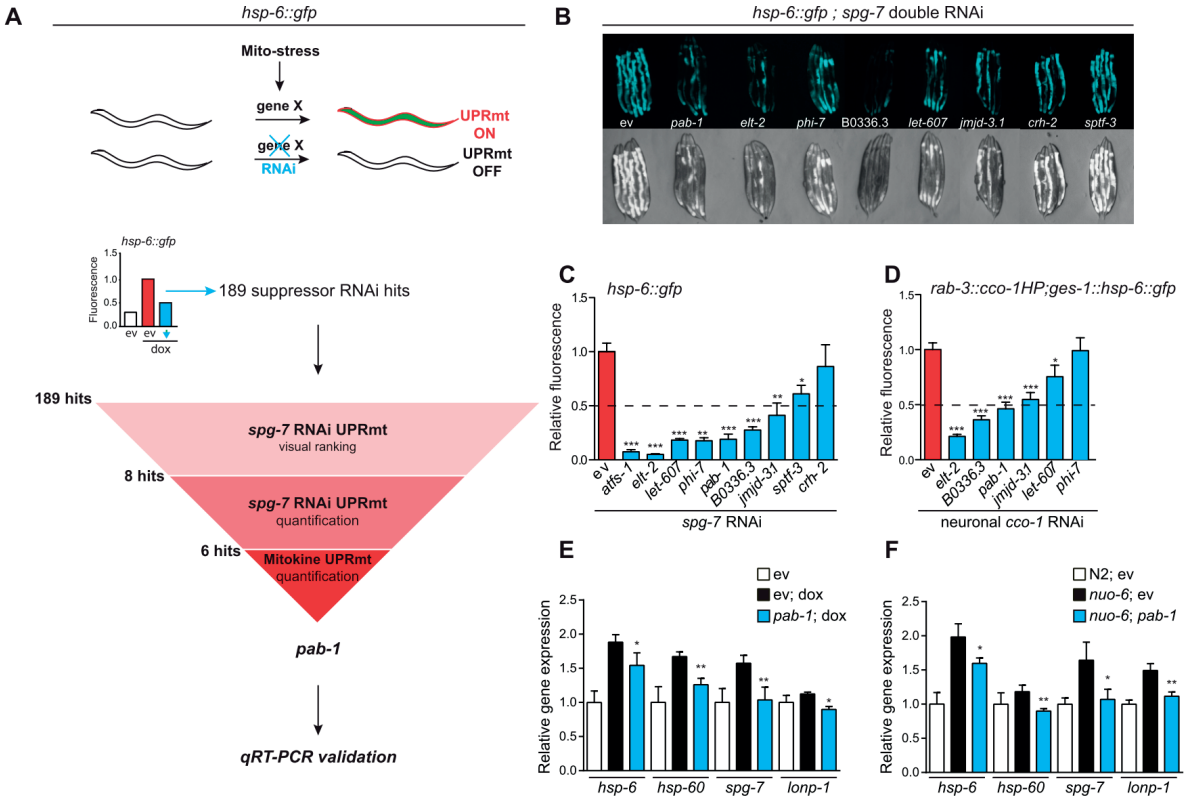

Figure 3.1 : Screening for mediators of UPR^{mt} response identifies *pab-1*

A. Schematic representation of the screening strategy to identify candidate regulators of mitochondrial stress. B. Representative pictures of *hsp-6::gfp* reporter worms fed with RNAi against the 8 top hits from our screen mixed in a ½ ratio with *spg-7* RNAi. C. Quantification of the suppressive effect on *hsp-6::gfp* fluorescence of RNAi against the 8 top hits mixed with *spg-7* RNAi. D. Quantification of the suppressive effect of the fluorescence of the mitokine-driven UPR^{mt} signalling reporter by the 6 top hits after quantification in 1C. C.D. Bars show mean±SEM, ***student t-test p-value P≤0.001 E and F. RT-qPCR validation of the suppressive effect of *pab-1* RNAi on the transcript levels of UPR^{mt} mediators induced by doxycycline treatment (E) *or nuo-6* mutation(F). Bars show mean±SD, *ANOVA p-value P≤0.05, **P≤0.01, *** P≤0.001. [a larger version of the figure can be found in Annexes]

3.3.2 The immune response is activated by mitochondrial stress in *nuo-6* mutants in a *pab-1* dependent manner

To gain insights into the molecular consequences of down-regulating *pab-1* in the context of mitochondrial stress, we analysed by RNA-Seq the impact of *pab-1* loss-of-function on transcript levels in both wild type N2 and *nuo-6* mutant worms. The 4 conditions were clearly segregated from each other by Principal Component Analysis (PCA) (Figure 3.2A), implying that the *nuo-6* mutation and *pab-1* silencing led to an extensive remodelling of gene expression, beyond the well-documented changes in the transcripts of the key UPR^{mt} genes (Supp.Figure 3.8C). To explore processes affected by *pab-1* LOF during mitochondrial stress, we focussed on those genes that were concomitantly up-regulated by the *nuo-6* mutation and down-regulated by *pab-1* LOF, eliminating from this group the genes down-regulated by *pab-1* KD in WT N2 (see green arrows in the scheme in Figure 3.2A). This analysis identified 417 genes fulfilling these filtering criteria. The top significant biological process terms that were enriched upon GO analysis were related to immunity, including “defence response”, “innate immune response”, “defence response to bacterium” (Figure 3.2B). Other enriched processes were linked to stress response, detoxification and metabolism, which corresponds to pathways usually induced by mitochondrial stress (Nargund et al., 2012). Further, the significantly enriched cellular component (CC) terms included several mitochondria-related terms, demonstrating the implication of the cytosolic *pab-1* protein in mitochondrial surveillance (Figure 3.2C). As an illustration of our selection process, *pab-1*-dependent genes belonging to the GO set “innate immune response” showed striking *nuo-6*- and *pab-1*- regulated changes in transcript levels (Figure 3.2D). Altogether, this analysis of gene expression patterns suggests that mitochondrial stress triggers the expression of innate immunity genes in a *pab-1*-dependent manner.

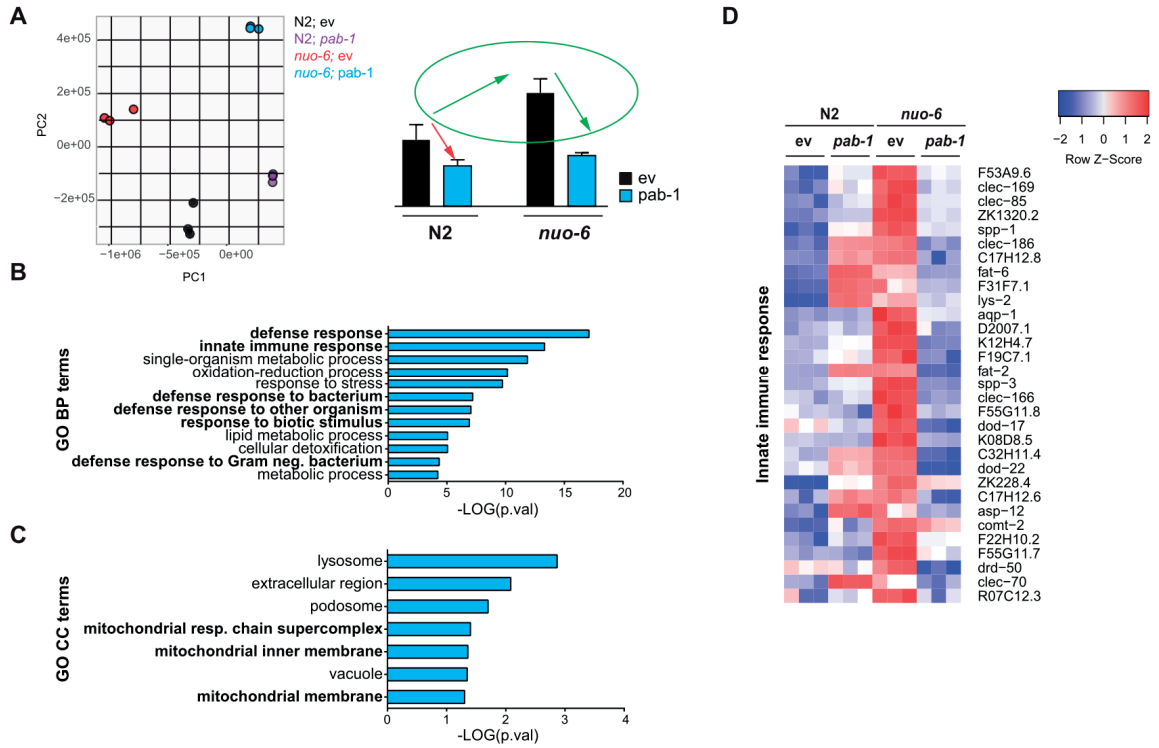

Figure 3.2 : *pab-1* drives the expression of immune genes in *nuo-6* mutants

A. Left: Principal component analysis of the RNA-Seq results from samples belonging to the 4 experimental conditions depicted in the legend. Right: The set of *pab-1*-dependent genes induced upon mito-stress comprises genes fulfilling three conditions: (i) being up-regulated by at least 1.5 fold in nuo-6 mutants compared to N2 worms (ii) being down-regulated by at least 1.5 fold by *pab-1* RNAi in *nuo-6* mutant background; and (iii) not being down-regulated by at least 1.5 fold by *pab-1* RNAi in N2 WT background (FDR≤0.05 for each condition). B. GO biological processes (GO BP) enriched in the *pab-1*-dependent gene set. C. GO cellular component (GO CC) enriched in the *pab-1*-dependent gene set. D. Heatmap representing the mRNA levels of the innate immunity genes in the RNA-Seq results in the 4 groups of worms.

3.3.3 The immune response as a major pathway activated by mitochondrial stress

Several studies already showed that immune response genes are triggered upon mitochondrial stress in *C. elegans* (Liu et al., 2014; Pellegrino et al., 2014). We wanted to extend this observation and ascertain that the immune response was a common pathway triggered by different mitochondrial stressors and hence we profiled transcript levels induced by three different mitochondrial stress conditions, i.e. *nuo-6* mutant worms, with an ETC Complex I subunit deletion, worms fed with an RNAi targeting the Complex IV protein *cco-1*, and worms treated with the bacterial and translational inhibitor, dox. We identified 667 genes that were commonly up-regulated amongst these 3 conditions (Figure 3.3A). The only significant GO term enriched in this common mitochondrial stress gene set was the “innate immune

response" (Figure 3.3B). Volcano plots of the differentially expressed genes in each of the three mito-stress conditions (Figure 3.3C), showed a clear induction of genes that are members of the mitochondrial stress geneset (from the Venn overlap; highlighted in orange), as well as members of the "innate immune response" (GO: 0045087; highlighted in green). Heatmaps representing the expression pattern of immune genes (Figure 3.3D) provide further convincing proof of their common activation by these three mito-stress conditions. Together, these data demonstrate that induction of immune genes is a common response to various types of mitochondrial stress (genetic as well as pharmacological) in *C.elegans* and are aligned with previous studies (Liu et al., 2014; Pellegrino et al., 2014).

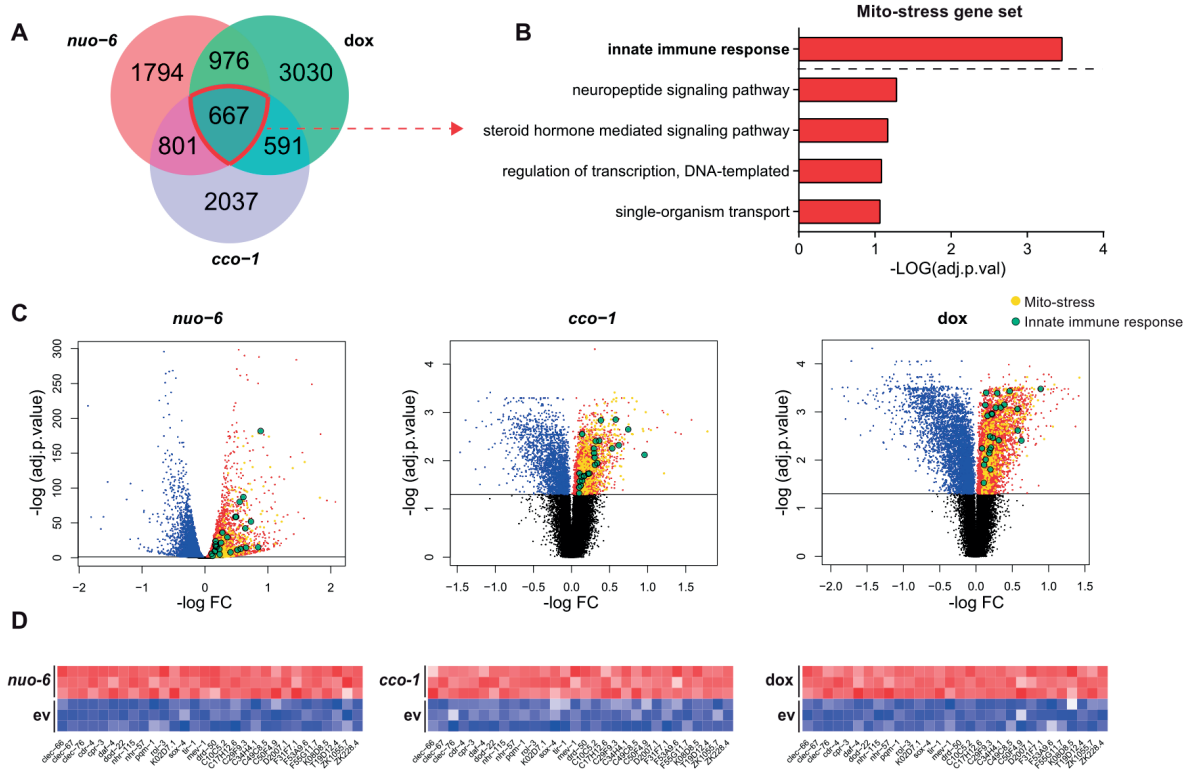

Figure 3.3 : Innate immunity genes are enriched in the common differentially expressed genes to three different triggers of mitochondrial stress

A. Venn diagram displaying the genes commonly up-regulated between 4 different conditions of mitochondrial stress : (i) RNA-Seq of *nuo-6* mutants *vs* N2 WT worms (fold change (FC)≥1.5, FDR≤0.05); (ii) microarray expression data of transcripts induced upon *cco-1* RNAi (fold change (FC)≥1.2, nom.p-value≤0.025); (iii) microarray expression data of transcripts induced by dox (fold change (FC)≥1.2, nom.p-value≤0.025. 667 genes in the middle represent the common set of genes induced by 3 independent mitochondrial stressors. B. GO biological processes (GO BP) enriched in the genes induced by mitochondrial stress. C. Volcano plots displaying –log(nom. p-value) and log(FC) of all genes for each of the three mitochondrial stress conditions. Orange dots represent the genes belonging to the mitochondrial stress gene set, whereas the green circles represent innate immunity genes (GO: 0045087). D. Heatmaps of the common innate immunity genes (30) induced in each of the 3 mitochondrial stress conditions. [a larger version of the figure can be found in Annexes]

3.3.4 *pab-1* is required for the expression of immune genes upon PA14 infection and dox treatment

To further ascertain the relevance of *pab-1* in the immune response, we overlapped the set of genes commonly up-regulated by mitochondrial stress (see Figure 3.3A) with the group of *pab-1*-regulated genes (Figure 3.2) and genes up-regulated upon infection of *C. elegans* with the Gram-negative, pathogenic bacterial strain *Pseudomonas aeruginosa* 14 (PA14) (Troemel et al., 2006) (Figure 3.4A). The resulting overlapping core set contained only 9 genes (Figure 3.4B), 7 of which were related to innate immunity (Figure 3.4B). As such the GO term analysis showed that the only significantly enriched process was innate immunity (Figure 3.4C). In accordance, *pab-1* RNAi robustly blunted the increased expression of this core set of immune genes upon infection of *C. elegans* by PA14 (Figure 3.4D and Supp. Figure 3.9A). *pab-1* LOF also inhibited the induction of the same transcripts following dox-induced mitochondrial stress.. Hence, these results demonstrate that *pab-1* is required to mount a proper transcriptional response involving immune genes, not only during mitochondrial stress, but also upon infection with the PA14 strain.

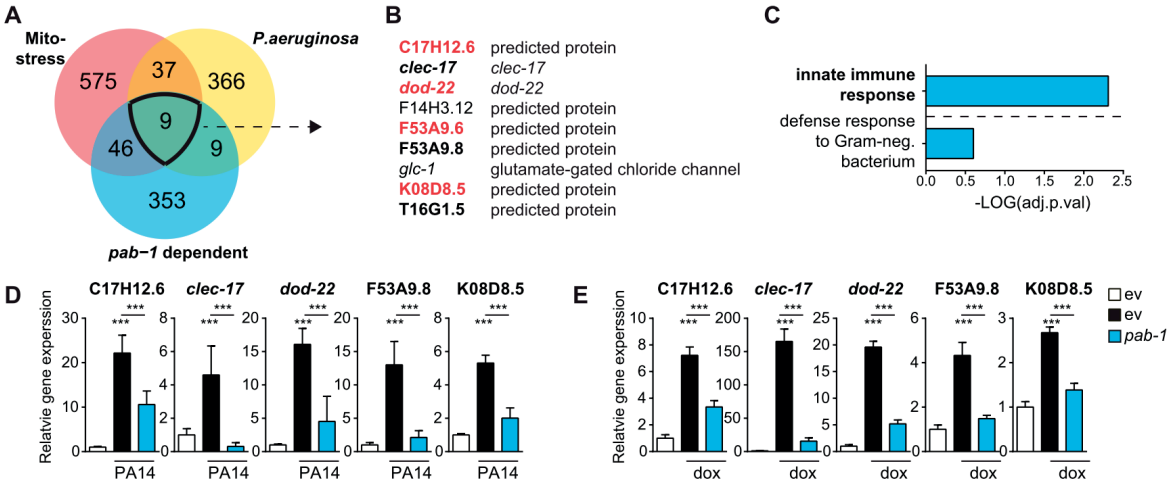

Figure 3.4 : Immune gene expression following dox or PA14 infection is dependent on *pab-1*

A. Venn diagram representing the 9 overlapping genes between (i) mitochondrial stress (from Fig.3A), (ii) the *pab-1*-dependent gene set (from Fig.2A) and (iii) the genes induced by *P.aeruginosa* PA14 infection, 4h and 8h post-infection (Troemel et al., 2006). B. List of the nine genes present in the core overlapping gene set. Four of these genes are known regulators of the immune response based on GO annotations (bold red) and three are linked to immunity based on their description on Wormbase (bold black). C. GO biological processes (GO BP) enriched in the core gene set. D. RT-qPCR results showing transcript levels of the core genes 24h post infection by *P.aeruginosa* PA14. Bars show mean±SD, *ANOVA p-value P≤0.05, **P≤0.01, *** P≤0.001. E. RT-qPCR results showing transcript levels of the core set genes after doxycycline treatment. Bars show mean±SD, *ANOVA p-value P≤0.05, **P≤0.01, *** P≤0.001.

3.3.5 *PABPC1*-correlated genes are enriched for immune and inflammation GO terms in human tissues

In order to gain insights into a possible conservation of this phenomenon in higher organisms, we carried out population-level gene set analysis (PGSA) for *PABPC1* in human population transcriptome data archived in the GTEx portal (Battle et al., 2017). This bioinformatic analysis provided an unbiased identification and quantification of the correlation between the expression of GO gene sets with the expression of *PABPC1*, the closest human orthologue to *pab-1*, across multiple tissues. Although GTEx does not provide expression data for immune cells *per se*, the clustering of immune terms amongst the most strongly correlated gene sets in aorta, liver, transverse colon, heart and oesophagus (Figure 3.5A) or in other tissues (Figure 3.5B), firmly suggests a conserved role of PABPC1 in controlling immune gene expression as part of the defence program against microorganisms or inflammation. These results point out an important and conserved role of *pab-1* and its human orthologue *PABPC1* in the expression of innate immune genes.

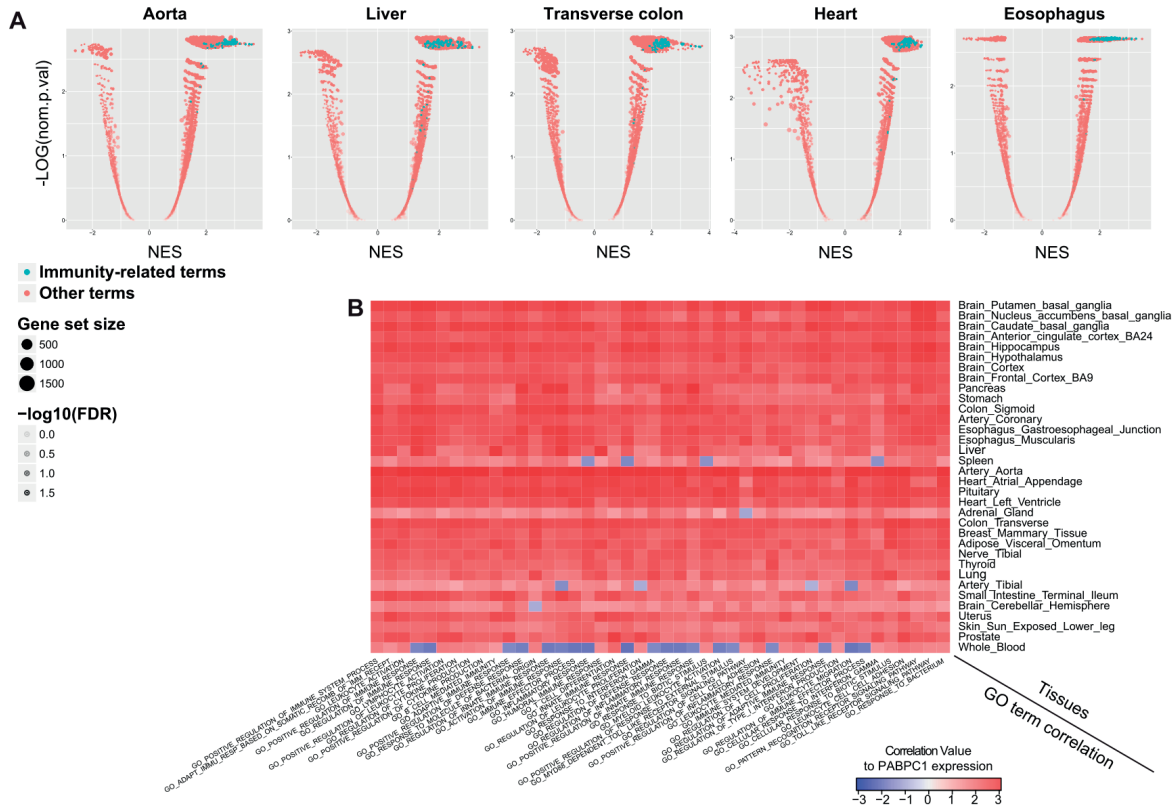

Figure 3.5 : The expression of human *PABPC1* correlates with immune and inflammatory gene sets

A. Volcano plots displaying the –log(nom. p-value) and normalized enrichment score (NES) in population gene set analysis (PGSA) results for *PABPC1*, respectively in each of the mentioned

tissues of human GTEx database samples. Immune-related GO terms are highlighted in turquoise. B. Heatmap showing the correlation of *PABPC1* with immune GO terms within the human tissues available in GTEx database. [a larger version of the figure can be found in Annexes]

3.3.6 *pab-1* LOF impairs survival to *P. aeruginosa* infection in an *atfs-1*-dependent manner

We next verified whether the robust impact of *pab-1* on immune genes translates into concrete effects on worm physiology and assessed the survival of worms in response to PA14 infection, in a slow-killing experimental set-up (Kirienko et al., 2014). WT N2 worms showed a mild, but significant, decrease in survival to bacterial infection upon *pab-1* RNAi feeding (Figure 3.6A). In addition, the exacerbated escaping behaviour of worms fed *pab-1* RNAi further demonstrated that they were suffering more than the control (Figure 3.6A, inset) (Battle et al., 2017).

Amongst the genes down-regulated by *pab-1* silencing in N2 worms in our RNA-Seq data, many relate to germline development (Supp. Figure 3.9B), which is line with the previous literature documenting a major role for *pab-1* in the development of the worm germline (Ko et al., 2013). Accordingly, we observed that *pab-1* LOF worms laid a significantly lower number of eggs than controls (Supp. Figure 3.9C), corroborating a disturbed development of their germline. Interestingly, germline impairment and the resulting signalling (Hsin and Kenyon, 1999; Lin et al., 2001), known as germline signalling, have been shown to increase worm resistance to PA14 (Alper et al., 2010). Therefore, we hypothesize that *pab-1* LOF leads to 2 opposite consequences: the activation of germline signalling and the reduction of immune genes expression, which respectively act as pro- and anti-survival signals during PA14 infection (Figure 3.6B). Hence, to avoid the confounding effects of germline signalling, we silenced *pab-1* by RNAi feeding in the *glp-1* mutants that are devoid of germline (Priess et al., 1987). As expected, when the germline was absent, the detrimental impact of *pab-1* LOF on the survival (Figure 3.6C) was accentuated.

As stated above, mitochondrial stress and immunity have already been shown to relate closely to each other, and exposing worms to mitochondrial stress primes them for an immune response and improves their resistance to a subsequent infection by PA14 (Pellegrino et al., 2014). *atfs-1* has been proven necessary for this particular type of stress-driven immunity. Interestingly, *pab-1* silencing disrupts the activation of *hsp-6::gfp* reporter following PA14 infection (Figure 3.6D). Since the *pab-1* LOF

phenotype combines alterations in both mitochondrial and immune responses, we hypothesized that it might at least in part require the action of *atfs-1*. Indeed, *pab-1* RNAi fails to impair the survival of *atfs-1* mutant worms when exposed to PA14 infection (Figure 3.6E). In line, the decrease of some UPR^{mt} genes observed in WT N2 worms upon *pab-1* RNAi feeding and PA14 infection is abrogated in the *atfs-1* mutant (Figure 3.6F). During PA 14 infection, *atfs-1* LOF also partially blunts the inhibitory effect of *pab-1* RNAi on some *pab-1*-dependent immune genes, such as *dod-22*, C17H12.6 and *glc-1* (Figure 3.6G). However, for some other genes, like K08D8.5 or F53A9.8 (Supp. Figure 3.9G), *atfs-1* LOF does not affect the down-regulation induced by *pab-1* silencing.

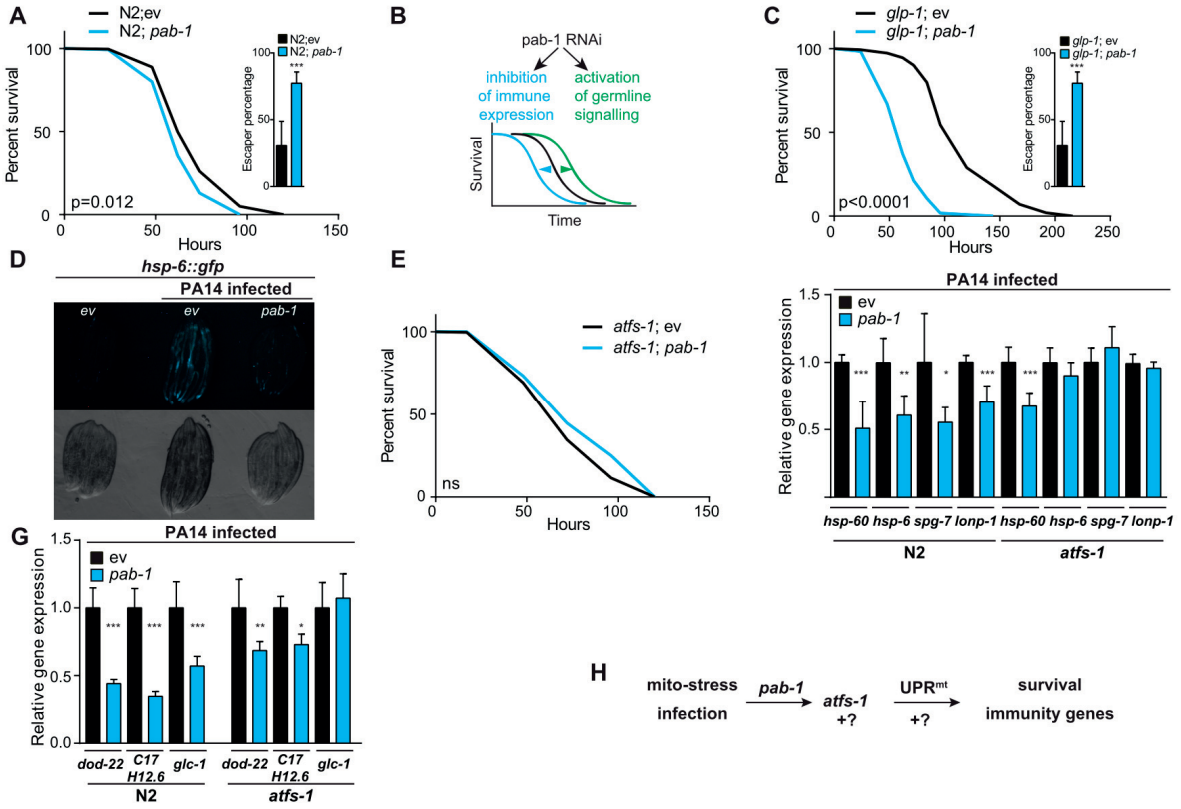

Figure 3.6 : *pab-1* is required for the survival upon *P. aeruginosa* infection

A. Survival curves of N2 WT worms exposed to *P.aeruginosa* PA14 (statistics with log-rank (Mantel-Cox) method) and percentage escapers per plate 24h post PA14 infection (Bars show mean±SD, ***student t-test p-value P≤0.001). B. Scheme illustrating the dual effect of *pab-1* silencing on worm survival upon *P.aeruginosa* PA14 infection: we show that *pab-1* LOF impairs immune gene expression, whereas it also activates germline signalling, a pro-survival intervention in the context of PA14 infection. C. Survival curves of *glp-1* mutant worms exposed to *P.aeruginosa* PA14 (statistics with log-rank (Mantel-Cox) method) and percentage escapers per plate 24h post-infection (Bars show mean±SD, ***student t-test p-value P≤0.001). D. Representative pictures of the *hsp-6::gfp* reporter worms treated with *P.aeruginosa* PA14 strain and *ev* (control empty vector) or *pab-1* RNAi. E. Survival curves of *atfs-1* mutant worms exposed to *P.aeruginosa* PA14 (statistics with log-rank (Mantel-Cox) method). F. RT-qPCR results showing the effect of *pab-1* RNAi on UPR^{mt} genes in N2 WT and *atfs-1*

mutant worms treated with *P.aeruginosa* PA14 strain. Bars show mean±SD, *student t-test p-value P≤0.05, **P≤0.01, *** P≤0.001. G. RT-qPCR results showing the effect of *pab-1* RNAi on UPR^{mt} genes in N2 WT and *atfs-1* mutant worms treated with *P.aeruginosa* PA14 strain. Bars show mean±SD, * ANOVA p-value P≤0.05, **P≤0.01, *** P≤0.001. H. Schematic model representing the main results shown in this study.

Taken together, these results demonstrate that *pab-1* is required for *C. elegans* defence against *P. aeruginosa* infection. In addition, *pab-1* RNAi affects the survival to *P. aeruginosa* through a mechanism that depends at least in part on *atfs-1* and UPR^{mt} gene expression (Figure 3.6H). However, at least when considering the expression of some immune transcripts (K08D8.5 or F53A9.8), *atfs-1* does not seem to be the only mediator, since the effect of *pab-1* LOF for these genes is similar in WT and in *atfs-1* mutant context, suggesting the involvement of other mediators (Figure 3.6H).

To get insights into the mechanism used by *pab-1* to regulate immune and mitochondrial stress responses, we searched into the literature for a role of its orthologues in stress conditions. Although PAB proteins are considered to mainly bind to the 3' poly(A)-tail of mRNAs (Smith et al., 2014), studies in plants (Xu et al., 2017), yeast (Gilbert et al., 2007) and mammalian cells (Kini et al., 2016; Sladic et al., 2004) report the ability of PAB proteins to bind A- and AU-rich regions all along mRNA sequences. Most interestingly, this special binding activity by PAB proteins seems to result in a dynamic regulation of mRNA translation, allowing the cell to react to abrupt environmental changes. Indeed, we found that the 5'UTR of the genes regulated by *pab-1* were significantly enriched in A-rich sequences (Figure 3.7 A). This suggests that these A-rich stretches might account for the mechanism of *pab-1*-driven regulation of mRNA levels.

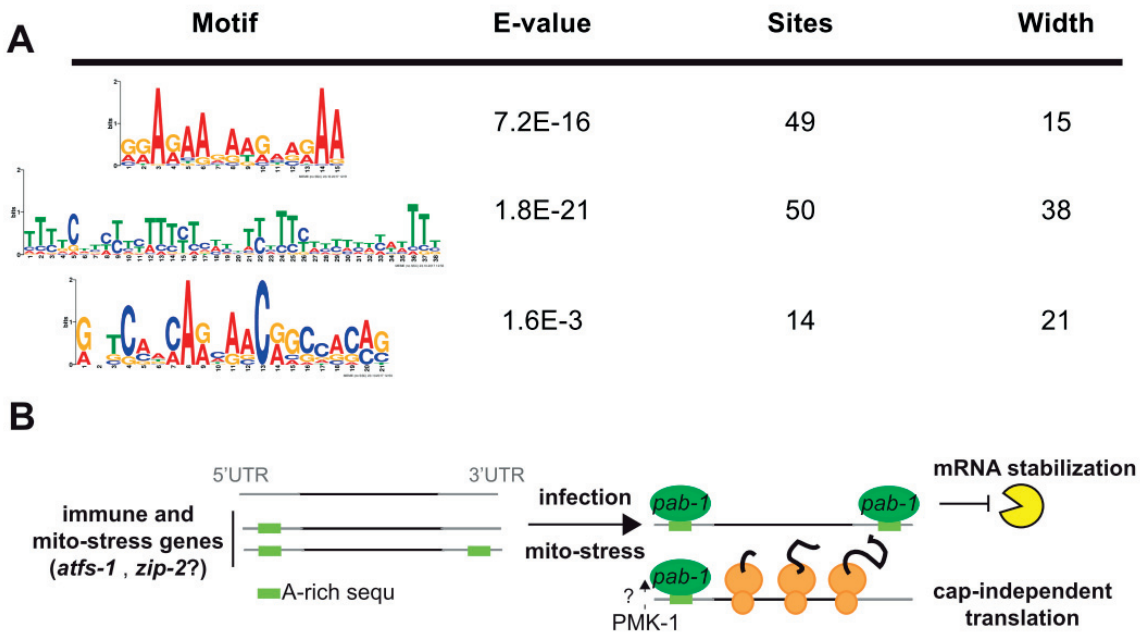

Figure 3.7 : A possible implication of A-rich sequences in the regulation of mRNAs by *pab-1* during stress

A. Enriched motifs in the 5' UTR of *pab-1*-dependent genes according to Multiple Em for Motif Elicitation (MEME) analysis from the MEME suite software. B. Model of a possible mechanism for the regulation exerted by *pab-1* in the context of innate immunity and mito-stress response.

3.4 Discussion

In this study, we establish *pab-1* as a new regulator of mitochondrial stress and immune response in *C. elegans*. We further show the physiological relevance of *pab-1* by demonstrating that it is required for the defence against the Gram-negative bacteria *P. aeruginosa*. Finally, we confirm that its role in both mitochondrial stress and infection response involves *atfs-1*, a transcription factor proven to regulate both mitochondrial stress and immunity genes (Nargund et al., 2012; Pellegrino et al., 2014). *atfs-1*, however, does not seem to be the only mediator of the transcriptional regulation exerted by *pab-1.*

The mammalian orthologue of *pab-1*, the cytoplasmic poly(A)-binding protein PABPC1, is known to bind non-specifically the poly(A)-tail of most mRNAs (Blobel, 1973), favouring their cap-dependent translation and their stability (Mangus et al., 2003; Smith et al., 2014). Paradoxically, it can also inhibit translation, regulate mRNA decay in a context- or mRNA-specific manner and it is involved in microRNA-silencing (Smith et al., 2014), as is *pab-1* in *C. elegans* (Flamand et al., 2016).

Therefore, one can speculate that *pab-1* most likely exerts its action post-transcriptionally and/or translationally.

The exact mechanism by which *pab-1* regulates immune genes is not fully understood. However, considering that we find an A-rich stretch enriched in transcripts regulated by *pab-1*, we can formulate two possible hypotheses. First, *pab-1* could bind to these A-rich regions in its target mRNAs, namely immune and mitochondrial stress genes, resulting in their stabilization during stress (Figure 3.6B). This is supported by the reduction we observe in mRNA levels upon *pab-1* silencing and by previous findings about PABPC1 in mammalian cells, where A-rich sequences also impact on mRNA stability (Kini et al., 2016). Indeed, during inflammation, PABPC1 antagonizes the recruitment of destabilizing proteins binding to AU-rich regions of unstable mRNAs such as that of tumour necrosis factor (TNF) in macrophages (Rowlett et al., 2008). A second mechanism could involve the regulation of cap-independent translation of stress response mRNAs by *pab-1*. When cells undergo infection (Lemaitre and Girardin, 2013) or mitochondrial stress (D'Amico et al., 2017), they display an extensive and rapid remodelling of their translational landscape in order to cope with the inducing insult. Canonical translation initiation occurs via the recruitment of the eIF4F complex on mRNAs and is referred to as “cap-dependent translation” (Jackson et al., 2010). Under stress, to save energy and adapt the metabolic fate of the cell, the cap-dependent translation is slowed down. However, stress-response genes have to be translated to restore homeostasis. To bypass the block of regular translation, these stress-responsive mRNAs are translated specifically by cap-independent mechanisms that rely on sequence-specific features, such as internal open reading frames (Jackson et al., 2010). Although it is more speculative, the regulation of cap-independent translation might constitute a conserved regulatory mechanism, since *pab-1* orthologues in plants and yeast exert such role. In yeast, several genes required for invasive growth under glucose deprivation contain A-rich stretches that are able to initiate cap-independent translation via the recruitment of Pab1 and ribosomal subunits (Gilbert et al., 2007). In the plant *Arabidopsis thaliana*, PAB2 was recently shown to bind to 5’UTR A-rich sequences to increase the translation efficiency of immune genes upon immune challenge (Xu et al., 2017).

Considering these striking similarities, we expect that the mechanism underlying our observations involves stabilization and/or translational regulation of stress-responsive mRNAs by *pab-1*, possibly through the interaction with A-rich regions of its target mRNAs (Figure 3.6B).

The mechanism of how *pab-1* senses the immune challenge still remains to be elucidated. Interestingly, K08D8.5, one of the genes not responding to *atfs-1* impairment (Figure 3.5G), is a target of the p38 MAPK/PMK-1, a well-defined regulator of *C. elegans* immunity (Troemel et al., 2006). Interestingly, a similar mechanism, recently described in plants, shows the phosphorylation of PAB2 by MAPK (Xu et al., 2017), whereas PABPC1 in mouse cells is also phosphorylated by p38 MAPK in macrophages (Rowlett et al., 2008). This strongly suggests a possible implication of *pmk-1* in the *pab-1*-driven immune regulation, although more experimental studies will be required to integrate all facets of this complex regulation. Further studies will be required to fully decipher the exact mechanism underlying our observations.

In accordance with our study, PAB proteins are implicated in stress response throughout evolution in various manners. Indeed, several studies associate PABPC1/Pab1 levels with stress tolerance (Ma et al., 2009). In addition, from yeast to mammals, Pab1/PAB-1/PABPC1 are components of stress-granules, structures that form dynamically in the cytoplasmic following a set of insults and that retain mRNAs intact and dormant until stress resolves (Anderson and Kedersha, 2006; Lechler et al., 2017; Riback et al., 2017). Interestingly, structural properties of the low complexity regions of yeast Pab1 confer a stress sensor activity to the protein: variations in temperature or pH modify the physical and assembly properties of Pab1, leading to extensive remodelling of stress granules and maintenance of fitness during prolonged stress (Riback et al., 2017). Since we did not explore this field, we cannot exclude our observations to be partially explained by changes in mRNA stability/ localization due the regulation exerted by *pab-1* on stress granules.

3.5 Materials and methods

C. elegans strains and RNAi experiments

All strains were provided by the *Caenorhabditis* genetics center (University of Minesota). Strains used were wild-type Bristol N2, MQ1333(*nuo-6(qm200)*), NL2099 (*rrf-3(pk1426*)II), SJ4100 (zcIs13[hsp-6::GFP]), SJ4005 (zcIs4[*hsp-4*::GFP]), CB4037(*glp-1(e2141ts))*. Strains were cultivated at 20°C, except *glp-1(e2141ts)* strain, which was kept at 15°C, on nematode growth media agar plates seeded with *E.coli* OP50. To perform the experiments, *glp-1(e2141ts)* eggs were seeded per plate and raised at 25°C (to eliminate germ cells) for ~40 hr, then shifted to 20°C for the rest of worm's life. *rab-3::cco-1HP;ges-1::hsp-6::gfp* strain was provided by the Dillin laboratory.

Bacterial feeding RNAi experiments were carried out essentially as described previously (Kamath et al., 2001). Clones used were HT115, *pab-1* (Y106G6H.2), *spg-7* (Y47G6A.10) and *mrps-5* (E02A10.1). Clones were purchased from GeneService and confirmed by sequencing.

UPR^{mt} screening

C. elegans were age synchronized by egg bleaching and cultivated in liquid culture in 96-well plates, exposed to RNAi to be screened and dox (15µg/ml) from hatching. Fluorescence was read at day 1 of adulthood using a large particle flow cytometry device (Copas plateform, Union biometrica). The screening library of RNAi-bacterial clones was assembled by combining subsets of the genome-wide, RNAi Ahringer's library, namely « transcription factors » (387 genes), « chromatin players» (263 genes) and «mitochondrial proteins » (680 genes) commercially available from GeneService, as well as a fourth subset of cherry-picked genes encoding for additional transcriptional regulators (479 genes) to complement the three other sets. Worms were synchronized at L1 larval stage just after hatching and treated with RNAi and doxycycline (15µg/ml) from that time until the fluorescence was read at day 1 of adulthood. To increase the sensitivity, the worm strain used for the screening was derived from a cross between the strain bearing the *hsp-6 ::gfp* reporter (SJ4100) and a strain hypersensitive to RNAi due to a *rrf-3* mutation (NL2099).

GFP reporter analysis

GFP expression and quantification was carried out according to the protocol previously described (Durieux et al., 2011). GFP expression was monitored in day 1 adults. Fluorimetric assays were performed using a Victor X4 multilabel plate reader (Perkin Elmer Life Science). Eighty worms per condition were randomly picked and analyzed in black-walled 96-well plate. An average of 20 worms were put per well filled with 100µL M9 medium. For fluorescence microscopy pictures, worms were randomly picked and immobilized with a 10 mM solution of tetramisole hydrochloride (Sigma) during picture acquisition. Each well was read 6 times, then averaged and normalized by the exact number of worms contained by the well. To trigger UPR^{ER}, tunicamycin 25ng/ul was added to the worm-containing M9 directly in wells. Fluorescence was read after 5 hours of incubation.

Pseudomonas survival assay

Culturing and seeding of *Pseudomonas aeruginosa* PA14 (obtained from CGC) on modified NGM agar plates, as well as the *C. elegans* slow killing assay were performed as described in (Kirienko et al., 2014). Briefly, worms were grown OP50 until L4 stage and then transferred to plates seeded with PA14. Survival was scored twice per day until all worms were dead. Worms that escaped on the side of the plate were censored. Prism 5 software was used for statistical analysis to determine significance calculated using the log-rank (Mantel-Cox) method.

RNA isolation and quantitative RT-PCR

For RT-qPCR analysis, *C. elegans* were age synchronized by egg bleaching and cultivated on NGM agar plates seeded with HT115 bacteria expressing RNAi constructs at 20°C and/or containing doxycycline hyclate 15µg/ml. L4 worms were infected with PA14 and recovered with M9 minimal liquid medium after 24h of exposure. Five biological replicates for each condition were prepared, consisting of ~600 worms per sample in M9. Before mRNA preparation, samples were washed twice with 5 mL M9 to eliminate residual bacteria. Total RNA was prepared using TRIzol (Invitrogen) according to the manufacturer's instructions. RNA was treated with DNase, and 1 µg of RNA was used for reverse transcription (RT). 15X diluted cDNA was used for RT- quantitative PCR (RT-qPCR) reactions. The RT-qPCR

reactions were performed using the LightCycler 480 System (Roche Applied Science) and a qPCR Supermix (QIAGEN) with the indicated primers. At least 2 housekeeping genes (* in the sequences below) were used as normalization control. Three technical replicates were used for each biological replicate.

The primers used for the *C. elegans* genes were the following:

spg-7 (Y47G6A.10): fw: aagtatgcaggacaaacgtgc, rv: tgaggtttgggatttcgcgt.
hsp-6 (C37H5.8): fw: aaccaccgtcaacaacgccg, rv: agcgatgatcttatctccagcgtcc.
hsp-60 (Y22D7AL.5): fw: ttctcgccagagccatcgcc, rv: tctcttcgggggtggtgaccttc.
lonp-1 (C34B2.6): fw: cgatgatggccattgtgcag, rv: cgctttgaaacatcaatttcatcca.
C17H12.6 : fw: accacaattccagcaggagc, rv: ggagaacgacttgaaacacgag
clec-17 (E03H4.10):fw: tggctctgcacagagttacg, rv: acagtcgtctgcatgagttgt
F14H3.12:fw: gctgatcaggaagatcaggcg, rv: agtgtgcagacctcgatatccc
F53A9.6:fw: atatgctccaccaccagtcc, rv: ggctttcgtagtgtcctccg
F53A9.8 :fw: catgaggaccatcacgagca, rv: cttcatgggagtcgtgagca
glc-1 (F11A5.10):fw: agcccaacaagctagaacga, rv: ggtcgcactcggaaatcgta
K08D8.5 :fw: aaaacccagtacgagtcggg, rv: tcccggaggatattttgaccag
T16G1.5 :fw: gtgaacaagtacgctggcat, rv: cctgtctgtcagcaccagag
**act-1* (T04C12.6): fw: gctggacgtgatcttactgattacc, rv: gtagcagagcttctccttgatgtc.
**pmp-3* (C54G10.3): fw: gttcccgtgttcatcactcat, rv: acaccgtcgagaagctgtaga
**cdc-42* (R07G3.1): fw:, *agccattctggccgctctcg rv: gcaaccgcttctcgtttggc*
**Y45F10D.4: fw: gtcgcttcaaatcagttcagc, rv: gttcttgtcaagtgatccgaca

RNA Sequencing and microarray analysis

N2 and *nuo-6* mutants were age synchronized by egg bleaching and cultivated on NGM agar plates seeded with HT115 bacteria expressing RNAi constructs or containing doxycycline hyclate 15µg/ml. Worms were harvested at L4 stage. Before RNA extraction, samples were washed twice with 5 mL M9 to eliminate residual bacteria. Total RNA was isolated using Trizol (Life Technologies) and purified using the RNeasy Mini Kit (Qiagen) in accordance with the manufacturer's instructions. It was then assessed for degradation using an Advanced Analytical Agilent Fragment Analyzer. For each condition, the 3 best quality samples were selected and taken further for microarray or RNA-Seq.

For RNA-Seq, all 12 samples had an RNA Quality Number >9.6. Ilumina Truseq stranded polyA-mRNA library was prepared and sequenced for 100 cycles at the Genome Technologies Facility at the University of Lausanne. The 12 samples were multiplexed and sequenced on two lanes of an Illumina Hiseq 2500, yielding a minimum of about 30 million reads per sample. All obtained results passed the quality

check and were subsequently quantified and mapped to the *C. elegans* reference genome using the Kallisto-Sleuth R package. Differentially expressed genes were determined using false discovery rate FDR<0.05 with DESeq R package (Anders and Huber, 2010).

Microarray analysis was performed using Affymetrix *C. elegans* Gene 1.0ST chips in triplicates per RNAi condition. Microarray data was normalized with RMA-sketch method and analyzed using the Affymetrix Expression and Transcriptome analysis consoles. Volcano plots, heatmaps and Venn diagrams were generated with R (www.r-project.org). GO terms enrichment was determined with the "goana" function from the limma R package (3.2BC) or using the DAVID online tool (Huang da et al., 2009) (3.3B, 3.4C), for both methods using Bonferroni adjusted p value < 0.05.

PGSA

Transcript expressions in human tissues were downloaded from the GTEx Portal (version v6p) [PMID: 23715323]. Gene expression residuals after removing covariates, including first three genetic principle components, gender, and other available covariates by PEER (probabilistic estimation of expression residuals) [PMID: 22343431] were used for the enrichment analysis. For gene set enrichment analysis (GSEA), genes were ranked based on their Pearson correlation coefficients with the expression residuals of *PABPC1*, and GSEA was performed to find the enriched gene sets co-expressed with *PABPC1* using the R/fgsea package [PMID: 16199517; doi: 10.1101/060012].

The gene-level statistics was performed based on the Pearson correlation coefficient of the expression of genes and the gene of interest in the transcriptome datasets. We calculated the gene set statistics through a Kolmogorov–Smirnov statistic [PMID: 16199517]. Assume that we have the set S with m genes along with computed statistics and corresponding p-values. All genes are ranked due to the correlations of expression level with expression of the gene-of-interest $\rho_1 \leq \rho_2 \leq \cdots \leq \rho_N$. Then the two running sums are constructed: S_1 is for the genes from the set and S_2 for all other genes:

$$S_1(S,i) = \sum_{\substack{g_j \in S \\ j \le i}} \frac{\left|R_j\right|^p}{\sum_{g_j \in S}\left|R_j\right|^p}$$

$$S_2(S,i) = \sum_{\substack{g_j \notin S \\ j \le i}} \frac{1}{N-m}, \quad i = 1, \ldots, N$$

Enrichment score (ES) is defined as the maximum deviation from zero of their difference $\mathrm{ES} = \max_i S_1(S,i) - S_2(S,i)$. Letting $p = 1$ here. Significance of the observed score is assessed using the null distribution formed of the statistics computed on permuted gene labels. The empirical p value is calculated based on the probability that the random gene sets statistics are equal or larger than the original gene set statistics. Normalized enrichment score (NES) is obtained by normalizing the size of each gene set to account for gene set size. The multiple testing problem given the high number of gene sets tested is corrected using false discovery rate (FDR) estimation.

For plotting, the logarithm of the empirical p values were plotted against the NES, with the size of the dots representing the gene set sizes, and the darkness of the dots indicating the FDR of the enrichment. Mitochondrial relevant gene sets were colored in green and immune relevant gene sets were colored in blue.

MEME analysis

5'UTR sequence of *pab-1*–regulated genes were retrieved using the biomaRt package on R (Durinck et al., 2005) and submitted to MEME website (http://meme-suite.org/tools/meme) for analysis of enriched sequences, using default parameters and "search on given strand only" option, since RNA was being analysed.

Statistical analysis

Survival analyses were performed using the Kaplan Meier method and the significance was calculated using the log rank test. Differences between two groups were assessed using two-tailed t-tests. Analysis of variance, assessed by Bonferroni's multiple comparison test, was used when comparing more than two groups. The statistical software used was GraphPad Prism 5 and $p<0,05$ was considered significant.

3.6 Supplementary tables and figures

Hit	Function	Orthologue	% reduction	
			by A	by B
pab-1	RBP	Pabpc1	95	95
elt-2	TF	Gata4/Gata6	100	98
phi-7	TF/RBP*	Cdc5l	90	90
B0336.3	RBP*	Rbm26	95	95
let-607	TF*	Creb3l3/CrebH	80	90
jmjd-3.1	KDM	Jmjd3/Utx/Uty	70-100	80
sptf-3	TF	Sp4, Sp3, Sp1	30-60	60
crh-2	TF	Creb3l2	30-60	50
sec-23	vesicular protein*	Sec23A/Sec23B	100	98
W01D2.1	ribosomal protein*	60S ribosomal protein L37	100	98
ceh-1	TF*	Nkx1-1, Nkx1-2	30	40
hmp-2	adhesion molecule	Ctnnb-1 (beta-catenin)	30	40
nhr-8	NHR	Vdr (Vit D receptor)	30	20
cep-1	TF	p53	10-20	10-20
nhr-66	NHR	RXR-beta	20-30	10-20
tbx-30	TF*	Mga (MAX-gene associated protein)	40	20
ztf-4	RBP*	Hnrnpc	0-10	10-20
oma-1	TF/RBP	Tristetraprolin (TTP) (Zfp36)	10	0-10
ceh-48	TF	HNF6/Onecut2	30	0-10
nhr-38	NHR	Nr5a1/ Nr5a2	20	0-10

Table 3.1 : UPR^{mt} screening hits

Ranking of the 20 top hits by relevance and their suppressive effect on hsp-6::gfp fluorescence upon spg-7 RNAi treatment by visual assessment by person A and B. (TF= transcription factor, NHR=nuclear hormone receptor, RBP=RNA-binding protein, KDM= histone lysine (K)-demethylase, Hnrpc= heterogenous nuclear ribonucleoproteins C1/C2, *=putative function)

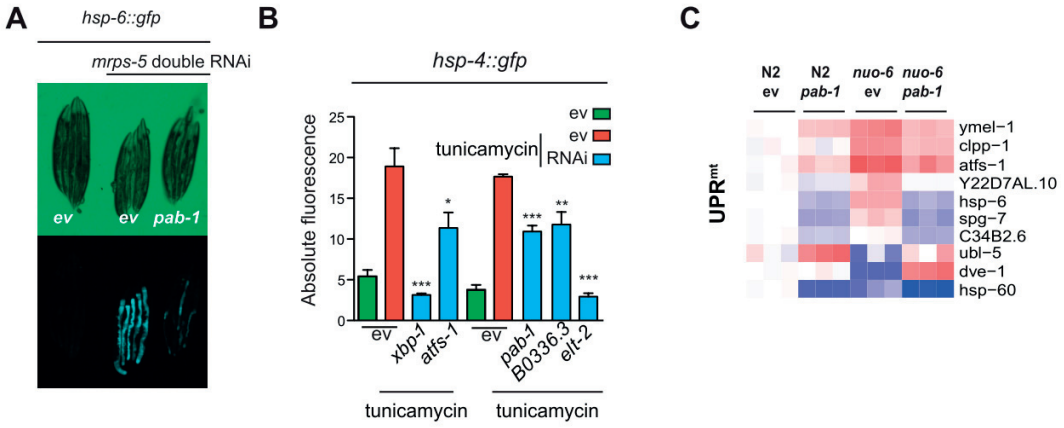

Supp. Figure 3.8

A. Representative pictures of the *hsp-6::gfp* reporter worms fed with RNAi mixed with *mrps-5* RNAi. B. Quantification of the suppressive effect of the fluorescence of the UPR^{ER} signalling reporter by the 3 top hits after treatment with tunicamycin 25ng/ul for 5 hours. Bars show mean±SEM, ANOVA p-value P≤0.05, **P≤0.01, *** P≤0.001. C. Heatmap representing the mRNA levels of the UPR^{mt} genes in the RNA-Seq results.

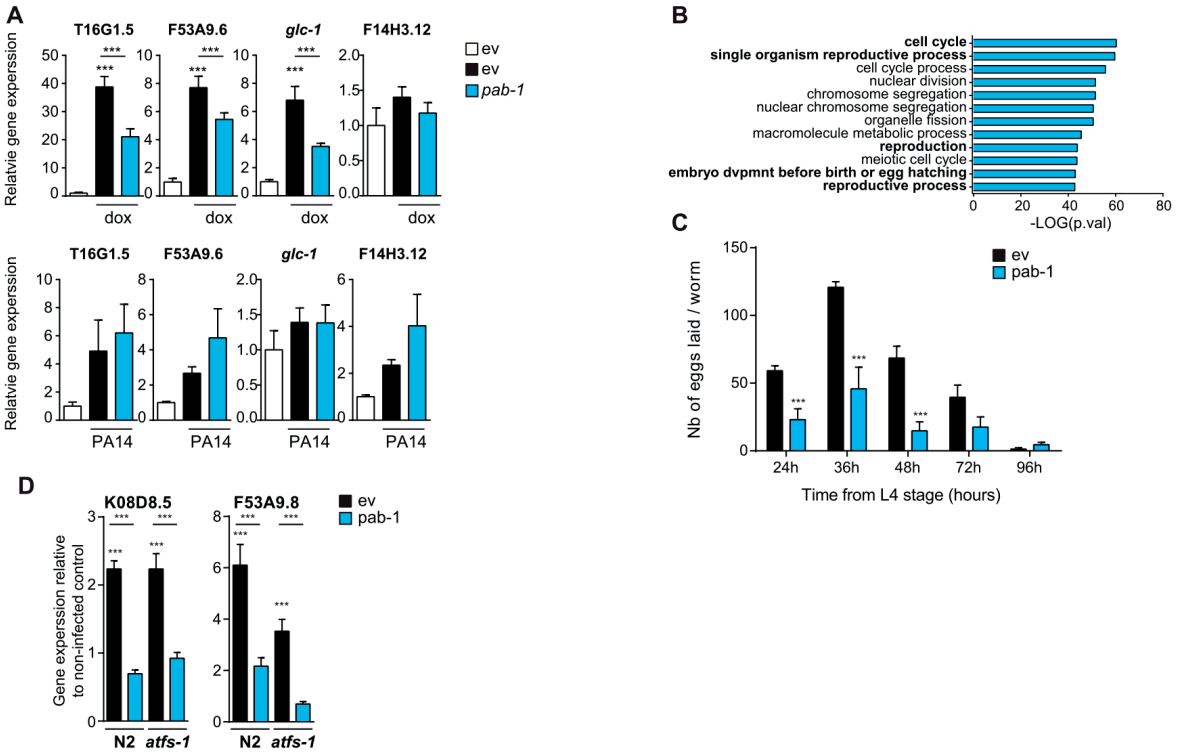

Supp. Figure 3.9

A. RT-qPCR results showing transcript levels of some of the core genes (Figure 3.4A) upon doxycycline treatment (top row) or infection by *P.aeruginosa* PA14 (bottom row). Bars show mean±SD, *ANOVA p-value P≤0.05, **P≤0.01, *** P≤0.001. B. GO biological processes (GO BP) enriched amongst genes down-regulated by *pab-1* silencing in N2 WT worms (RNA-Seq experiment (Figure 3.2A), by at least 1.5 fold decrease, FDR≤0.05. C. The effect of *pab-1* silencing on egg laying of N2 WT worms. Bars show mean±SEM, student t-test p-value, *** P≤0.001. D. RT-qPCR results showing the effect of *pab-1* RNAi on UPR^{mt} genes in N2 WT and *atfs-1* mutant worms treated with *P.aeruginosa* PA14 strain. Bars show mean±SD, * ANOVA p-value,*** P≤0.001.

	p-value	mean survival(h)	SEM	deaths	total
N2; ev		68.8	2.4	46	150
N2; pab-1	0.0118*	64.5	3.09	29	150
***glp-1;* ev**		111.5	3.06	70	150
glp-1; pab-1	< 0.0001***	70.9	3	24	150
atfs-1; ev		62.4	3.96	50	200
atfs-1; pab-1	0.1138	76.2	3.51	65	200

Table 3.2 : Survival statistics for the PA14 slow killing assay

Chapter 4 Exploring the conservation of the mitochondrial unfolded protein response (UPR^{mt}) in mammals

4.1 Multilayered genetic and omics dissection of mitochondrial activity in a mouse reference population

Adapted from

Wu Y*, Williams EG*, Dubuis S, Mottis A, Jovaisaite V, Houten SM, Argmann CA, Faridi P, Wolski W, Kutalik Z, Zamboni N, Auwerx J§, Aebersold R§. Multilayered Genetic and Omics Dissection of Mitochondrial Activity in a Mouse Reference Population. 2014, Cell 158, 1415-1430. doi: 10.1016

* Co-first author

§ Co-corresponding author

In this study, I achieved the *C. elegans* experiments and contributed in the experimental design and the writing of the figure about UPR^{mt}. I include here only the parts of the above-mentioned article that are needed for a clear understanding of how this study relates to UPR^{mt}.

4.1.1 Introduction

The central dogma of molecular biology states that genetic information encoded in DNA is first transcribed by RNA polymerase, then translated by ribosomes into proteins. However, the DNA sequence of a gene provides little information for predicting when, where, and to what extent its associated RNA and protein products will be expressed. Since the advent of microarray technology, comprehensive gene expression patterns—i.e. the transcriptome—can be precisely and comprehensively quantified across large populations. Unfortunately, transcript levels generally have only modest correlation with the levels of corresponding proteins (Ghazalpour et al., 2011; Gygi et al., 1999; Schwanhausser et al., 2011), and genetic variants similarly affecting both the transcript and peptide levels of a gene are relatively uncommon

(Albert et al., 2014; Skelly et al., 2013). As proteins in most cases are more directly responsible than transcripts in the regulation of cellular pathways—and ultimately phenotypic traits—there is a critical need for efficient, large-scale and accurately quantitative proteomics methods to complement transcriptomic datasets.

Over the past decade, the development of discovery mass spectrometry ("shotgun") has allowed the first large-scale studies on quantitative proteomics. In this approach, protein extracts are cleaved into short peptide sequences, which are then chromatographically separated and analyzed by tandem mass spectrometry. This allows the untargeted discovery of thousands of peptides, but if the number of unique peptide fragments in a sample significantly exceeds the number of available sequencing cycles (as in whole proteome extracts), any individual peptide will be inconsistently sampled across repeat analyses. This reduces the technical reproducibility, but moreover means that the number of peptides consistently quantified across all (or most) samples decreases as the study size increases (Karpievitch et al., 2012). Consequently, discovery mass spectrometry strategy has yielded mixed results in large population studies (Ghazalpour et al., 2011; Holdt et al., 2013), particularly as specific peptides of interest cannot be targeted, and the most consistently identified peptides are biased towards those of higher abundance (Callister et al., 2006). To overcome these hurdles, selected reaction monitoring (SRM) was developed, which perfects technical reproducibility and allows consistent multiplexed quantitation of target proteins by deploying a mass spectrometric measurement assay that is specific for each targeted peptide (Lange et al., 2008). Thus, hundreds of target peptides can be consistently and accurately quantified across large populations of samples. Recent studies in yeast have shown that the proteins and transcripts of genes are typically controlled by different, distinct mechanisms (Albert et al., 2014; Picotti et al., 2013). However, these hypotheses have not been well tested in mammalian genetic reference populations (GRPs) through multilayered transcriptomic and proteomic strategies.

Large GRPs are frequently used to determine to which extent phenotypic variation is driven by genetic variants (i.e. heritability), and to subsequently identify genes driving such variation. These genes can be identified by genome-wide association (GWA) or by quantitative trait locus (QTL) mapping, approaches that have been applied to various species and have led to the successful identification of dozens of major allelic

variants (Andreux et al., 2012; De Luca et al., 2003; Deeb et al., 1998; Yvert et al., 2003). In mammals, the murine BXD family is the largest and best studied GRP, consisting of ~150 recombinant inbred strains descended from C57BL/6J (B6) and DBA/2J (D2) (Andreux et al., 2012). Using 40 strains of this population on both chow (CD) and high fat (HFD) diets, we have obtained major metabolic phenotypes and established a multilayered dataset focused on 192 metabolic genes expressed in the liver. For all genes, we know the sequence variants, transcript levels, and protein levels in all cohorts. We further used the integrated molecular profiles to characterize complex pathways, as illustrated with the mitochondrial unfolded protein response (UPR^{mt}). UPR^{mt} shows strikingly variant responses at the transcript and protein level that are remarkably conserved between C.elegans, mice, and humans. Overall, these examples demonstrate the value of an integrated multilayered omics approach to characterize complex metabolic phenotypes.

4.1.2 Protein targeting across a genetically & environmentally diverse murine population

We first selected 192 metabolic proteins for study, with particular focus on genes regulating mitochondria and general energy metabolism. For each gene, synthetic peptides were generated based on established assays (Picotti et al., 2010) (Figure 4.1A) to accurately quantify each protein across all cohorts.

It has been well-established that transcriptomic networks of many metabolic processes covary quite well, e.g. within the electron transport chain or within the citric acid cycle (Ihmels et al., 2002). On protein level, proteins which function in common biological processes or which localize to the same functional modules are also reported to be subject to similar regulatory process and generally co-vary (Foster et al., 2006). To validate and identify which of these 192 proteins vary synchronously, we computed the robust Spearman correlation network for all protein pairs using the full SRM dataset (Figure 4.1B). The resulting network contained 82 correlated nodes (proteins) with 211 edges in 3 main enrichment clusters. As expected, many of the mitochondrial proteins and proteins involved in lipid metabolism are highly correlated (Figure 4.1B, cluster a and b). Within cluster a. are five of the six measured proteins involved in mitochondrial unfolded protein response (UPR^{mt}) (HSPD1, HSPE1, HSPA9, CLPP, and LONP1 indicated in red), along with three of the four measured NADH dehydrogenase genes (NDUFA1, NDUFB3 and NDUFS6—in blue), and four

of the eight measured mitochondrial-encoded proteins (MT-CYB, MT-CO2, MT-CO3, and MT-ND3 in black). Meanwhile, proteins involved in carbohydrate metabolism are enriched in the same cluster (Figure 4.1B, cluster c). These results show that functionally-related proteins tend to be coordinately regulated at a protein level, and that coregulation of protein abundance is strongly maintained for certain processes. To validate biological significance of these function-based covariation clusters, we further investigated one, the UPR^{mt} network (elaborated in Figure 4.2).

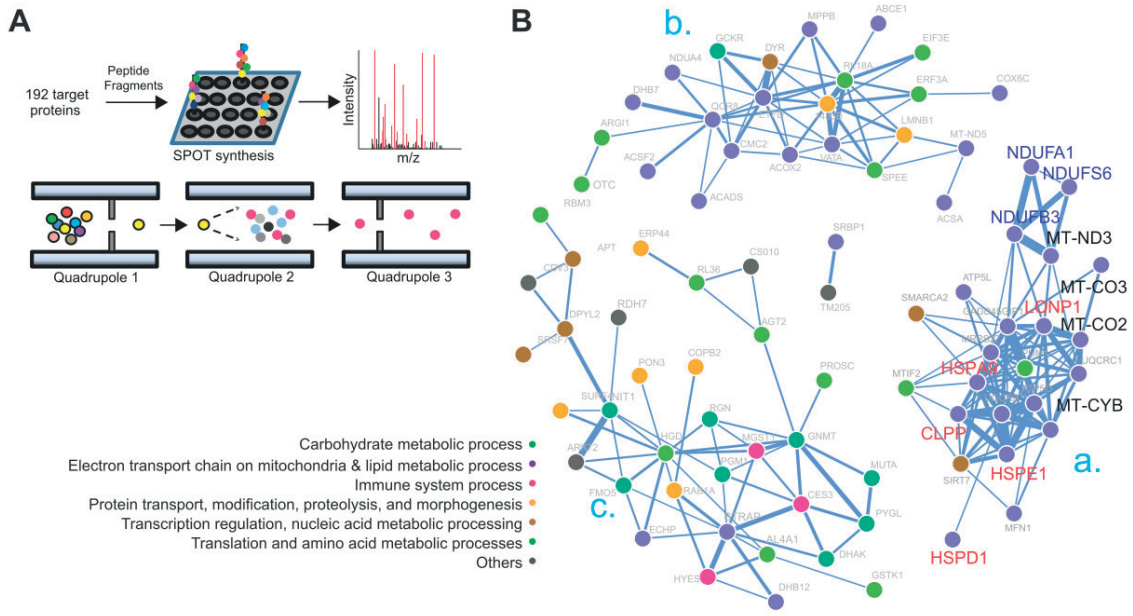

Figure 4.1 : SRM-based Protein Quantification and Covariation Network

A. SRM assay development for targeted proteomic measurements. 309 peptides corresponding to 192 genes were designed and synthesized via SPOT synthesis. Fragment ion spectra were generated on a triple-quadrupole MS with SRM-triggered MS2 mode, then ions were selected based on their relative intensities. Dot colors indicate different amino acids. m/z, mass-to-charge ratio. Mouse liver homogenate combined with the heavy reference proteome was analyzed with SRM on a triple-quadrupole MS. Different dot colors represent different peptides (Quadrupole 1) or product ions (Quadrupole 3). B. Protein association network based on robust Spearman correlation measures for all protein pairs. Statistically significant and strong positive associations ($p < 0.01$ & $r > 0.6$) are edges. The largest correlation clusters are labeled “a.”, “b.”, and “c.”. Nodes are labeled with protein names and colored according to their biological process, as reported by DAVID (Huang da et al., 2009).

4.1.3 The mitochondrial unfolded protein response

The UPR^{mt} is a mitochondrial stress response pathway that is activated by proteostatic stress, such as by accumulation of unassembled or unfolded proteins in the mitochondria (Zhao et al., 2002), by the presence of an imbalance between mitochondrial and nuclear encoded proteins (Houtkooper et al., 2013), or by electron transport chain defects (Durieux et al., 2011b; Runkel et al., 2013). The activation of

UPR^{mt} in turn leads to the transcription/translation of nuclear-encoded protective genes such as mitochondrial chaperones and proteases to reestablish mitochondrial proteostasis (reviewed in (Haynes et al., 2013; Jovaisaite et al., 2014; Wolff et al., 2014)). The bulk of research on UPR^{mt} has taken place using *C. elegans* and mammalian cell lines, thus little is known about when or how UPR^{mt} occurs *in vivo* in mammals. Furthermore, as the UPR^{mt} is a stress response tied to maintaining mitochondrial protein balance, we hypothesized that its protein correlation networks may be different than those generally examined at the transcriptional level.

In the worm, two "classical" approaches have been typically used to induce UPR^{mt}: loss-of-function of *cco-1*, a nuclear encoded component of the electron transport chain (Durieux et al., 2011b), or loss of function of *spg-7*, a mitochondrial protein quality-control protease (Yoneda et al., 2004). We confirmed that the knockdown of either gene by RNAi triggers the UPR^{mt} response in *C. elegans*, by strong induction of the mitochondrial chaperone *hsp-6* and of the proteases *lonp-1* and *clpp-1* (Figure 6A). Moreover, we linked this UPR^{mt} activation to specific phenotypes—a major reduction in size and mobility, as well as a decrease in oxygen consumption—which are consequences of mitochondrial stress (Figure 6B). However, whether this coordinated regulation of UPR^{mt} genes is conserved in mammals *in vivo*, has not been previously shown.

In the BXDs, we investigated the expression of six members of the UPR^{mt} pathway, which are well-conserved from *C. elegans*: mitochondrial chaperones (*Hspd1, Hspe1, Hspa9*), proteases (*Clpp, Lonp1*), and a transcriptional regulator involved in UPR^{mt} (*Ubl5*). These UPR^{mt} genes are also coordinately regulated at both mRNA and protein level in the BXDs, but with much stronger connections among proteins (Figure 6C). Moreover, the UPR^{mt} network correlates negatively with *Cox5b* and *Spg7* (mouse orthologues of worm *cco-1* and *spg-7*, respectively), indicating that low abundance of these genes amplifies UPR^{mt} in mammals as in *C. elegans* (Figure 6D). The network is also influenced in part by diet. While *Cox5b* expression patterns are similar between CD and HFD, *Spg7* covariation is disjointed between the dietary cohorts (Figure 6E). This may explain why, despite a similar overall UPR^{mt} response in both diets (Figure 6D & F), *Spg7* trends positively in HFD cohorts, while *Cox5b* remains consistent (Figure 6G). Using four large transcriptional studies of human tissue biopsies, we observe similar transcriptional links, particularly including a strong

network between all the UPR^{mt} genes (Figure 6H). In humans, *SPG7* is a consistent negative correlate of this network, in contrast to *COX5B,* which generally has positive covariation with the UPR^{mt} response (Figure 6I). Thus, while many of the overall regulators of UPR^{mt} remain coregulated across species—worm, mouse and human—particular nuances of its activation pathways appear variable dependent on species, environment, tissue, and likely other factors.

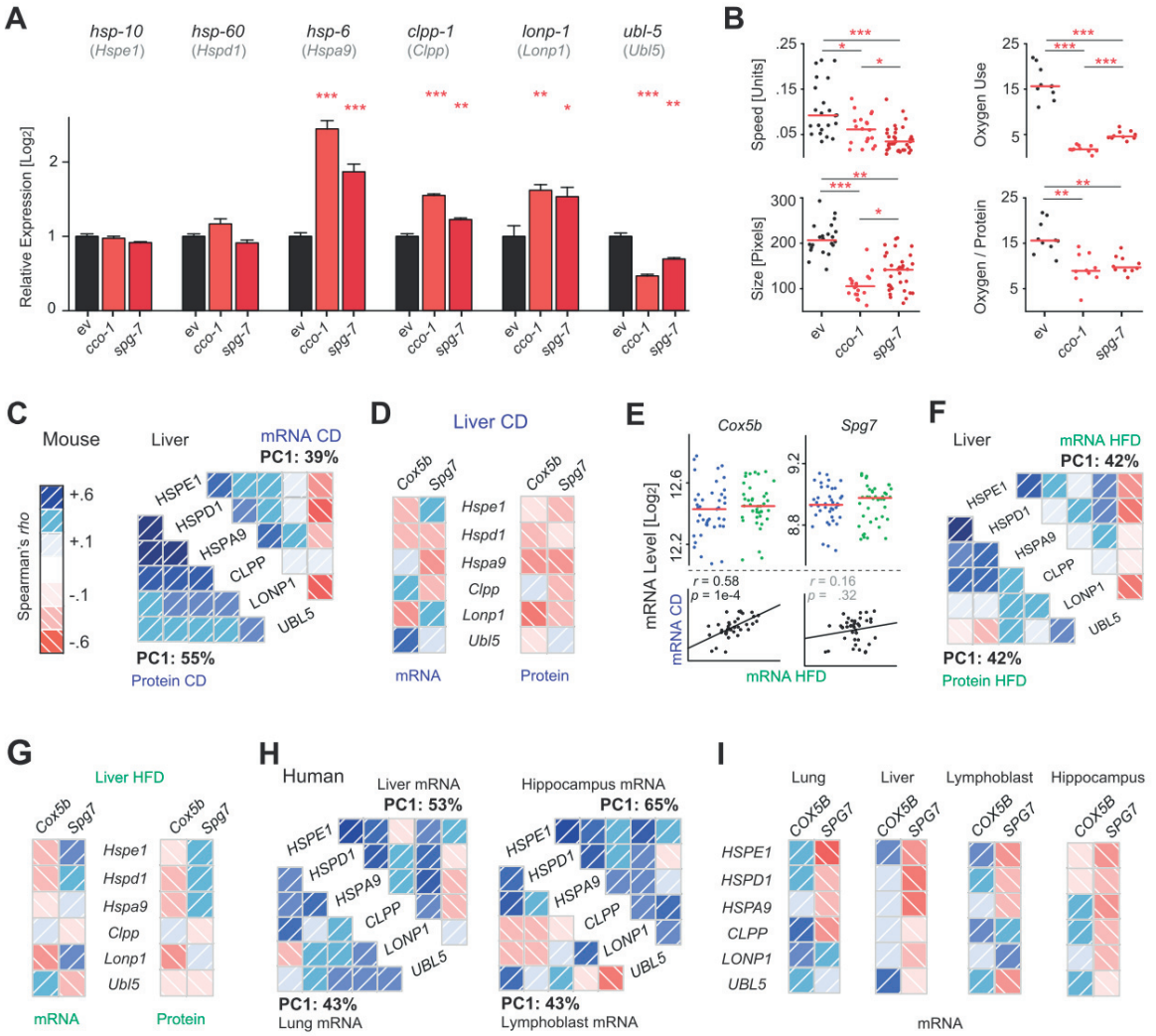

Figure 4.2 : The Mitochondrial Unfolded Protein Response

A. UPR^{mt} induction in *C. elegans* triggered by interference with ETC (RNAi of *cco-1*) or mitochondrial proteostasis (RNAi for *spg-7*). These triggers result in upregulation of UPR^{mt} effectors *hsp-6*, *clpp-1*, and *lonp-1* and a reduction in *ubl-5*. The orthologous mouse genes are indicated below the respective *C. elegans* gene symbol. Error bars represent mean + SEM. B. UPR^{mt} induction in *C. elegans* decreases movement, size, and oxygen consumption. C. UPR^{mt} genes and proteins form a network of coordinately expressed mRNAs and proteins *in vivo* in mice, which is stronger at the protein than at the mRNA level. D. *Cox5b* and *Spg7* (orthologs of *C. elegans cco-1* and *spg-7*), are generally negatively associated with the levels of all UPR^{mt} genes in CD cohorts, particularly at the protein level, in line with observations in the worm. E. While the levels of *Cox5b* and *Spg7* are not affected by diet,

expression is consistent by strain across the two diets only for *Cox5b*. F. The UPR^{mt} network in HFD livers is similar to that observed in CD, but somewhat weaker. *Ubl5* remains a striking negative correlate at the mRNA level. G. In HFD, *Cox5b* remains a negative correlate of UPRmt transcripts and proteins, while *Spg7* does not. H. The features of the UPR^{mt} network are also conserved in 427 human liver biopsies (Schadt et al., 2008), 405 lung biopsies (Ding et al., 2004), 180 lymphoblast lines (Monks et al., 2004), and 43 hippocampi (Berchtold et al., 2008). I. In humans, *SPG7* is a consistent negative correlate of the UPR^{mt} transcripts.

4.1.4 Discussion

Due to major differences in transcript and protein regulation, it has become increasingly clear that systems proteomics is essential for the analysis of complex systems such as metabolism (Khan et al., 2013; Skelly et al., 2013). In this study, we quantified 192 metabolism genes at the transcript and protein level in livers from 77 cohorts of the BXD GRP under two different dietary conditions.

It is worth stressing that novel regulatory mechanisms can be found either through QTL analysis and their equivalent from GWAS, SNP analysis, or through network analyses, which are a complementary and powerful approach to dissect complex traits. The network approach is particularly viable when backed by high-depth multilayered datasets such as illustrated by our example on UPR^{mt}. UPR^{mt} is a reparative pathway activated by mitochondrial proteotoxic stress that has been primarily studied in the *C. elegans* and in cultured cells, but little is known about whether it occurs *in vivo* in mammals. We examined six genes that are known to be major regulators of *C. elegans* UPR^{mt} and which are conserved in mammals. These six genes form a robust coexpression network in both diets at the transcriptional and proteomic levels, with the proteomic connections being stronger, befitting the role of UPR^{mt} as a sensor and regulator of protein stress. One observation that stood out in the analysis of the UPR^{mt}, was the striking “contradiction” between the *Ubl5* transcript and UBL5 protein correlations to the UPR^{mt} network. *Ubl5* is a transcriptional regulator known to induce UPR^{mt}, yet in both worms and mice, its transcript levels decrease when UPR^{mt} is activated. Conversely, the UBL5 protein is increased with UPR^{mt} activation in the BXDs, an observation also previously reported in *C. elegans* (Benedetti et al., 2006). This discordance in protein/transcript regulation suggests the existence of posttranscriptional mechanisms or a negative feedback loop, which could not be detected at the transcript or protein level alone. While there remains a great deal of this pathway left to be explored, it is clear that accurate, systems-scale

protein measurements are essential to effectively model complex protein response networks like UPR^{mt}.

4.2 Assessing the effects of doxycycline on murine physiology and longevity

Data and text of paragraph 4.2.2 adapted from

Moullan N*, Mouchiroud L*, Wang X, Ryu D, Williams EG, Mottis A, Jovaisaite V, Frochaux MV, Quiros PM, Deplancke B, Houtkooper RH[§] and Auwerx J[§]. Tetracyclines disturb mitochondrial function across eukaryotic models: a call for caution in Biomedical Research. 2015, Cell reports, pii: S2211-1247(15)00180-1. doi: 10.1016

* Co-first author

[§] Co-corresponding author

This chapter combines published results from a study where I contributed (4.2.2, see below for details) and unpublished results (4.2.3, post-natal dox study, that I achieved in collaboration with another PhD student, V.Jovaisaite).

4.2.1 Introduction

Bioinformatic studies revealed a marked trend of coexpression of UPR^{mt} genes in genomics and proteomics data from both mice and human (Chapter 4.1) (Wu et al., 2014). This suggests a conserved coregulation of this pathway in mammals in normal physiological state. We hypothesized that studying the features and effects of the mitochondrial response when triggering a stress *in vivo* would complement our understanding. For this purpose, we used the well-characterized antibiotic doxycycline (dox) from the tetracycline class, targeting bacterial translation. Dox leads to the specific inhibition of mitochondrial translation in eukaryotic cells due the bacterial origin of this organelle (Clark-Walker and Linnane, 1966). Dox therefore blocks the production of mitochondria-encoded OXPHOS complex subunits. Since nuclear-encoded subunits are still produced, it disturbs the stoichiometry of respiratory complexes and the proteostasis in the mitochondria (Houtkooper et al., 2013). This state of mitonuclear imbalance causes mitochondrial stress and the activation of UPR^{mt}, which has been more extensively characterized in *C.elegans*. Moreover, when worms are subjected to UPR^{mt} activation during a particular developmental window, it leads to their lifespan extension (Durieux et al., 2011a).

Epigenetic remodeling of histone marks by the histone demethylases *jmjd-3.1* and *phf-8* was shown to mediate this long-lasting effect on longevity (Merkwirth et al., 2016). Additionally, in theBXDs, expression of the mammalian orthologues *Jmjd3* and *Phf8* correlates with that of UPR^{mt} genes (Merkwirth et al., 2016). Mitochondrial stress is at the origin of lifespan extension in several genetic models, including mammals (Quiros et al., 2016). Finally, like knocking-down mitochondrial ribosomal proteins (MRPs) extends lifespan in worms, and *Mrps5* was found in a genomic loci regulating lifespan in mice and its expression correlates negatively with longevity in the BXDs (Houtkooper et al., 2013). All these evidences suggest that pharmacological disturbance of mitochondrial function early in life might be epigenetically imprinted and have long-lasting effect on physiology and longevity. To this purpose, we investigated the effects of post-natal dox treatment in mice.

4.2.2 Doxycycline disturbs mitochondrial proteostasis and function in mice

Adapted from (Moullan et al., 2015). In this study, I contributed in performing and analysing the in vivo experiments in mice.

Male C57BL/6J mice were treated with 50- or 500-mg /kg/day of dox dissolved in their drinking water supplemented with sucrose for 14 days. We used 50-mg/kg/day amoxicillin as a control, since this antibiotic does not interfere with bacterial/mitochondrial translation, but disrupts the bacterial cell wall. Dox dose-dependently induced mitonuclear protein imbalance in different mouse tissues including liver, heart, and brain (Figure 4.3A, B, C). We analysed the physiological consequences of dox treatment in mice. The treatment did not affect body weight or food intake, suggesting no overt toxicity for the treatment timeframe and dosage used (Figure 4.3D, E). At the whole-body level, these short-term treatments did not affect body composition in either lean or fat mass between the amoxicillin and dox groups (Figure 4.3F, G). The decreased oxygen consumption of dox-treated mice, indicative for reduced energy expenditure (Figure 4.3H), and the marked increase in physical activity (Figure 4.3I) are, however, clear indicators for altered physiological fitness.

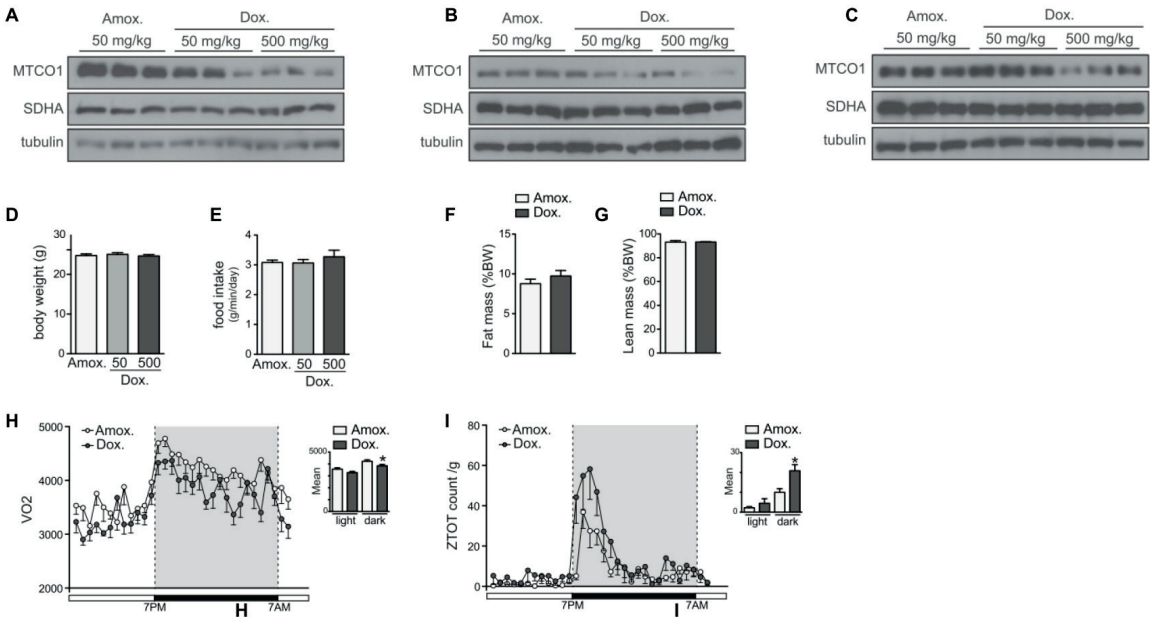

Figure 4.3 : Dox *in vivo* treatment in mice impairs OXPHOS proteostasis and energy expenditure.

A-C. Dox (at 50 and 500 mg/kg/day in the drinking water) induces mitonuclear protein imbalance in liver (A), heart (B), and brain (C), as shown by the reduced ratio between mtDNA-encoded MTCO1 and nDNA-encoded SDHA when compared with amoxicillin (at 50 mg/kg/day) after 14 days of treatment. D-E. Dox treatment (500 mg/kg/day in drinking water for 14 days) in mice does not affect body weight (BW) (D) or food intake (E) compared to mice treated with amoxicillin (at 50 mg/kg/day). F-G. Fat mass (F) and lean mass (G) were not affected by dox. H-I. Dox treatment reduced energy expenditure (H), but increases locomotor activity (I) in dox- compared to amoxicillin-treated mice. The gray area shows the time when lights in the animal facility were switched off. Bar graphs are expressed as mean + SEM, *p % 0.05

4.2.3 Post-natal doxycycline does not show long-term effects on physiology and longevity

We subjected C57BL/6J males to post-natal (from the morning following their birth) treatment with dox 500-mg /kg/day in the drinking water supplemented with sucrose during 6 weeks. Since dox is excreted in the milk (Aupee et al., 2009), the treatment was dependent on the mother until weaning at week 3 after birth. We phenotyped the mice at 6 months of age to analyse the long-lasting physiological consequences of post-natal dox treatment, in comparison with control mice (Suc, receiving sucrose only) and amoxicillin-treated mice (50-mg/kg/day). No difference was observed in body weight of the mice at 6 months (Figure 4.4A). Similarly, food intake, fat and lean mass were not changed (Figure 4.4B, C, D). While dox treatment impacts on oxygen consumption (Figure 4.3H), post-natal administration of dox did not cause sustainable negative or positive effects on VO_2 (Figure 4.4E). However, we found

that dox, as well as amoxicillin, significantly reduced the activity of 6-months old mice subjected to these drugs at birth (Figure 4.4F, G, H). Finally, post-natal dox administration, did not impact on longevity of the mice neither when compared to control nor to amoxicillin-treated mice (Figure 4.4I). Altogether, these results suggest that post-natal dox treatment did not have a major long-term impact on health- and life-span. However, mice treated post-natally with dox, as well as amoxicillin, displayed decreased activity compared to control mice, suggesting that some effects of the post-natal intervention persisted in time.

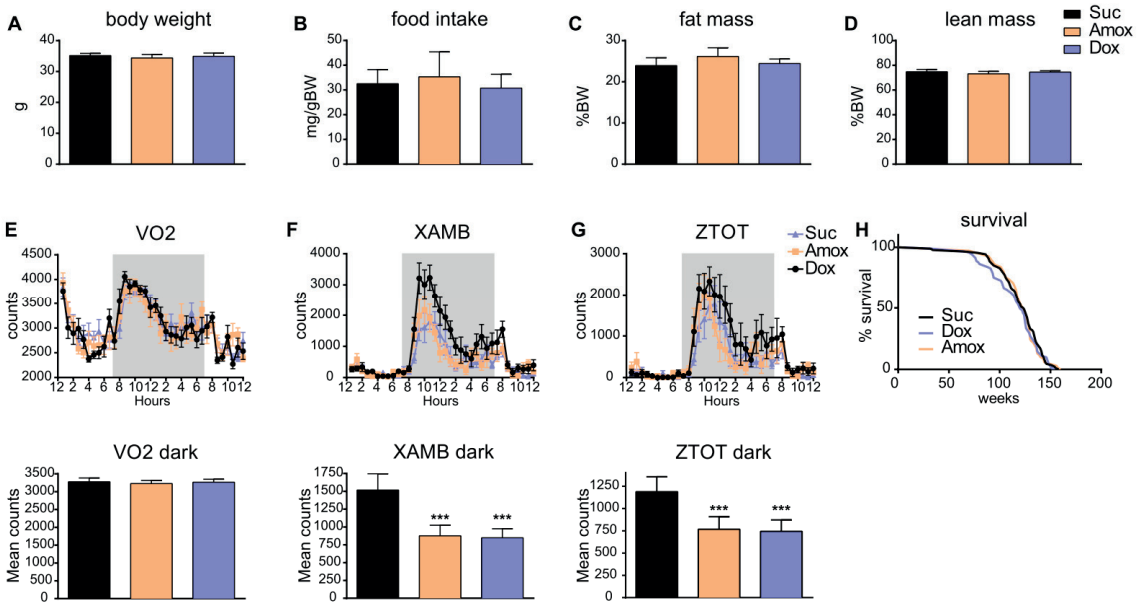

Figure 4.4 : Post-natal dox treatment does not show specific consequences on physiology and longevity over the long term

A-E. Dox and amoxicillin (Amox) treatment in mice for 6 weeks (from their time of birth) do not affect body weight (BW) (A), food intake (B), lean (C), fat mass (D) and oxygen consumption (VO2) (E) in comparison to control mice (Suc) at 6 months of age. F-H. Post-natal dox (Dox) and amoxicillin (Amox) treatment decreased the locomotor activity at 6 months of age. Top panel: counts in function of time. Bottom panel: Mean counts during dark phase (gray area), i.e. when lights are switched off. I. Post-natal dox (Dox) and amoxicillin (Amox) treatment do not affect mouse lifespan. Bar graphs are expressed as mean + SEM, ***p <0.001

4.2.4 Discussion

Here, we showed that dox induces mitonuclear imbalance *in vivo* and impacts on mitochondrial function and whole body physiology; namely, it reduces oxygen consumption and increases mobility, as it does in flies and worms (Moullan et al., 2015). In *C. elegans,* dox and mitochondrial stress signaled by UPR^{mt} prolong lifespan through the intervention of epigenetic modifications mediated by conserved demethylases (Houtkooper et al., 2013; Jovaisaite et al., 2014). Although it is tempting to speculate that physiological effects of mitochondrial stress may be long-lasting, we found that they do not persist in mice subjected to dox postnatally. Longevity also was not impacted by early life dox treatment.

Decreased physical activity was the only long-term consequence of post-natal dox treatment, which, however, was also observed in mice treated with amoxicillin. As amoxicillin does not affect mitochondria, we concluded that the reduced activity probably resulted from the alteration of their gut microbiota due to the antibiotic treatment. A decrease in general locomotor activity can also be a sign of anxiety and depressive behavior. Indeed, many studies demonstrated that alterations of the gut microbiota, especially in early life, affect the gut-brain axis, leading to anxiety and depression (Foster and McVey Neufeld, 2013). This observation therefore highlights the physiological impact of altering the microbiota post-natally through treatment with antibiotics (Cho and Blaser, 2012; Cho et al., 2012). The fact that similar data were obtained with two antibiotics that have a divergent impact on the mitochondria also suggest that an accurate assessment of mitochondrial stress induced by dox should be performed in an experimental set-up which is free of microbiota, such as in mice raised in a germ-free environment.

4.3 Materials and methods

4.3.1 Materials and Methods to corresponding to section 4.1

Animals

40 strains of the BXD population—40 on CD, 37 on HFD—with ~10 male animals from each strain were separated into two cohorts of five for each diet. Food access was *ad libitum* for CD—Harlan 2018 6% kCal/fat, 74% carbohydrates, 20% protein—or for HFD—Harlan 06414 (60% kCal/fat, 20% carbohydrate, 20% protein). HFD cohorts received the diet from week 8 until sacrifice. Each cohort was communally

housed until wk 23, after which animals were single caged until tissues collection at 29 wks after an overnight fast. Tissues were collected from 183 CD and 168 HFD animals, with at least 3 biological replicates for all cohorts.

Sample Preparation and Analysis

For liver analyses, three ~100 mg pieces were taken from cold storage for each individual, then weighed and sorted for mRNA, protein, and metabolite measurements. For microarray, mRNA from 3–5 individuals per cohort were prepared separately then pooled equally after nanodrop quantification and run on the Affymetrix Mouse Gene 1.0 ST array platform. For proteomics, protein was prepared from one to three biological replicates per cohort.

SRM Assay Development and Protein Quantification

Generation of peptide library and development of SRM assays were performed as described (Picotti et al., 2010). Identical SRM assays for all 192 target proteins were run on all 77 cohorts. SRM traces were manually checked according to established criteria (Lange et al., 2008). For relative quantification of each protein across the set of different cohorts, the raw intensity of transitions of the native and ($^{13}C_6$, $^{15}N_4$)-Arginine, ($^{13}C_6$, $^{15}N_2$)-Lysine peptides were considered. Technical reproducibility of SRM-based quantification was validated by measuring the individual samples with three independent mass-spectrometry injections.

General Informatic Analyses

Correlations are Pearson's *r* or Spearman's *rho*, depending on the absence or presence of outliers. Student's *t*-test was used for comparing two groups in normalized data (all protein and mRNA are normalized). Bonferroni's correction for multiple testing was performed, and cutoffs for both nominal significance ($p < 0.05$) and corrected significance ($p < 0.05/n\text{-}tests$) are displayed. Except for QTL plots, graphs and analyses were performed in R.

C. elegans experiments

Wild-type Bristol N2 *C. elegans* provided by the *Caenorhabditis* Genetics Center (University of Minnesota) were cultured at 20°C and sustained on the OP50 *E. coli* strain. Bacterial feeding RNAi experiments were carried out as described (Kamath et

al., 2001). *cco-1* (F26E4.9) and *spg-7* (Y47G6A.10) clones were purchased from GeneService and sequenced.

For qPCR analysis, five biological replicates for each condition were prepared, consisting of ~600 worms per sample in M9 minimal liquid medium. Before mRNA preparation, samples were washed twice with 5 mL M9 to eliminate residual bacteria. Total RNA was prepared using TRIzol (Invitrogen) according to the manufacturer's instructions. RNA was treated with DNase, and 1 µg of RNA was used for reverse transcription (RT). 15X diluted cDNA was used for RT- quantitative PCR (RT-qPCR) reactions. The RT-qPCR reactions were performed using the LightCycler 480 System (Roche Applied Science) and a qPCR Supermix (QIAGEN) with the indicated primers. *act-1* was used as normalization control. Three technical replicates were used for each biological replicate.

The primers used for the *C. elegans* genes were as follows:

cco-1 (F26E4.9): fw: gctcgtcttgctggagatgatcgtt, rv: ggtcggcgtcgactcccttg.
spg-7 (Y47G6A.10): fw: aagtatgcaggacaaacgtgc, rv: tgaggtttgggatttcgcgt.
hsp-6 (C37H5.8): fw: aaccaccgtcaacaacgccg, rv: agcgatgatcttatctccagcgtcc.
hsp-60 (Y22D7AL.5): fw: ttctcgccagagccatcgcc, rv: tctcttcgggggtggtgaccttc.
hsp-10(Y22D7AL.10): fw: gggaaaagtccttgaagccac, rv: ctccgagaagatcagactcgc.
clpp-1 (ZK970.2): fw: tgcacagggaacctgctcgg, rv: ttgagagcttcgtgggcgct.
lonp-1 (C34B2.6): fw: cgatgatggccattgtgcag, rv: cgctttgaaacatcaatttcatcca.
ubl-5 (F46F11.4): fw: acgaatcaagtgcaatccatcag, rv: gctcgaaattgaatccctcgtg.
act-1 (T04C12.6): fw: gctggacgtgatcttactgattacc, rv: gtagcagagcttctccttgatgtc.

For *C. elegans* phenotyping, oxygen consumption was measured using the Seahorse XF96 equipment (Seahorse Bioscience Inc.) as described previously (Yamamoto et al., 2011). Typically, 100 worms per condition were recovered from plates with Nematode Growth Medium (NGM), then washed three times in 2 mL of M9 liquid medium to eliminate residual bacteria, and resuspended again in 500 µL of M9. Worms were transferred in 96-well standard Seahorse plates (#100777-004) (10 worms per well) and oxygen consumption was measured 6 times. Respiration rates were normalized to the number of worms in each individual well.

Movement was recorded for 45 seconds at day 2 of adulthood using a Nikon DS-L2 / DS-Fi1 camera and controller setup, attached to a computerized Nikon bright field

microscope. Five plates of worms, with 20 worms per plate, were measured in each condition. The movement of worms during this time was calculated by following the worm centroids using the same modified version of the freely-available for the Parallel Worm Tracker in MATLAB (Ramot et al., 2008).

4.3.2 Materials and Methods corresponding to section 4.2

Mouse experiments

Male C57BL/6J mice at 8 weeks of age were treated for 14 days with 50 or 500 mg/kg/day doxycycline hyclate (Sigma) or 50 mg/kg/day amoxicillin (Mepha) in drinking water. As doxycycline is bitter we supplemented the water for all the conditions (treatments and controls) with 50 g/L sucrose. Drinking water was changed every 48 hours.

For post-natal dox treatment, female mice were put in the empty cage of their breeder 3 days before mating in order to stimulate their fertility, therefore ensuring a good synchronization of the breeding mothers housed in the same cage. The day pups were born, they were treated with 500 mg/kg/day doxycycline (Sigma) or 50 mg/kg/day amoxicillin (Mepha) supplemented in drinking water. Drinking water for both dox and control groups was supplemented with 50 g/L sucrose. As doxycycline is bitter we supplemented the water for all the conditions (treatments and controls) with 50 g/L sucrose. Drinking water was changed every 48 hours. Male pups were treated for 6 weeks after birth.

At 6 months of age, indirect calorimetry to monitor O2 consumption and measurement of activity was assessed using Comprehensive Lab Animal Monitoring System (CLAMS; Columbus Instruments). Lean and fat mass was measured by echoMRI. About 75 animals per conditions were used to monitor survival. Mouse experiments were performed in accordance with Swiss law and institutional guidelines.

Western blotting

Proteins were extracted from liver and cells in protein extraction buffer containing 25 mM Tris-HCl, 150 mM NaCl, 1% NP-40, 1% sodium deoxycholate, 0.1% SDS withadded protease inhibitor cocktail (Roche). We used 20 µg of total protein lysate to detect mitochondrial protein imbalance. Antibodies against MTCO1, SDHA (both

from Abcam) and β tubulin, GAPDH (both from Santa-Cruz) were used for immunoblotting.

Chapter 5 Doxycycline-induced mitochondrial stress in microbiota-free mice reveals organ-specific response

Adapted from

Mottis A, D'Amico D, Williams EG, Quiros PM, Moullan N, Jovaisaite V, Harris N, Zamboni N, Aebersold R, §Auwerx J. In preparation.

§ Co-corresponding author

I initially conceived this project. I supervised the *in vivo* experiment (achieved in germ-free incubator of Harris laboratory) and harvested/extracted all samples for the different analysis. Proteomics and metabolomics analyses were done in collaboration with laboratories that are expert in these techniques. I analyzed the data, conceived and wrote the manuscript with guidance from JA and advices from DD.

5.1 Introduction

Mitochondria have long been considered as simple "energy factories" that host cellular respiration and ATP production. Studies over the last decades have expanded the functions of the mitochondria and have shown that they crucially contribute to the homeostasis of the cell and the whole organism, far beyond the simple fact of harvesting energy. Mitochondria house numerous pathways with both anabolic as well as catabolic functions and hence directly control metabolite balance, and by extension also control a number of epigenetic modifications (Matilainen et al., 2017a). In addition, an ever-growing importance is being attributed to the role of mitochondria in immunity (Mills et al., 2017). Their outer membrane constitutes a central platform for intracellular immune signalling, containing key players such as the mitochondrial antiviral signalling protein (MAVS), which is activated by the viral RNA sensors RIG-I and MDA5 (Mills et al., 2017). Mitochondria can also engage in a sentinel function by sending danger signals when they are being targeted and damaged by infectious microorganisms, a so called danger-associated molecular

pattern (DAMP). For instance, the release of mtDNA into the cytosol is sensed by the cyclic GMP-AMP synthase-stimulator of interferon genes (cGAS-STING) DNA-sensing system, which subsequently triggers anti-viral and inflammatory cascades, such as type 1 interferon (IFN) or NF-κB (West and Shadel, 2017).

Mitochondria are therefore in constant communication with the other subcellular compartments, such as the nucleus and the endoplasmic reticulum (ER) (Friedman and Nunnari, 2014; Quiros et al., 2016). When facing a stress that disrupts mitochondrial homeostasis, mitochondria send signals to the nucleus to activate stress resistance genes. Doxycycline (dox) is an antibiotic agent that blocks bacterial protein synthesis. This compound was also found to affect mitochondrial function across the eukaryotic kingdom due to the similarities of the mitochondrial translation machinery with their bacterial ancestor (Houtkooper et al., 2013; Moullan et al., 2015). Dox impedes mitochondrial protein synthesis and the production of the mtDNA-encoded OXPHOS subunits, leading to an accumulation of orphan nuclear-encoded OXPHOS subunits that cannot assemble into complexes with their mitochondria-encoded partner subunits. This so called mito-nuclear protein imbalance imposes a mitochondrial proteotoxic stress, leading to the activation of the UPR^{mt}. This transcriptional, reparative response has been well characterized in *C. elegans*, but the adaptations to mitochondrial stress in mammals still remain poorly characterized. Characterizing the effects of *in vivo* administration of mitochondrial stressors will provide a better understanding of the responses that help to restore or ameliorate mitochondrial function in normal physiology, as well as in the context of disease. Indeed, it is now commonly accepted that mitochondrial dysfunction participates in the pathology of a wide range of common disorders, such as diabetes, neurodegenerative diseases, cancer and muscular dystrophies (Andreux et al., 2013).

Since mitochondria evolved from bacterial ancestors, most of the drugs that generate mitochondrial stress also will impact on bacteria. Higher metazoans have coevolved in a symbiotic relationship with the bacteria that constitute their flora. As a result, microbiota influence many aspects of mammalian physiology, ranging from metabolism, inflammation, immunity, to the function of the nervous system (Cho and Blaser, 2012). In this study, we describe the *in vivo* consequences of a pure mitochondrial stress that is void of any interference caused by an impact on the

microbiota. We therefore treated germ-free mice with dox and characterized the change in the transcriptome and proteome in their liver, kidney, heart and muscle—metabolic organs with high mitochondrial activity. Our results show distinct organ specific signatures in response to doxycycline and allow us to distinguish the effects of dox on the so-called “mitobiome” from those on the “microbiome”.

5.2 Results

5.2.1 Microbiota-independent transcriptomic signatures of doxycycline treatment show differential organ responses

We treated 9-week old mice C57BL/6J mice raised in a germ-free environment during 16 days with 500mkd doxycycline (dox) in drinking water supplemented with sucrose. Germ-free mice allow the study mitochondrial stress induced by dox *in vivo*, independent of an eventual impact of the compound on the microbiota (Figure 5.1A). Mice were sacrificed in the non-fasted state. Body weight at the time of the sacrifice was not different between the groups, suggesting the absence of obvious adverse effects attributable to the dox treatment or to the germ-free status (Supp. Figure 5.9B) We assessed changes in whole genome transcript levels elicited by dox in 4 organs, i.e. kidney, liver, heart and a skeletal muscle, gastrocnemius by microarray profiling (Figure 5.1A). The number and distribution of differentially expressed genes represented by volcano plots for each tissue indicated differential effects of dox treatment. Liver and kidney, the two main metabolic organs, display more differentially expressed genes than do cardiac and skeletal muscles (Figure 5.1B). Venn diagrams displaying the number of significantly up- and down-regulated genes in common among these organs, showed that there was no common up-regulated gene and only one gene was down-regulated in common across these tissues with the most stringent significance threshold (Figure 5.1C); similar results were obtained when a lower stringency cut-off was used (Supp. Figure 5.1B). Of note and in common, however, was the low percentage of mitochondrial genes amongst the differentially expressed genes in the 4 tissues (only 3% or 6%; Figure 5.1D). Together, these results suggest that the changes in transcript levels elicited by the dox are different among the kidney, liver, heart and gastrocnemius and are hence organ-specific. Moreover, perturbation of mitochondrial gene expression does not appear as the main component of the response to mitochondrial stress.

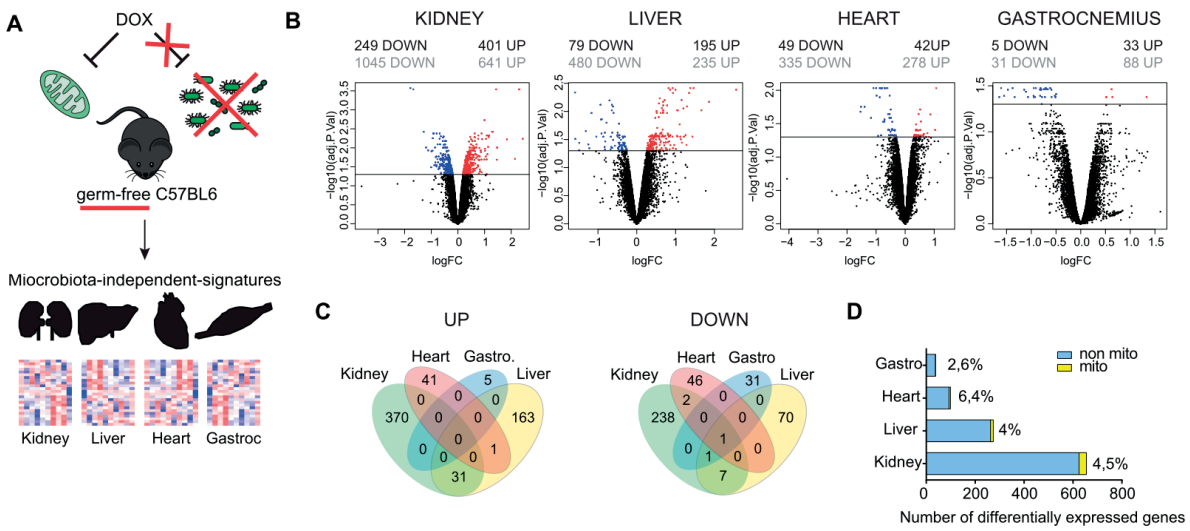

Figure 5.1 : Transcriptomics analysis of doxycycline treatment in germ-free mice

A. Schematic representation of the present study: C57BL/6J mice raised and maintained in a germ-free environment were treated with doxycycline (dox) and the resulting transcript signatures were analyzed in kidney, liver, heart and gastrocnemius. B. Volcano plots displaying –log(nom. p-value) and the log fold change (FC) of all genes in each organ. Above the graph, the number of differentially expressed genes is indicated (in black, genes with adjusted p value adj.pval<0.05, in gray with adj.pval<0.01 with Benjamini-Hochberg correction). C. Venn diagrams displaying the genes commonly up and down-regulated between 4 different tissues upon mitochondrial stress (differentially expressed genes with adj.pval<0.05). D. Barplot displaying the total number and percentage of mitochondrial versus non-mitochondrial differentially expressed genes in each organ (differentially expressed genes with adj.pval<0.05). [a larger version of the figure can be found in Annexes]

5.2.2 Mitochondrial proteins are differentially regulated in liver compared to kidney

We used SWATH-MS proteomics (Bai et al., 2017) measurements to analyse the changes in the liver and kidney proteome of dox-treated mice. Volcano plots (Figure 5.2A), supported by the counts in the Venn diagrams (Figure 5.2B), demonstrated a striking contrast of the effect of dox on protein levels in liver versus kidney. Although there were a relatively comparable number of down-regulated proteins, few of them are common to both organs. In addition, a lot more proteins were up-regulated by dox in kidney compared to liver. This general trend is further illustrated by scatterplots putting in relation protein versus transcript levels for each measured protein (Figure 5.2C). However, assessing the Pearson correlation between proteomic and the transcriptomic data revealed that proteins levels in the liver have a higher chance to directly reflect changes at the transcript level, compared to kidney. The correlation for the blue subgroup (i.e. significantly changed upon dox at the mRNA level only), as well as the purple line for overall correlation, was significant in liver; in the kidney, the transcript correlation was not significant and even showed a trend towards an inverse

correlation (Figure 5.2C). This suggests that there are extensive compensatory or post-transcriptional mechanisms causing a discrepancy between transcript and protein levels in the kidney.

Assessing the differentially expressed proteins either localized in the mitochondria versus protein not in the mitochondria, indicated that mitochondrial proteins had a tendency to be down-regulated in the liver, while being up-regulated in the kidney following dox (Figure 5.2D). Together, these results suggest that dox-driven mitochondrial stress leads to a higher proportion of down-regulated proteins in liver compared to kidney, especially when considering mitochondrial proteins.

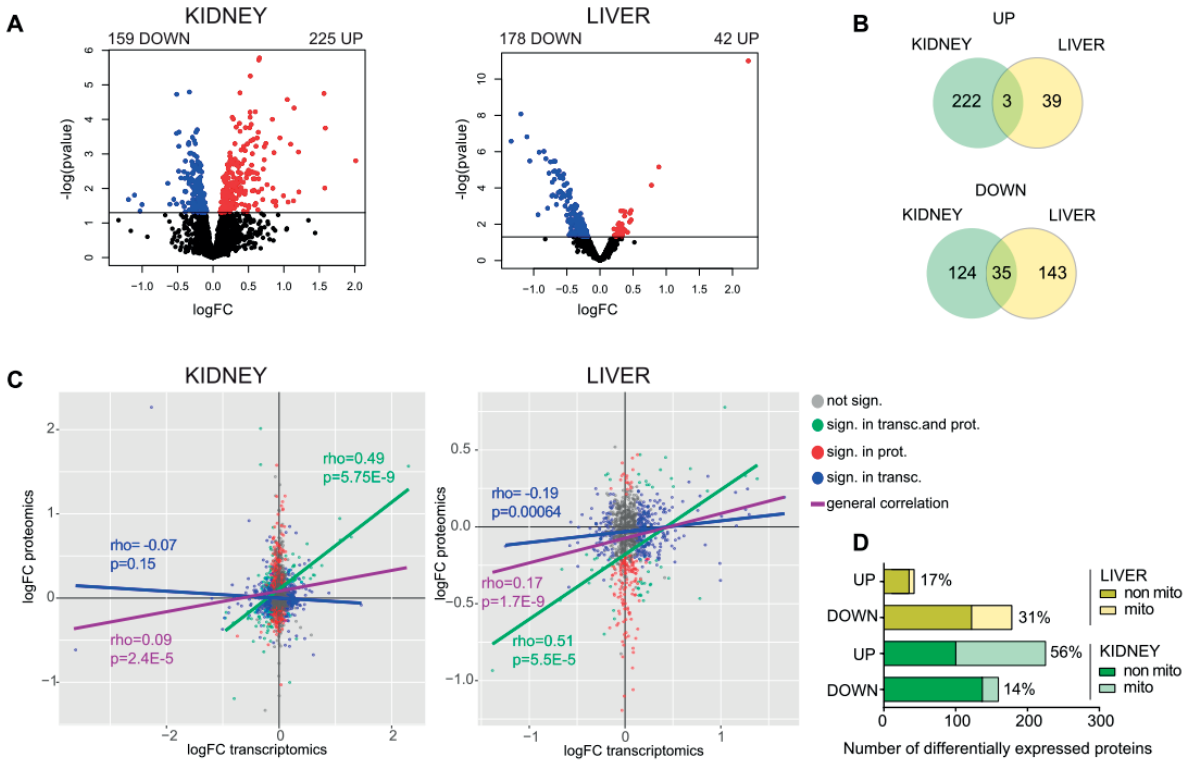

Figure 5.2 : Proteomics analysis of doxycycline treatment in germ-free mice

A. Volcano plots displaying –log(nom. p-value) and log(FC) of all measured proteins in kidney and liver (threshold set at nominal pval<0.05 for colored genes and the number of genes indicated above the graph). B. Venn diagrams displaying the genes commonly up and down-regulated between the different tissues upon mitochondrial stress (proteins with <0.05). C. Scatterplot displaying the relation between log(FC) of transcriptomics and of proteomics measurements for each of the measured proteins in kidney and liver. Blue, red and green correspond to significance at transcriptomics, proteomics and both levels, respectively (nom. pvalue<0.05). Lines represent the Pearson correlation of each group of genes accordingly to the color, with rho value and p value, purple corresponding to the general correlation of all dots together. D. Barplot displaying the total number and percentage of mitochondrial versus non-mitochondrial differentially expressed proteins in each organ (differentially expressed genes with nom. pval<0.05). [a larger version of the figure can be found in Annexes]

5.2.3 Dox does not affect OXPHOS activity in the liver despite a decrease in their protein levels

In order to understand which processes were affected by dox treatment, we searched for enriched gene ontology biological process (GO BP) terms in the list of all measured proteins, ranked from the most to the least down-regulated proteins. Several mitochondria-related terms, such as “mitochondrial respiratory chain complex assembly” and “NADH dehydrogenase complex assembly” were enriched (Figure 5.3A). A heatmap showing levels of OXPHOS proteins (Figure 5.3B), complemented by immunoblots (Figure 5.3C), confirms that respiratory complexes are down-regulated upon dox in the liver. This result validated previous findings showing that, although dox initially impairs mitochondrial translation, the consequent mitonuclear imbalance leads, in a second phase, to a general decrease in OXPHOS complex levels independently of the nuclear or mitochondrial origin of the proteins (Quiros et al., 2017). The scatterplot of the OXPHOS subunits shows that this general decrease of their protein levels is apparently not driven by a down-regulation of their transcripts levels, since none of them is decreased at the mRNA level, most of them rather displaying an up-regulation of their transcripts levels (Figure 5.3D). Surprisingly, there were no consequences of the changes in OXPHOS protein levels on the activity of the individual OXPHOS complexes or on the activity of citrate synthase, and ATP levels in the liver (Figure 5.3E). In fact, complex I and ATP levels rather showed tendencies towards an increase. Together, proteomics measurements confirm the negative effect of dox-driven mitochondrial stress on OXPHOS protein levels in vivo, but OXPHOS activity and ATP production remained intact or even tended to increase, suggesting the existence of compensatory mechanisms.

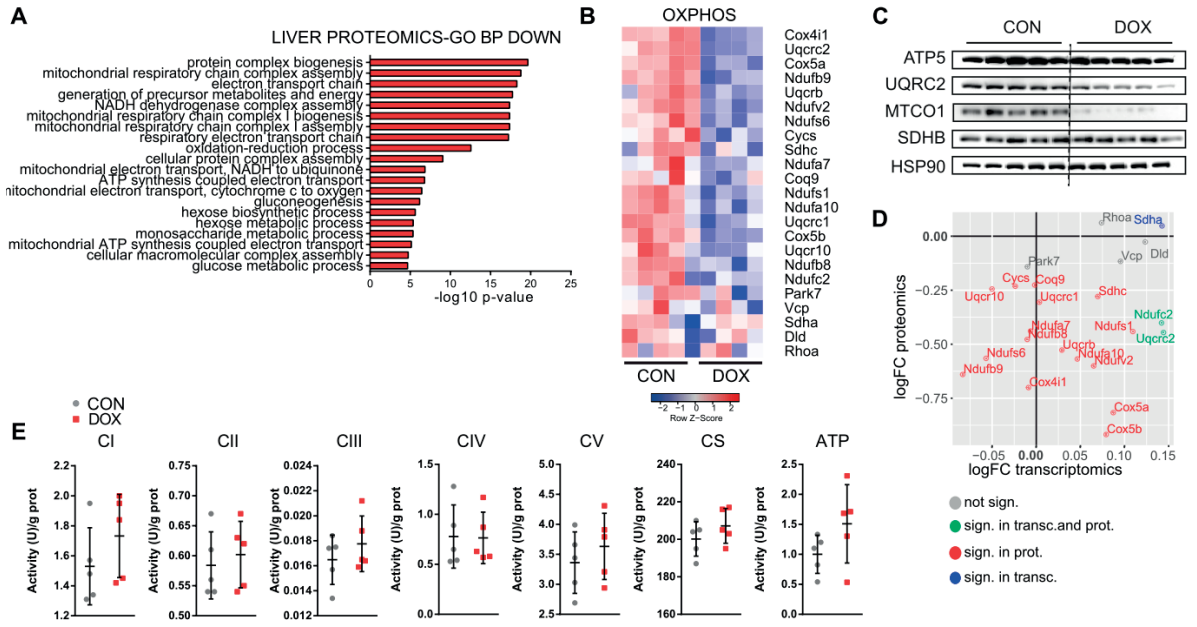

Figure 5.3 : The effect of dox treatment on OXPHOS proteins and activity in liver

A. Up-regulated gene ontology biological processes (GO BP) terms enriched from the list of measured proteins ranked by their decreasing fold change upon dox treatment in liver. B. Heatmap representing the protein levels of the OXPHOS proteins in control (CON) versus dox-treated mice (DOX). C. Immunoblots of OXPHOS protein levels in liver of control and dox-treated germ-free mice. D. Scatterplot displaying the relation between log(FC) of transcriptomics and of proteomics measurements for each measured OXPHOS proteins in liver (based on GO: 0006119). Blue, red and green correspond to significance at transcriptomics, proteomics and both levels, respectively (nom. pvalue<0.05). E. Activity measurements of OXPHOS complexes I to V, of citrate synthase (CS) and measurement of ATP levels in liver of control and dox-treated germ-free mice.

5.2.4 Dox remodels liver metabolism

Although only few proteins were significantly increased in the liver, exploring the GO BP enrichment of the list of measured proteins (ranked in a decreasing order by their fold change) identified several lipid-related processes: GO BP terms such as “lipid metabolic process”, “fatty acid catabolic process” or “lipid biosynthetic process” were enriched (Figure 5.4A). The scatterplot for all proteins belonging to the “lipid metabolic process” showed a robust correlation, reflecting a good probability for these changes to be transcriptionally driven (Figure 5.4B). Some proteins implicated in both catabolic and biosynthetic lipid pathways, such as fatty acid oxidation (FAO), fatty acid synthesis (FAS) or cholesterol synthesis were amongst the most induced proteins. Of note, amongst the top induced transcripts are those encoding for the FAS genes, *Fasn* and *Acss2*, the FAO genes, *Acaa1a* and *Acaa1b* as well as the cholesterol synthesis gene, *Hmgcs1* (Figure 5.4B). To assess the physiological impact of this regulation, we measured triglyceride (TG), free fatty acid (FFA) and

cholesterol levels in liver and plasma (Figure 5.4C). Liver and plasma TG, FFA and cholesterol levels were not affected by dox. In the liver, however, several phospholipids were increased, as highlighted by metabolomic measurements (Figure 5.4C). Similarly, levels of several intermediates of the TCA cycle were increased (Figure 5.4C). Therefore, our results suggest that selected lipid and metabolic pathways are remodelled by dox, without any clear commitment towards either anabolic or catabolic lipid metabolism. On top, immunoblotting of phosphorylated adenosine monophosphate-activated protein kinase (AMPK), which constitutes a sensor of cellular energy level, was not changed upon dox treatment (data not shown). It hence suggests that the observed lipid remodelling does not simply result from the regulation imposed by the cellular energy (nutrient) state.

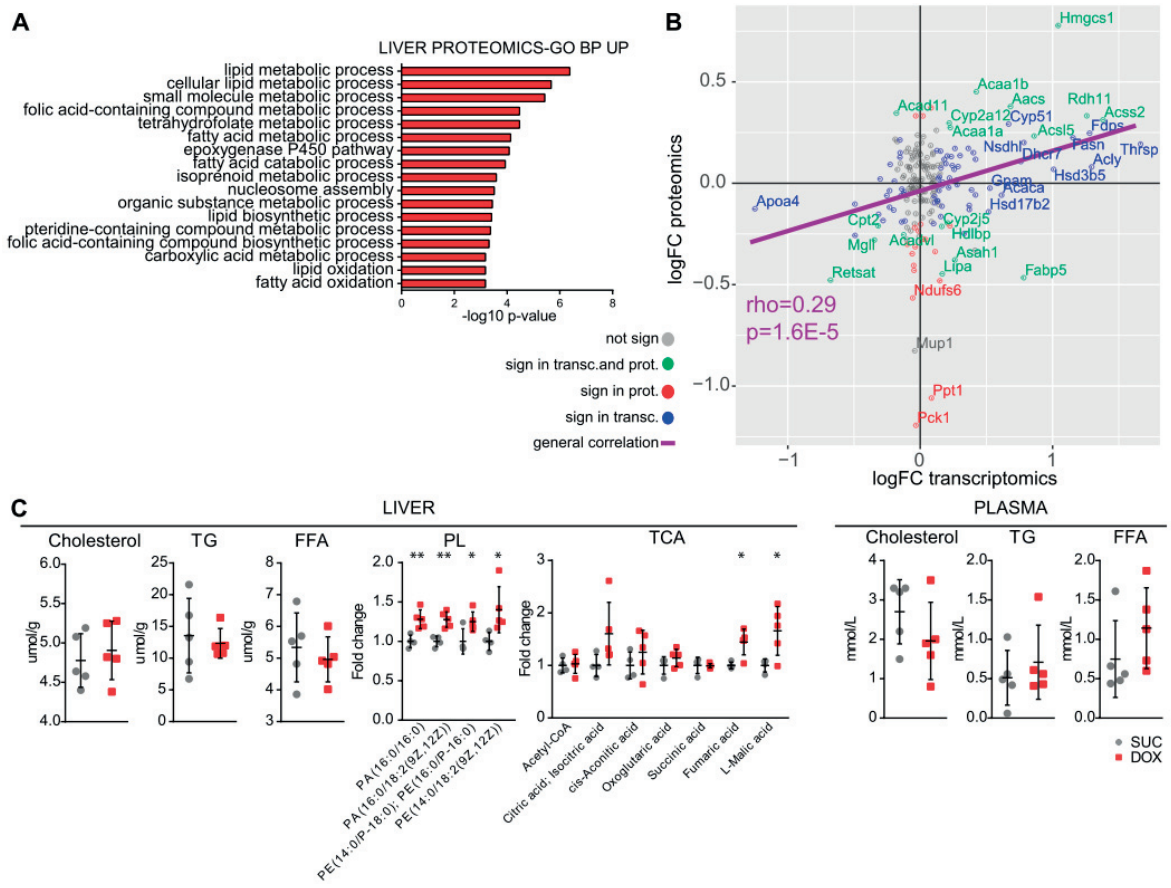

Figure 5.4 : The effect of dox treatment on lipid metabolism in liver

A. Up-regulated GO BP terms enriched from the list of measured proteins ranked by their decreasing fold change upon dox treatment in liver. B. Scatterplot displaying the relation between log(FC) of transcriptomics and of proteomics measurements for each measured lipid-metabolism proteins in liver (based on GO: 0006629). Blue, red and green correspond to significance at transcriptomics, proteomics and both levels, respectively (nom. pvalue<0.05). The purple line shows the general Pearson correlation of all dots. C. Measurements of cholesterol, triglyceride (TG), free fatty acids (FA),

phospholipids (PL) and TCA cycle intermediates, in liver and plasma of control and dox-treated germ-free mice. [a larger version of the figure can be found in Annexes]

5.2.5 Liver transcriptome data shows activation of ER and cytosolic stress responses as well as the type I interferon response in dox-treated mice

To further explore the processes and pathways modulated in response to dox in the liver, we performed Gene Set Enrichment Analysis (GSEA) using several gene set compendia: Reactome pathways, GO biological processes, KEGG pathways gene sets and transcription factors motifs. Among the most induced pathways, several lipid-related gene sets (in blue) and the “KEGG TCA cycle” were enriched, consistent with our previous observations (Figure 5.5A, 5.5B, Supp. Figure 5.10B, 5.11A, 5.12C, highlighted in blue). Another noteworthy response was the enrichment of the unfolded protein response in the endoplasmic reticulum (Figure 5.5A, 5.5B, Supp. Figure 5.10B, 5.11A, in red). The enrichment of “XBP1_01” among the top motifs, also supported the involvement of the X-box protein protein 1 (XBP1) (Supp. Figure 5.10A), a master regulator of ER stress response. Along the same line, the only transcription factors motif significantly enriched was “TTCNRGNNNNTTC_HSF_Q6” (Supp. Figure 5.10A), supporting that the heat shock factor (HSF) response, a transcriptional program governing the expression of cytosolic chaperones subsequent to heat stress, was activated. ROS ensuing from disturbed mitochondrial function are a major trigger of cellular stress pathways. Interestingly, several metabolites from the glutathione (GSH) pathway were increased by dox in the liver (Figure 5.5C, Supp. Figure 5.12D), consistent with the observation that “glutathione metabolism” was amongst the top upregulated terms in metabolite set enriched analysis (MSEA) (Supp. Figure 5.12A). The GSH pathway constitutes one of the major buffering systems for ROS and the increase in GSS-GSSH can therefore be seen as another layer of cellular adaptation to increased oxidative stress. The enrichment of “NRF2_01” the top motifs (Figure 5.5C, Supp. Figure 5.10A), i.e. genes activated by the nuclear factor erythroid 2-related factor 2 (NFE2L2 or NRF2), a major antioxidant response, also reinforces this hypothesis. These observations are therefore in line with several studies that indicated that mitochondrial stress is often signalled to other cellular stress networks in several species (Kim et al., 2016; Matilainen et al., 2017b) (reviewed in (D'Amico et al., 2017)).

Amongst the dox-induced enriched up-regulated Reactome and GO BP pathways were those related to virus infection, such as “Reactome Influenza viral RNA transcription and replication” (Figure 5.5A), “GO viral life cycle” or “GO defence response to virus” (Supp. Figure 5.10B), as well as several immune function-related terms (Figure 5.5A, 5B, Supp. Figure 10B, 5.11A,, in green). Notably, the interferon regulatory factor 7 (Irf7) was one of the few genes commonly up-regulated in liver and kidney (Figure 5.1C). This transcription factor activates inflammatory and antiviral genes downstream of viral nucleic acid-sensing pathways (Chen et al., 2016). On top, “IRF_Q6”, which is the motif recognised by the IRF family transcription factors was one of the highest enriched transcription factor binding motifs (Supp. Figure 5.10A). IRF7 is one of the transcription factors that mediates the gene expression program induced upon sensing of dsDNA in the cytosol and the downstream signalling of the antiviral cytokines type I interferon (IFNα and IFNβ). IRF7 binding induces its target genes by binding to IFN-stimulated response element (ISRE) DNA sequences, another motif enriched in GSEA results (Supp. Figure 5.10A). Indeed, type I IFN related terms are enriched in both Reactome and GO BP GSEA upon dox (Figure 5.5A, Supp. Figure 5.10B). In combination all this suggests that dox induces an antiviral response orchestrated by type I IFN, possibly due to a leakage of mtDNA in the cytosol or in the circulation.

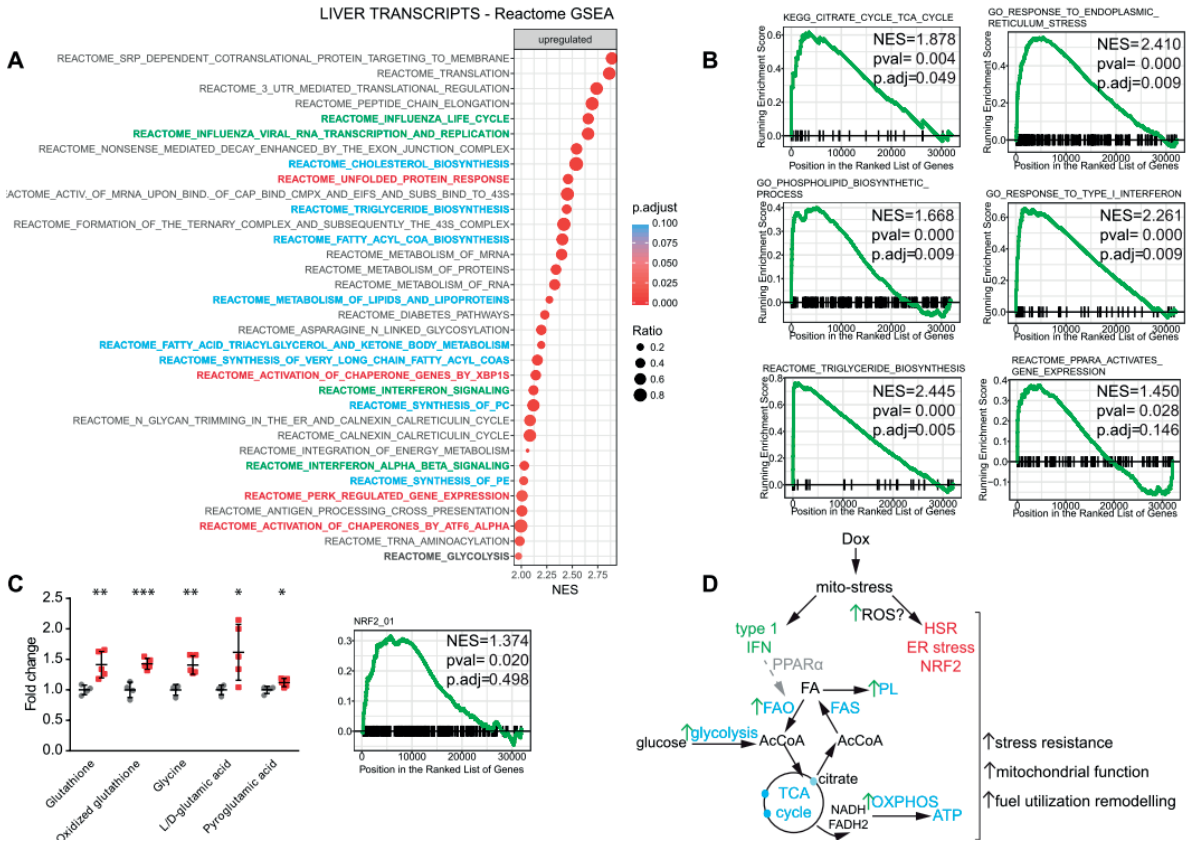

Figure 5.5 : GSEA of the liver transcript signature of dox treatment in germ-free mice

A. Graph representing the top significant pathways enriched in GSEA analysis using Reactome pathways term library, ordered by decreasing adjusted p value. The horizontal axis corresponds the normalized enrichment score (NES). The size of the dots corresponds to the ratio. B. Enrichment score plot for each of the mentioned terms. C. Metabolomics measurements of the gluthatione pathway intermediates. Please refer to Supp. Figure 12D for their occurrence in the pathways. Enrichment score plot for the NRF2 motif. Bars show mean±SD, * Student t-test p-value P≤0.05, **P≤0.01, *** P≤0.001. D. Scheme summarizing the observed changes in the liver of germ-free dox-treated mice (green arrows represent the known effects of type I IFN). In A. and D. blue highlight corresponds to lipid-related, terms, pathways and processes; green to terms and pathways related to virus infection; red to ER and heat shock (HSR) stress. [a larger version of the figure can be found in Annexes]

A major arm of the type I IFN response consists in counteracting the metabolic modulations elicited by a viral infection (Fritsch and Weichhart, 2016). Since the replication of viruses is an energy-demanding process, they hijack cellular metabolism to sustain their need in protein and nucleotide synthesis, pathways that are also upregulated in our metabolomics data (Supp. Figure 5.12A). Type I IFN metabolic modulation mainly include an activation of glycolysis, as we saw amongst up-regulated terms of GSEA and MSEA (Figure 5.5A, Supp. Figure 5.12A), as well as an increase in OXPHOS activity sustained by increased FAO rates dependent on *de novo* FAS (Wu et al., 2016). These type 1 IFN-driven metabolic changes are

orchestrated by the nuclear receptor PPARα (Wu et al., 2016). Interestingly, the enrichment of “KEGG PPAR signalling pathway” and “Reactome PPARa activates gene expression”, although just not significant, may suggest a possible involvement of PPARα (Figure 5.5B, Supp. Figure 5.12C). On top, both type 1 IFN and PPARα induce lipolysis, which could explain the tendency towards an increase of plasma FFAs (Figure 5.4C). As seen in the context of viral infection and subsequent type I IFN activation (Fritsch and Weichhart, 2016; Wu et al., 2016), FFAs arising from induced *de novo* FAS may be used directly by FAO and and the resulting acetyl-coA may be funneled into the TCA cycle, which could explain the moderate impact on steady lipid levels in liver (Figure 5.4C, 5.5D). In accordance, marked changes in transcript levels of lipid gene sets, but sometimes in opposite directions (Figure 5.5A, Supp. Figure 5.10B versus Supp. Figure 5.10C), reflect the ambivalent activation of both catabolic and anabolic lipid metabolic pathways (Figure 5.5D).

Additionally, some phospholipid species were increased in liver (Figure 5.4C), in line with the extensive remodeling of membrane lipids dynamics caused by viruses and IFN (Fritsch and Weichhart, 2016).

Together, these results suggest that the response to dox in the liver is multifaceted and involves of the activation of cellular stress pathways, such as the ER and heat shock stress responses, probably triggered by increased oxidative stress (Figure 5.5D). In addition, the hepatic, metabolic response to mitochondrial stress *in vivo* seems to be driven by innate immunity and inflammation induced by dox. The induction of pathways such as glycolysis, TCA cycle, OXPHOS activity, FAO, FAS, cholesterol and phospholipid synthesis may result from a mimicry of a viral infection and the resulting action of type 1 IFN on metabolism, potentially mediated by PPARα (Figure 5.5D).

5.2.6 Dox treatment impairs OXPHOS activity in the kidney

We then analysed the kidney proteomics data by searching for enriched gene sets in the list of the most to the least up- and down-regulated proteins upon dox treatment. OXPHOS-related terms, in particular complex I, were down-regulated (Figure 5.6A), whereas several mitochondrial terms, such as “mitochondrion organization”, “cristae formation” or “mitochondrial translation” were enriched amongst the up-regulated terms (Figure 5.6B). The corresponding heatmaps confirmed these results, OXPHOS

proteins showing both tendencies to down- or up-regulation and “mitochondrial membrane organization“ genes being overall up-regulated (Figure 5.6C). The scatterplot for OXPHOS proteins, however, demonstrated that most of their transcripts were down-regulated (Figure 5.6D). In coherence with the proteomics measurements, the activity of complex I and IV, as well as ATP levels were down-regulated in the kidney, and a clear tendency towards decreased complex V activity was observed (Figure 5.6E). Thus, proteomics and activity measurements together demonstrate that the activity and the protein level of some OXPHOS complexes are impaired by dox treatment, while some other mitochondrial proteins, involved in mitochondrial membrane organization are increased.

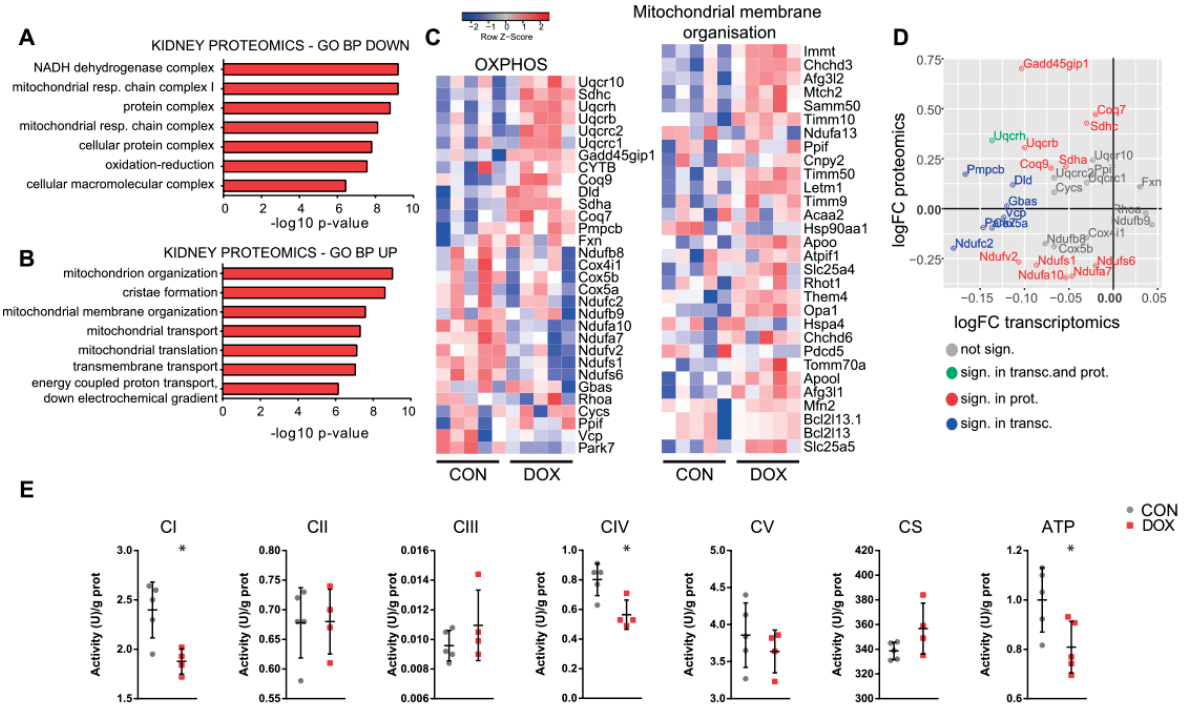

Figure 5.6 : The effect of dox treatment on OXPHOS proteins and activity in kidney

A. Up-regulated GO BP terms enriched from the list of measured proteins ranked by their decreasing fold change upon dox treatment in kidney. B. Down-regulated GO BP terms enriched from the list of measured proteins ranked by their increasing fold change upon dox treatment in kidney. C. Heatmap representing the expression of OXPHOS (left) and mitochondrial membrane organization (right; GO:0007006) proteins in control (CON) versus dox-treated mice (DOX), respectively. D. Scatterplot displaying the relation between log(FC) of transcriptomics and of proteomics measurements for each measured OXPHOS proteins in kidney (based on GO:0006119) (significance nom. P val<0.05). E. Activity measurements of OXPHOS complexes I to V and citrate synthase (CS) and measurement of ATP levels in kidney of control and dox-treated germ-free mice. * Student t-test p-value P≤0.05

5.2.7 The transcriptomics response of dox treatment in the kidney features ER stress and a marked down-regulation of mitochondrial genes

To characterize the transcript signature underpinning the proteomic changes observed following mitochondrial stress triggered by dox, we performed GSEA on the kidney transcriptomics data. We found similarities to the changes seen in liver: terms related to virus defence and type 1 IFN were enriched (Figure 5.7A, 5.7B, Supp. Figure 5.14, in green), and the motifs of STAT3 and NFKB (Supp. Figure 5.13A), other down-stream transcriptional mediators of type 1 IFN response were amongst the top ranked motifs. Also, the cytosolic and ER stress and quality control pathways (Figure 5.7A, 5.7B, Supp. Figure 5.14, in red) were enriched in the up-regulated terms, together with some up-regulated transcription factor motifs, such as HSF1 as mentioned above, or another ER stress transducer, CHOP (Supp. Figure 5.13A).

Interestingly, many of the sets that were positively modulated in the liver transcriptome, such as the lipid-related (catabolic and anabolic), “PPAR”-, “TCA cycle”-, “pyruvate”- and “oxidative phosphorylation”-containing terms were strongly down-regulated in the kidney (Figure 5.7A, 5.7B, Supp. Figure 5.13B, 5.14, in blue). In line, GSEA analysis for GO cellular component (GO CC) terms confirmed the enrichment of mitochondrial components (Supp. Figure 5.15A) in the most down-regulated sets, which clearly differs from the liver transcriptome data (Supp. Figure 5.15B). We therefore concluded that mitochondrial mRNAs levels decreased upon dox treatment in the kidney, which seems as a paradox given that several mitochondrial proteins displayed increased proteins levels (Figure 5.6B, 5.6C, 5.6D). The scatterplot of all measured mitochondrial proteins confirmed this trend as a particularity of the kidney, i.e. that transcriptomic and proteomic measurements for mitochondrial proteins did not correlate in the kidney (Figure 5.7D), as opposed to in the liver (Supp. Figure 5.15C). Of note, genes significantly modulated at the mRNA level only were showing an inverse correlation approaching significance (Figure 5.7D). However, a significant positive correlation existed amongst the genes for which both transcriptomics and proteomics data were significant (Figure 5.7D, in green). In particular, the chaperone *Hspa9*, the protease *Lonp1* and the mitochondrial inner membrane protein *Phb2* were part of this group. *Hspa9* and *Lonp1* are the respective orthologues of the UPR^{mt} genes *hsp-6* and *lonp-1* in *C. elegans*, demonstrating a robust mitochondrial stress.

A possible explanation for the decreased mRNAs levels of mitochondrial proteins could be their active repression by inhibitory transcriptional mechanisms, a hypothesis that we cannot reject nor support with our data. Alternatively, some post-transcriptional mechanisms could account for the decrease in mRNAs levels of mitochondrial proteins and a general remodeling of the RNA landscape. For instance, during stress, the activation of nonsense-mediated mRNA decay mitigates the ISR and contributes to restore homeostasis and prevent apoptosis(Nasif et al., 2017). Supporting this, we found several terms in the up-regulated processes in kidney, such as “Reactome nonsense mediated decay […]”, “Reactome metabolism of mRNA” and “GO RNA catabolic process” (Figure 5.7A, 5.7B, Supp. Figure 5.14, in orange). Similar terms (Figure 5.5A, 5.5B, Supp. Figure 5.10B, 5.11A, 5.12C, in orange), or other related terms like “Reactome regulation of mRNA stability by proteins that bind AU-rich elements” were also enriched in the liver (Supp. Figure 5.11A, in orange).

Together, the results indicated that a particularity of the renal response to dox was a down-regulation of mitochondrial gene sets. Similarly to liver, however, ER and heat shock stress response, as well as the antiviral type IFN 1 response were induced.

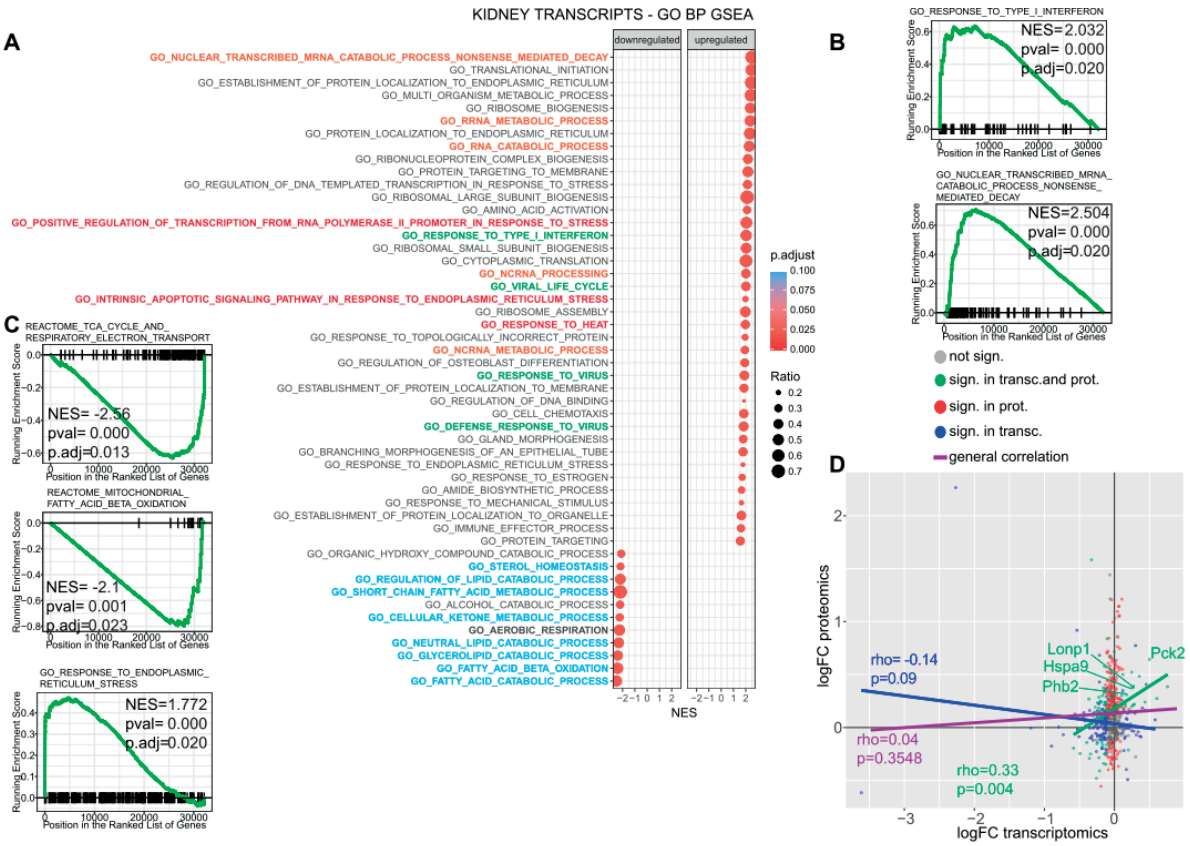

Figure 5.7 : GSEA of the kidney transcript signature of dox treatment in germ-free mice

A. Graph representing the top significant pathways enriched in GSEA analysis using GO BP pathways term library, ordered by decreasing adjusted p value. The horizontal axis corresponds the normalized enrichment score (NES). The size of the dots corresponds to the ratio of the number of genes in the leading edge over the total number of genes in the term. Blue highlight corresponds to lipid-related, terms, pathways and processes; green to terms and pathways related to virus infection; red to ER and heat shock (HSR) stress; orange to RNA regulation–related pathways. B-C. Enrichment score plot for each of the mentioned terms. D. Scatterplot displaying the relation between log(FC) of transcriptomics and of proteomics measurements for each measured mitochondrial protein in kidney of dox treated germ-free mice. Blue, red and green correspond to significance at transcriptomics, proteomics and both levels, respectively (nom. pvalue<0.05). Lines represent the Pearson correlation of each group of genes accordingly to the color, with rho value and p value, purple corresponding to the general correlation of all dots without any group taken into consideration. [a larger version of the figure can be found in Annexes]

5.2.8 The ATF4/ISR response is activated specifically in the kidney and is accompanied by an inhibition of cytosolic translation

As stated above, the increased protein levels of some mitochondrial genes, such as *Pck2*, *Hspa9*, *Lonp1* and *Phb2*, seem to result from increased transcript expression following dox-induced mitochondrial stress (Figure 5.7D, in green). Each of these proteins are confirmed or predicted targets of the ATF4 and ATF5 transcription factors, which activate the integrated stress response (ISR) in response to various stressors (Teske et al., 2013), including mitochondrial stress (Baker et al., 2012;

Fiorese et al., 2016; Munch and Harper, 2016; Quiros et al., 2017). Of note, GSEA scores a significant enrichment for “Reactome activation of genes by ATF4” (Supp. Figure 5.16B). In addition, the motif of ATF3, a target of ATF4, was amongst the top up-regulated motifs (Supp. Figure 5.13A). Dox furthermore increased the expression of other ATF4 targets, such as the endocrine peptides *Fgf21* and *Adm2* and of the anaplerotic genes *Asns* and *Pck2* (Figure 5.8A). Western blot also showed that protein levels of ASNS, HSPA9 and LONP1 were increased (Figure 5.8B). The elevated expression and protein levels of ATF4 targets upon dox-treatment was confirmed also in mice that were raised in conventional, non-germ-free, conditions (Figure 5.8C,D), indicating that this response is independent to the presence and effect of dox to the microbiota. *Ddit3/Chop* and its target, *Gdf15*, recently identified as myomitokine induced by the mitochondrial stress response in mammalian cells (Chung et al., 2017), were up-regulated by dox in kidney (Supp. Figure 5.16C,D). However, these *Atf4*-, *Atf5*- and ISR-associated transcripts are not modulated by dox in the liver (Supp. Figure 5.16C,D).

The increase in mitochondrial ribosomes in the kidney upon treatment with dox was a striking trend in the mitochondrial proteomic data, as illustrated by a heatmap of proteomics results (Figure 5.8E). Cytosolic ribosomes however, rather showed an opposite tendency (Figure 5.8E). The activation of the ATF4 response is directly regulated by the translational status of the cell (Jackson et al., 2010). Although a multitude of stressors can trigger the ISR, a common point of convergence is the phosphorylation of the eukaryotic translation initiation factor 2 (eIF2α). This event results in a reduced availability of the ternary complex eIF2-tRNA^{Met}-GTP, which has two consequences: (1) a general slow-down of the cytosolic cap-dependent translation, which represents an energy-costly process when cells have to save their resources to cope with the stress, and (2) an increase in the translation of the transcripts that contain an alternative ORF; ATF4 is one of the best characterized mRNAs with this feature (Jackson et al., 2010). This form of translational regulation was also evident in the dox-treated kidneys, since dox induced eIF2α phosphorylation (Figure 5.8F). The absence of eIF2α modulation in the liver was in coherence with the fact that the ATF4 response was not activated in the liver (Figure 5.8G). Upon mitochondrial stress, the eiF2α-dependent ISR crosstalks also with the mechanistic target of rapamycin (mTOR) pathway, although is not clear yet exactly

how this happens. mTOR is an integrator of cellular energy metabolism, which promotes cap-dependent translation and blocks autophagy depending on the abundance of growth factors and amino acids. A downstream effector of mTOR is the kinase of the ribosomal protein S6 (S6K), whose phosphorylation correlates with increase cap-dependent translation. Immunobloting of S6 phosphorylation proved that dox inhibited mTOR, in line with a blockade of cap-dependent translation in the context of an ATF4 response in the kidney (Figure 5.8F), whereas the unchanged phosphorylation levels of S6 and eIF2α corroborate that the translational block and subsequent activation of the ISR were more discrete in the liver (Figure 5.8G). Thus, these results suggest that in the kidney, dox inhibited mTOR signalling and slowed cap-dependent translation, resulting in the induction of the ATF4 response (Figure 5.8H). Concomitantly, we observed an increase of mitochondrial and a mild decrease of cytosolic ribosomes.

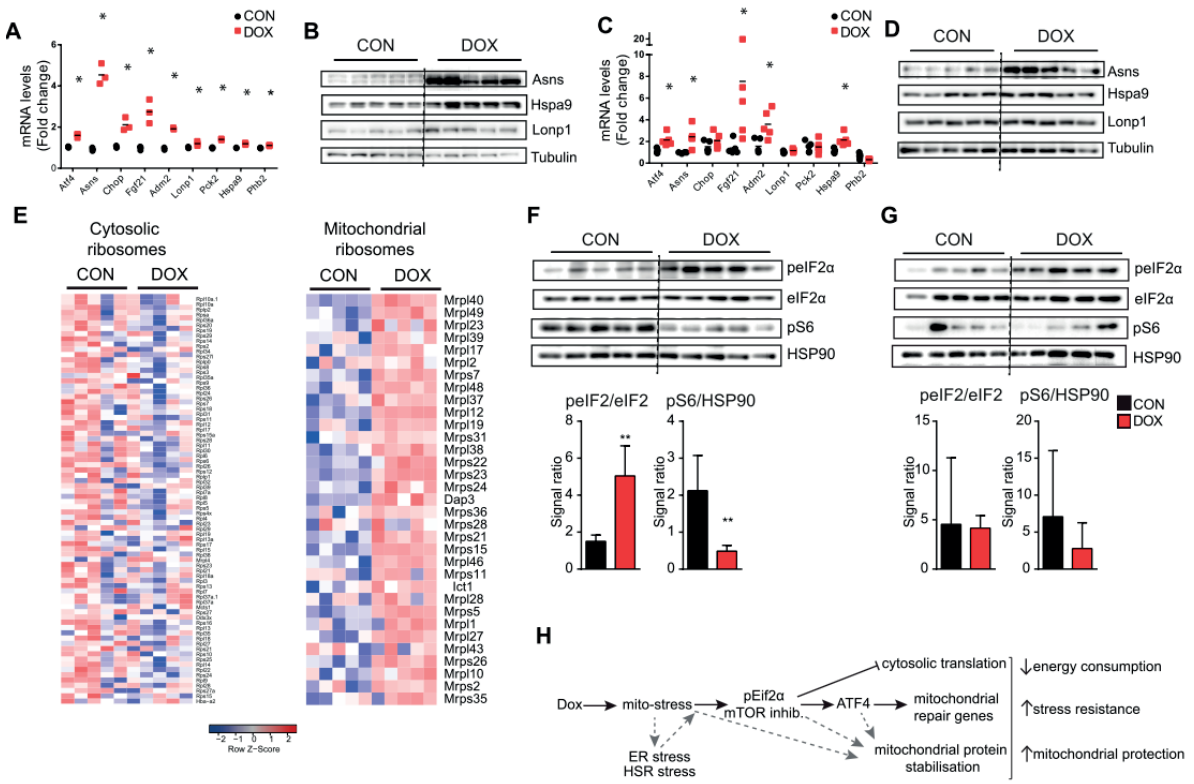

Figure 5.8 : Dox activates the ATF4-ISR response in the kidney of dox-treated germ-free and non-germ-free mice

A. mRNA levels of ATF4 targets in the kidney of control and dox-treated germ-free mice analyzed by microarray. * Student t-test p-value P≤0.05 B. Immunoblots of ATF4 targets in the kidney of control and dox-treated germ-free mice. C. mRNA levels of ATF4 targets in the kidney of control and dox-treated germ-free mice analysed by RT-qPCR.* Student t-test p-value P≤0.05 D. Immunoblots of ATF4 targets in the kidney of control and dox-treated non germ-free mice. E. Heatmap representing the protein levels of the cytosolic (left) and mitochondrial (right) ribosomal proteins in the kidney of control

(CON) versus dox-treated mice (DOX). F-G. Immunoblots of phosphorylated eIF2α (peIF2α) and phosphorylated S6 (pS6) in the kidney (F) and liver (G) of control and dox-treated germ-free mice. Quantification of the results is shown underneath the blots. H. Scheme summarizing the observed changes in the kidney of germ-free dox-treated mice. Dashed arrows represent unexplored relations.

Pathways	Liver	Kidney
Transcriptomics		
ER and HSR stresses	UP	UP
type I IFN	UP	UP
mitochondrial genes	-	DOWN
lipid metabolism	UP	DOWN
ATF4 response	-	UP
TCA cycle	UP	DOWN
glycolysis and pyruvate	UP	DOWN
Proteomics		
OXPHOS	DOWN	UP/DOWN
peIF2α	-	UP
mTOR (pS6)	-	DOWN
mitoribosomes	-	UP

Table 5.1 : Summary of the main changes observed upon dox in liver versus kidney

(-) represents no changes

5.3 Discussion

In this study, we performed a multi-omics characterization of the response elicited by *in vivo* treatment with the mitochondrial stressor, dox, in C57BL/6J mice raised in a germ-free environment. Transcriptomics and proteomics analysis demonstrated that organs highly dependent on mitochondria did not show a uniform response to mitochondrial stress. In the kidney, OXPHOS activity was clearly impeded, but the expression of several mitochondrial ribosomal and OXPHOS proteins was increased. In the liver, however, mitochondrial respiration was maintained and ATP production even marginally increased, despite a general decrease in OXPHOS and mitochondrial protein levels.

Profiling the hepatic response at the level of gene and protein expression completed by metabolomics and lipid measurements demonstrated an increase in glycolysis, TCA cycle, ROS metabolism, as well as in lipid anabolic and catabolic pathways. Several similarities with the metabolic modulations caused by viral infection and the subsequent activation of type 1 IFN response, were evident in GSEA results in both liver and kidney. The precise trigger, the exact mechanism and consequences of the induction of the type 1 IFN response still require further characterization. Knowing

that mtDNA constitutes a potent DAMP (West et al., 2015), it is tempting to speculate that a release of mtDNA occurs when mitochondria are stressed by dox. This could activate the cGAS-STING cytosolic DNA sensor pathway, culminating into a type 1 IFN response, as previously reported in other contexts (Bai et al., 2017; Oka et al., 2012; Rath et al., 2012). However, since mitochondria constitute signalling platforms for other immune pathways such as RIG-I, these cascades could potentially also be (co-)activated as a consequence of disrupted mitochondrial membrane integrity. An example of such indirect activation can happen in the context of stress in the ER, whose membrane hosts the key mediator, STING, of the DNA sensing response (Chen et al., 2016; Petrasek et al., 2013; Smith et al., 2008). A detailed lipidomics profiling to assess how single lipid species are modulated in liver and plasma by dox could therefore provide insight, considering that lipids play a crucial signalling role in the communication of mitochondrial stress (Kim et al., 2016; Liu et al., 2014), and are central to mediating innate immunity and pathogen resistance (Liu et al., 2014).

Another common trend in the hepatic and renal responses to mitochondrial stress was the induction of the HSF and ER stress responses. ER stress can on its turn also trigger the ATF4 and ISR response. Consistent with the fact that the ATF4 program is an integral part of the defence against mitochondrial stress in mammals (Munch and Harper, 2016; Quiros et al., 2017), we here show that a major arm of the renal response to dox *in vivo* is the ATF4-mediated activation of the ISR and the activation of a subset of mitochondrial proteases. Our work hence supports the observation that ATF4 targets are more typifying of the mammalian response to mitochondrial stress than the induction of the mammalian orthologues of the *hsp-60, hsp-10* or *clpp-1* genes, the targets of the canonical UPR^{mt} in *C. elegans*. We however observe in the kidney increased transcript and protein levels of *Hspa9* and Lonp1, orthologues of worm *hsp-6* and *lonp-1* respectively. It has also been proposed that ATF4 and ATF5 targets could be considered as the hallmark mammalian UPR^{mt} (Shpilka and Haynes, 2017). In liver however, we could not observe the induction of the UPR^{mt}. Future investigations should decipher these differences in mitochondrial stress response between these tissues and analyze other aspects, such as the timing of the response or starvation state of the organ.

Finally, some open questions remain concerning the tissue-specific differences in the responses to dox. As distinct organs, they obviously have their respective metabolic

and functional specializations and a similar stress could have a different outcome in liver and kidney. On the basis of our data, one cannot reject that these differences could also be attributed in part to the respective tissue exposure to dox and the resulting level of stress, as well as to the chronology of the response in these tissues. Definitely, the tissue energy status has a major influence on their respective response. The kidney is characterized by an attenuated mTOR pathway, decreased levels ATP and OXPHOS activity, and a shutdown of metabolism and translation upon dox. On the opposite, the liver shows a tendency towards increased ATP levels, with replenishment of TCA intermediates and an anabolic metabolic signature. The remodelling of hepatic metabolism contrasted with regulatory changes in the kidney that rather underpinned a general metabolic shut-down, in line with the disruption of anabolic processes requiring a lot of energy such as cap-dependant translation. In line with this, the marked down-regulation of mitochondrial transcripts and their paradoxical increase at protein level in the kidney were corroborated by the absence of overall correlation between mitochondrial proteins and mRNAs. This phenomenon suggests the existence of mechanisms favouring the stabilization of existent mitochondrial proteins, while hampering the production and import of new mitochondrial proteins, which comes at a high energy cost and could potentially aggravate the situation (Figure 5.8H). Of importance, this mechanism is capable of discriminating and still allowing the transcription and translation of mitochondrial effector proteins participating in the reparative response, such the as the ATF4 targets and the Lonp1 protease and the Hspa9 chaperone. Further mechanistic studies are hence warranted to identify the signals that result in such diverse outcomes, as a metabolic shut-down in the kidney versus processes oriented towards energy production in the liver.

5.4 Materials and Methods

Mouse experiments

Male C57BL/6J mice at 9 weeks old of age were treated for 16 days with 500 mg/kg/day doxycycline hyclate (Sigma) in drinking water. As doxycycline is bitter we supplemented the water for both conditions (treatments and controls) with 50 g/L sucrose. Drinking water was changed every 48 hours. Germ-free C57BL/6J mice were obtained from the Clean Mouse Facility, University of Bern (Bern, Switzerland),

and compared with specific pathogen-free (SPF) C57BL/6J mice from Janvier Labs. Mouse experiments were performed in accordance with Swiss law and institutional guidelines.

RNA extraction and microarray analysis

Total RNA was isolated using Trizol (Life Technologies) and purified using the RNeasy Mini Kit (Qiagen) in accordance with the manufacturer's instructions. Microarray analysis was performed using Affymetrix *mouse MAT1.0* chips in triplicates per condition. Microarray data was normalized with RMA-sketch method of the Affymetrix Expression console and analyzed using limma R package(Ritchie et al., 2015). Bonferroni adjusted p value<0.05 was used to determine the differentially expressed genes. Volcano plots, scatterplots, heatmaps and Venn diagrams were generated with R (www.r-project.org).

GO enrichment

GO enrichement was done using GOrilla online tool (http://cbl-gorilla.cs.technion.ac.il/) using the mode allowing to search for terms densely enriched at the top of a ranked gene list. All measured proteins were listed by their logFC in the decreasing order to search for enriched terms in the up-regulated genes (respectively in the increasing order to look using Bonferroni adjusted p value < 0.05.

GSEA

GSEA was performed using the clusterProfiler package(Yu et al., 2012). GO genesets in gmt format were obtained from the MSigDB Collections website from the Broad Institute website. For each organ, all expressed genes were ordered by decreasing fold change based on the differential expression analysis upon dox. We used GO BP, GO CC, KEGG pathways, Reactome pathways and transcription factor targets gene set categories. For each organ and gene category, we performed 10'000 permutations using the "fgsea" option, a minimum gene set size of 10, and a maximum of 1000. False discovery rate-adjusted P-values calculated using the Benjamini–Hochberg method were considered to determine significance of the enrichments.

qRT-PCR

RNA from cells and tissues and worms was extracted using TRIzol and then transcribes in cDNA by the QuantiTect Reverse Transcription Kit (Qiagen) following the manufacturer's instructions. The RT-qPCR reactions were performed using the Light-Cycler system (Roche Applied Science) and the expression of selected genes was analyzed using the LightCycler 480 System (Roche) and SYBR Green chemistry. All quantitative polymerase chain reaction (PCR) results were presented relative to the mean of *housekeeping genes* ($\Delta\Delta C_t$ method). mRNA levels were normalized over 36B4 for gene expression for cell and tissue samples.

The following primers were used :

gene	forward	reverse
Atf4	gcc ggt tta agt tgt gtg ct	ctg gat tcg agg aat gtg ct
Asns	gag aaa ctc ttc cca ggc tttg	caa gcg ttt ctt gat agc gtt gt
Chop/Ddit3	cgg aac ctg agg aga gag tg	cgt ttc ctg ggg atg aga ta
Fgf21	cctctaggtttctttgccaacag	aagctgcaggcctcaggat
Adm2	tgcatcagcctcctctacct	ggaaggaatcttagctgggg
Lonp1	atgaccgtcccggatgtgt	cctccacgatcttgataaagcg
Pck2	gctatgctccttccttccccg	agcccgtgccggctaa
Hspa9	acaggccactaaggatgctggc	tgccgcaacaaagcttggtcaa
Phb2	cgtgcagcaggacacg	cgcagggagatgttcacca
36B4	tgt gtc cgt cgt gga tct ga	cct gct tca cca cct tct tgat

SWATH-MS Proteomics

About 30-50mg of frozen tissue were used to prepare protein and peptides for SWATH-MS as described in(Wu et al., 2017).

Western blotting

Cells and tissues were lysed in RIPA buffer [50 mM tris (pH 7.4), 150 mM KCl, 1 mM EDTA, 0,1% SDS, 1% NP40, 100 mM NaF, 5mg/ml Sodium deoxycholate] with

Halt™ protease (78430, Thermo Fisher Scientific) and phosphatase (78442, Thermo Fisher Scientific) inhibitor cocktails. Proteins were separated by SDS-PAGE and transferred onto polyvinylidene difluoride membranes. Proteins were detected using commercial antibodies against eIF2α, phospho-eIF2α, phospho-S6 (all from Cell signalling), HP90 (Santa Cruz), ASNS (Atlas antibodies), HSPA9 (Antibodies Online), LONP1 (Sigma), OXPHOS proteins (Mitoprofile Total OXPHOS Rodent WB Antibody Cocktail , Mitoscience) and β tubulin (Santa Cruz). In addition to the housekeeping proteins, loading was monitored by Ponceau Red to ensure a homogeneous loading.

Lipid measurements

Hepatic lipids were extracted according to the Bligh & Dyer protocol(Bligh and Dyer, 1959). TG, FFA and cholesterol contents in plasma and hepatic lipid fractions were quantified using enzymatic assays (Roche). BUN and ALAT concentrations in blood were determined using standard clinical chemistry methods.

Respiratory complex activity

All respiratory chain complex assays were based on methods described by Kramer (Kramer & Nowak, 1988) and Krakenbuhl (Krahenbuhl et al., 1994), both modified to match our apparatus requirements. The activities of all the complexes in each sample were normalized by the amount of protein or referred to citrate synthase activity to allow sample comparison.

- Complex I activity measurement

Briefly, reduced nicotinamide adenine dinucleotide phosphate (NADPH)-ubiquinone reductase activity (complex I) was measured by following the disappearance of NADPH using rotenone as a specific inhibitor to ensure the specificity of the assay.

- Complex II activity measurement

Complex II activity, succinate-ubiquinone reductase, was assayed through the reduction of 2,6-dichlorophenolindophenol, a final electron acceptor, after the addition of succinate.`

- Complex III activity measurement

The activity of complex III, ubiquinone-cytochrome c reductase, was determined by assaying the rate of reduction of cytochrome c.

- Complex IV activity measurement

The cytochrome c oxidase (complex IV) activity was based on the same assay as for complex III using potassium cyanide to inhibit the activity of this enzyme.

- Complex V activity measurement

Complex V activity was measured according to a method coupling ADP production to NADH disappearance through the conversion of phosphoenol-pyruvate into pyruvate then into lactate (Rustin et al., 1993).

- Citrate synthase (CS) activity measurement

The activity of CS was assayed as described previously (Itoh and Srere, 1970) with the reduction of DTNB caused by the de-acetylation of acetyl-CoA.

ELISA measurements of FGF21

FGF21 levels in the plasma were measured by commercial ELISA kit (Millipore) following the manufacturer's instructions.

Metabolomics analysis

Approximatively 20 mg of liver tissue was used for metabolites extraction by adding ice-cold acetonitrile/methanol/water (40:40:20, vol/vol). To remove cell debris, tubes were centrifuged (4°C, 13,000 rpm, 2 min), and the supernatants collected were assayed by flow injection analysis using time-of-flight mass spectrometry (6550 QTOF; Agilent Technologies) operated in the negative ionization mode. High-resolution mass spectra were recorded from 50–1,000 m/z and analyzed as described previously (Fuhrer et al., 2011). Detected ions were putatively annotated by as searching matching metabolites in the Kyoto Encyclopedia of Genes and Genomes (KEGG;(Kanehisa et al., 2006)) using an m/z tolerance of 0.001 and including all common electrospray derivatives. Metabolites set analysis was done using the Metaboanalyst website (http://www.metaboanalyst.ca)

ATP quantification

Total ATP content was measured by the CellTiter-Glo luminescent cell viability assays (Promega) in protein lysate of tissue. Typically, the luminescence was recorded with a Victor X4 plate reader (PerkinElmer) and values are normalized by the total protein concentration determined using a Bradford assay.

Statistics

Differences between two groups were assessed using two-tailed t-tests. GraphPad Prism 5 (GraphPad Software, Inc.) was used for all statistical analyses, and $p<0.05$ was considered significant.

5.5 Supplementary figures

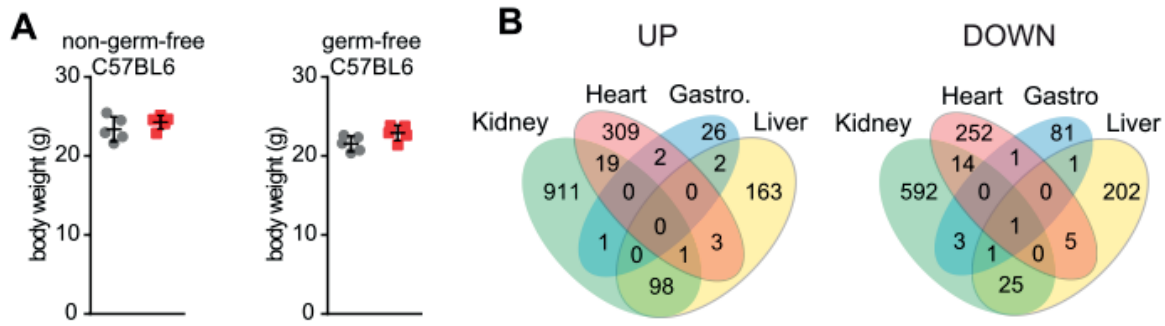

Supp. Figure 5.9

A. Body weight at the time of sacrifice of germ and non-germ-free mice, upon dox treatment. B. Venn diagrams displaying the genes commonly up and down-regulated between the 4 different tissues (differentially expressed genes with adj.p val<0.01).

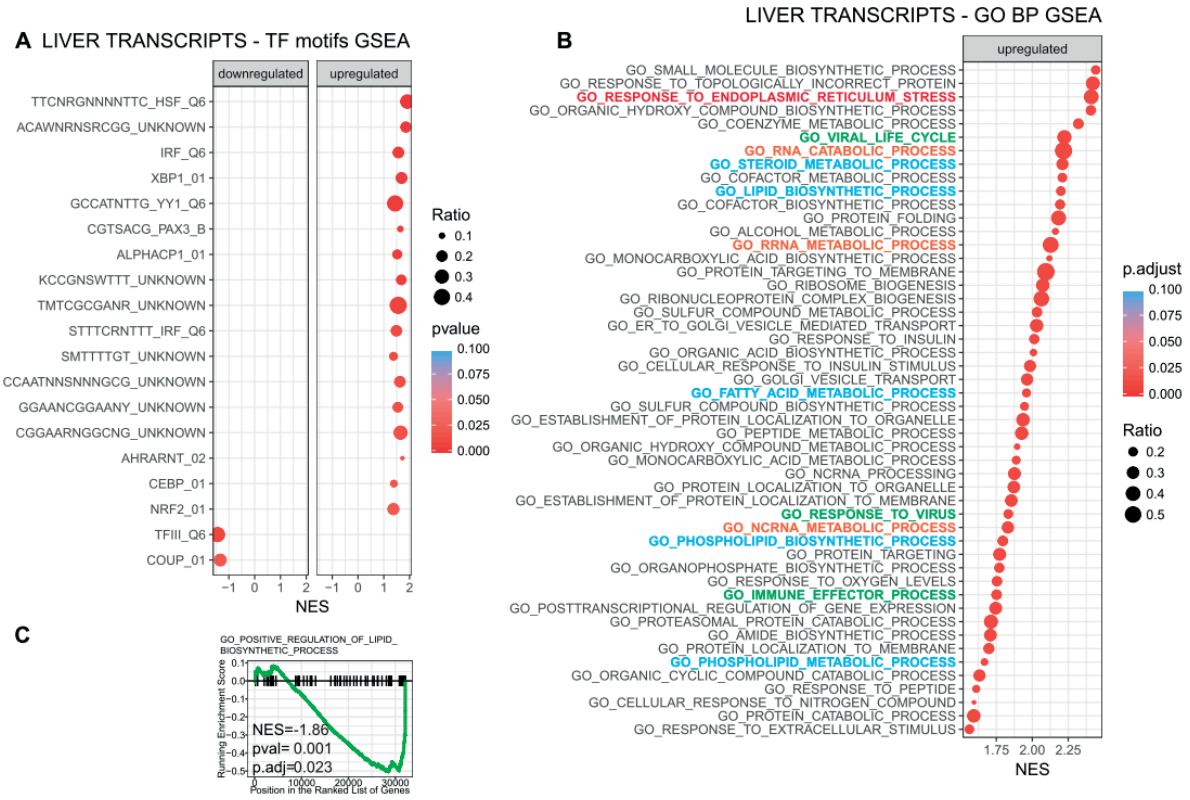

Supp. Figure 5.10

A. Graph representing the top significant pathways enriched in GSEA analysis using transcription factor motif library, ordered by decreasing nominal p value, in liver of germ-free dox-treated mice. B. Graph representing the top significant pathways enriched in GSEA analysis using GO BP pathways library, ordered by decreasing adjusted p value, in liver of germ-free dox-treated mice. The horizontal axis corresponds the normalized enrichment score (NES). The size of the dots corresponds to the ratio of the number of genes in the leading edge over the total number of genes in the term. Blue highlight corresponds to lipid-related, terms, pathways and processes; green to terms and pathways related to virus infection; red to ER and heat shock (HSR) stress; orange to RNA regulation –related pathways. C. Enrichment plot for the down-regulated term

“GO_POSITIVE_REGULATION_OF_LIPID_BIOSYNTHETIC_PROCESS”. [a larger version of the figure can be found in Annexes]

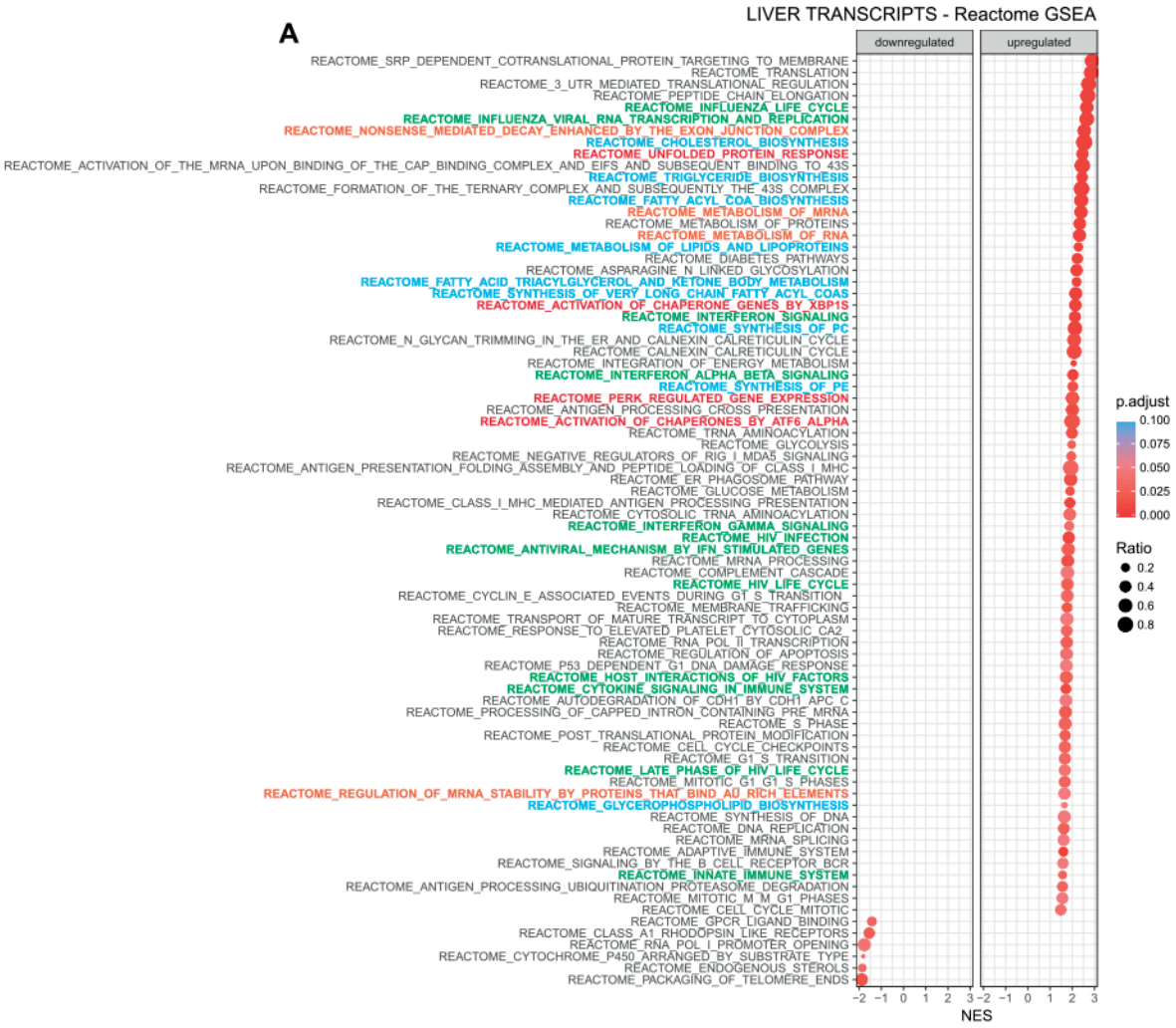

Supp. Figure 5.11

A. Graph representing the top significant pathways enriched in GSEA analysis using Reactome pathways library, ordered by decreasing adjusted p value, in liver of germ-free dox-treated mice. The horizontal axis corresponds the normalized enrichment score (NES). The size of the dots corresponds to the ratio of the number of genes in the leading edge over the total number of genes in the term. Blue highlight corresponds to lipid-related, terms, pathways and processes; green to terms and pathways related to virus infection; red to ER and heat shock (HSR) stress; orange to RNA regulation–related pathways. [a larger version of the figure can be found in Annexes]

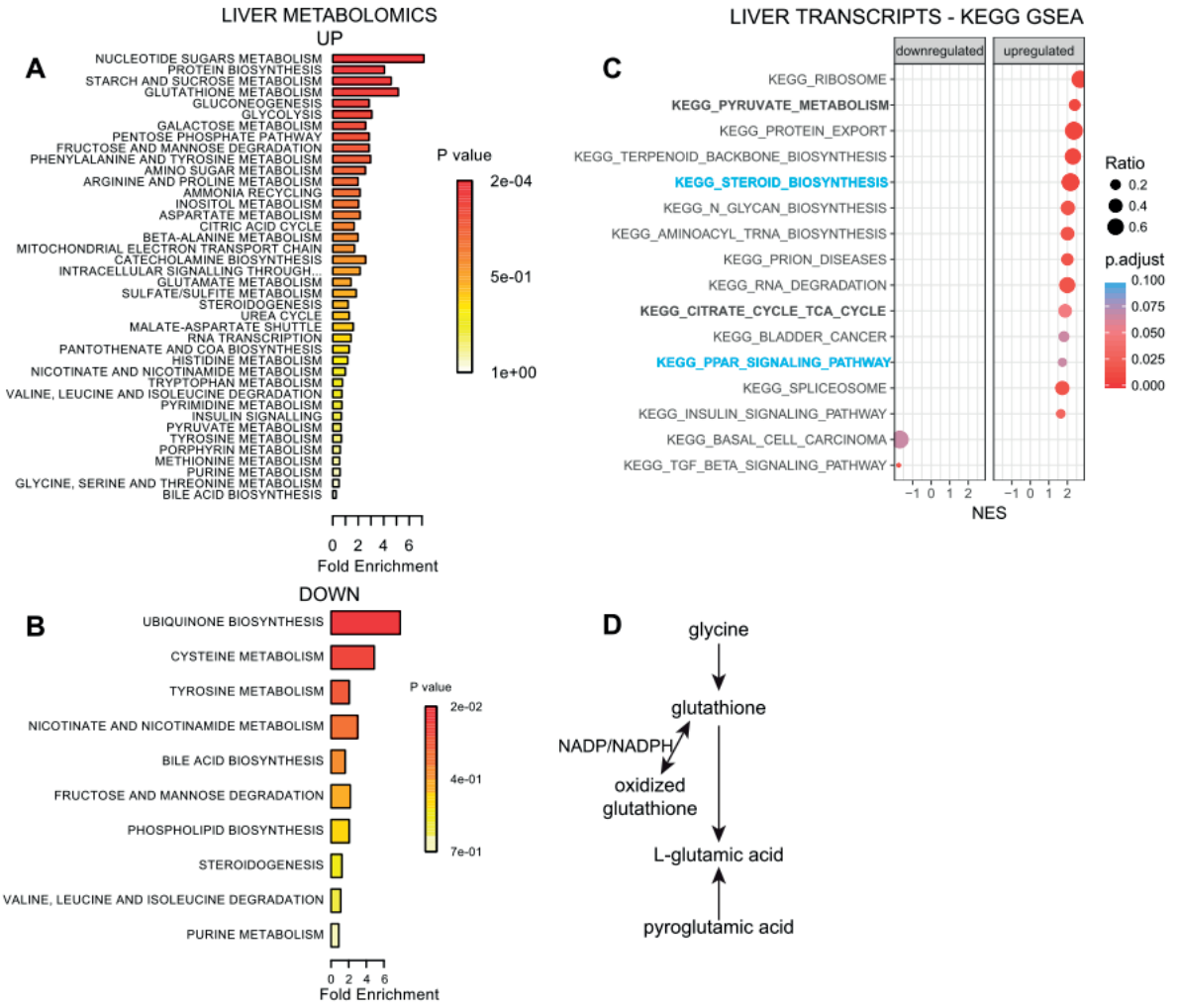

Supp. Figure 5.12

A-B. Metabolite set enrichment analysis (MSEA) results from the liver of germ-free dox-treated mice, of respectively up- (A) and down-regulated (B) metabolites. Color scale represents the nominal p value. C. Graph representing the top significant pathways enriched in GSEA analysis using KEGG pathways library, ordered by decreasing adjusted p value, in liver of germ-free dox-treated mice. The horizontal axis corresponds the normalized enrichment score (NES). The size of the dots corresponds to the ratio of the number of genes in the leading edge over the total number of genes in the term. Blue highlight corresponds to lipid-related, terms, pathways and processes.

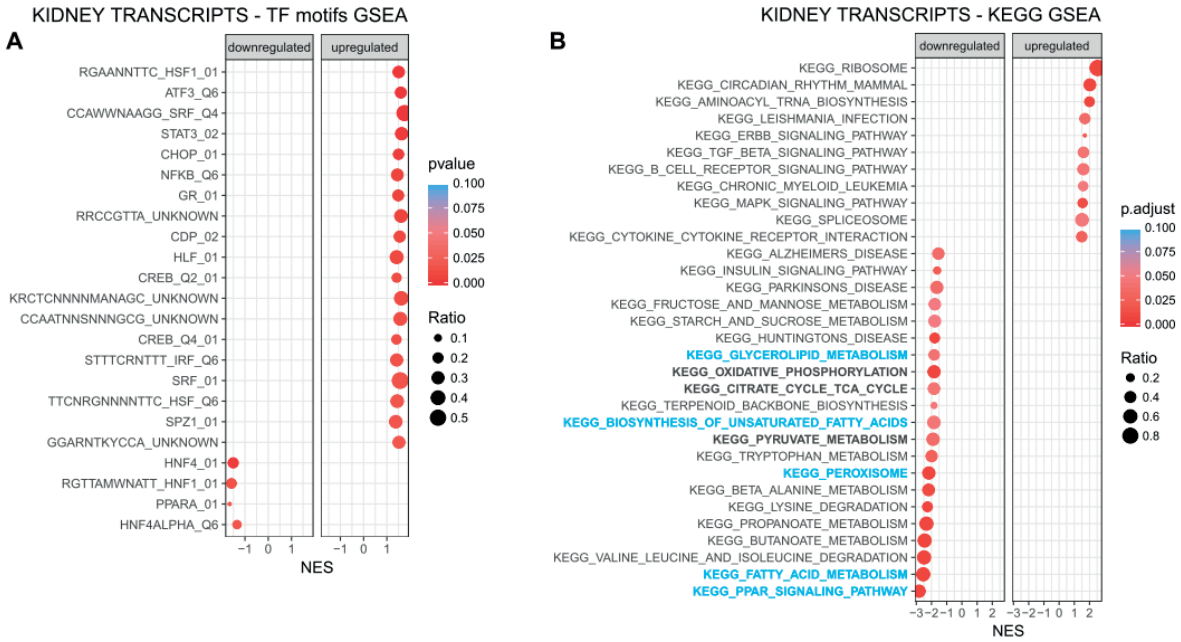

Supp. Figure 5.13

A. Graph representing the top significant pathways enriched in GSEA analysis using transcription factor motif library, ordered by decreasing nominal p value, in kidney of germ-free dox-treated mice. B. Graph representing the top significant pathways enriched in GSEA analysis using KEGG pathways library, ordered by decreasing adjusted p value, in kidney of germ-free dox-treated mice. The horizontal axis corresponds the normalized enrichment score (NES). The size of the dots corresponds to the ratio of the number of genes in the leading edge over the total number of genes in the term. Blue highlight corresponds to lipid-related, terms, pathways and processes. [a larger version of the figure can be found in Annexes]

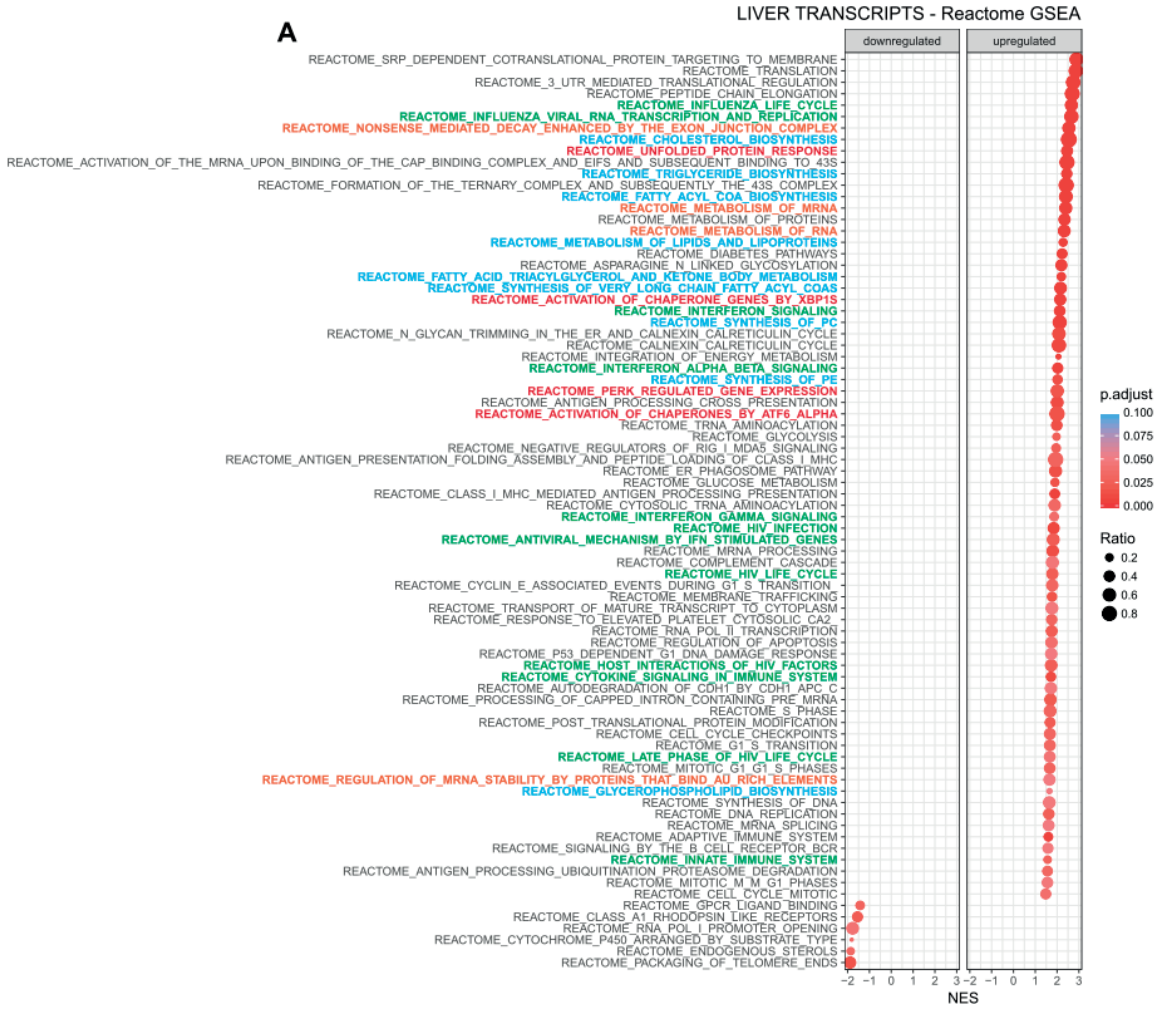

Supp. Figure 5.14

A. Graph representing the top significant pathways enriched in GSEA analysis using Reactome pathways library, ordered by decreasing adjusted p value, in kidney of germ-free dox-treated mice. The horizontal axis corresponds the normalized enrichment score (NES). The size of the dots corresponds to the ratio of the number of genes in the leading edge over the total number of genes in the term. Blue highlight corresponds to lipid-related, terms, pathways and processes; green to terms and pathways related to virus infection; red to ER and heat shock (HSR) stress; orange to RNA regulation–related pathways. [a larger version of the figure can be found in Annexes]

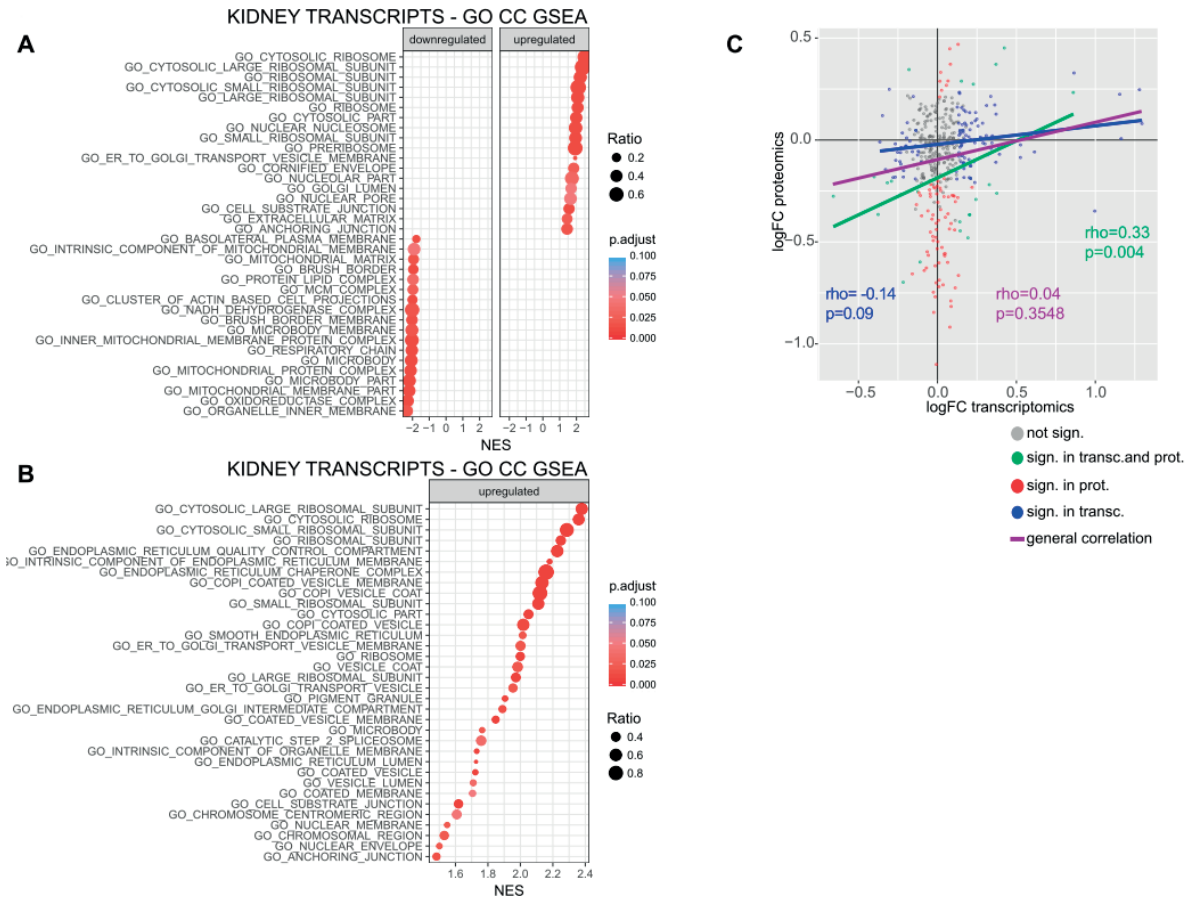

Supp. Figure 5.15

A-B. Graph representing the top significant pathways enriched in GSEA analysis using GO cellular component (CC) pathways library, ordered by decreasing adjusted p value, in kidney (resp. liver B.) of germ-free dox-treated mice. The horizontal axis corresponds the normalized enrichment score (NES). The size of the dots corresponds to the ratio of the number of genes in the leading edge over the total number of genes in the term. C. Scatterplot displaying the relation between log(FC) of transcriptomics and proteomics measurements for each measured mitochondrial protein in kidney of dox treated germ-free mice. Blue, red and green correspond to significance at transcriptomics, proteomics and both levels, respectively (nom. pvalue<0.05). Lines represent the Pearson correlation of each group of genes accordingly to the color, with rho value and p value, purple corresponding to the general correlation of all dots together. [a larger version of the figure can be found in Annexes]

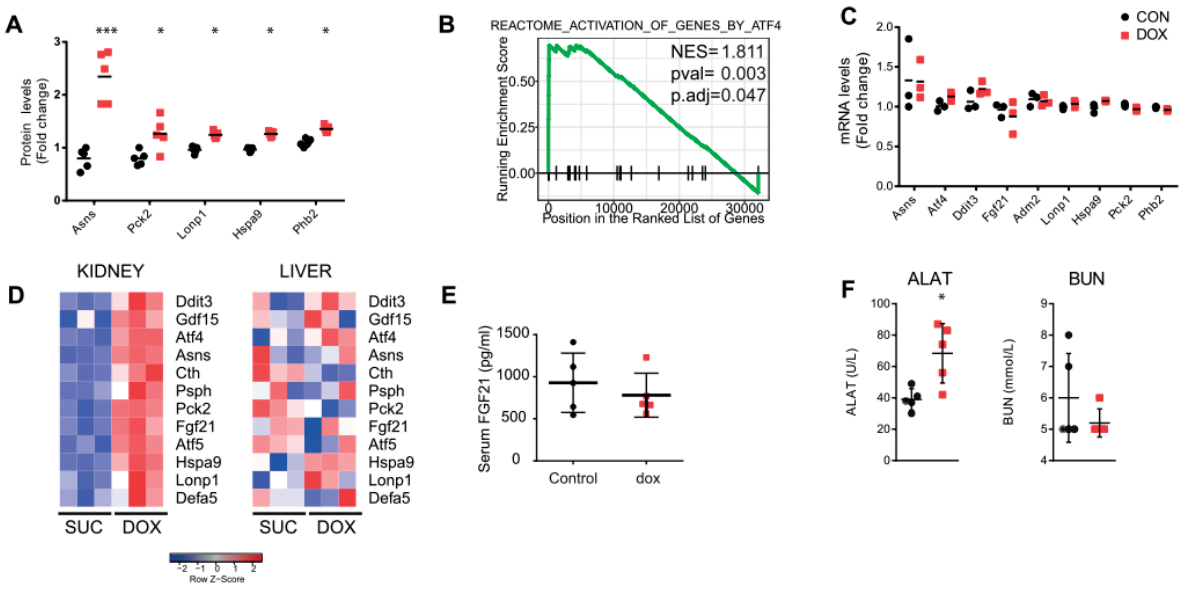

Supp. Figure 5.16

A. Proteomics measurements of ATF4 targets in kidney of germ-free mice. B. Enrichment of "Reactome_ACTIVATION_OF_GENES_BY_ATF4". C. mRNA levels of ATF4 targets in the liver of control and dox-treated germ-free mice analyzed by microarray. D. Heatmap displaying the gene expression of mammalian UPR^{mt} genes in kidney and liver. E. Serum levels of FGF21 in control and dox-treated germ-free mice. F. Plasma levels of alanine aminotransferase (ALAT) and blood urea nitrogen (BUN). Bars show mean±SD,* Student t-test p-value P≤0.05, **P≤0.01, *** P≤0.001.

Chapter 6 Conclusions and future perspectives

6.1 Results achieved

Beyond energy harvesting, mitochondria play a crucial role in cellular and organismal homeostasis. Therefore, proteostasis in mitochondria has to be closely monitored to ensure their optimal function. In my thesis project I investigated the signalling pathways activated by mitochondrial stress and in particular by the UPR^{mt} and studied their physiological impact.

In *C. elegans,* we screened for new members of the UPR^{mt} signalling. We identified the cytosolic poly(A)-binding protein *pab-1* as a novel regulator of mitochondrial stress and innate immunity. We demonstrated that *pab-1* is required for the resistance of nematodes to *P. aeruginosa* infection and that it requires *atfs-1*, the master regulator of UPR^{mt}, to regulate innate immunity. Using human transcriptomic data, we showed that the expression of immune genes correlates with that of *PABPC1*, the orthologue of *pab-1*, across multiple tissues. This suggests a conserved role of poly(A)-binding proteins in mammalian immunity and fuels optimism for future investigations in mammalian models to validate these findings.

In mice, we used the BXD GRP to explore the conservation of UPR^{mt} at the transcript and protein level. Using bioinformatics approaches, we found that the network of UPR^{mt} genes is tightly co-regulated in mice under normal physiological conditions. As a complementary approach, we investigated the physiological impact of mitochondrial stress triggered by treatment of mice with doxycycline (dox) either at the *adult* stage of their life or in the immediate *post-natal* period. Although dox impacts on mitochondrial proteostasis and oxygen consumption, our study did not report any dox-specific, long-term consequences on physiology and longevity.

Using multi-omics profiling of germ-free mice, we characterized the dox-induced mitochondrial stress response, as such controlling for any confounding influences of dox on the microbiota. We found that organs highly dependent on mitochondria show specific transcriptomic and proteomic signatures following dox treatment. Kidney displayed a general attenuation of metabolism and translation with the resulting activation of the ATF4 integrated stress response (ISR). Liver on the contrary

exhibited a remodelling of lipid metabolism with an activation of energy-producing pathways.

Taken together, my work demonstrates that mitochondrial stress leads to a multi-faceted response with commonly recurring themes like innate immunity and post-transcriptional regulation, across species, tissues and conditions.

6.2 Conclusions across projects

6.2.1 Mitochondrial stress and immunity

The major highlight of this thesis is that two different projects in evolutionary distant organisms (Chapter 3 and 5) independently unveiled an intimate interplay between mitochondrial stress and innate immunity. In *C. elegans*, several studies showed that bacterial infection triggers UPR^{mt} and that *atfs-1* participates in the resistance to infection (Liu et al., 2014; Pellegrino et al., 2014). Inversely, by comparing several mitochondrial stressors, we confirmed that the induction of innate immunity genes is a hallmark of mitochondrial stress response at the transcriptome level. We identified *pab-1* at the regulatory crossroad between these two responses, a role possibly conserved for human PABPC1. Investigating the crosstalk of *pab-1 w*ith well-defined immune pathways in *C. elegans* will help to identify the exact mechanism underlying our observations and guide future studies of the role its mammalian orthologues.

Also in germ-free mice, the type I IFN response was amongst the pathways commonly activated in liver and kidney upon treatment with the mitochondrial translation inhibitor and stressor, dox, and IRF7 is amongst the few commonly up-regulated genes (5.2.5), although further validation of this tantalizing observation is required. The cGAS-cGAMP-STING mtDNA-sensing pathway is known to be activated upon infection-induced release of mtDNA into the cytosol as a DAMP mechanism (West and Shadel, 2017). Recent studies however report cases, where physiological responses are driven by the sensing of mtDNA. In obese mice, mtDNA release upon high-fat diet feeding was shown to trigger cGAS-cGAMP-STING in adipose tissue (Bai et al., 2017). Inversely, overexpression of the DsbA-L chaperone-like protein in the mitochondrial matrix prevented mtDNA release and protected against obesity-induced inflammation. cGAS-cGAMP-STING signalling is also elicited by LOF of the mtDNA-binding protein TFAM (the transcription factor A, mitochondrial)(West et al., 2015). TFAM deficiency leads to moderate mtDNA

instability, as seen upon mitochondrial dysfunction linked to aging or various disorders. Future studies should characterize the exact trigger inducing cGAS-cGAMP-STING and type I interferon upon dox treatment in mice and whether it participates in a systemic signalling of mitochondrial stress. A possible mechanism could be an opening of mitochondrial membrane pores leading to mitochondrial permeability, as it was observed in some stress conditions such as ischemia/reperfusion injury (Halestrap and Richardson, 2015).

Due to their bacterial ancestry, mitochondria induce innate immunity and hence, a tight regulation of mitochondrial permeability and mitophagy participated in the evolution of the host tolerance to mitochondria (Rongvaux, 2017). Commonly, our study and these examples demonstrate that innate immune pathways conserved some reactivity towards mitochondria as a means to detect abnormal mitochondrial "behaviour". Reinterpreting and targeting the crosstalk between mitochondrial stress and innate immunity might allow a better understanding and novel therapeutic strategies for disorders, such as neurodegenerative and autoimmune diseases. It is furthermore tempting to speculate and interesting to explore whether the induction of type I interferon signalling plays a role in the bacteriostatic actions of antibiotic agents, such as doxycycline that inhibit mitochondrial translation.

6.2.2 Post-transcriptional and translational regulation

The studies reported in this thesis identified *pab-1* as the first RBP taking part in UPR^{mt} signalling. The regulation of mitochondrial stress responses and of the UPR^{mt} at the post-transcriptional and translational level remains poorly studied. However, as also observed in the renal response to dox (chapter 5), a block in translation is a common consequence of various types of stresses (D'Amico et al., 2017). Hence, pleiotropic mechanisms, extending beyond strict regulation of transcription, have to ensure the proper translation of specific mRNAs needed to cope with and resolve the stress, like the well-documented ATF4 response. In line with this premise, UPR^{mt} genes correlate in a much tighter manner in the BXD GRP at the protein level than at the level of mRNA. This indeed suggests that mechanisms at the post-transcriptional and/or translational level might account for the tighter correlation of the network at protein level (Figure 4.2).

Only few RBPs regulating mitochondrial protein expression have been characterized sofar (Jourdain et al., 2013; Jourdain et al., 2017; Schatton et al., 2017). However, ongoing research in our lab identified the worm and mouse orthologues of the yeast pumilio factor PUF3p as an important player in regulation of mitochondrial function (unplublished data). This RBP was shown to play pleiotropic roles in the regulation of mitochondrial biogenesis and proteins in *Saccharomyces cerevisiae* (Rowe et al., 2013; Tu et al., 2005). Therefore, it appears that post-transcriptional regulatory mechanism endorsed by RBPs shows a striking conservation across species.

Our studies on *pab-1* are another example of the conservation of post-transcriptional regulatory mechanisms governing mitochondrial and immune functions (Chapter 3). A recent study in *A. thaliana* described the binding of the plant *pab-1* orthologue PAB2 to A-rich sequences in stress-responsive mRNAs, which were preferentially translated upon immune challenge (Xu et al., 2017). Our data documented the influence of *pab-1* on transcript levels of immune and mitochondrial stress genes. However, the enrichment of an A-rich motif among *pab-1*-regulated mRNAs suggests that *pab-1* may regulate translation of mitochondrial stress and immune proteins, similar to plant PAB2. Alternatively, the binding by *pab-1* might also regulate mRNA stability (Figure 3.7B). Indeed, both liver and kidney transcript signatures upon dox treatment showed the enrichment of terms related to RNA metabolism, decay and stabilization (in orange in GSEA figures of chapter 5). Interestingly, liver transcript showed the enrichment for “Reactome_regulation_of_mRNA_stability_by_proteins_that_bind_AU_rich_elements ”, which contains Pabpc1, the mouse *pab-1* ortholog.

We therefore think that RBP-driven post-transcriptional/translational processes might constitute conserved regulatory mechanisms playing crucial, though poorly characterized, roles in the mitochondrial stress response. Thus, a promising strategy may lie in characterizing the translational signature caused by mitochondrial stress, using polysome profiling.

Finally, *pab-1* and its orthologues, from yeast to human, are well-documented members of stress granules. A recent study documented that aging and reduced fitness in *C. elegans* result from impaired stress granules dynamics (Lechler et al., 2017). PAB-1 and other stress granules RBPs contain low complexity regions

causing the formation of deleterious aggregates upon aging. Mitochondrial stress triggered by RNAi against the OXPHOS subunit *cyc-1* delayed the age-dependent aggregation of PAB-1 (Lechler et al., 2017). Along the same line, the induction of mitochondrial stress and mitophagy has recently been shown to impede the formation of β-amyloid aggregates in Alzheimer's disease (Sorrentino et al., 2017). Therefore, it may be relevant to explore whether *pab-1* takes part in mitophagy or in aggregate formation in the context of mitochondrial stress and neurodegeneration.

6.2.3 Evolution of the UPR^{mt} and the mitochondrial stress response

One of the initial goals of this thesis was to explore the conservation of the UPR^{mt} in mammals, where it is less extensively characterized than in *C.elegans*. Examining the liver transcript and protein levels of the mouse orthologues of the canonical UPR^{mt} in the BXD GRP supported a good co-regulation of this network in mammals (Chapter 4.1). In the organ-specific response to dox in germ-free mice, levels of *Hspa9* and *Lonp1* (orthologues of *hsp-6* and *lonp-1* respectively in worms), were clearly induced at the transcript and protein level. Other members of the mammalian UPR^{mt}, such as CHOP, ATF4, ATF5 and their targets were also robustly induced in the kidney, proving a conservation of this response. However, they were not changed in the liver, although modulation of numerous transcripts and proteins was clearly observed in this organ upon dox treatment. This therefore suggests that the signalling of UPR^{mt} might depend on multiple parameters such as timing of the response, the organ, the fasting/feeding state or perhaps even the age of the animal. We indeed cannot exclude, for example, that liver would also display a similar UPR^{mt} activation after a shorter or longer exposure or an exposure during a different developmental window to dox. One can also speculate that the UPR^{mt} and the mitochondrial stress response rather behave like a multi-arm response, the canonical UPR^{mt} being one arm more easily responsive in the kidney *in vivo* upon dox treatment. Although ATF5 has been proposed as the mammalian functional orthologue of *atfs-1* (Fiorese et al., 2016; Nargund et al., 2012), three additional transcription factors, i.e. ATF4, ATF5, CHOP, are already known to regulate the mammalian equivalent response. Therefore, this indicates that the mammalian response to mitochondrial stress probably evolved into a more complex and advanced version of the nematode UPR^{mt}.

Another conserved aspect of the mitochondrial stress response is its crosstalk with other proteostatic networks. We found that mitochondrial stress elicited by dox in germ-free mice induced the transcripts of the heat shock cytosolic and ER stress response in liver and kidney (5.2.5 and 5.2.7). In *C. elegans,* mitochondrial stress and UPR^{mt} are also coupled to the HSF-1-dependent activation of cytosolic chaperones (Kim et al., 2016; Matilainen et al., 2017b). This communication can be mediated by (1) an impaired balance of histone protein levels and the chromatin remodeling ISW-1 (Matilainen et al., 2017b) and (2) an accumulation in lipid and cardiolipin species (Kim et al., 2016). The need for lipid species to signal mitochondrial stress has already been reported. Ceramides are required for the role of UPR^{mt} in immune mitochondrial surveillance (Liu et al., 2014). Thus, the remodeling of lipid metabolism seen in liver after dox *in vivo* treatment could also potentially play a signalling role and be linked to the HSR and ER stress. Indeed, impaired balance of membrane phospholipids triggered by choline deficiency in cells, called “membrane stress response”, activated the UPR^{ER} and the cytosolic HSR (Thibault et al., 2012). Therefore, more in-depth lipidomics profiling of mitochondrial stresses may open new research avenues. To conclude, the interaction of the mitochondrial stress response with other proteostatic networks reflects that mitochondrial function impacts on multiple aspects of cellular homeostasis.

6.3 Perspectives

This thesis highlights the versatile and intricate nature of the response to mitochondrial stress and its interconnectivity with other well-documented pathways and processes. I therefore hope that my work contributes to mitigate the perception that the mitochondrial stress response should have a single definition across species and conditions. Indeed, the outcome and the set of players involved in it may highly depend on the organ, the developmental and energy status, the species, as well as many other parameters. Since mitochondria take part in multiple processes, future research should further consider the globality of the consequences of mitochondrial stress on the cell and the organism. Therefore, the use of omics technologies to monitor mitochondrial stress-driven modulations at multiple cellular and systemic levels, and in multiple conditions, will help characterizing and integrate trends that appear difficult to detect and explain in single contexts. In addition, studying the

implications of mitochondrial stress in pathological conditions might lead to important therapeutic advances.

List of abbreviations

AMPK	Adenosine monophosphate-activated protein kinase
ATF4	Activating transcription factor
ATFS-1	Activating transcription factor associated with stress 1
ATP	Adenosine triphosphate
BXD	recombinant inbred mouse cross (C57BL/6J x DBA/2J)
CD	chow diet
CHOP	C/EBP homologous protein
DAMP	Damage-associated molecular pattern
DAMP	Danger-associated molecular pattern
eIF2α	α subunit of eukaryotic translation initiation factor 2
ER	Endoplasmic reticulum
ESRE	Ethanol and Stress Response Element
ETC	Electron transport chain
FAO	Fatty acid oxidation
FAS	Fatty acid synthesis
FFA	Free fatty acid
GADD34	growth arrest and DNA damage-inducible protein
GCN2	General control non-derepressible 2
GFP	green fluorescent protein
GO	Gene ontology
GO BP	gene ontology biological process
GO CC	gene ontology cellular component
GRP	Genetic reference population
GSEA	Gene Set Enrichment Analysis
GWAS	genome-wide association study
HFD	high fat diet
HIF-1	Hypoxia-inducible factor 1
HSF	heat shock factor
HSR	heat shock response
IFN	interferon
ISR	Integrated stress response
JNK	c-Jun amino-terminal kinase
KD	knock-down
LOF	loss of function
MAPK	mitogen-activated protein kinase
MSEA	metabolite set enrichment analysis
mtDNA	mammalian mitochondrial DNA
mTOR	mammalian target of rapamycin
NADH	Nicotinamide adenine dinucleotide, reduced
ND75	NADH-ubiquinone oxidoreductase 75 kDa
nDNA	nuclear DNA
NFATc	Nuclear factor of activated T cells
NFE2L2/NRF2	Nuclear factor erythroid 2-related factor 2

NHR	Nuclear hormone receptor
NLP	Neuropeptide-like protein
NLR	NOD-like receptor
OXPHOS	Oxidative phosphorylation
p38 MAPK	p38 mitogen-activated protein kinase
PAB	Poly(A)-binding protein
PAMP	Pathogen-associated molecular pattern
PCA	Principal Component Analysis
PGSA	Population-level gene set analysis
PL	phospholipid
PPAR	Peroxisome proliferator-activated receptor
PQC	Protein quality control
PRR	Pattern recognition receptor
QTL	Quantitative trait locus
RBP	RNA-binding protein
RLRs	RIG-I-like receptors
RNAi	RNA interference
ROS	reactive oxygen species
RTG	Retrograde response genes
SKN-1	Skinhead-1
SNP	single nucleotide polymorphism
SRM	Selected reaction monitoring
SRM	selected reaction monitoring
SSBP1	Single-stranded DNA-binding protein 1
TCA cycle	tricarboxylic acid cycle
TF	Transcription factor
TFAM	Transcription factor A mitochondrial
TG	Triglyceride
TLR	Toll-like receptor
TNF	Tumour necrosis factor
TORC1	Target of rapamycin complex 1
TRIB3	Tribbles homolog 3
UPR^{ER}	Unfolded protein response of the endoplasmic reticulum
UPR^{mt}	mitochondrial unfolded protein response
WT	wild type

Curriculum Vitae

Adrienne Mottis
mottis.adrienne@hotmail.com
Chemin d'En-Perrey 30, CH-1616 Attalens

EDUCATION

Ph.D. in Biotechnology and Bioengineering, 2012-2017
Ecole Polytechnique Fédérale de Lausanne (CH)

Master in Life Sciences and Technology, Specialization in Molecular Medicine, 2010-2012
Ecole Polytechnique Fédérale de Lausanne (CH)

Bachelor of Science in Biochemistry, 2007-2010
Faculty of Science, University of Fribourg (CH)

Swiss Matriculation Certificate ("Biology-Chemistry", "Advanced mathematics"), 2003-2007
Collège du Sud, Bulle (CH)

RESEARCH EXPERIENCE

Doctoral thesis in Biotechnology and Bioengineering, since 2013

Title : "Mitochondrial stress signalling and its impacts on animal physiology"

Supervision by Prof. Johan Auwerx, in the Laboratory of Integrative Systems Physiology (LISP) Swiss Federal Institute of Technology (EPFL), Lausanne (Switzerland)

Mater thesis in Life Sciences and Technology, Specialization in Molecular Medicine, 2011-2012

Title : "Characterization of the role of *gei-8*, the *C.elegans* orthologue of NCoR1/SMRT co-repressors"

Supervision by Prof. Johan Auwerx, in the Laboratory of Integrative Systems Physiology (LISP) Swiss Federal Institute of Technology (EPFL), Lausanne (Switzerland)

> *Experimental work in the model organism C.elegans, with the initial aim of confirming the conservation of the role that NCoR/SMRT exerts on mammalian metabolism and mitochondrial regulation*

COMPLEMENTARY EXPERIENCES

EPFL, Course in Management of Innovation and Technology Transfer (MINTT), 2014

Accelerating training in the field of academic results industrialization, patenting, invention management, license negotiation, assessment of potential and start-up strategy evaluation.
Practical case study on a start-up from EPFL (confidential), supervised by Technology Transfer Office (TTO) of EPFL

EPFL, School of Life Sciences, 2011-2015

Assistantship and teaching:

- organization and teaching of exercises sessions for the course « Biological chemistry » to Bachelor students 2nd year (by Prof. Kristina Schoonjans), during 3 semesters
- teaching of Physiology practicals (by André Pexieder)
- supervision of a student group for a Project in Translational Biomedical research (by Prof. Johan Auwerx)
- ex-cathedra teaching for 1st student in "General Biology" course (by Prof. Johan Auwerx)

Diagnoplex SA, 2010-2011

Team work for Business strategy course, Collège des Humanités, EPFL

- analysis of the market, the statistics and current practice in colon cancer screening in Switzerland, complemented by interviews of stakeholders
- development of a strategy advice for the launching on the Swiss market of a molecular test for colon cancer screening

Program for International Student Assessment (PISA), Conference Intercantonale de l'Instruction Publique (Swiss office for public education), 2009

Administrator of test sessions in middle school classes in the Canton de Fribourg

AWARDS AND HONORS

Award for the best final average mark amongst students in MSc in Life Sciences and Technologies, 2012

EPFL, Lausanne (CH)

Award for the best master thesis amongst students in Molecular Medicine specialization (Master in Life Sciences and Technologies), 2012

EPFL, Lausanne (CH)

PUBLICATIONS

Mottis A., Mouchiroud L. and Auwerx J. (2013). Emerging roles of the corepressors NCoR1 and SMRT in homeostasis. Genes and Development.

Mouchiroud L, Houtkooper RH, Moullan N, Katsyuba E, Ryu D, Cantó C, Mottis A., Jo YS, Viswanathan M, Schoonjans K, Guarente L, Auwerx J. (2013). The NAD(+)/Sirtuin Pathway Modulates Longevity through Activation of Mitochondrial UPR and FOXO Signaling. Cell.

Andreux P.A., Mouchiroud L., Wang X., Jovaisaite V., Mottis A., Bichet S., Moullan N., Houtkooper, R.H., and Auwerx, J. (2014). A method to identify and validate mitochondrial modulators using mammalian cells and the worm C. elegans. Scientific reports.

Lo Sasso G, Menzies KJ*, Mottis A.*, Piersigilli A, Perino A, Yamamoto H, Schoonjans K, Auwerx J. (2014) SIRT2 deficiency modulates macrophage polarization and susceptibility to experimental colitis. Plos one.

Mottis A., Jovaisaite V. and Auwerx, J. (2014). The mitochondrial unfolded protein response in mammalian physiology. Mammalian genome.

Wu Y, Williams EG, Dubuis S, Mottis A, Jovaisaite V, Houten SM, Argmann CA, Faridi P, Wolski W, Kutalik Z, Zamboni N, Auwerx J, Aebersold R. (2014) Multilayered genetic and omics dissection of mitochondrial activity in a mouse reference population. Cell.

Moullan N., Mouchiroud L., Wang X., Ryu D., Williams E. G., Mottis A., Jovaisaite V., Frochaux M. V., Quiros P. M., Deplancke B., Houtkooper, R. H. and Auwerx J. (2015). Tetracyclines Disturb

Mitochondrial Function across Eukaryotic Models: A Call for Caution in Biomedical Research. Cell reports.

Quiros PM*, Mottis A* and Auwerx J. (2016). Mitonuclear communication in homeostasis and stress. Nature Reviews Molecular Cell Biology.

LANGUAGES

French
Native proficiency

English
Highly proficient (Level C1, Cambridge Certificate in Advanced English (CAE) in 2012)

German
Proficient verbal and especially written (Level B2, German-French Bachelor level from the bilingual Faculty of Sciences, Fribourg CH)

References

(1998). Genome sequence of the nematode C. elegans: a platform for investigating biology. Science *282*, 2012-2018.

Acin-Perez, R., Carrascoso, I., Baixauli, F., Roche-Molina, M., Latorre-Pellicer, A., Fernandez-Silva, P., Mittelbrunn, M., Sanchez-Madrid, F., Perez-Martos, A., Lowell, C.A.*, et al.* (2014). ROS-triggered phosphorylation of complex II by Fgr kinase regulates cellular adaptation to fuel use. Cell metabolism *19*, 1020-1033.

Akerfelt, M., Morimoto, R.I., and Sistonen, L. (2010). Heat shock factors: integrators of cell stress, development and lifespan. Nature reviews Molecular cell biology *11*, 545-555.

Al-Furoukh, N., Ianni, A., Nolte, H., Holper, S., Kruger, M., Wanrooij, S., and Braun, T. (2015). ClpX stimulates the mitochondrial unfolded protein response (UPRmt) in mammalian cells. Biochimica et biophysica acta *1853*, 2580-2591.

Albert, F.W., Treusch, S., Shockley, A.H., Bloom, J.S., and Kruglyak, L. (2014). Genetics of single-cell protein abundance variation in large yeast populations. Nature.

Aldridge, J.E., Horibe, T., and Hoogenraad, N.J. (2007). Discovery of genes activated by the mitochondrial unfolded protein response (mtUPR) and cognate promoter elements. PloS one *2*, e874.

Alper, S., McElwee, M.K., Apfeld, J., Lackford, B., Freedman, J.H., and Schwartz, D.A. (2010). The Caenorhabditis elegans germ line regulates distinct signaling pathways to control lifespan and innate immunity. The Journal of biological chemistry *285*, 1822-1828.

Amuthan, G., Biswas, G., Ananadatheerthavarada, H.K., Vijayasarathy, C., Shephard, H.M., and Avadhani, N.G. (2002). Mitochondrial stress-induced calcium signaling, phenotypic changes and invasive behavior in human lung carcinoma A549 cells. Oncogene *21*, 7839-7849.

Amuthan, G., Biswas, G., Zhang, S.Y., Klein-Szanto, A., Vijayasarathy, C., and Avadhani, N.G. (2001). Mitochondria-to-nucleus stress signaling induces phenotypic changes, tumor progression and cell invasion. The EMBO journal *20*, 1910-1920.

Anders, S., and Huber, W. (2010). Differential expression analysis for sequence count data. Genome biology *11*, R106.

Anderson, P., and Kedersha, N. (2006). RNA granules. The Journal of cell biology *172*, 803-808.

Andreux, P.A., Houtkooper, R.H., and Auwerx, J. (2013). Pharmacological approaches to restore mitochondrial function. Nature reviews Drug discovery *12*, 465-483.

Andreux, P.A., Williams, E.G., Koutnikova, H., Houtkooper, R.H., Champy, M.F., Henry, H., Schoonjans, K., Williams, R.W., and Auwerx, J. (2012). Systems genetics of metabolism: the

use of the BXD murine reference panel for multiscalar integration of traits. Cell *150*, 1287-1299.

Apfeld, J., O'Connor, G., McDonagh, T., DiStefano, P.S., and Curtis, R. (2004). The AMP-activated protein kinase AAK-2 links energy levels and insulin-like signals to lifespan in C. elegans. Genes & development *18*, 3004-3009.

Arnould, T., Vankoningsloo, S., Renard, P., Houbion, A., Ninane, N., Demazy, C., Remacle, J., and Raes, M. (2002). CREB activation induced by mitochondrial dysfunction is a new signaling pathway that impairs cell proliferation. The EMBO journal *21*, 53-63.

Arnoult, D., Soares, F., Tattoli, I., and Girardin, S.E. (2011). Mitochondria in innate immunity. EMBO reports *12*, 901-910.

Aupee, O., Almeras, D., Le Garlantezec, P., and Bohand, X. (2009). [Doxycycline]. Medecine tropicale : revue du Corps de sante colonial *69*, 556-558.

Bai, J., Cervantes, C., Liu, J., He, S., Zhou, H., Zhang, B., Cai, H., Yin, D., Hu, D., Li, Z.*, et al.* (2017). DsbA-L prevents obesity-induced inflammation and insulin resistance by suppressing the mtDNA release-activated cGAS-cGAMP-STING pathway. Proceedings of the National Academy of Sciences of the United States of America *114*, 12196-12201.

Baixauli, F., Acin-Perez, R., Villarroya-Beltri, C., Mazzeo, C., Nunez-Andrade, N., Gabande-Rodriguez, E., Ledesma, M.D., Blazquez, A., Martin, M.A., Falcon-Perez, J.M.*, et al.* (2015). Mitochondrial Respiration Controls Lysosomal Function during Inflammatory T Cell Responses. Cell metabolism *22*, 485-498.

Baker, B.M., Nargund, A.M., Sun, T., and Haynes, C.M. (2012). Protective coupling of mitochondrial function and protein synthesis via the eIF2alpha kinase GCN-2. PLoS genetics *8*, e1002760.

Battle, A., Brown, C.D., Engelhardt, B.E., and Montgomery, S.B. (2017). Genetic effects on gene expression across human tissues. Nature *550*, 204-213.

Benedetti, C., Haynes, C.M., Yang, Y., Harding, H.P., and Ron, D. (2006). Ubiquitin-like protein 5 positively regulates chaperone gene expression in the mitochondrial unfolded protein response. Genetics *174*, 229-239.

Berchtold, N.C., Cribbs, D.H., Coleman, P.D., Rogers, J., Head, E., Kim, R., Beach, T., Miller, C., Troncoso, J., Trojanowski, J.Q.*, et al.* (2008). Gene expression changes in the course of normal brain aging are sexually dimorphic. Proceedings of the National Academy of Sciences of the United States of America *105*, 15605-15610.

Biswas, G., Adebanjo, O.A., Freedman, B.D., Anandatheerthavarada, H.K., Vijayasarathy, C., Zaidi, M., Kotlikoff, M., and Avadhani, N.G. (1999). Retrograde Ca2+ signaling in C2C12 skeletal myocytes in response to mitochondrial genetic and metabolic stress: a novel mode of inter-organelle crosstalk. The EMBO journal *18*, 522-533.

Biswas, G., Anandatheerthavarada, H.K., Zaidi, M., and Avadhani, N.G. (2003). Mitochondria to nucleus stress signaling: a distinctive mechanism of NFkappaB/Rel activation through calcineurin-mediated inactivation of IkappaBbeta. The Journal of cell biology *161*, 507-519.

Bligh, E.G., and Dyer, W.J. (1959). A rapid method of total lipid extraction and purification. Canadian journal of biochemistry and physiology *37*, 911-917.

Blobel, G. (1973). A protein of molecular weight 78,000 bound to the polyadenylate region of eukaryotic messenger RNAs. Proceedings of the National Academy of Sciences of the United States of America *70*, 924-928.

Brenner, S. (1974). The genetics of Caenorhabditis elegans. Genetics *77*, 71-94.

Bretscher, A.J., Busch, K.E., and de Bono, M. (2008). A carbon dioxide avoidance behavior is integrated with responses to ambient oxygen and food in Caenorhabditis elegans. Proceedings of the National Academy of Sciences of the United States of America *105*, 8044-8049.

Bruning, A., Brem, G.J., Vogel, M., and Mylonas, I. (2014). Tetracyclines cause cell stress-dependent ATF4 activation and mTOR inhibition. Experimental cell research *320*, 281-289.

Caballero, A., Ugidos, A., Liu, B., Oling, D., Kvint, K., Hao, X., Mignat, C., Nachin, L., Molin, M., and Nystrom, T. (2011). Absence of mitochondrial translation control proteins extends life span by activating sirtuin-dependent silencing. Molecular cell *42*, 390-400.

Callister, S.J., Barry, R.C., Adkins, J.N., Johnson, E.T., Qian, W.J., Webb-Robertson, B.J., Smith, R.D., and Lipton, M.S. (2006). Normalization approaches for removing systematic biases associated with mass spectrometry and label-free proteomics. Journal of proteome research *5*, 277-286.

Chae, S., Ahn, B.Y., Byun, K., Cho, Y.M., Yu, M.H., Lee, B., Hwang, D., and Park, K.S. (2013). A systems approach for decoding mitochondrial retrograde signaling pathways. Science signaling *6*, rs4.

Chen, Q., Sun, L., and Chen, Z.J. (2016). Regulation and function of the cGAS-STING pathway of cytosolic DNA sensing. Nature immunology *17*, 1142-1149.

Chen, X.L., and Kunsch, C. (2004). Induction of cytoprotective genes through Nrf2/antioxidant response element pathway: a new therapeutic approach for the treatment of inflammatory diseases. Current pharmaceutical design *10*, 879-891.

Chin, R.M., Fu, X., Pai, M.Y., Vergnes, L., Hwang, H., Deng, G., Diep, S., Lomenick, B., Meli, V.S., Monsalve, G.C.*, et al.* (2014). The metabolite alpha-ketoglutarate extends lifespan by inhibiting ATP synthase and TOR. Nature *510*, 397-401.

Cho, I., and Blaser, M.J. (2012). The human microbiome: at the interface of health and disease. Nature reviews Genetics *13*, 260-270.

Cho, I., Yamanishi, S., Cox, L., Methe, B.A., Zavadil, J., Li, K., Gao, Z., Mahana, D., Raju, K., Teitler, I.*, et al.* (2012). Antibiotics in early life alter the murine colonic microbiome and adiposity. Nature *488*, 621-626.

Chung, H.K., Ryu, D., Kim, K.S., Chang, J.Y., Kim, Y.K., Yi, H.S., Kang, S.G., Choi, M.J., Lee, S.E., Jung, S.B.*, et al.* (2017). Growth differentiation factor 15 is a myomitokine governing systemic energy homeostasis. The Journal of cell biology *216*, 149-165.

Clark-Walker, G.D., and Linnane, A.W. (1966). In vivo differentiation of yeast cytoplasmic and mitochondrial protein synthesis with antibiotics. Biochemical and biophysical research communications *25*, 8-13.

Cohen, L.B., and Troemel, E.R. (2015). Microbial pathogenesis and host defense in the nematode C. elegans. Current opinion in microbiology *23*, 94-101.

Corsi, A.K., Wightman, B., and Chalfie, M. (2015). A Transparent window into biology: A primer on Caenorhabditis elegans. WormBook : the online review of C elegans biology, 1-31.

Curtis, R., O'Connor, G., and DiStefano, P.S. (2006). Aging networks in Caenorhabditis elegans: AMP-activated protein kinase (aak-2) links multiple aging and metabolism pathways. Aging cell *5*, 119-126.

D'Amico, D., Sorrentino, V., and Auwerx, J. (2017). Cytosolic Proteostasis Networks of the Mitochondrial Stress Response. Trends in biochemical sciences *42*, 712-725.

De Luca, M., Roshina, N.V., Geiger-Thornsberry, G.L., Lyman, R.F., Pasyukova, E.G., and Mackay, T.F. (2003). Dopa decarboxylase (Ddc) affects variation in Drosophila longevity. Nature genetics *34*, 429-433.

Deeb, S.S., Fajas, L., Nemoto, M., Pihlajamaki, J., Mykkanen, L., Kuusisto, J., Laakso, M., Fujimoto, W., and Auwerx, J. (1998). A Pro12Ala substitution in PPARgamma2 associated with decreased receptor activity, lower body mass index and improved insulin sensitivity. Nature genetics *20*, 284-287.

Ding, L., Quinlan, K.B., Elliott, W.M., Hamodat, M., Pare, P.D., Hogg, J.C., and Hayashi, S. (2004). A lung tissue bank for gene expression studies in chronic obstructive pulmonary disease. Copd *1*, 191-204.

Dogan, S.A., Pujol, C., Maiti, P., Kukat, A., Wang, S., Hermans, S., Senft, K., Wibom, R., Rugarli, E.I., and Trifunovic, A. (2014). Tissue-specific loss of DARS2 activates stress responses independently of respiratory chain deficiency in the heart. Cell metabolism *19*, 458-469.

Donnelly, N., Gorman, A.M., Gupta, S., and Samali, A. (2013). The eIF2alpha kinases: their structures and functions. Cellular and molecular life sciences : CMLS *70*, 3493-3511.

Dunbar, T.L., Yan, Z., Balla, K.M., Smelkinson, M.G., and Troemel, E.R. (2012). C. elegans detects pathogen-induced translational inhibition to activate immune signaling. Cell host & microbe *11*, 375-386.

Durieux, J., Wolff, S., and Dillin, A. (2011a). The cell-non-autonomous nature of electron transport chain-mediated longevity. Cell *144*, 79-91.

Durieux, J., Wolff, S., and Dillin, A. (2011b). The cell-non-autonomous nature of electron transport chain-mediated longevity. Cell *144*, 79-91.

Durinck, S., Moreau, Y., Kasprzyk, A., Davis, S., De Moor, B., Brazma, A., and Huber, W. (2005). BioMart and Bioconductor: a powerful link between biological databases and microarray data analysis. Bioinformatics *21*, 3439-3440.

Edwards, C.B., Copes, N., Brito, A.G., Canfield, J., and Bradshaw, P.C. (2013). Malate and fumarate extend lifespan in Caenorhabditis elegans. PloS one *8*, e58345.

Egan, D.F., Shackelford, D.B., Mihaylova, M.M., Gelino, S., Kohnz, R.A., Mair, W., Vasquez, D.S., Joshi, A., Gwinn, D.M., Taylor, R.*, et al.* (2011). Phosphorylation of ULK1 (hATG1) by AMP-activated protein kinase connects energy sensing to mitophagy. Science *331*, 456-461.

Engelmann, I., and Pujol, N. (2010). Innate immunity in C. elegans. Advances in experimental medicine and biology *708*, 105-121.

Ermolaeva, M.A., Segref, A., Dakhovnik, A., Ou, H.L., Schneider, J.I., Utermohlen, O., Hoppe, T., and Schumacher, B. (2013). DNA damage in germ cells induces an innate immune response that triggers systemic stress resistance. Nature *501*, 416-420.

Evans, E.A., Kawli, T., and Tan, M.W. (2008). Pseudomonas aeruginosa suppresses host immunity by activating the DAF-2 insulin-like signaling pathway in Caenorhabditis elegans. PLoS pathogens *4*, e1000175.

Evstafieva, A.G., Garaeva, A.A., Khutornenko, A.A., Klepikova, A.V., Logacheva, M.D., Penin, A.A., Novakovsky, G.E., Kovaleva, I.E., and Chumakov, P.M. (2014). A sustained deficiency of mitochondrial respiratory complex III induces an apoptotic cell death through the p53-mediated inhibition of pro-survival activities of the activating transcription factor 4. Cell death & disease *5*, e1511.

Ewbank, J.J., and Pujol, N. (2016). Local and long-range activation of innate immunity by infection and damage in C. elegans. Current opinion in immunology *38*, 1-7.

Fiorese, C.J., Schulz, A.M., Lin, Y.F., Rosin, N., Pellegrino, M.W., and Haynes, C.M. (2016). The Transcription Factor ATF5 Mediates a Mammalian Mitochondrial UPR. Current biology : CB *26*, 2037-2043.

Flamand, M.N., Wu, E., Vashisht, A., Jannot, G., Keiper, B.D., Simard, M.J., Wohlschlegel, J., and Duchaine, T.F. (2016). Poly(A)-binding proteins are required for microRNA-mediated silencing and to promote target deadenylation in C. elegans. Nucleic acids research *44*, 5924-5935.

Formentini, L., Sanchez-Arago, M., Sanchez-Cenizo, L., and Cuezva, J.M. (2012). The mitochondrial ATPase inhibitory factor 1 triggers a ROS-mediated retrograde prosurvival and proliferative response. Molecular cell *45*, 731-742.

Foster, J.A., and McVey Neufeld, K.A. (2013). Gut-brain axis: how the microbiome influences anxiety and depression. Trends in neurosciences *36*, 305-312.

Foster, L.J., de Hoog, C.L., Zhang, Y., Zhang, Y., Xie, X., Mootha, V.K., and Mann, M. (2006). A mammalian organelle map by protein correlation profiling. Cell *125*, 187-199.

Friedman, J.R., and Nunnari, J. (2014). Mitochondrial form and function. Nature *505*, 335-343.

Friis, R.M., Glaves, J.P., Huan, T., Li, L., Sykes, B.D., and Schultz, M.C. (2014). Rewiring AMPK and mitochondrial retrograde signaling for metabolic control of aging and histone acetylation in respiratory-defective cells. Cell reports *7*, 565-574.

Fritsch, S.D., and Weichhart, T. (2016). Effects of Interferons and Viruses on Metabolism. Frontiers in immunology *7*, 630.

Fuhrer, T., Heer, D., Begemann, B., and Zamboni, N. (2011). High-throughput, accurate mass metabolome profiling of cellular extracts by flow injection-time-of-flight mass spectrometry. Analytical chemistry *83*, 7074-7080.

Gallo, M., Park, D., and Riddle, D.L. (2011). Increased longevity of some C. elegans mitochondrial mutants explained by activation of an alternative energy-producing pathway. Mechanisms of ageing and development *132*, 515-518.

Garcia-Roves, P.M., Osler, M.E., Holmstrom, M.H., and Zierath, J.R. (2008). Gain-of-function R225Q mutation in AMP-activated protein kinase gamma3 subunit increases mitochondrial

biogenesis in glycolytic skeletal muscle. The Journal of biological chemistry *283*, 35724-35734.

Gariani, K., Menzies, K.J., Ryu, D., Wegner, C.J., Wang, X., Ropelle, E.R., Moullan, N., Zhang, H., Perino, A., Lemos, V.*, et al.* (2015). Eliciting the mitochondrial unfolded protein response via NAD repletion reverses fatty liver disease. Hepatology.

Garsin, D.A., Villanueva, J.M., Begun, J., Kim, D.H., Sifri, C.D., Calderwood, S.B., Ruvkun, G., and Ausubel, F.M. (2003). Long-lived C. elegans daf-2 mutants are resistant to bacterial pathogens. Science *300*, 1921.

Ghazalpour, A., Bennett, B., Petyuk, V.A., Orozco, L., Hagopian, R., Mungrue, I.N., Farber, C.R., Sinsheimer, J., Kang, H.M., Furlotte, N.*, et al.* (2011). Comparative analysis of proteome and transcriptome variation in mouse. PLoS Genet *7*, e1001393.

Gilbert, W.V., Zhou, K., Butler, T.K., and Doudna, J.A. (2007). Cap-independent translation is required for starvation-induced differentiation in yeast. Science *317*, 1224-1227.

Guha, M., Fang, J.K., Monks, R., Birnbaum, M.J., and Avadhani, N.G. (2010). Activation of Akt is essential for the propagation of mitochondrial respiratory stress signaling and activation of the transcriptional coactivator heterogeneous ribonucleoprotein A2. Molecular biology of the cell *21*, 3578-3589.

Gygi, S.P., Rochon, Y., Franza, B.R., and Aebersold, R. (1999). Correlation between protein and mRNA abundance in yeast. Molecular and cellular biology *19*, 1720-1730.

Halestrap, A.P., and Richardson, A.P. (2015). The mitochondrial permeability transition: a current perspective on its identity and role in ischaemia/reperfusion injury. Journal of molecular and cellular cardiology *78*, 129-141.

Harding, H.P., Novoa, I., Zhang, Y., Zeng, H., Wek, R., Schapira, M., and Ron, D. (2000). Regulated translation initiation controls stress-induced gene expression in mammalian cells. Molecular cell *6*, 1099-1108.

Harding, H.P., Zhang, Y., Zeng, H., Novoa, I., Lu, P.D., Calfon, M., Sadri, N., Yun, C., Popko, B., Paules, R.*, et al.* (2003). An integrated stress response regulates amino acid metabolism and resistance to oxidative stress. Molecular cell *11*, 619-633.

Haynes, C.M., Fiorese, C.J., and Lin, Y.F. (2013). Evaluating and responding to mitochondrial dysfunction: the mitochondrial unfolded-protein response and beyond. Trends Cell Biol *23*, 311-318.

Haynes, C.M., Petrova, K., Benedetti, C., Yang, Y., and Ron, D. (2007). ClpP mediates activation of a mitochondrial unfolded protein response in C. elegans. Developmental cell *13*, 467-480.

Haynes, C.M., Yang, Y., Blais, S.P., Neubert, T.A., and Ron, D. (2010). The matrix peptide exporter HAF-1 signals a mitochondrial UPR by activating the transcription factor ZC376.7 in C. elegans. Molecular cell *37*, 529-540.

Hedgecock, E.M., Sulston, J.E., and Thomson, J.N. (1983). Mutations affecting programmed cell deaths in the nematode Caenorhabditis elegans. Science *220*, 1277-1279.

Heeren, G., Rinnerthaler, M., Laun, P., von Seyerl, P., Kossler, S., Klinger, H., Hager, M., Bogengruber, E., Jarolim, S., Simon-Nobbe, B.*, et al.* (2009). The mitochondrial ribosomal

protein of the large subunit, Afo1p, determines cellular longevity through mitochondrial back-signaling via TOR1. Aging *1*, 622-636.

Holdt, L.M., von Delft, A., Nicolaou, A., Baumann, S., Kostrzewa, M., Thiery, J., and Teupser, D. (2013). Quantitative trait loci mapping of the mouse plasma proteome (pQTL). Genetics *193*, 601-608.

Horibe, T., and Hoogenraad, N.J. (2007). The chop gene contains an element for the positive regulation of the mitochondrial unfolded protein response. PloS one *2*, e835.

Houtkooper, R.H., Mouchiroud, L., Ryu, D., Moullan, N., Katsyuba, E., Knott, G., Williams, R.W., and Auwerx, J. (2013). Mitonuclear protein imbalance as a conserved longevity mechanism. Nature *497*, 451-457.

Hsin, H., and Kenyon, C. (1999). Signals from the reproductive system regulate the lifespan of C. elegans. Nature *399*, 362-366.

Huang da, W., Sherman, B.T., and Lempicki, R.A. (2009). Systematic and integrative analysis of large gene lists using DAVID bioinformatics resources. Nature protocols *4*, 44-57.

Hwang, A.B., Ryu, E.A., Artan, M., Chang, H.W., Kabir, M.H., Nam, H.J., Lee, D., Yang, J.S., Kim, S., Mair, W.B.*, et al.* (2014). Feedback regulation via AMPK and HIF-1 mediates ROS-dependent longevity in Caenorhabditis elegans. Proceedings of the National Academy of Sciences of the United States of America *111*, E4458-4467.

Ihmels, J., Friedlander, G., Bergmann, S., Sarig, O., Ziv, Y., and Barkai, N. (2002). Revealing modular organization in the yeast transcriptional network. Nature genetics *31*, 370-377.

Inoue, H., Hisamoto, N., An, J.H., Oliveira, R.P., Nishida, E., Blackwell, T.K., and Matsumoto, K. (2005). The C. elegans p38 MAPK pathway regulates nuclear localization of the transcription factor SKN-1 in oxidative stress response. Genes & development *19*, 2278-2283.

Irazoqui, J.E., Urbach, J.M., and Ausubel, F.M. (2010). Evolution of host innate defence: insights from Caenorhabditis elegans and primitive invertebrates. Nature reviews Immunology *10*, 47-58.

Itoh, H., and Srere, P.A. (1970). A new assay for glutamate-oxaloacetate transaminase. Analytical biochemistry *35*, 405-410.

Jackson, R.J., Hellen, C.U., and Pestova, T.V. (2010). The mechanism of eukaryotic translation initiation and principles of its regulation. Nature reviews Molecular cell biology *11*, 113-127.

Jazwinski, S.M. (2013). The retrograde response: when mitochondrial quality control is not enough. Biochimica et biophysica acta *1833*, 400-409.

Jazwinski, S.M., and Kriete, A. (2012). The yeast retrograde response as a model of intracellular signaling of mitochondrial dysfunction. Frontiers in physiology *3*, 139.

Jin, S.M., and Youle, R.J. (2013). The accumulation of misfolded proteins in the mitochondrial matrix is sensed by PINK1 to induce PARK2/Parkin-mediated mitophagy of polarized mitochondria. Autophagy *9*, 1750-1757.

Jones, J.D., and Dangl, J.L. (2006). The plant immune system. Nature *444*, 323-329.

Jourdain, A.A., Koppen, M., Wydro, M., Rodley, C.D., Lightowlers, R.N., Chrzanowska-Lightowlers, Z.M., and Martinou, J.C. (2013). GRSF1 regulates RNA processing in mitochondrial RNA granules. Cell metabolism *17*, 399-410.

Jourdain, A.A., Popow, J., de la Fuente, M.A., Martinou, J.C., Anderson, P., and Simarro, M. (2017). The FASTK family of proteins: emerging regulators of mitochondrial RNA biology. Nucleic acids research *45*, 10941-10947.

Jovaisaite, V., Mouchiroud, L., and Auwerx, J. (2014). The mitochondrial unfolded protein response, a conserved stress response pathway with implications in health and disease. The Journal of experimental biology *217*, 137-143.

Kaletta, T., and Hengartner, M.O. (2006). Finding function in novel targets: C. elegans as a model organism. Nature reviews Drug discovery *5*, 387-398.

Kamath, R.S., and Ahringer, J. (2003). Genome-wide RNAi screening in Caenorhabditis elegans. Methods *30*, 313-321.

Kamath, R.S., Martinez-Campos, M., Zipperlen, P., Fraser, A.G., and Ahringer, J. (2001). Effectiveness of specific RNA-mediated interference through ingested double-stranded RNA in Caenorhabditis elegans. Genome biology *2*, RESEARCH0002.

Kanehisa, M., Goto, S., Hattori, M., Aoki-Kinoshita, K.F., Itoh, M., Kawashima, S., Katayama, T., Araki, M., and Hirakawa, M. (2006). From genomics to chemical genomics: new developments in KEGG. Nucleic acids research *34*, D354-357.

Karpievitch, Y.V., Dabney, A.R., and Smith, R.D. (2012). Normalization and missing value imputation for label-free LC-MS analysis. BMC Bioinformatics *13 Suppl 16*, S5.

Kenyon, C.J. (2010). The genetics of ageing. Nature *464*, 504-512.

Khan, N.A., Auranen, M., Paetau, I., Pirinen, E., Euro, L., Forsstrom, S., Pasila, L., Velagapudi, V., Carroll, C.J., Auwerx, J.*, et al.* (2014). Effective treatment of mitochondrial myopathy by nicotinamide riboside, a vitamin B3. EMBO molecular medicine *6*, 721-731.

Khan, Z., Ford, M.J., Cusanovich, D.A., Mitrano, A., Pritchard, J.K., and Gilad, Y. (2013). Primate transcript and protein expression levels evolve under compensatory selection pressures. Science *342*, 1100-1104.

Kim, H.E., Grant, A.R., Simic, M.S., Kohnz, R.A., Nomura, D.K., Durieux, J., Riera, C.E., Sanchez, M., Kapernick, E., Wolff, S.*, et al.* (2016). Lipid Biosynthesis Coordinates a Mitochondrial-to-Cytosolic Stress Response. Cell *166*, 1539-1552 e1516.

Kini, H.K., Silverman, I.M., Ji, X., Gregory, B.D., and Liebhaber, S.A. (2016). Cytoplasmic poly(A) binding protein-1 binds to genomically encoded sequences within mammalian mRNAs. Rna *22*, 61-74.

Kirienko, N.V., Ausubel, F.M., and Ruvkun, G. (2015). Mitophagy confers resistance to siderophore-mediated killing by Pseudomonas aeruginosa. Proceedings of the National Academy of Sciences of the United States of America *112*, 1821-1826.

Kirienko, N.V., Cezairliyan, B.O., Ausubel, F.M., and Powell, J.R. (2014). Pseudomonas aeruginosa PA14 pathogenesis in Caenorhabditis elegans. Methods Mol Biol *1149*, 653-669.

Kirienko, N.V., and Fay, D.S. (2010). SLR-2 and JMJC-1 regulate an evolutionarily conserved stress-response network. The EMBO journal *29*, 727-739.

Kirienko, N.V., Kirienko, D.R., Larkins-Ford, J., Wahlby, C., Ruvkun, G., and Ausubel, F.M. (2013). Pseudomonas aeruginosa disrupts Caenorhabditis elegans iron homeostasis, causing a hypoxic response and death. Cell host & microbe *13*, 406-416.

Ko, S., Kawasaki, I., and Shim, Y.H. (2013). PAB-1, a Caenorhabditis elegans poly(A)-binding protein, regulates mRNA metabolism in germline by interacting with CGH-1 and CAR-1. PloS one *8*, e84798.

Kohler, F., Muller-Rischart, A.K., Conradt, B., and Rolland, S.G. (2015). The loss of LRPPRC function induces the mitochondrial unfolded protein response. Aging *7*, 701-717.

Kops, G.J., Dansen, T.B., Polderman, P.E., Saarloos, I., Wirtz, K.W., Coffer, P.J., Huang, T.T., Bos, J.L., Medema, R.H., and Burgering, B.M. (2002). Forkhead transcription factor FOXO3a protects quiescent cells from oxidative stress. Nature *419*, 316-321.

Krahenbuhl, S., Talos, C., Fischer, S., and Reichen, J. (1994). Toxicity of bile acids on the electron transport chain of isolated rat liver mitochondria. Hepatology *19*, 471-479.

Lange, V., Picotti, P., Domon, B., and Aebersold, R. (2008). Selected reaction monitoring for quantitative proteomics: a tutorial. Molecular systems biology *4*, 222.

Lechler, M.C., Crawford, E.D., Groh, N., Widmaier, K., Jung, R., Kirstein, J., Trinidad, J.C., Burlingame, A.L., and David, D.C. (2017). Reduced Insulin/IGF-1 Signaling Restores the Dynamic Properties of Key Stress Granule Proteins during Aging. Cell reports *18*, 454-467.

Lee, R.C., Feinbaum, R.L., and Ambros, V. (1993). The C. elegans heterochronic gene lin-4 encodes small RNAs with antisense complementarity to lin-14. Cell *75*, 843-854.

Lee, S.J., Hwang, A.B., and Kenyon, C. (2010). Inhibition of respiration extends C. elegans life span via reactive oxygen species that increase HIF-1 activity. Current biology : CB *20*, 2131-2136.

Lemaitre, B., and Girardin, S.E. (2013). Translation inhibition and metabolic stress pathways in the host response to bacterial pathogens. Nature reviews Microbiology *11*, 365-369.

Lerner, C., Bitto, A., Pulliam, D., Nacarelli, T., Konigsberg, M., Van Remmen, H., Torres, C., and Sell, C. (2013). Reduced mammalian target of rapamycin activity facilitates mitochondrial retrograde signaling and increases life span in normal human fibroblasts. Aging cell *12*, 966-977.

Liberati, N.T., Fitzgerald, K.A., Kim, D.H., Feinbaum, R., Golenbock, D.T., and Ausubel, F.M. (2004). Requirement for a conserved Toll/interleukin-1 resistance domain protein in the Caenorhabditis elegans immune response. Proceedings of the National Academy of Sciences of the United States of America *101*, 6593-6598.

Lim, J.H., Lee, J.I., Suh, Y.H., Kim, W., Song, J.H., and Jung, M.H. (2006). Mitochondrial dysfunction induces aberrant insulin signalling and glucose utilisation in murine C2C12 myotube cells. Diabetologia *49*, 1924-1936.

Lin, K., Hsin, H., Libina, N., and Kenyon, C. (2001). Regulation of the Caenorhabditis elegans longevity protein DAF-16 by insulin/IGF-1 and germline signaling. Nature genetics *28*, 139-145.

Liu, Y., Samuel, B.S., Breen, P.C., and Ruvkun, G. (2014). Caenorhabditis elegans pathways that surveil and defend mitochondria. Nature *508*, 406-410.

Liu, Z., and Butow, R.A. (2006). Mitochondrial retrograde signaling. Annual review of genetics *40*, 159-185.

Lu, W., Chen, Z., Zhang, H., Wang, Y., Luo, Y., and Huang, P. (2012). ZNF143 transcription factor mediates cell survival through upregulation of the GPX1 activity in the mitochondrial respiratory dysfunction. Cell death & disease *3*, e422.

Luo, Y., Bond, J.D., and Ingram, V.M. (1997). Compromised mitochondrial function leads to increased cytosolic calcium and to activation of MAP kinases. Proceedings of the National Academy of Sciences of the United States of America *94*, 9705-9710.

Ma, S., Bhattacharjee, R.B., and Bag, J. (2009). Expression of poly(A)-binding protein is upregulated during recovery from heat shock in HeLa cells. The FEBS journal *276*, 552-570.

Mangus, D.A., Evans, M.C., and Jacobson, A. (2003). Poly(A)-binding proteins: multifunctional scaffolds for the post-transcriptional control of gene expression. Genome biology *4*, 223.

Manzanillo, P.S., Ayres, J.S., Watson, R.O., Collins, A.C., Souza, G., Rae, C.S., Schneider, D.S., Nakamura, K., Shiloh, M.U., and Cox, J.S. (2013). The ubiquitin ligase parkin mediates resistance to intracellular pathogens. Nature *501*, 512-516.

Marsh, E.K., and May, R.C. (2012). Caenorhabditis elegans, a model organism for investigating immunity. Applied and environmental microbiology *78*, 2075-2081.

Martinez-Reyes, I., Sanchez-Arago, M., and Cuezva, J.M. (2012). AMPK and GCN2-ATF4 signal the repression of mitochondria in colon cancer cells. The Biochemical journal *444*, 249-259.

Matilainen, O., Quiros, P.M., and Auwerx, J. (2017a). Mitochondria and Epigenetics - Crosstalk in Homeostasis and Stress. Trends in cell biology *27*, 453-463.

Matilainen, O., Sleiman, M.S.B., Quiros, P.M., Garcia, S., and Auwerx, J. (2017b). The chromatin remodeling factor ISW-1 integrates organismal responses against nuclear and mitochondrial stress. Nature communications *8*, 1818.

McEwan, D.L., Kirienko, N.V., and Ausubel, F.M. (2012). Host translational inhibition by Pseudomonas aeruginosa Exotoxin A Triggers an immune response in Caenorhabditis elegans. Cell host & microbe *11*, 364-374.

Melo, J.A., and Ruvkun, G. (2012). Inactivation of conserved C. elegans genes engages pathogen- and xenobiotic-associated defenses. Cell *149*, 452-466.

Mercer, T.R., Neph, S., Dinger, M.E., Crawford, J., Smith, M.A., Shearwood, A.M., Haugen, E., Bracken, C.P., Rackham, O., Stamatoyannopoulos, J.A.*, et al.* (2011). The human mitochondrial transcriptome. Cell *146*, 645-658.

Merkwirth, C., Jovaisaite, V., Durieux, J., Matilainen, O., Jordan, S.D., Quiros, P.M., Steffen, K.K., Williams, E.G., Mouchiroud, L., Tronnes, S.U.*, et al.* (2016). Two Conserved Histone Demethylases Regulate Mitochondrial Stress-Induced Longevity. Cell *165*, 1209-1223.

Michel, S., Canonne, M., Arnould, T., and Renard, P. (2015). Inhibition of mitochondrial genome expression triggers the activation of CHOP-10 by a cell signaling dependent on the integrated stress response but not the mitochondrial unfolded protein response. Mitochondrion *21*, 58-68.

Mills, E.L., Kelly, B., and O'Neill, L.A.J. (2017). Mitochondria are the powerhouses of immunity. Nature immunology *18*, 488-498.

Miyadera, H., Amino, H., Hiraishi, A., Taka, H., Murayama, K., Miyoshi, H., Sakamoto, K., Ishii, N., Hekimi, S., and Kita, K. (2001). Altered quinone biosynthesis in the long-lived clk-1 mutants of Caenorhabditis elegans. The Journal of biological chemistry *276*, 7713-7716.

Mohrin, M., Shin, J., Liu, Y., Brown, K., Luo, H., Xi, Y., Haynes, C.M., and Chen, D. (2015). Stem cell aging. A mitochondrial UPR-mediated metabolic checkpoint regulates hematopoietic stem cell aging. Science *347*, 1374-1377.

Moisoi, N., Klupsch, K., Fedele, V., East, P., Sharma, S., Renton, A., Plun-Favreau, H., Edwards, R.E., Teismann, P., Esposti, M.D.*, et al.* (2009). Mitochondrial dysfunction triggered by loss of HtrA2 results in the activation of a brain-specific transcriptional stress response. Cell death and differentiation *16*, 449-464.

Monaghan, R.M., Barnes, R.G., Fisher, K., Andreou, T., Rooney, N., Poulin, G.B., and Whitmarsh, A.J. (2015). A nuclear role for the respiratory enzyme CLK-1 in regulating mitochondrial stress responses and longevity. Nature cell biology *17*, 782-792.

Monks, S.A., Leonardson, A., Zhu, H., Cundiff, P., Pietrusiak, P., Edwards, S., Phillips, J.W., Sachs, A., and Schadt, E.E. (2004). Genetic inheritance of gene expression in human cell lines. American journal of human genetics *75*, 1094-1105.

Mottis, A., Jovaisaite, V., and Auwerx, J. (2014). The mitochondrial unfolded protein response in mammalian physiology. Mammalian genome : official journal of the International Mammalian Genome Society.

Mouchiroud, L., Houtkooper, R.H., Moullan, N., Katsyuba, E., Ryu, D., Canto, C., Mottis, A., Jo, Y.S., Viswanathan, M., Schoonjans, K.*, et al.* (2013). The NAD(+)/Sirtuin Pathway Modulates Longevity through Activation of Mitochondrial UPR and FOXO Signaling. Cell *154*, 430-441.

Moullan, N., Mouchiroud, L., Wang, X., Ryu, D., Williams, E.G., Mottis, A., Jovaisaite, V., Frochaux, M.V., Quiros, P.M., Deplancke, B.*, et al.* (2015). Tetracyclines Disturb Mitochondrial Function across Eukaryotic Models: A Call for Caution in Biomedical Research. Cell reports.

Munch, C., and Harper, J.W. (2016). Mitochondrial unfolded protein response controls matrix pre-RNA processing and translation. Nature *534*, 710-713.

Nargund, A.M., Fiorese, C.J., Pellegrino, M.W., Deng, P., and Haynes, C.M. (2015). Mitochondrial and nuclear accumulation of the transcription factor ATFS-1 promotes OXPHOS recovery during the UPR(mt). Molecular cell *58*, 123-133.

Nargund, A.M., Pellegrino, M.W., Fiorese, C.J., Baker, B.M., and Haynes, C.M. (2012). Mitochondrial import efficiency of ATFS-1 regulates mitochondrial UPR activation. Science *337*, 587-590.

Nasif, S., Contu, L., and Muhlemann, O. (2017). Beyond quality control: The role of nonsense-mediated mRNA decay (NMD) in regulating gene expression. Seminars in cell & developmental biology.

Newton, K., and Dixit, V.M. (2012). Signaling in innate immunity and inflammation. Cold Spring Harbor perspectives in biology *4*.

Nguyen, T., Nioi, P., and Pickett, C.B. (2009). The Nrf2-antioxidant response element signaling pathway and its activation by oxidative stress. The Journal of biological chemistry *284*, 13291-13295.

Novoa, I., Zeng, H., Harding, H.P., and Ron, D. (2001). Feedback inhibition of the unfolded protein response by GADD34-mediated dephosphorylation of eIF2alpha. The Journal of cell biology *153*, 1011-1022.

Ohoka, N., Yoshii, S., Hattori, T., Onozaki, K., and Hayashi, H. (2005). TRB3, a novel ER stress-inducible gene, is induced via ATF4-CHOP pathway and is involved in cell death. The EMBO journal *24*, 1243-1255.

Oka, T., Hikoso, S., Yamaguchi, O., Taneike, M., Takeda, T., Tamai, T., Oyabu, J., Murakawa, T., Nakayama, H., Nishida, K.*, et al.* (2012). Mitochondrial DNA that escapes from autophagy causes inflammation and heart failure. Nature *485*, 251-255.

Owusu-Ansah, E., Song, W., and Perrimon, N. (2013). Muscle mitohormesis promotes longevity via systemic repression of insulin signaling. Cell *155*, 699-712.

Owusu-Ansah, E., Yavari, A., Mandal, S., and Banerjee, U. (2008). Distinct mitochondrial retrograde signals control the G1-S cell cycle checkpoint. Nature genetics *40*, 356-361.

Pagliarini, D.J., Calvo, S.E., Chang, B., Sheth, S.A., Vafai, S.B., Ong, S.E., Walford, G.A., Sugiana, C., Boneh, A., Chen, W.K.*, et al.* (2008). A mitochondrial protein compendium elucidates complex I disease biology. Cell *134*, 112-123.

Palam, L.R., Baird, T.D., and Wek, R.C. (2011). Phosphorylation of eIF2 facilitates ribosomal bypass of an inhibitory upstream ORF to enhance CHOP translation. The Journal of biological chemistry *286*, 10939-10949.

Papa, L., and Germain, D. (2014). SirT3 regulates the mitochondrial unfolded protein response. Molecular and cellular biology *34*, 699-710.

Papp, D., Csermely, P., and Soti, C. (2012). A role for SKN-1/Nrf in pathogen resistance and immunosenescence in Caenorhabditis elegans. PLoS pathogens *8*, e1002673.

Pellegrino, M.W., Nargund, A.M., Kirienko, N.V., Gillis, R., Fiorese, C.J., and Haynes, C.M. (2014). Mitochondrial UPR-regulated innate immunity provides resistance to pathogen infection. Nature *516*, 414-417.

Petrasek, J., Iracheta-Vellve, A., Csak, T., Satishchandran, A., Kodys, K., Kurt-Jones, E.A., Fitzgerald, K.A., and Szabo, G. (2013). STING-IRF3 pathway links endoplasmic reticulum stress with hepatocyte apoptosis in early alcoholic liver disease. Proceedings of the National Academy of Sciences of the United States of America *110*, 16544-16549.

Picotti, P., Clement-Ziza, M., Lam, H., Campbell, D.S., Schmidt, A., Deutsch, E.W., Rost, H., Sun, Z., Rinner, O., Reiter, L.*, et al.* (2013). A complete mass-spectrometric map of the yeast proteome applied to quantitative trait analysis. Nature *494*, 266-270.

Picotti, P., Rinner, O., Stallmach, R., Dautel, F., Farrah, T., Domon, B., Wenschuh, H., and Aebersold, R. (2010). High-throughput generation of selected reaction-monitoring assays for proteins and proteomes. Nature methods *7*, 43-46.

Pimenta de Castro, I., Costa, A.C., Lam, D., Tufi, R., Fedele, V., Moisoi, N., Dinsdale, D., Deas, E., Loh, S.H., and Martins, L.M. (2012). Genetic analysis of mitochondrial protein misfolding in Drosophila melanogaster. Cell death and differentiation *19*, 1308-1316.

Pirinen, E., Canto, C., Jo, Y.S., Morato, L., Zhang, H., Menzies, K.J., Williams, E.G., Mouchiroud, L., Moullan, N., Hagberg, C*., et al.* (2014). Pharmacological Inhibition of poly(ADP-ribose) polymerases improves fitness and mitochondrial function in skeletal muscle. Cell metabolism *19*, 1034-1041.

Pradel, E., Zhang, Y., Pujol, N., Matsuyama, T., Bargmann, C.I., and Ewbank, J.J. (2007). Detection and avoidance of a natural product from the pathogenic bacterium Serratia marcescens by Caenorhabditis elegans. Proceedings of the National Academy of Sciences of the United States of America *104*, 2295-2300.

Priess, J.R., Schnabel, H., and Schnabel, R. (1987). The glp-1 locus and cellular interactions in early C. elegans embryos. Cell *51*, 601-611.

Quiros, P.M., Langer, T., and Lopez-Otin, C. (2015). New roles for mitochondrial proteases in health, ageing and disease. Nature reviews Molecular cell biology *16*, 345-359.

Quiros, P.M., Mottis, A., and Auwerx, J. (2016). Mitonuclear communication in homeostasis and stress. Nature reviews Molecular cell biology *17*, 213-226.

Quiros, P.M., Prado, M.A., Zamboni, N., D'Amico, D., Williams, R.W., Finley, D., Gygi, S.P., and Auwerx, J. (2017). Multi-omics analysis identifies ATF4 as a key regulator of the mitochondrial stress response in mammals. The Journal of cell biology *216*, 2027-2045.

Rainbolt, T.K., Atanassova, N., Genereux, J.C., and Wiseman, R.L. (2013). Stress-Regulated Translational Attenuation Adapts Mitochondrial Protein Import through Tim17A Degradation. Cell metabolism *18*, 908-919.

Ramot, D., Johnson, B.E., Berry, T.L., Jr., Carnell, L., and Goodman, M.B. (2008). The Parallel Worm Tracker: a platform for measuring average speed and drug-induced paralysis in nematodes. PloS one *3*, e2208.

Rath, E., Berger, E., Messlik, A., Nunes, T., Liu, B., Kim, S.C., Hoogenraad, N., Sans, M., Sartor, R.B., and Haller, D. (2012). Induction of dsRNA-activated protein kinase links mitochondrial unfolded protein response to the pathogenesis of intestinal inflammation. Gut *61*, 1269-1278.

Reddy, K.C., Dunbar, T.L., Nargund, A.M., Haynes, C.M., and Troemel, E.R. (2016). The C. elegans CCAAT-Enhancer-Binding Protein Gamma Is Required for Surveillance Immunity. Cell reports *14*, 1581-1589.

Riback, J.A., Katanski, C.D., Kear-Scott, J.L., Pilipenko, E.V., Rojek, A.E., Sosnick, T.R., and Drummond, D.A. (2017). Stress-Triggered Phase Separation Is an Adaptive, Evolutionarily Tuned Response. Cell *168*, 1028-1040 e1019.

Richardson, C.E., Kooistra, T., and Kim, D.H. (2010). An essential role for XBP-1 in host protection against immune activation in C. elegans. Nature *463*, 1092-1095.

Ritchie, M.E., Phipson, B., Wu, D., Hu, Y., Law, C.W., Shi, W., and Smyth, G.K. (2015). limma powers differential expression analyses for RNA-sequencing and microarray studies. Nucleic acids research *43*, e47.

Rizzuto, R., De Stefani, D., Raffaello, A., and Mammucari, C. (2012). Mitochondria as sensors and regulators of calcium signalling. Nature reviews Molecular cell biology *13*, 566-578.

Rongvaux, A. (2017). Innate immunity and tolerance toward mitochondria. Mitochondrion.

Rowe, W., Kershaw, C.J., Castelli, L.M., Costello, J.L., Ashe, M.P., Grant, C.M., Sims, P.F., Pavitt, G.D., and Hubbard, S.J. (2013). Puf3p induces translational repression of genes linked to oxidative stress. Nucleic acids research.

Rowlett, R.M., Chrestensen, C.A., Schroeder, M.J., Harp, M.G., Pelo, J.W., Shabanowitz, J., DeRose, R., Hunt, D.F., Sturgill, T.W., and Worthington, M.T. (2008). Inhibition of tristetraprolin deadenylation by poly(A) binding protein. American journal of physiology Gastrointestinal and liver physiology *295*, G421-430.

Runkel, E.D., Liu, S., Baumeister, R., and Schulze, E. (2013). Surveillance-activated defenses block the ROS-induced mitochondrial unfolded protein response. PLoS genetics *9*, e1003346.

Rustin, P., Chretien, D., Bourgeron, T., LeBidois, J., Sidi, D., Rotig, A., and Munnich, A. (1993). Investigation of respiratory chain activity in human heart. Biochemical medicine and metabolic biology *50*, 120-126.

Ryu, D., Jo, Y.S., Lo Sasso, G., Stein, S., Zhang, H., Perino, A., Lee, J.U., Zeviani, M., Romand, R., Hottiger, M.O.*, et al.* (2014). A SIRT7-dependent acetylation switch of GABPbeta1 controls mitochondrial function. Cell metabolism *20*, 856-869.

Schadt, E.E., Molony, C., Chudin, E., Hao, K., Yang, X., Lum, P.Y., Kasarskis, A., Zhang, B., Wang, S., Suver, C.*, et al.* (2008). Mapping the genetic architecture of gene expression in human liver. PLoS Biol *6*, e107.

Schatton, D., Pla-Martin, D., Marx, M.C., Hansen, H., Mourier, A., Nemazanyy, I., Pessia, A., Zentis, P., Corona, T., Kondylis, V.*, et al.* (2017). CLUH regulates mitochondrial metabolism by controlling translation and decay of target mRNAs. The Journal of cell biology *216*, 675-693.

Schieber, M., and Chandel, N.S. (2014). ROS function in redox signaling and oxidative stress. Current biology : CB *24*, R453-462.

Schmeisser, S., Schmeisser, K., Weimer, S., Groth, M., Priebe, S., Fazius, E., Kuhlow, D., Pick, D., Einax, J.W., Guthke, R.*, et al.* (2013). Mitochondrial hormesis links low-dose arsenite exposure to lifespan extension. Aging cell *12*, 508-517.

Schwanhausser, B., Busse, D., Li, N., Dittmar, G., Schuchhardt, J., Wolf, J., Chen, W., and Selbach, M. (2011). Global quantification of mammalian gene expression control. Nature *473*, 337-342.

Sekito, T., Thornton, J., and Butow, R.A. (2000). Mitochondria-to-nuclear signaling is regulated by the subcellular localization of the transcription factors Rtg1p and Rtg3p. Molecular biology of the cell *11*, 2103-2115.

Shadel, G.S., and Horvath, T.L. (2015). Mitochondrial ROS Signaling in Organismal Homeostasis. Cell *163*, 560-569.

Shi, S.Y., Lu, S.Y., Sivasubramaniyam, T., Revelo, X.S., Cai, E.P., Luk, C.T., Schroer, S.A., Patel, P., Kim, R.H., Bombardier, E.*, et al.* (2015). DJ-1 links muscle ROS production with metabolic reprogramming and systemic energy homeostasis in mice. Nature communications *6*, 7415.

Shivers, R.P., Youngman, M.J., and Kim, D.H. (2008). Transcriptional responses to pathogens in Caenorhabditis elegans. Current opinion in microbiology *11*, 251-256.

Shpilka, T., and Haynes, C.M. (2017). The mitochondrial UPR: mechanisms, physiological functions and implications in ageing. Nature reviews Molecular cell biology.

Siegelin, M.D., Dohi, T., Raskett, C.M., Orlowski, G.M., Powers, C.M., Gilbert, C.A., Ross, A.H., Plescia, J., and Altieri, D.C. (2011). Exploiting the mitochondrial unfolded protein response for cancer therapy in mice and human cells. The Journal of clinical investigation *121*, 1349-1360.

Silva, J.M., Wong, A., Carelli, V., and Cortopassi, G.A. (2009). Inhibition of mitochondrial function induces an integrated stress response in oligodendroglia. Neurobiology of disease *34*, 357-365.

Singh, V., and Aballay, A. (2006). Heat-shock transcription factor (HSF)-1 pathway required for Caenorhabditis elegans immunity. Proceedings of the National Academy of Sciences of the United States of America *103*, 13092-13097.

Skelly, D.A., Merrihew, G.E., Riffle, M., Connelly, C.F., Kerr, E.O., Johansson, M., Jaschob, D., Graczyk, B., Shulman, N.J., Wakefield, J.*, et al.* (2013). Integrative phenomics reveals insight into the structure of phenotypic diversity in budding yeast. Genome research *23*, 1496-1504.

Sladic, R.T., Lagnado, C.A., Bagley, C.J., and Goodall, G.J. (2004). Human PABP binds AU-rich RNA via RNA-binding domains 3 and 4. European journal of biochemistry / FEBS *271*, 450-457.

Smith, J.A., Turner, M.J., DeLay, M.L., Klenk, E.I., Sowders, D.P., and Colbert, R.A. (2008). Endoplasmic reticulum stress and the unfolded protein response are linked to synergistic IFN-beta induction via X-box binding protein 1. European journal of immunology *38*, 1194-1203.

Smith, R.W., Blee, T.K., and Gray, N.K. (2014). Poly(A)-binding proteins are required for diverse biological processes in metazoans. Biochemical Society transactions *42*, 1229-1237.

Song, M., Mihara, K., Chen, Y., Scorrano, L., and Dorn, G.W., 2nd (2015). Mitochondrial fission and fusion factors reciprocally orchestrate mitophagic culling in mouse hearts and cultured fibroblasts. Cell metabolism *21*, 273-285.

Sorrentino, V., Romani, M., Mouchiroud, L., Beck, J.S., Zhang, H., D'Amico, D., Moullan, N., Potenza, F., Schmid, A.W., Rietsch, S.*, et al.* (2017). Enhancing mitochondrial proteostasis reduces amyloid-beta proteotoxicity. Nature.

Srinivasan, S., Guha, M., Dong, D.W., Whelan, K.A., Ruthel, G., Uchikado, Y., Natsugoe, S., Nakagawa, H., and Avadhani, N.G. (2015). Disruption of cytochrome c oxidase function induces the Warburg effect and metabolic reprogramming. Oncogene.

Sulston, J.E., and Horvitz, H.R. (1977). Post-embryonic cell lineages of the nematode, Caenorhabditis elegans. Developmental biology *56*, 110-156.

Tan, K., Fujimoto, M., Takii, R., Takaki, E., Hayashida, N., and Nakai, A. (2015). Mitochondrial SSBP1 protects cells from proteotoxic stresses by potentiating stress-induced HSF1 transcriptional activity. Nature communications *6*, 6580.

Tan, W.Q., Wang, K., Lv, D.Y., and Li, P.F. (2008). Foxo3a inhibits cardiomyocyte hypertrophy through transactivating catalase. The Journal of biological chemistry *283*, 29730-29739.

Tang, H., and Pang, S. (2016). Proline Catabolism Modulates Innate Immunity in Caenorhabditis elegans. Cell reports *17*, 2837-2844.

Teske, B.F., Fusakio, M.E., Zhou, D., Shan, J., McClintick, J.N., Kilberg, M.S., and Wek, R.C. (2013). CHOP induces activating transcription factor 5 (ATF5) to trigger apoptosis in response to perturbations in protein homeostasis. Molecular biology of the cell *24*, 2477-2490.

Thibault, G., Shui, G., Kim, W., McAlister, G.C., Ismail, N., Gygi, S.P., Wenk, M.R., and Ng, D.T. (2012). The membrane stress response buffers lethal effects of lipid disequilibrium by reprogramming the protein homeostasis network. Molecular cell *48*, 16-27.

Tjahjono, E., and Kirienko, N.V. (2017). A conserved mitochondrial surveillance pathway is required for defense against Pseudomonas aeruginosa. PLoS genetics *13*, e1006876.

Troemel, E.R., Chu, S.W., Reinke, V., Lee, S.S., Ausubel, F.M., and Kim, D.H. (2006). p38 MAPK regulates expression of immune response genes and contributes to longevity in C. elegans. PLoS genetics *2*, e183.

Tu, B.P., Kudlicki, A., Rowicka, M., and McKnight, S.L. (2005). Logic of the yeast metabolic cycle: temporal compartmentalization of cellular processes. Science *310*, 1152-1158.

Viader, A., Sasaki, Y., Kim, S., Strickland, A., Workman, C.S., Yang, K., Gross, R.W., and Milbrandt, J. (2013). Aberrant Schwann cell lipid metabolism linked to mitochondrial deficits leads to axon degeneration and neuropathy. Neuron *77*, 886-898.

Wallace, D.C. (2009). Mitochondria, bioenergetics, and the epigenome in eukaryotic and human evolution. Cold Spring Harbor symposia on quantitative biology *74*, 383-393.

Wang, D., Malo, D., and Hekimi, S. (2010). Elevated mitochondrial reactive oxygen species generation affects the immune response via hypoxia-inducible factor-1alpha in long-lived Mclk1+/- mouse mutants. J Immunol *184*, 582-590.

Wang, D., Wang, Y., Argyriou, C., Carriere, A., Malo, D., and Hekimi, S. (2012). An enhanced immune response of Mclk1(+)/(-) mutant mice is associated with partial protection from fibrosis, cancer and the development of biomarkers of aging. PloS one *7*, e49606.

Wang, X., and Chen, X.J. (2015). A cytosolic network suppressing mitochondria-mediated proteostatic stress and cell death. Nature *524*, 481-484.

West, A.P., Brodsky, I.E., Rahner, C., Woo, D.K., Erdjument-Bromage, H., Tempst, P., Walsh, M.C., Choi, Y., Shadel, G.S., and Ghosh, S. (2011). TLR signalling augments macrophage bactericidal activity through mitochondrial ROS. Nature *472*, 476-480.

West, A.P., Khoury-Hanold, W., Staron, M., Tal, M.C., Pineda, C.M., Lang, S.M., Bestwick, M., Duguay, B.A., Raimundo, N., MacDuff, D.A*., et al.* (2015). Mitochondrial DNA stress primes the antiviral innate immune response. Nature *520*, 553-557.

West, A.P., and Shadel, G.S. (2017). Mitochondrial DNA in innate immune responses and inflammatory pathology. Nature reviews Immunology *17*, 363-375.

Wolff, S., Weissman, J.S., and Dillin, A. (2014). Differential scales of protein quality control. Cell *157*, 52-64.

Woods, A., Dickerson, K., Heath, R., Hong, S.P., Momcilovic, M., Johnstone, S.R., Carlson, M., and Carling, D. (2005). Ca2+/calmodulin-dependent protein kinase kinase-beta acts upstream of AMP-activated protein kinase in mammalian cells. Cell metabolism *2*, 21-33.

Wrobel, L., Topf, U., Bragoszewski, P., Wiese, S., Sztolsztener, M.E., Oeljeklaus, S., Varabyova, A., Lirski, M., Chroscicki, P., Mroczek, S*., et al.* (2015). Mistargeted mitochondrial proteins activate a proteostatic response in the cytosol. Nature *524*, 485-488.

Wu, D., Sanin, D.E., Everts, B., Chen, Q., Qiu, J., Buck, M.D., Patterson, A., Smith, A.M., Chang, C.H., Liu, Z*., et al.* (2016). Type 1 Interferons Induce Changes in Core Metabolism that Are Critical for Immune Function. Immunity *44*, 1325-1336.

Wu, H., Kanatous, S.B., Thurmond, F.A., Gallardo, T., Isotani, E., Bassel-Duby, R., and Williams, R.S. (2002). Regulation of mitochondrial biogenesis in skeletal muscle by CaMK. Science *296*, 349-352.

Wu, Y., Williams, E.G., and Aebersold, R. (2017). Application of SWATH Proteomics to Mouse Biology. Current protocols in mouse biology *7*, 130-143.

Wu, Y., Williams, E.G., Dubuis, S., Mottis, A., Jovaisaite, V., Houten, S.M., Argmann, C.A., Faridi, P., Wolski, W., Kutalik, Z*., et al.* (2014). Multilayered genetic and omics dissection of mitochondrial activity in a mouse reference population. Cell *158*, 1415-1430.

Xu, G., Greene, G.H., Yoo, H., Liu, L., Marques, J., Motley, J., and Dong, X. (2017). Global translational reprogramming is a fundamental layer of immune regulation in plants. Nature *545*, 487-490.

Yamamoto, H., Williams, E.G., Mouchiroud, L., Canto, C., Fan, W., Downes, M., Heligon, C., Barish, G.D., Desvergne, B., Evans, R.M*., et al.* (2011). NCoR1 is a conserved physiological modulator of muscle mass and oxidative function. Cell *147*, 827-839.

Yates, S.P., Jorgensen, R., Andersen, G.R., and Merrill, A.R. (2006). Stealth and mimicry by deadly bacterial toxins. Trends in biochemical sciences *31*, 123-133.

Yoneda, T., Benedetti, C., Urano, F., Clark, S.G., Harding, H.P., and Ron, D. (2004). Compartment-specific perturbation of protein handling activates genes encoding mitochondrial chaperones. Journal of cell science *117*, 4055-4066.

Yu, G., Wang, L.G., Han, Y., and He, Q.Y. (2012). clusterProfiler: an R package for comparing biological themes among gene clusters. Omics : a journal of integrative biology *16*, 284-287.

Yvert, G., Brem, R.B., Whittle, J., Akey, J.M., Foss, E., Smith, E.N., Mackelprang, R., and Kruglyak, L. (2003). Trans-acting regulatory variation in Saccharomyces cerevisiae and the role of transcription factors. Nature genetics *35*, 57-64.

Zarse, K., Schmeisser, S., Groth, M., Priebe, S., Beuster, G., Kuhlow, D., Guthke, R., Platzer, M., Kahn, C.R., and Ristow, M. (2012). Impaired insulin/IGF1 signaling extends life span by promoting mitochondrial L-proline catabolism to induce a transient ROS signal. Cell metabolism *15*, 451-465.

Zhang, Y., Lu, H., and Bargmann, C.I. (2005). Pathogenic bacteria induce aversive olfactory learning in Caenorhabditis elegans. Nature *438*, 179-184.

Zhao, Q., Wang, J., Levichkin, I.V., Stasinopoulos, S., Ryan, M.T., and Hoogenraad, N.J. (2002). A mitochondrial specific stress response in mammalian cells. The EMBO journal *21*, 4411-4419.

Zou, C.G., Ma, Y.C., Dai, L.L., and Zhang, K.Q. (2014). Autophagy protects C. elegans against necrosis during Pseudomonas aeruginosa infection. Proceedings of the National Academy of Sciences of the United States of America *111*, 12480-12485.

Annexes

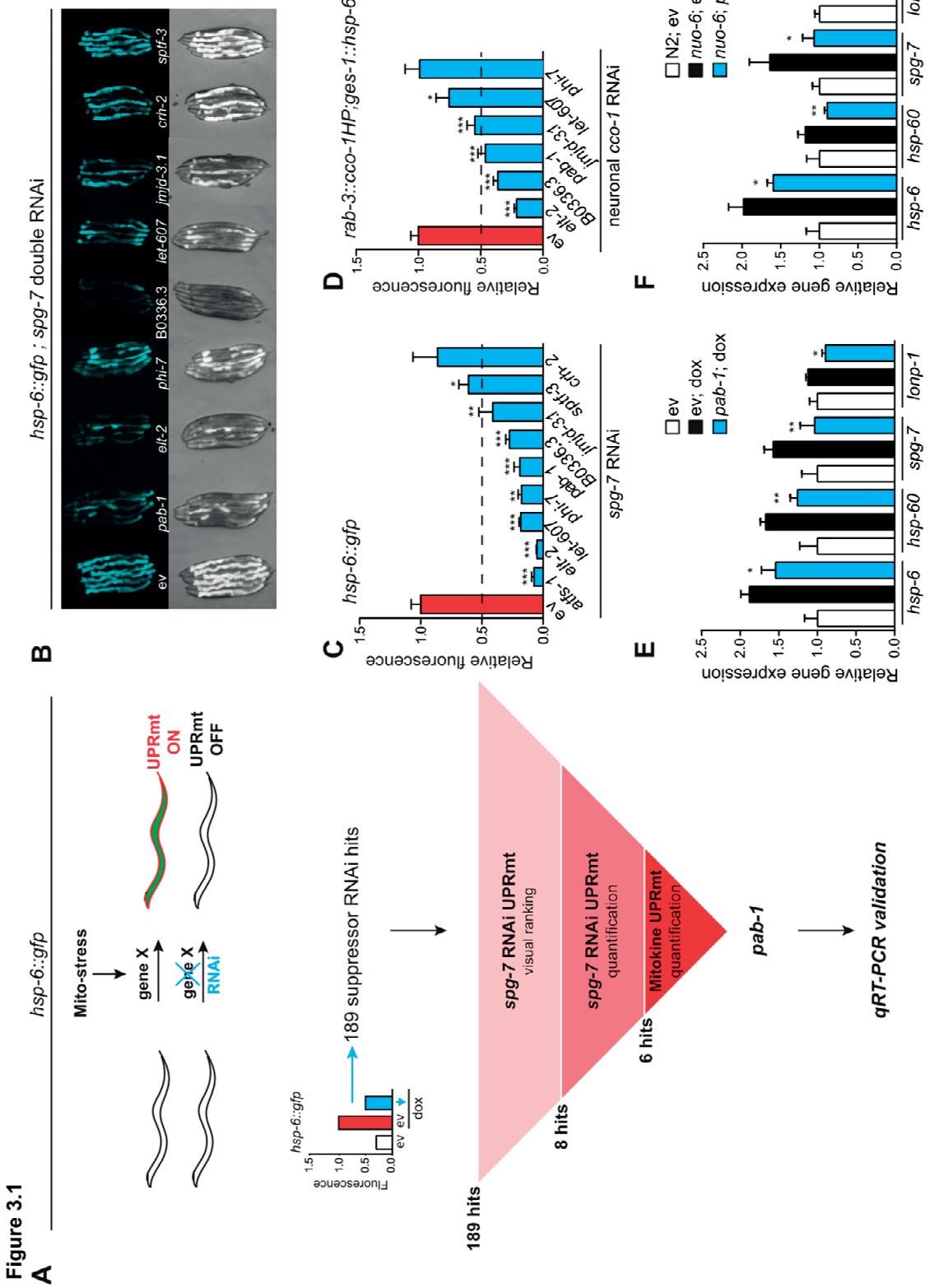
Figure 3.1
A
hsp-6::gfp
Mito-stress
gene X
gene X
RNAi
UPRmt ON
UPRmt OFF
hsp-6::gfp
Fluorescence
ev
ev
dox
189 suppressor RNAi hits
189 hits
spg-7 RNAi UPRmt
visual ranking
8 hits
spg-7 RNAi UPRmt
quantification
6 hits
Mitokine UPRmt
quantification
pab-1
qRT-PCR validation
B
hsp-6::gfp ; spg-7 double RNAi
ev
pab-1
elt-2
phi-7
B0336.3
let-607
jmjd-3.1
crh-2
sptf-3
C
hsp-6::gfp
Relative fluorescence
spg-7 RNAi
D
rab-3::cco-1HP;ges-1::hsp-6::gfp
Relative fluorescence
neuronal cco-1 RNAi
E
ev
ev; dox
pab-1; dox
Relative gene expression
hsp-6
hsp-60
spg-7
lonp-1
F
N2; ev
nuo-6; ev
nuo-6; pab-1
Relative gene expression
hsp-6
hsp-60
spg-7
lonp-1

Figure 3.3

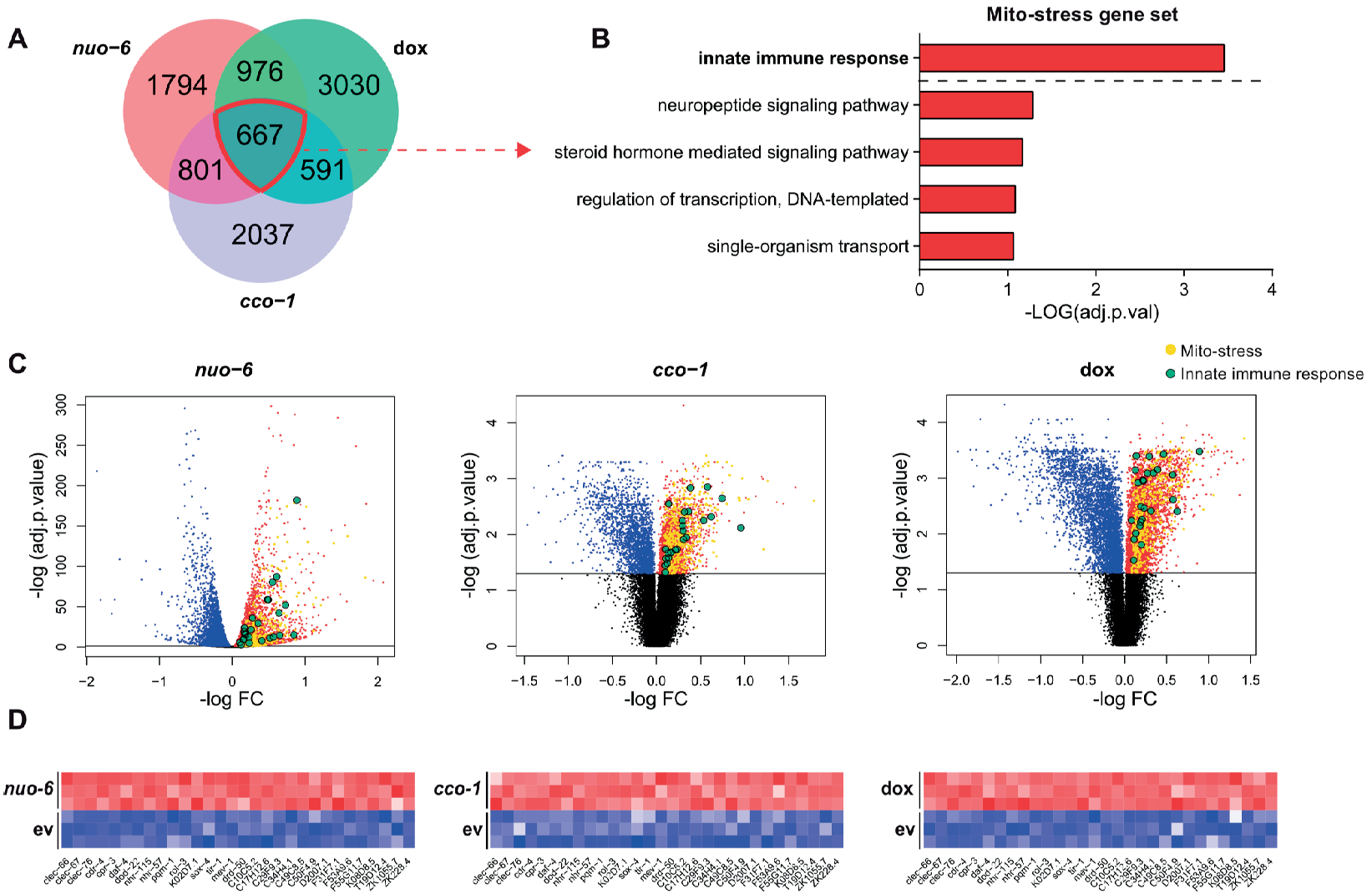
A
nuo−6
dox
cco−1
1794
976
3030
667
801
591
2037
B
Mito-stress gene set
innate immune response
neuropeptide signaling pathway
steroid hormone mediated signaling pathway
regulation of transcription, DNA-templated
single-organism transport
0
1
2
3
4
-LOG(adj.p.val)
C
nuo−6
cco−1
dox
Mito-stress
Innate immune response
-log (adj.p.value)
-log FC
D
nuo-6
cco-1
dox
ev

Figure 3.5

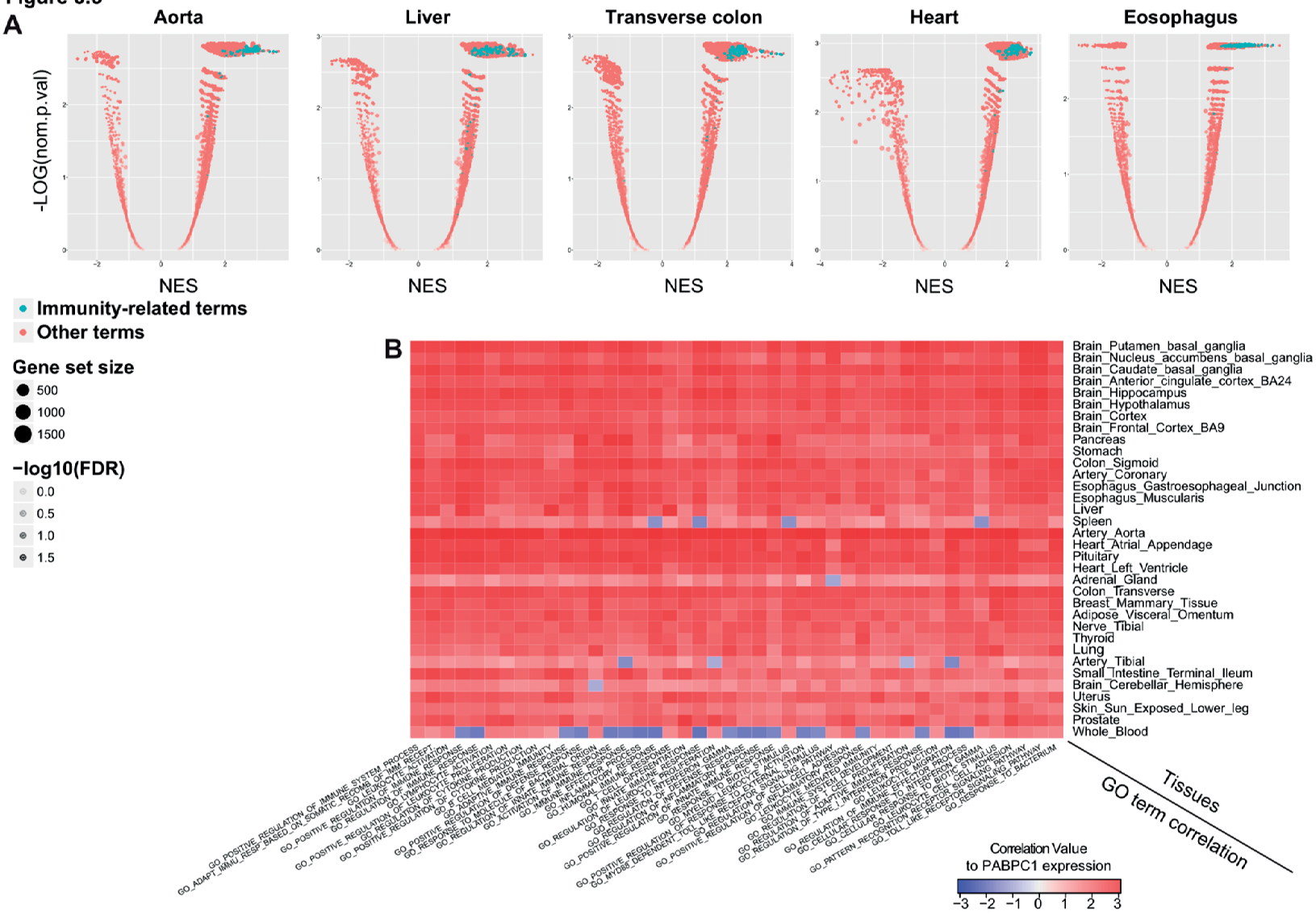
A
Aorta
Liver
Transverse colon
Heart
Eosophagus
-LOG(nom.p.val)
NES
Immunity-related terms
Other terms
Gene set size
500
1000
1500
−log10(FDR)
0.0
0.5
1.0
1.5
B
Brain_Putamen_basal_ganglia
Brain_Nucleus_accumbens_basal_ganglia
Brain_Caudate_basal_ganglia
Brain_Anterior_cingulate_cortex_BA24
Brain_Hippocampus
Brain_Hypothalamus
Brain_Cortex
Brain_Frontal_Cortex_BA9
Pancreas
Stomach
Colon_Sigmoid
Artery_Coronary
Esophagus_Gastroesophageal_Junction
Esophagus_Muscularis
Liver
Spleen
Artery_Aorta
Heart_Atrial_Appendage
Pituitary
Heart_Left_Ventricle
Adrenal_Gland
Colon_Transverse
Breast_Mammary_Tissue
Adipose_Visceral_Omentum
Nerve_Tibial
Thyroid
Lung
Artery_Tibial
Small_Intestine_Terminal_Ileum
Brain_Cerebellar_Hemisphere
Uterus
Skin_Sun_Exposed_Lower_leg
Prostate
Whole_Blood
Tissues
GO term correlation
Correlation Value
to PABPC1 expression
−3 −2 −1 0 1 2 3

Figure 5.1

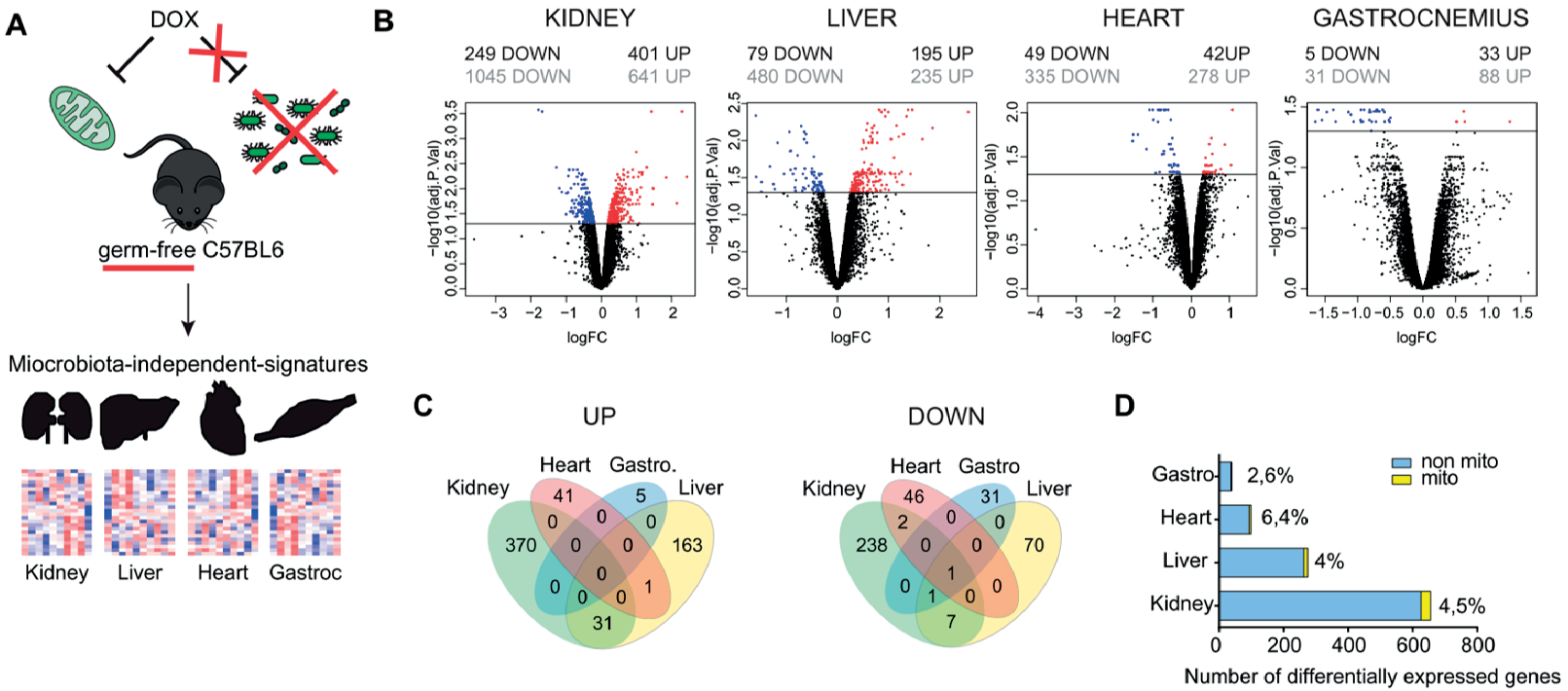
A
DOX
germ-free C57BL6
Miocrobiota-independent-signatures
Kidney
Liver
Heart
Gastroc
B
KIDNEY
249 DOWN
1045 DOWN
401 UP
641 UP
LIVER
79 DOWN
480 DOWN
195 UP
235 UP
HEART
49 DOWN
335 DOWN
42UP
278 UP
GASTROCNEMIUS
5 DOWN
31 DOWN
33 UP
88 UP
−log10(adj.P.Val)
logFC
C
UP
Kidney
Heart
Gastro.
Liver
41
5
370
163
31
1
DOWN
Kidney
Heart
Gastro
Liver
46
31
2
238
70
1
7
D
Gastro
Heart
Liver
Kidney
2,6%
6,4%
4%
4,5%
non mito
mito
0
200
400
600
800
Number of differentially expressed genes

Figure 5.2

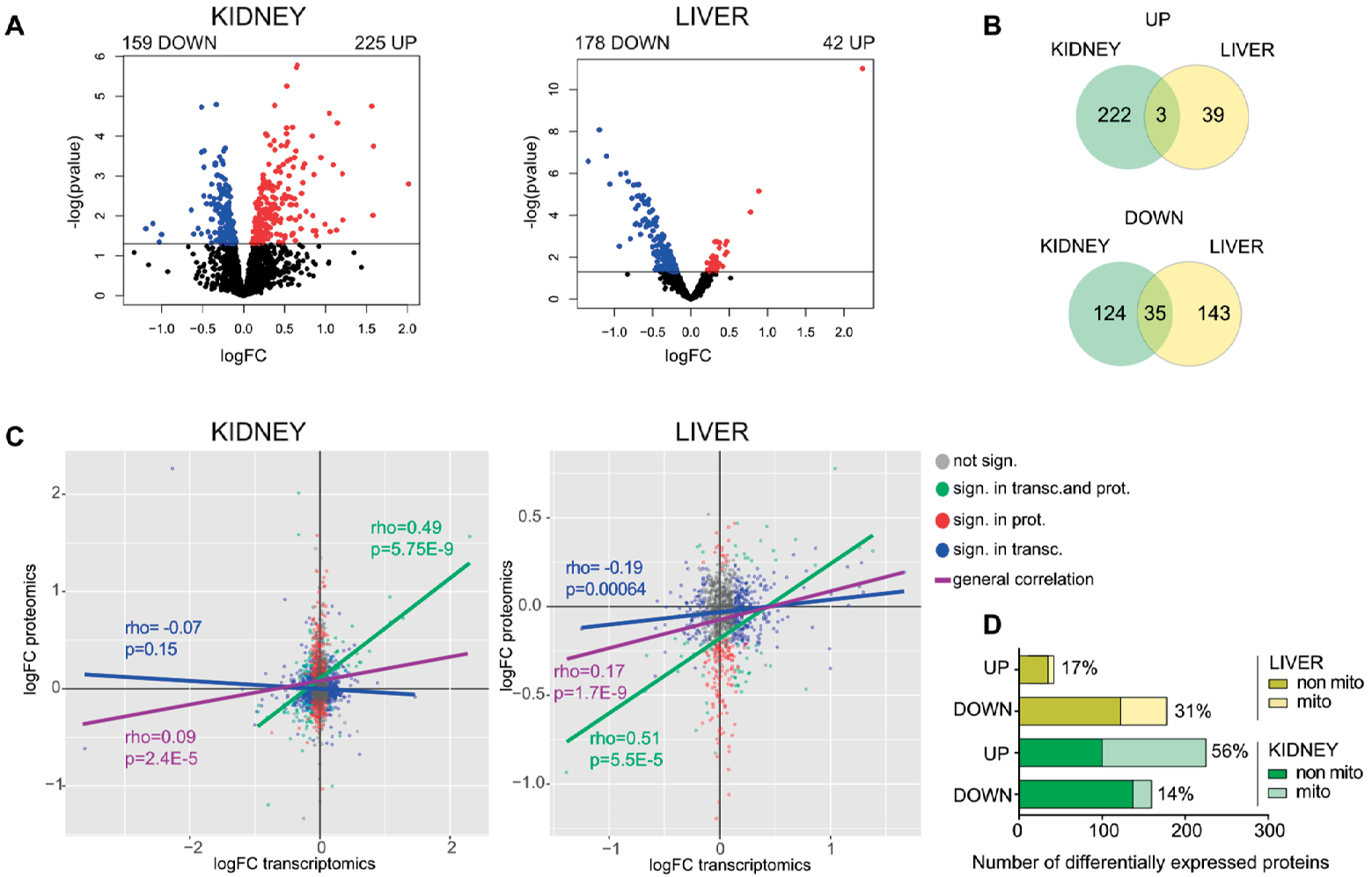
A
KIDNEY
159 DOWN
225 UP
-log(pvalue)
logFC
LIVER
178 DOWN
42 UP
-log(pvalue)
logFC
B
UP
KIDNEY
LIVER
222
3
39
DOWN
KIDNEY
LIVER
124
35
143
C
KIDNEY
rho=0.49
p=5.75E-9
rho= -0.07
p=0.15
rho=0.09
p=2.4E-5
logFC proteomics
logFC transcriptomics
LIVER
rho= -0.19
p=0.00064
rho=0.17
p=1.7E-9
rho=0.51
p=5.5E-5
logFC proteomics
logFC transcriptomics
not sign.
sign. in transc.and prot.
sign. in prot.
sign. in transc.
general correlation
D
UP
DOWN
UP
DOWN
17%
31%
56%
14%
LIVER
non mito
mito
KIDNEY
non mito
mito
Number of differentially expressed proteins

Figure 5.3

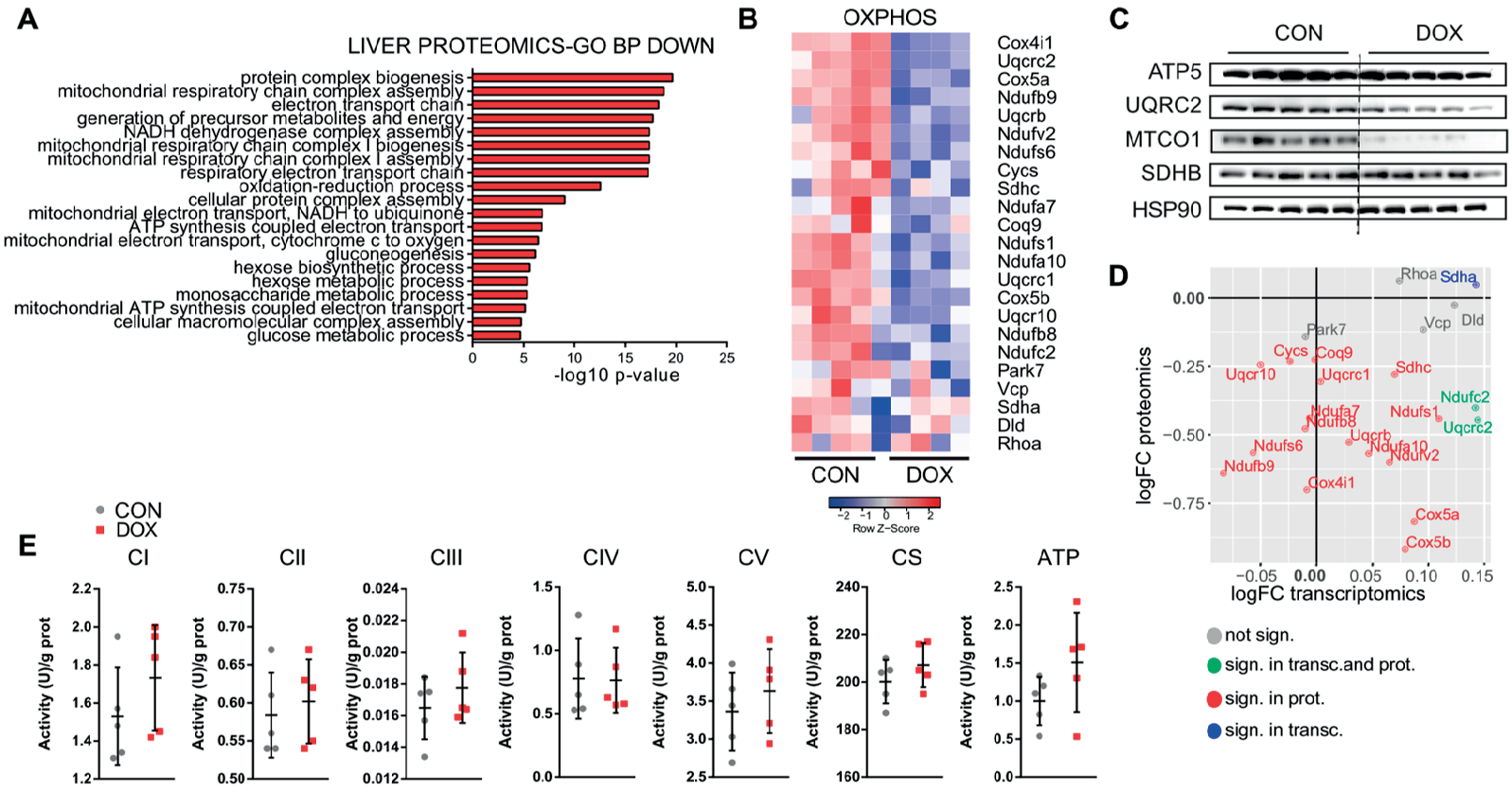
A
LIVER PROTEOMICS-GO BP DOWN
protein complex biogenesis
mitochondrial respiratory chain complex assembly
electron transport chain
generation of precursor metabolites and energy
NADH dehydrogenase complex assembly
mitochondrial respiratory chain complex I biogenesis
mitochondrial respiratory chain complex I assembly
respiratory electron transport chain
oxidation-reduction process
cellular protein complex assembly
mitochondrial electron transport, NADH to ubiquinone
ATP synthesis coupled electron transport
mitochondrial electron transport, cytochrome c to oxygen
gluconeogenesis
hexose biosynthetic process
hexose metabolic process
monosaccharide metabolic process
mitochondrial ATP synthesis coupled electron transport
cellular macromolecular complex assembly
glucose metabolic process
0 5 10 15 20 25
-log10 p-value
B
OXPHOS
Cox4i1
Uqcrc2
Cox5a
Ndufb9
Uqcrb
Ndufv2
Ndufs6
Cycs
Sdhc
Ndufa7
Coq9
Ndufs1
Ndufa10
Uqcrc1
Cox5b
Uqcr10
Ndufb8
Ndufc2
Park7
Vcp
Sdha
Dld
Rhoa
CON
DOX
−2 −1 0 1 2
Row Z-Score
C
CON
DOX
ATP5
UQRC2
MTCO1
SDHB
HSP90
D
logFC proteomics
logFC transcriptomics
0.00
−0.25
−0.50
−0.75
−0.05 0.00 0.05 0.10 0.15
Rhoa
Sdha
Vcp
Dld
Park7
Cycs
Coq9
Uqcr10
Uqcrc1
Sdhc
Ndufc2
Ndufa7
Ndufb8
Ndufs1
Uqcrc2
Uqcrb
Ndufa10
Ndufs6
Ndufv2
Ndufb9
Cox4i1
Cox5a
Cox5b
not sign.
sign. in transc.and prot.
sign. in prot.
sign. in transc.
E
CON
DOX
CI
CII
CIII
CIV
CV
CS
ATP
Activity (U)/g prot

Figure 5.4

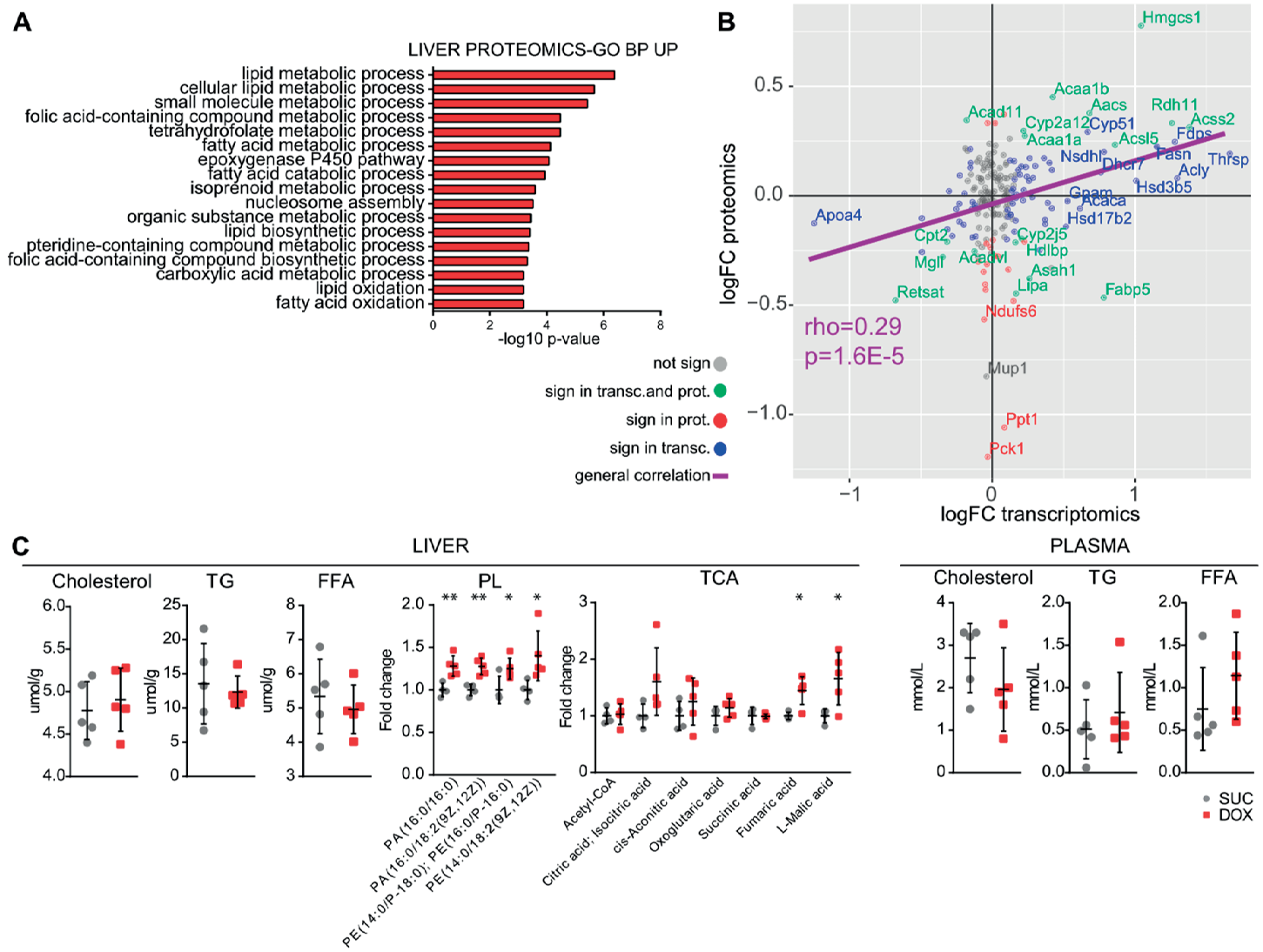
A
LIVER PROTEOMICS-GO BP UP
lipid metabolic process
cellular lipid metabolic process
small molecule metabolic process
folic acid-containing compound metabolic process
tetrahydrofolate metabolic process
fatty acid metabolic process
epoxygenase P450 pathway
fatty acid catabolic process
isoprenoid metabolic process
nucleosome assembly
organic substance metabolic process
lipid biosynthetic process
pteridine-containing compound metabolic process
folic acid-containing compound biosynthetic process
carboxylic acid metabolic process
lipid oxidation
fatty acid oxidation
0 2 4 6 8
-log10 p-value
not sign
sign in transc.and prot.
sign in prot.
sign in transc.
general correlation
B
logFC proteomics
logFC transcriptomics
rho=0.29
p=1.6E-5
Hmgcs1
Acaa1b
Aacs
Rdh11
Acad11
Acss2
Cyp2a12
Cyp51
Fdps
Acaa1a
Acsl5
Nsdhl
Fasn
Thrsp
Dhcr7
Acly
Hsd3b5
Gpam
Acaca
Apoa4
Hsd17b2
Cpt2
Cyp2j5
Hdlbp
Mgll
Acadvl
Asah1
Lipa
Retsat
Fabp5
Ndufs6
Mup1
Ppt1
Pck1
C
LIVER
Cholesterol
TG
FFA
PL
TCA
umol/g
Fold change
PA(16:0/16:0)
PA(16:0/18:2(9Z,12Z))
PE(14:0/P-18:0); PE(16:0/P-16:0)
PE(14:0/18:2(9Z,12Z))
Acetyl-CoA
Citric acid; Isocitric acid
cis-Aconitic acid
Oxoglutaric acid
Succinic acid
Fumaric acid
L-Malic acid
PLASMA
mmol/L
SUC
DOX

Figure 5.5

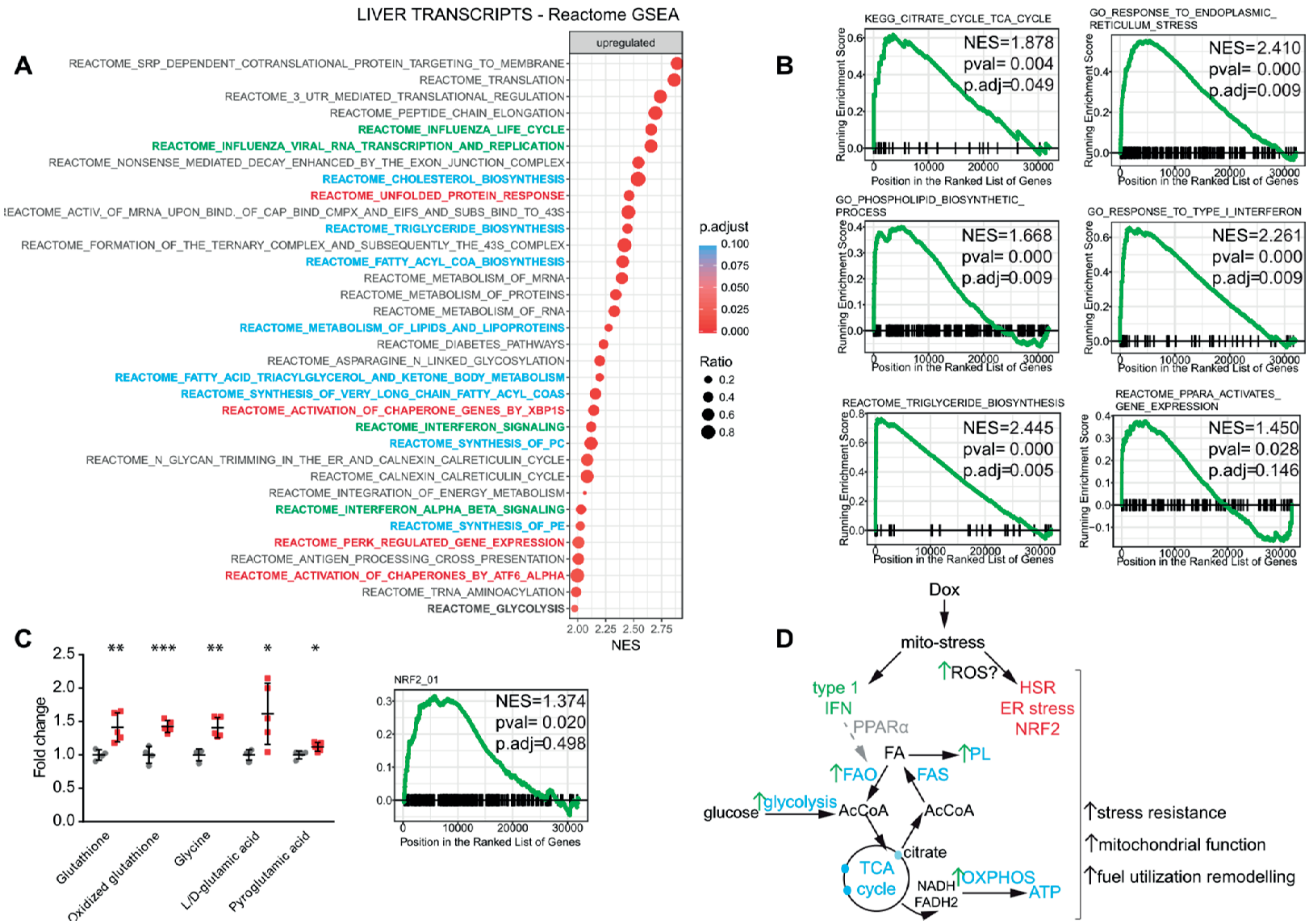
LIVER TRANSCRIPTS - Reactome GSEA
A
upregulated
REACTOME_SRP_DEPENDENT_COTRANSLATIONAL_PROTEIN_TARGETING_TO_MEMBRANE
REACTOME_TRANSLATION
REACTOME_3_UTR_MEDIATED_TRANSLATIONAL_REGULATION
REACTOME_PEPTIDE_CHAIN_ELONGATION
REACTOME_INFLUENZA_LIFE_CYCLE
REACTOME_INFLUENZA_VIRAL_RNA_TRANSCRIPTION_AND_REPLICATION
REACTOME_NONSENSE_MEDIATED_DECAY_ENHANCED_BY_THE_EXON_JUNCTION_COMPLEX
REACTOME_CHOLESTEROL_BIOSYNTHESIS
REACTOME_UNFOLDED_PROTEIN_RESPONSE
REACTOME_ACTIV._OF_MRNA_UPON_BIND._OF_CAP_BIND_CMPX_AND_EIFS_AND_SUBS_BIND_TO_43S
REACTOME_TRIGLYCERIDE_BIOSYNTHESIS
REACTOME_FORMATION_OF_THE_TERNARY_COMPLEX_AND_SUBSEQUENTLY_THE_43S_COMPLEX
REACTOME_FATTY_ACYL_COA_BIOSYNTHESIS
REACTOME_METABOLISM_OF_MRNA
REACTOME_METABOLISM_OF_PROTEINS
REACTOME_METABOLISM_OF_RNA
REACTOME_METABOLISM_OF_LIPIDS_AND_LIPOPROTEINS
REACTOME_DIABETES_PATHWAYS
REACTOME_ASPARAGINE_N_LINKED_GLYCOSYLATION
REACTOME_FATTY_ACID_TRIACYLGLYCEROL_AND_KETONE_BODY_METABOLISM
REACTOME_SYNTHESIS_OF_VERY_LONG_CHAIN_FATTY_ACYL_COAS
REACTOME_ACTIVATION_OF_CHAPERONE_GENES_BY_XBP1S
REACTOME_INTERFERON_SIGNALING
REACTOME_SYNTHESIS_OF_PC
REACTOME_N_GLYCAN_TRIMMING_IN_THE_ER_AND_CALNEXIN_CALRETICULIN_CYCLE
REACTOME_CALNEXIN_CALRETICULIN_CYCLE
REACTOME_INTEGRATION_OF_ENERGY_METABOLISM
REACTOME_INTERFERON_ALPHA_BETA_SIGNALING
REACTOME_SYNTHESIS_OF_PE
REACTOME_PERK_REGULATED_GENE_EXPRESSION
REACTOME_ANTIGEN_PROCESSING_CROSS_PRESENTATION
REACTOME_ACTIVATION_OF_CHAPERONES_BY_ATF6_ALPHA
REACTOME_TRNA_AMINOACYLATION
REACTOME_GLYCOLYSIS
2.00 2.25 2.50 2.75
NES
p.adjust
0.100
0.075
0.050
0.025
0.000
Ratio
0.2
0.4
0.6
0.8
B
KEGG_CITRATE_CYCLE_TCA_CYCLE
NES=1.878
pval= 0.004
p.adj=0.049
GO_RESPONSE_TO_ENDOPLASMIC_RETICULUM_STRESS
NES=2.410
pval= 0.000
p.adj=0.009
GO_PHOSPHOLIPID_BIOSYNTHETIC_PROCESS
NES=1.668
pval= 0.000
p.adj=0.009
GO_RESPONSE_TO_TYPE_I_INTERFERON
NES=2.261
pval= 0.000
p.adj=0.009
REACTOME_TRIGLYCERIDE_BIOSYNTHESIS
NES=2.445
pval= 0.000
p.adj=0.005
REACTOME_PPARA_ACTIVATES_GENE_EXPRESSION
NES=1.450
pval= 0.028
p.adj=0.146
Running Enrichment Score
Position in the Ranked List of Genes
C
Fold change
Glutathione
Oxidized glutathione
Glycine
L/D-glutamic acid
Pyroglutamic acid
NRF2_01
NES=1.374
pval= 0.020
p.adj=0.498
Position in the Ranked List of Genes
D
Dox
mito-stress
↑ROS?
HSR
ER stress
NRF2
type 1
IFN
PPARα
FA
↑PL
↑FAO
FAS
glucose
↑glycolysis
AcCoA
AcCoA
citrate
TCA
cycle
NADH
FADH2
↑OXPHOS
ATP
↑stress resistance
↑mitochondrial function
↑fuel utilization remodelling

Figure 5.6

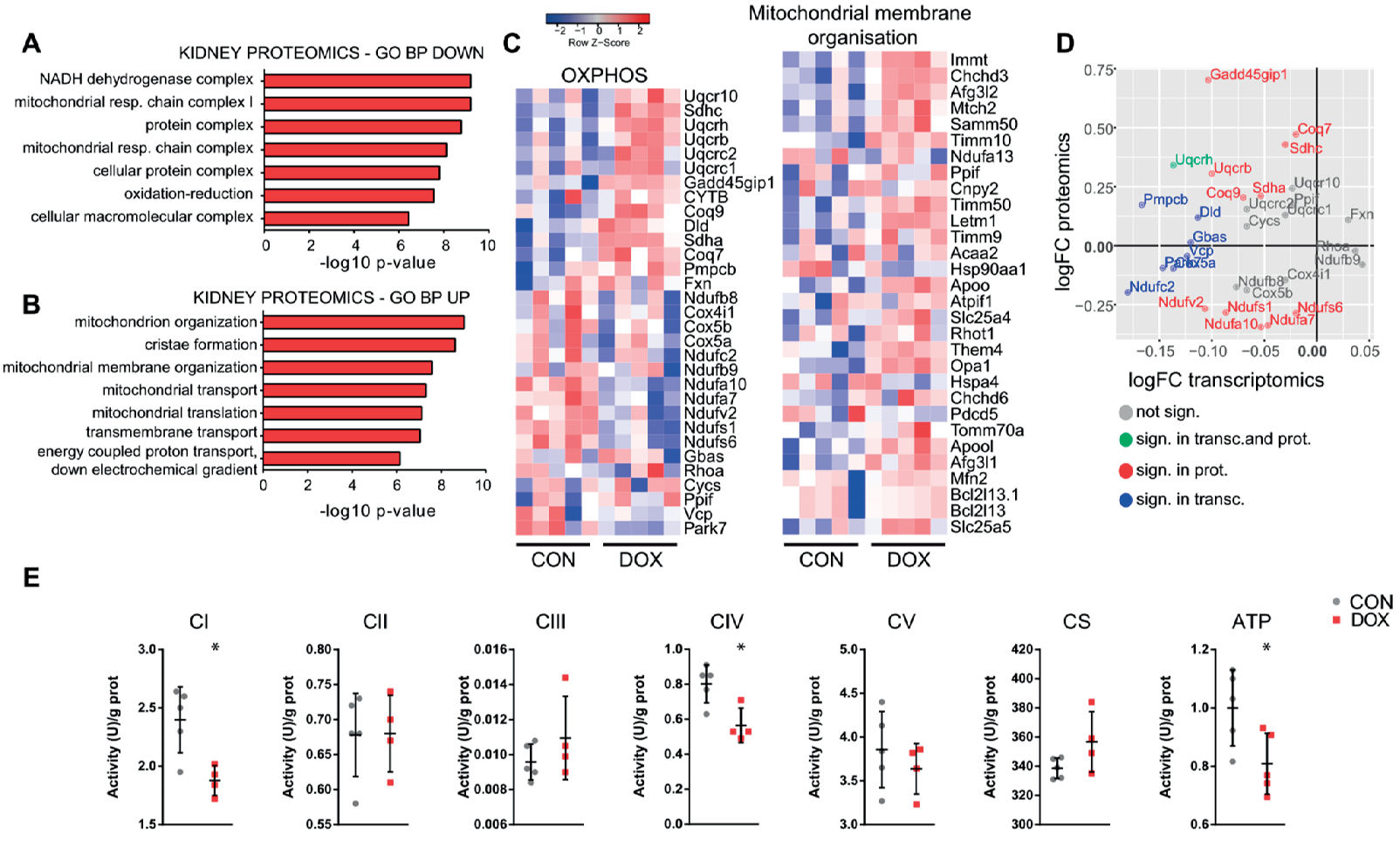
A
KIDNEY PROTEOMICS - GO BP DOWN
NADH dehydrogenase complex
mitochondrial resp. chain complex I
protein complex
mitochondrial resp. chain complex
cellular protein complex
oxidation-reduction
cellular macromolecular complex
0 2 4 6 8 10
-log10 p-value
B
KIDNEY PROTEOMICS - GO BP UP
mitochondrion organization
cristae formation
mitochondrial membrane organization
mitochondrial transport
mitochondrial translation
transmembrane transport
energy coupled proton transport, down electrochemical gradient
0 2 4 6 8 10
-log10 p-value
C
Row Z-Score
OXPHOS
Uqcr10
Sdhc
Uqcrh
Uqcrb
Uqcrc2
Uqcrc1
Gadd45gip1
CYTB
Coq9
Dld
Sdha
Coq7
Pmpcb
Fxn
Ndufb8
Cox4i1
Cox5b
Cox5a
Ndufc2
Ndufb9
Ndufa10
Ndufa7
Ndufv2
Ndufs1
Ndufs6
Gbas
Rhoa
Cycs
Ppif
Vcp
Park7
CON
DOX
Mitochondrial membrane organisation
Immt
Chchd3
Afg3l2
Mtch2
Samm50
Timm10
Ndufa13
Ppif
Cnpy2
Timm50
Letm1
Timm9
Acaa2
Hsp90aa1
Apoo
Atpif1
Slc25a4
Rhot1
Them4
Opa1
Hspa4
Chchd6
Pdcd5
Tomm70a
Apool
Afg3l1
Mfn2
Bcl2l13.1
Bcl2l13
Slc25a5
CON
DOX
D
logFC proteomics
logFC transcriptomics
0.75
0.50
0.25
0.00
−0.25
−0.15 −0.10 −0.05 0.00 0.05
Gadd45gip1
Coq7
Sdhc
Uqcrh
Uqcrb
Sdha
Uqcr10
Coq9
Pmpcb
Ppif
Uqcrc2
Uqcrc1
Dld
Cycs
Fxn
Gbas
Vcp
Rhoa
Ndufb9
Cox4i1
Ndufc2
Cox5b
Ndufb8
Ndufv2
Ndufs1
Ndufs6
Ndufa10
Ndufa7
not sign.
sign. in transc.and prot.
sign. in prot.
sign. in transc.
E
CI
CII
CIII
CIV
CV
CS
ATP
CON
DOX
Activity (U)/g prot
*

Figure 5.7

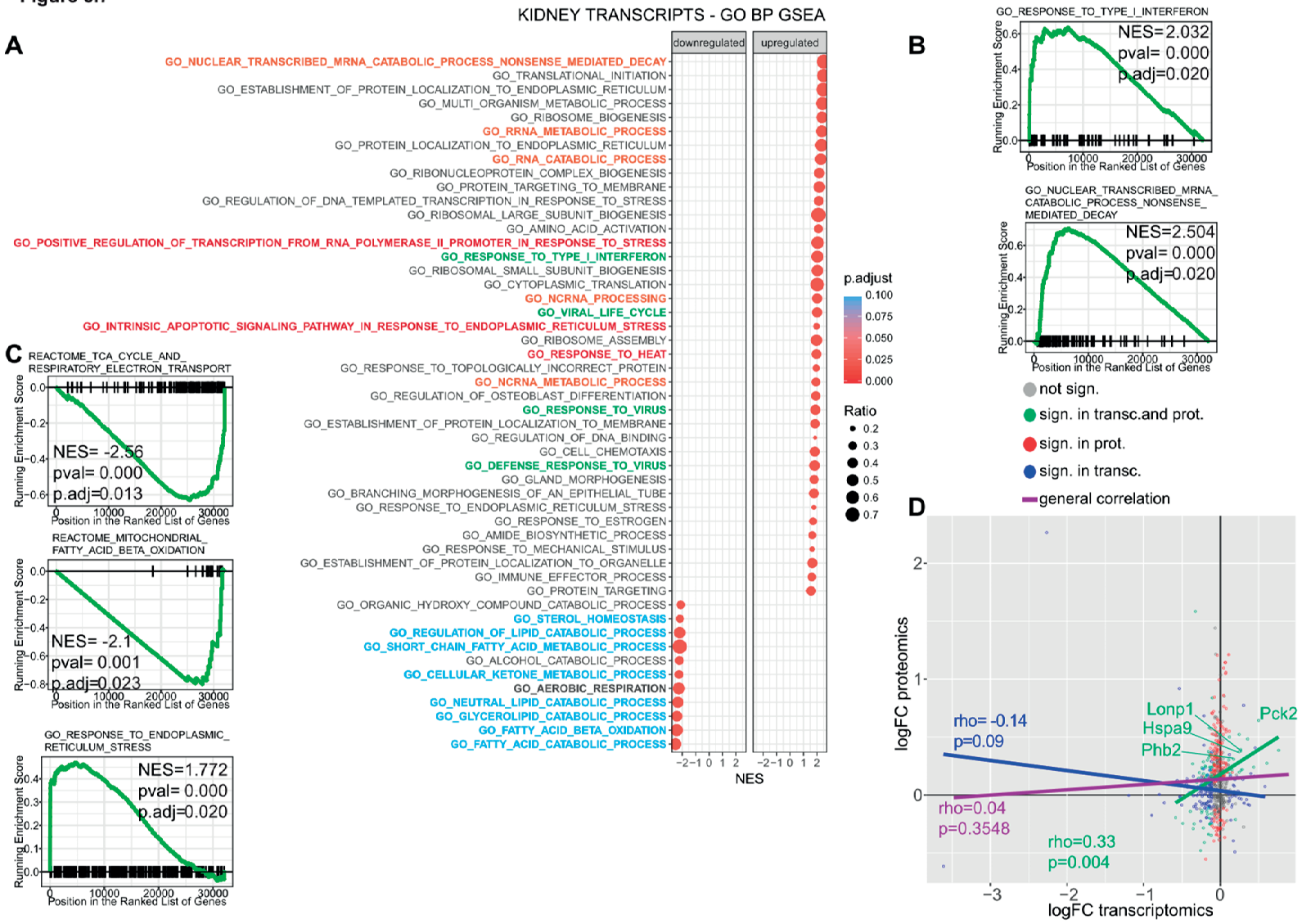
A
KIDNEY TRANSCRIPTS - GO BP GSEA
downregulated
upregulated
GO_NUCLEAR_TRANSCRIBED_MRNA_CATABOLIC_PROCESS_NONSENSE_MEDIATED_DECAY
GO_TRANSLATIONAL_INITIATION
GO_ESTABLISHMENT_OF_PROTEIN_LOCALIZATION_TO_ENDOPLASMIC_RETICULUM
GO_MULTI_ORGANISM_METABOLIC_PROCESS
GO_RIBOSOME_BIOGENESIS
GO_RRNA_METABOLIC_PROCESS
GO_PROTEIN_LOCALIZATION_TO_ENDOPLASMIC_RETICULUM
GO_RNA_CATABOLIC_PROCESS
GO_RIBONUCLEOPROTEIN_COMPLEX_BIOGENESIS
GO_PROTEIN_TARGETING_TO_MEMBRANE
GO_REGULATION_OF_DNA_TEMPLATED_TRANSCRIPTION_IN_RESPONSE_TO_STRESS
GO_RIBOSOMAL_LARGE_SUBUNIT_BIOGENESIS
GO_AMINO_ACID_ACTIVATION
GO_POSITIVE_REGULATION_OF_TRANSCRIPTION_FROM_RNA_POLYMERASE_II_PROMOTER_IN_RESPONSE_TO_STRESS
GO_RESPONSE_TO_TYPE_I_INTERFERON
GO_RIBOSOMAL_SMALL_SUBUNIT_BIOGENESIS
GO_CYTOPLASMIC_TRANSLATION
GO_NCRNA_PROCESSING
GO_VIRAL_LIFE_CYCLE
GO_INTRINSIC_APOPTOTIC_SIGNALING_PATHWAY_IN_RESPONSE_TO_ENDOPLASMIC_RETICULUM_STRESS
GO_RIBOSOME_ASSEMBLY
GO_RESPONSE_TO_HEAT
GO_RESPONSE_TO_TOPOLOGICALLY_INCORRECT_PROTEIN
GO_NCRNA_METABOLIC_PROCESS
GO_REGULATION_OF_OSTEOBLAST_DIFFERENTIATION
GO_RESPONSE_TO_VIRUS
GO_ESTABLISHMENT_OF_PROTEIN_LOCALIZATION_TO_MEMBRANE
GO_REGULATION_OF_DNA_BINDING
GO_CELL_CHEMOTAXIS
GO_DEFENSE_RESPONSE_TO_VIRUS
GO_GLAND_MORPHOGENESIS
GO_BRANCHING_MORPHOGENESIS_OF_AN_EPITHELIAL_TUBE
GO_RESPONSE_TO_ENDOPLASMIC_RETICULUM_STRESS
GO_RESPONSE_TO_ESTROGEN
GO_AMIDE_BIOSYNTHETIC_PROCESS
GO_RESPONSE_TO_MECHANICAL_STIMULUS
GO_ESTABLISHMENT_OF_PROTEIN_LOCALIZATION_TO_ORGANELLE
GO_IMMUNE_EFFECTOR_PROCESS
GO_PROTEIN_TARGETING
GO_ORGANIC_HYDROXY_COMPOUND_CATABOLIC_PROCESS
GO_STEROL_HOMEOSTASIS
GO_REGULATION_OF_LIPID_CATABOLIC_PROCESS
GO_SHORT_CHAIN_FATTY_ACID_METABOLIC_PROCESS
GO_ALCOHOL_CATABOLIC_PROCESS
GO_CELLULAR_KETONE_METABOLIC_PROCESS
GO_AEROBIC_RESPIRATION
GO_NEUTRAL_LIPID_CATABOLIC_PROCESS
GO_GLYCEROLIPID_CATABOLIC_PROCESS
GO_FATTY_ACID_BETA_OXIDATION
GO_FATTY_ACID_CATABOLIC_PROCESS
−2 −1 0 1 2
NES
p.adjust
0.100
0.075
0.050
0.025
0.000
Ratio
0.2
0.3
0.4
0.5
0.6
0.7
B
GO_RESPONSE_TO_TYPE_I_INTERFERON
NES=2.032
pval= 0.000
p.adj=0.020
Running Enrichment Score
Position in the Ranked List of Genes
GO_NUCLEAR_TRANSCRIBED_MRNA_CATABOLIC_PROCESS_NONSENSE_MEDIATED_DECAY
NES=2.504
pval= 0.000
p.adj=0.020
not sign.
sign. in transc.and prot.
sign. in prot.
sign. in transc.
general correlation
C
REACTOME_TCA_CYCLE_AND_RESPIRATORY_ELECTRON_TRANSPORT
NES= -2.56
pval= 0.000
p.adj=0.013
REACTOME_MITOCHONDRIAL_FATTY_ACID_BETA_OXIDATION
NES= -2.1
pval= 0.001
p.adj=0.023
GO_RESPONSE_TO_ENDOPLASMIC_RETICULUM_STRESS
NES=1.772
pval= 0.000
p.adj=0.020
D
logFC proteomics
logFC transcriptomics
rho= -0.14
p=0.09
rho=0.04
p=0.3548
rho=0.33
p=0.004
Lonp1
Hspa9
Phb2
Pck2

Supp figure 5.10

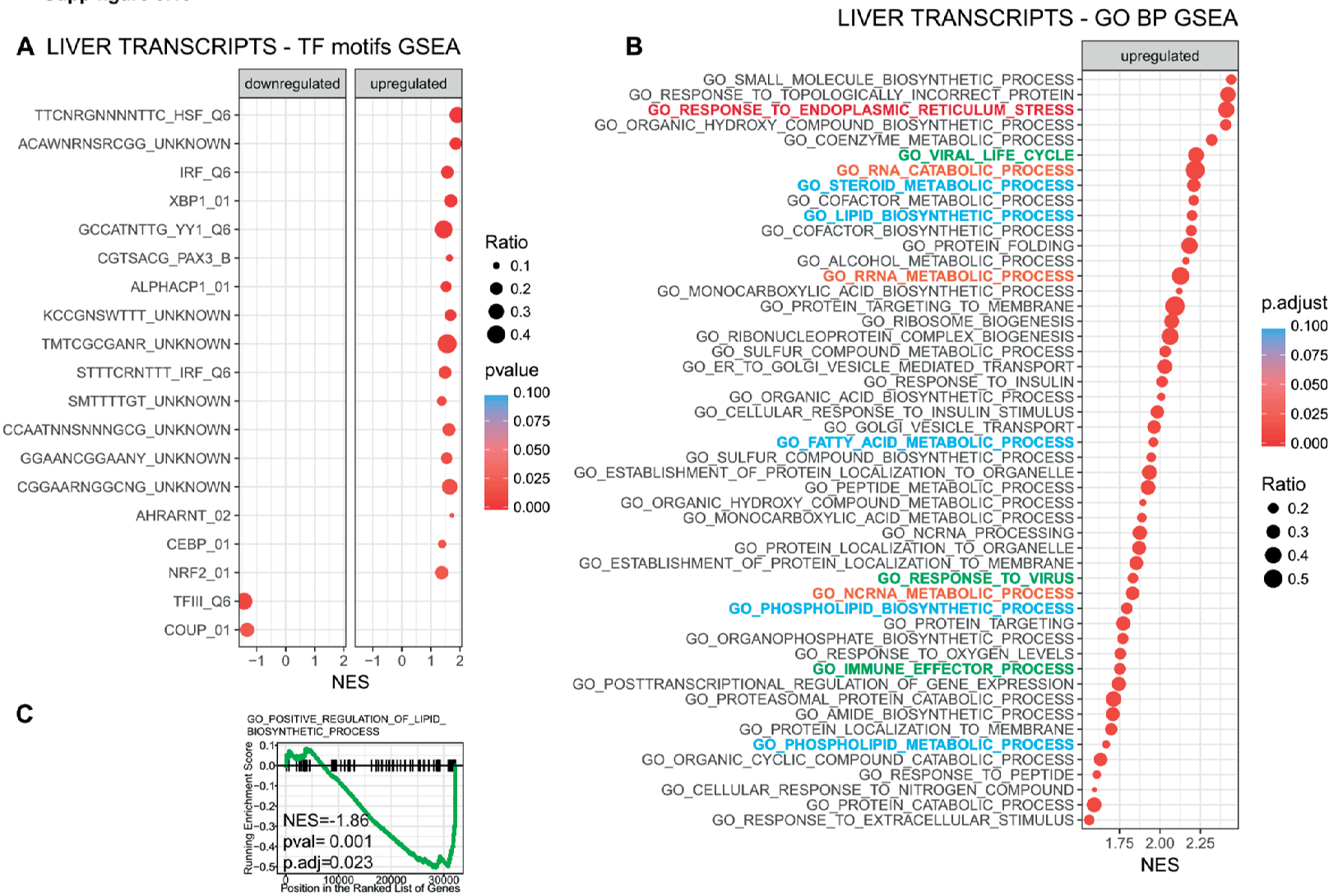

Supp figure 5.11

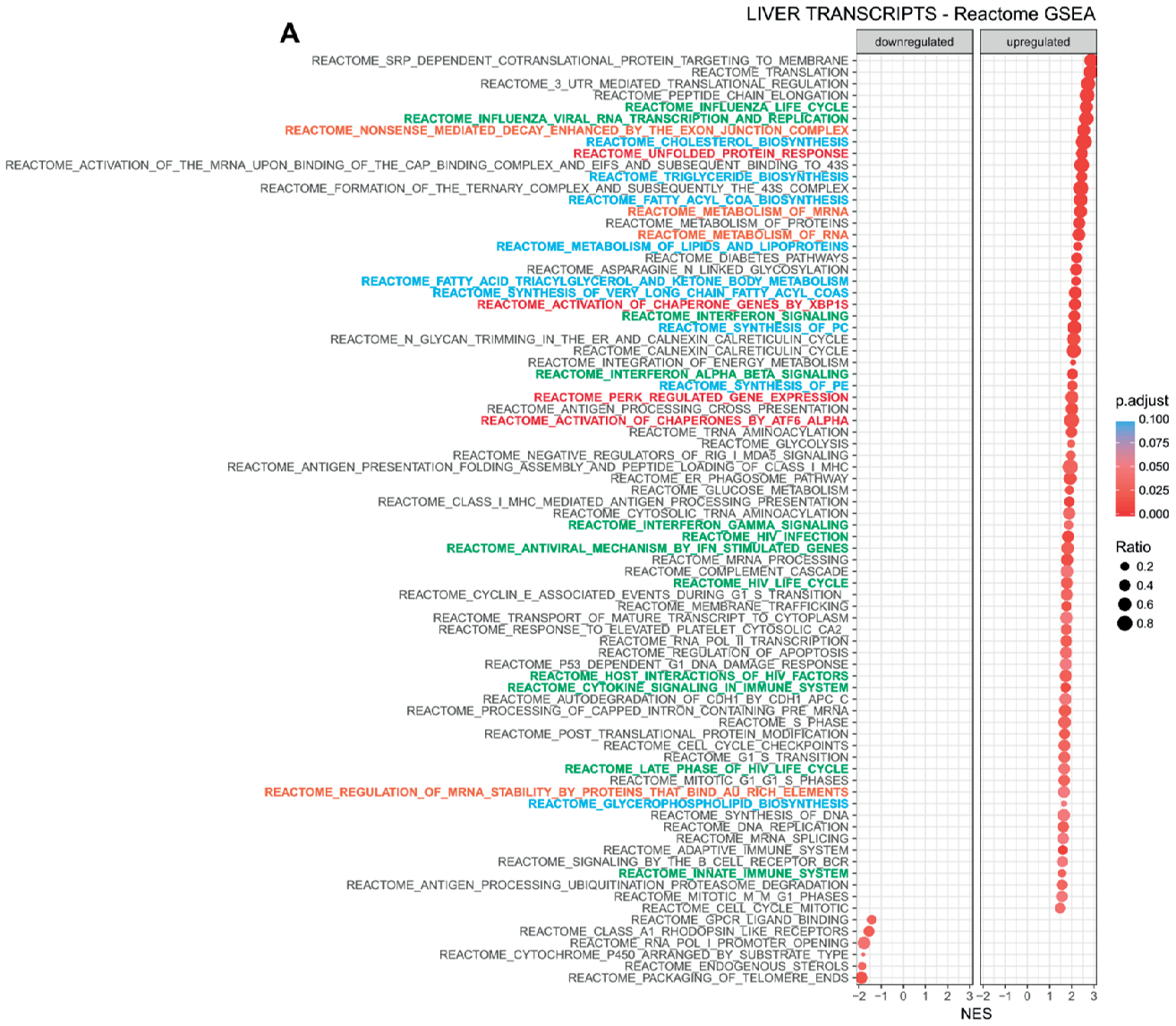

Supp figure 5.12

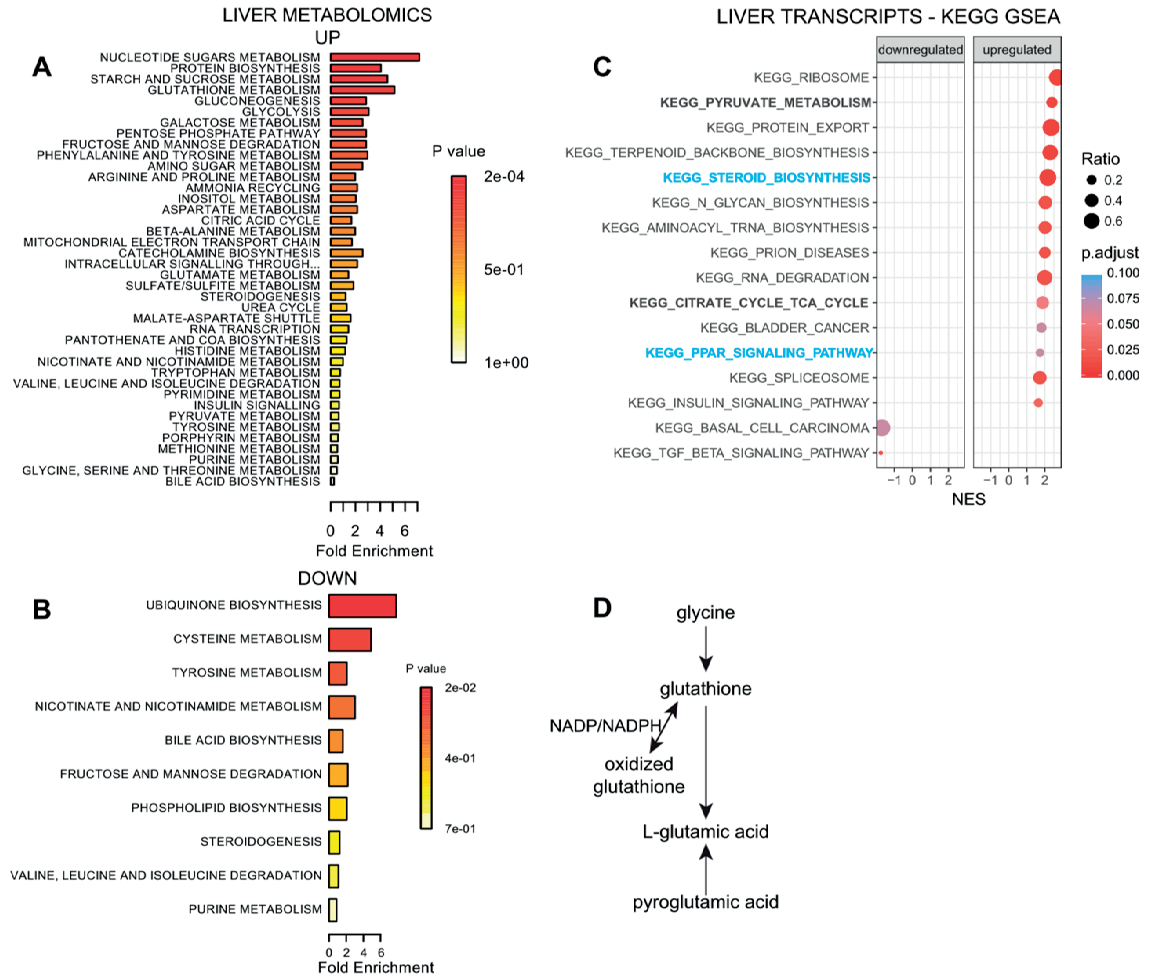

Supp figure 5.13

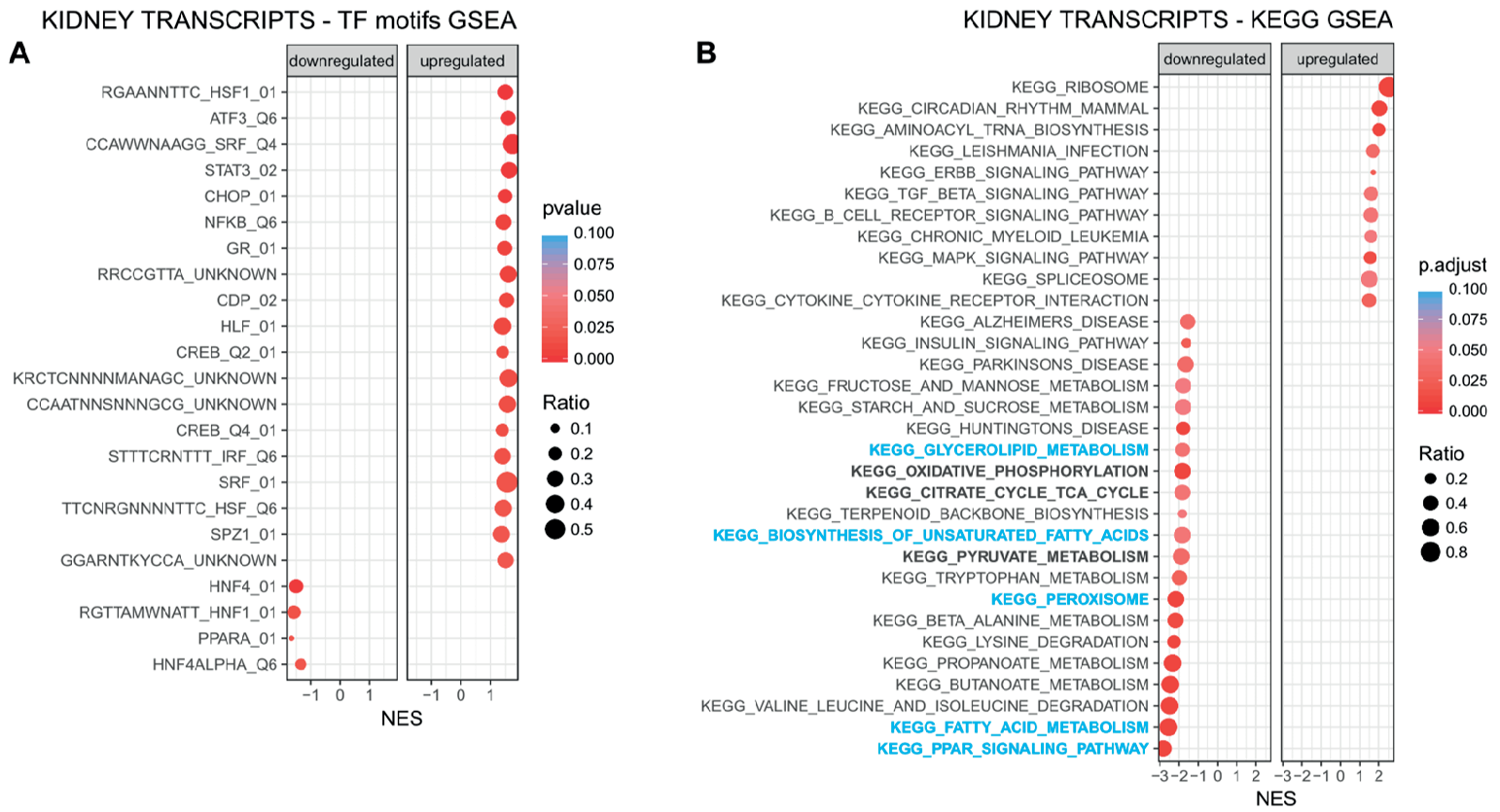

Supp figure 5.14

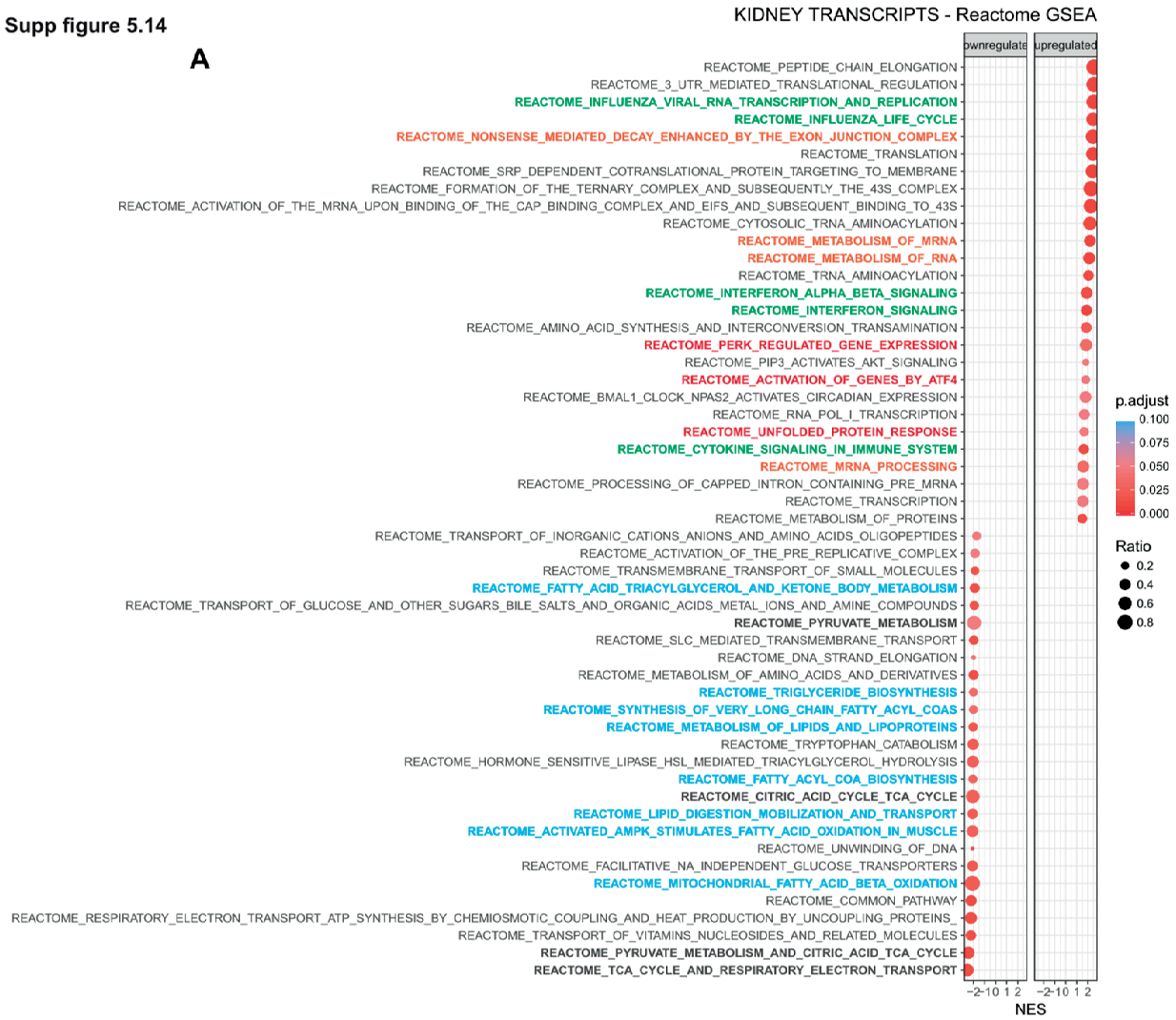

Supp figure 5.15